https://theses.gla.ac.uk/

Theses Digitisation:

https://www.gla.ac.uk/myglasgow/research/enlighten/theses/digitisation/

This is a digitised version of the original print thesis.

Copyright and moral rights for this work are retained by the author

A copy can be downloaded for personal non-commercial research or study, without prior permission or charge

This work cannot be reproduced or quoted extensively from without first obtaining permission in writing from the author

The content must not be changed in any way or sold commercially in any format or medium without the formal permission of the author

When referring to this work, full bibliographic details including the author, title, awarding institution and date of the thesis must be given

Enlighten: Theses
https://theses.gla.ac.uk/
research-enlighten@glasgow.ac.uk

RELIABILITY ANALYSIS OF CONTINUOUS STRUCTURAL SYSTEMS

A Thesis Submitted

for the Degree of Doctor of Philosophy

in the Faculty of Engineering at the University of Glasgow

by

Joo - Sung Lee, B.Sc., M.Sc.

Department of Naval Architecture and Ocean Engineering

University of Glasgow

© Joo-Sung Lee, 1989

ProQuest Number: 10999338

All rights reserved

INFORMATION TO ALL USERS
The quality of this reproduction is dependent upon the quality of the copy submitted.

In the unlikely event that the author did not send a complete manuscript
and there are missing pages, these will be noted. Also, if material had to be removed,
a note will indicate the deletion.

ProQuest 10999338

Published by ProQuest LLC (2018). Copyright of the Dissertation is held by the Author.

All rights reserved.
This work is protected against unauthorized copying under Title 17, United States Code
Microform Edition © ProQuest LLC.

ProQuest LLC.
789 East Eisenhower Parkway
P.O. Box 1346
Ann Arbor, MI 48106 – 1346

To

My Parents, Late Father - In - Law and Family

ACKNOWLEDGEMENTS

The thesis is based on the study carried out during the period of October 1986 to January 1989 in the Department of Naval Architecture and Ocean Engineering at the University of Glasgow. The author wishes to express his warmest gratitude

To Professor Douglas Faulkner, his supervisor and Head of the Department of Naval Architecture and Ocean Engineering, for his expertised guidance, advice and timely encouragement throughout the duration of the author's study, and also for his strong support to get the University Scholarship which enabled the author's study.

To My colleagues in the Department of Naval Architecture, Shipbuilding and Ocean Engineering at the University of Ulsan in Korea for their continual encouragement, especially to Dr. S.-R. Cho for his fruitful discussion about subjects of each other during the time spent together.

and the author's warmest thanks are due to Mrs. Isobel Faulkner for her editing the draft of the author's thesis.

Finally, many thanks should go to all of my families for their endurance, especially to my beloved wife, Yun-Hee, and two lovely boys, Kyoung-Seop and Yun-Seop, for their endless love and mental support. It is not an overstatement to say that they have nearly lost their husband and daddy at least for the last two and half years. The author have nothing to have done for them and all he could do is to put their names on just here ...

Joo-Sung Lee,
Glasgow,
March 1989

TABLE OF CONTENTS

SUMMARY

This study mainly deals with developing another approximate method for system reliability analysis and its applications to the continuous structures such as an assembly of stiffened cylindrical and rectangular sections used in Tension Leg Platform (TLP). Various methods developed for the structural system reliability analysis are reviewed

The developed system reliability method, called herein the "Extended Incremental Load Method", is an extended approach of the conventional incremental load method. It has been developed in order to extend its applicability to the system reliability analysis of a structure under multiple loadings. It directly uses existing component strength formulae in the system analysis and more realistically takes account of the post-ultimate (post-failure) behaviour of a failed component when assessing the system reliability and ultimate strength. This is an important merit of the method over other methods.

The method allows for load re-distribution during the development of elasto-plastic moments in large cross-sections under the action of axial and bending forces and in the presence of lateral hydrostatic and hydrodynamic pressure. The effects of shearing actions are ignored. A search is made for the most important failure modes to give the lowest system safety index.

In the method the modified safety margin equation, which has been proposed to use existing strength formulae for principle components of a floating offshore structure, is employed in which the strength modelling parameter is treated as a basic random variable in system reliability analysis as well as component reliability analysis and the concept of the first-order second moment method is adopted to obtain the resistance coefficients and the loading coefficients in the safety margin equation.

Details about deriving the safety margin equation by the proposed reliability method, calculation of the total load factor, the procedure of identifying the most

important failure modes and flow vectors of principle component are described in the Appendices.

Applications to discrete structures are demonstrated to show the validity of the proposed method. The method has been applied to the Hutton TLP and two variants, TLP-A and TLP-B, which are modified models of the Hutton TLP and of the design using TLP Rule Case Committee type loading and improved strength models, under the design environmental loading conditions. Components and systems safety indices of the models, Hutton TLP, TLP-A and TLP-B, are illustrated with three dimensional collapse mechanisms figures. Reserve and reserve strength characteristics are derived for the design as built and for more economical and efficient variations of the design. The TLP form is shown to possess high redundancy and systems safety.

Sensitivity studies to changes in stochastic parameters of resistance and loading variables have been carried out. For this purpose the strength modelling parameter, yield stress and certain member sizes are selected as resistance variables, and effects of their mean values and/or coefficients of variation on the system, as well as on the component reliability index, have been investigated. The effects of mean bias and coefficient of variation of load effects, namely, static, quasi-static and dynamic component, on the the system as well as on the component reliability index have also been investigated. The results are discussed with regard to effects of various parameters on safety, with illustrating figures, from which the relative importance of random variables can be seen.

As an another important resistance variable, the post-ultimate behaviour of failed components has been taken account of in system reliability assessment, which should be the most important resistance variable affecting the system reliability and the effective residual strength of a structure. Some case studies have been carried out with the simplified non-linear model which has a form of piecewise multi-state (more than two states) and is characterised by the post-ultimate slope and the residual strength. The results are illustrated in figures and tables and discussion made about its effects on the

system reliability level. The analysis, using two-state model which has only the residual strength characteristic, has also been carried out using the proposed approach of calculating the artificial force vector due the unloading effect of a failed component of which behaviour is not ductile. The results using multi-state model and two state model have been compared.

The results of sensitivity studies show the importance of coefficient of variation of the strength modelling parameter and post ultimate-behaviour as resistance variables, and the mean bias and coefficients of variation of static and dynamic load effect. Among resistance variables in the sensitivity studies, the COV of yield stress and certain geometric variables has relatively small influence on the resulting system reliability index. The post-ultimate behaviour has significant influence on the system safety and seems to be more influential than the strength modelling parameter and even loading variables. Hence, it should be considered in system reliability analysis using a more refined and realistic model.

The present sensitivity study is useful and important in assessing the parameters perturbation effects on the component and system reliability and the results can provide valuable information about the relative importance of random variables in the context of reliability analysis. Therefore, in order to provide the designer with useful criteria or information as an aid to decision making in the design stage, it is recommended that certain types of sensitivity studies to change in the stochastic parameters of resistance and loading variables, as illustrated, must be carried out.

A few basic ideas about reliability-based design are addressed and a simple procedure of evaluating the system safety level has been introduced. An attempt has been made of to link component and system safety to structural redundancy as an aid to choice of acceptable component and system safety levels in the design stage. The study indicates that some acceptable safety levels may well be lower than the present levels used in design. The basic concept of the reliability-based optimal design and optimal inspection and maintenance strategy are briefly described.

The thesis ends with a summary of the present work drawn from the proposed approach for system reliability analysis and its application to continuous structures (TLPs) as well as discrete structures not only in the context of structural design (for minimum weight and/or cost) but also for in-service re-assessment purposes. Future research and extensions of the present work are recommended in the context of reliability-based limit state design.

NOMENCLATURE

A_k : cross sectional area of component r_k or k

a_{ki} : utilisation ratio of component r_k utilised in the i th load increment

A_{st} : stiffener sectional area

A_T : total sectional area

b, b_e, b_e' : flat panel width between stiffeners and its effective width and reduced effective width

B : bias or breadth

B_{ml} : loading coefficient of the l th loading for the m th failure mode in the safety margin equation

b_f, t_f : width and thickness of flange

C_a : added mass coefficient

C_D : drag coefficient

C_{DL} : equivalent linear drag coefficient

C_f : expected cost of failure

C_I : cost of inspection

C_o : initial cost

C_M : inertia coefficient ($= 1 + C_a$)

C_{mk} : resistance coefficients in the safety margin equation

C_R : cost of repair

C_s : shape coefficient for wind force

C_T : total cost

$CF^{(l)}$: contribution factor of the l th loading case

D : diameter

E : elastic modulus

E' : unloading rate or normalised post-ultimate slope of load-displacement curve

E^* : effective tangential modulus of stiffened plating

E_i : tangential stiffness of element i

F_c : current force

F_D : wave drift force

F_W : wind force

F_x : axial force

F_{xu} : ultimate axial compressive force

F_y, F_z : shear force in y- and z-direction

$f_X(\cdot)$: probability density function of random variable X

$F_X(\cdot)$: probability distribution function of random variable X

h_w, t_w : height and thickness of web

H_w : wave height

I_k : moment of inertia of component r_k or k

K_c : buckling coefficient

m : element mass

m_a : added mass of element

M_{min} : minimum required number of important failure modes to be identified

M_u : ultimate bending moment

M_x : torsional moment

M_y, M_z : bending moment about y- and z-axis

N_i : number of failed components in a failure path

N_{det} : prescribed number to limit the number of interim modes of which determinants are to be checked

N_{max} : maximum number of failed components in the interim failure mode for all possible modes

N_{Limit} : the number to limit the number of interim modes to be considered

n : reserve strength ratio for system

P : radial pressure (MPa)

P_c : collapse radial pressure

P_{ij} : joint probability of failure between mode i and j

P_f : probability of failure

P_{f_j} : failure probability of the j th failure mode

$(P_f)_{sys}$: probability of system failure

P_k : load increment to fail the component, r_k

$P^{(l)}$, P_l : the l th loading

p_s : ratio of the structural proportional limit to yield stress

P_s : probability of survival

$(P_s)_{sys}$: probability of system survival (reliability)

P_u : ultimate axial compression

Q_k : load effect of component k or r_k

R : radius of cylindrical component

r_k or k : component number failed at the k th failure (or incremental) stage

R_k : resistance of component k or r_k

R_r : residual stress reduction factor

R_{sys} : system resistance

RI : redundancy index

RDI : residual strength index or residual resistance factor (RIF)

RSI : reserve strength index or reserve resistance factor (REF)

RDI_β : β-measure of residual strength of structural system

s, s_e, s_e' : curved panel width between stringer, and its effective width and reduced effective width

s_i : feasible direction of variable X_i

T_w : wave period (sec)

u_p, u_p : velocity and acceleration of water particle

U_r : amplitude of relative velocity of water particle and structural element

$\underline{U}_r$: square root of relative velocity variance of water particle and structural element

u_r : relative velocity of water particle and structural element

u_s, u_s : velocity and acceleration of structural element

V : volume

V_C : current velocity

V_{X_i} : COV of random variable X_i

V_{X_M} : modelling uncertainty (COV) of strength modelling parameter

V_z : wind velocity at z m above sea level

V_{10} : wind velocity at 10 m above sea level

w' : non-dimensional lateral pressure

X_i : random variable

$\underline{X}_i$: mean value of random variable X_i

X_i^* : design point of random variable X_i

X_M : strength modelling parameter

$\underline{X}_M$: mean bias of strength modelling parameter

X_{M_k} : strength modelling parameter of component k or r_k

Z : safety margin or section modulus

Z^{eq} : equivalent safety margin

Z_L or Z : Batdorf length parameter

Z_m : safety margin for the mth failure mode

Z'_m : non-dimensional safety margin for the mth failure mode

Z_p : plastic sectional modulus

Z_s : Batdorf width parameter

α_i : sensitivity to random variable X_i

α_i^{eq} : equivalent sensitivity to random variable X_i

β : reliability index or plate slenderness

β^{eq} : equivalent reliability index

β^o : allowable reliability index (target reliability index)

β_{comp} : component reliability index

β_m : reliability index for the m th failure mode

β_{path} : path reliability index

β_{sys} : system reliability index

$\beta_{sys,R}$: residual system reliability index

γ_i : partial safety factor for variable X_i

δ_o : initial deflection of plate

ε : strain

ε' : normalised strain

ε_{det} : prescribed small number used to judge the singularity of the structural stiffness matrix

ε_{r_k} : strain of the component, r_k

ε_u : ultimate strain

ε_{utr} : prescribed small number to discard the deterministically less important modes

ε_{sys} : prescribed value used to check the convergence of bounds of system reliability index

ε_Y : yield strain

Φ : standard normal distribution function

ϕ : standard normal density function or compressive strength parameter of stiffened panel

ϕ_{sys} : system factor (system partial safety factor)

ϕ_y, ϕ_z : curvature associated with bending about y- and z-axis

η : residual strength parameter or welding tension block parameter

λ : slenderness of stiffener-plate combination

λ_{CLF} : central load factor

λ_j : mean load factor to fail the j th component

λ_T : total load factor or reserve strength index

ν : Poissons ratio

θ : central safety factor

ρ : density of water

ρ_a : density of air

ρ_{ij} : correlation coefficient between variables X_i and X_j

ρ_n, ρ_x, ρ_θ : knock-down factor

σ' : normalised stress

σ_{eff} : effective stress

ψ : imperfect elastic buckling parameter

σ_r : compressive residual stress

σ_u : ultimate stress

σ_{X_i} : standard deviation of random variable, X_i

σ_{xu} : ultimate axial stress

σ_Y : yield stress

σ_θ : hoop stress

$\sigma_{\theta u}$: ultimate hoop stress

χ : wave direction (degree)

ζ_s : systematic error

[A] : total mean utilisation matrix

{a} : flow vector

[a] : utilisation matrix

[B] : unloading matrix or damping matrix or unloading matrix

{f} : nodal force vector

$\{f\}_{eq}$: equivalent nodal force vector

[H] : hydrostatic stiffness matrix

[K] : structural stiffness matrix

Det. [K] : determinant of the structural stiffness matrix

$[k_o]$: elastic stiffness matrix of an element

$[k_r]$: reduced stiffness matrix of an element

[M] : total mass matrix

$[M_a]$: added mass matrix

$[M_s]$: structural mass matrix

$\{Q\}_l$: loading variable vector of the l th loading case

$\{R\}_k$: resistance variable vector of component k or r_k

[T] : tendon stiffness matrix

{u} : nodal displacement vector

under bar : mean value of random variable

Δ : incremental quantity

bold or {·} : vector

[·] : matrix

Unit : force = MN or Tonne

length = m or mm

pressure = MPa (= N/mm^2)

CHAPTER 1 INTRODUCTION

1.1 General

In the context of structural design, a major goal is to achieve a balance between structural safety and cost in which the construction cost, maintenance costs and the costs increased as a consequence of failure are included, i.e., a minimum total cost design for a required overall safety level.

Since there are too many uncertainties in natural phenomena, man has tried to treat the uncertainties more rationally in structural design. There may be no "true" solution within the context of structural design. As Plinty the Elder said "*The only thing that is certain is that nothing is certain*". This means that since there are too many uncertainties and randomness in natural phenomena, the solution may be regarded as a product of uncertainties and/or randomness. Many efforts gave birth to the traditional safety factor concept, i.e., working stress design. In this context the design loads are usually unfactored and are close to the maximum probable loads which occur during the specified life time of a structure. The elastically computed stresses arising from these loads are limited to the allowable stress, which is usually a specified fraction of the yield stress. But, as has been well recognised, this approach cannot provide a balanced safety distribution within the entire structure, because the uncertainties in resistance, load and analysis cannot be treated rationally. This limitation has been overcome by using the concept of probability in design which enables one to treat the uncertainties more rationally.

As stated by Ellingwood and Galambos[1], the development of probability-based limit state design has been motivated by a desire to quantify performance of structures and to treat uncertainties in loads, resistance and analysis in a more rational way.

The probability of failure or, alternatively, reliability index (safety index) is the quantitative measure of risk, or safety or serviceability and the basis for achieving uniform performance in probability-based limit state design. This probability has an absolute meaning[2] "the likelihood of occurrence of some pre-defined limit state" : it may be a serviceability limit state, e.g. excessive deflection or rotation, initial yielding, or an ultimate limit state, e.g., partial or total collapse, instability.The reliability is defined as the probability of non-failure and adequately performing the intended function of a structure, when operating under stated environmental conditions during the service life.

In contrast to working stress design, which is a deterministic approach, the reliability-based limit state design is a behaviour-oriented design method which requires specification writers and designers to consider explicitly the structural requirements for function and safety at service and extreme load levels. The probabilistic approach is suggested by the observation that many of the design variables exhibit statistical irregularity[1]. The conceptional framework for probability-based limit state design is provided by the classical theory of structural reliability which is based on full-distribution procedures. The trend to reliability-based codes is based upon important considerations arising from research and experience. These include[3]:

- the statistical nature and especially the randomness of design variables associated with both loading and strength.
- the recognition of the importance of a limit state approach to failure as distinct from a purely working stress approach.
- the acceptance that weight and cost benefits exist if we take advantage of improved knowledge and lower notional safety levels which to some extent have been based on past ignorance
- the advantage resulting from a more uniform reliability or safety throughout a structure and over a range of similar structures.

Errors which give rise to risk can be classified as follows:

Systematic errors : related to ignorance of real physical phenomena in the analysis

and design process, i.e. the unknown bias in analytical models used is a systematic error.

Random errors : associated with statistical variations. For example, maximum wave heights experienced by different platforms within a given area may vary widely due to inherent randomness of wave formation within a given storm or within storms experienced during the lifetime of the population of platforms, i.e. the randomness nature in strength and loading variables.

Gross error : human error or blunders which may result from mis-calculation or omissions by the designer, engineer, etc.

Reliability analysis is primarily concerned with systematic and random errors.

A particularly interesting use of reliability-based design procedure is that of tools to help decision making, and the advantages of reliability-based structural design procedure are[4,5]:

- it can treat the uncertainties or errors of all variabilities in strength and loading in a more rational way, and thus provide a better framework for safety evaluation of a structure
- it tends to lead to a balanced design and allows the engineer to check the design (or the code) against the influence of the stochastic parameters of resistance, loading variables, etc.
- it provides a logical framework for the choice between alternative solutions with a subjective acceptance of the estimated probabilities as degree of belief in the reliability of the structure.

In this we acknowledge the pioneering work on this subject by Pugsley for World War II aircraft[6]. Structural reliability theory has been concerned with the rational treatment of uncertainties in structural engineering and with the methods for assessing the safety and serviceability of structures. This apparently contrasts with the traditional deterministic view of structural bahaviour where, for example, design calculations are carried out using fixed values of the variables.

The application of the reliability analysis concept to a structure was initiated in the field of aircraft, civil engineering structures and so on[5], and it is widely applied in the marine, civil, electronic, electrical, aeronautical and nuclear fields. Structural reliability theory has grown rapidly during the last two decades and has evolved from academic research to practical applications, and becomes a design decision tool based on scientific methods rather than being a scientific theory[7]. The object of its application to design is to give a uniform and consistent reliability within a structural system. Tremendous advances have been made in the area of structural reliability, theoretically and practically, and more recently in the incorporation of probabilistic concepts into codifiable design of marine and civil structures. Since the mid 1970's, the concept of the reliability analysis has been extensively applied to the design of marine structures[5] and recent trends in developing a new design code is based on the reliability analysis[3,8-10]. The existing codes are re-developed based on this concept.

Where there has been none or not much service experience for a structure, such as a tension leg platform (TLP), the reliability approach has been successfully applied[9] as a suitable means of dealing with uncertainties and satisfying the designer and/or the owner that the structure will perform satisfactorily and is not over designed.

As offshore platform development moves into deeper and more hostile water, there is an increasing interest in having methods available for calculating the reliability of such structures. Most applications are, however, dealing with the reliability analysis of structural components. It has been recognised for many years that a more complete estimate of the reliability of a structure must include a structural system reliability analysis. Furthermore, it is needed to develop system "partial safety factors" to related component safety to system safety[11]. Possibilities of its application would then exist for[12]:

- 'tuning' new design concepts to calculated reliability levels in existing structures
- making more rational decisions in repair or upgrading situations
- developing improved guidelines for inspection and maintenance purposes.

In the case of statically determinant structures, it is sufficient and reasonable to estimate the reliability of the individual components of a structural system because the failure of any single component will result in the failure of the total structural system. However, in the case of statically indeterminant structures, this is not true because the remaining components will be able to sustain further external load because of load re-distribution after any component fails. In other words, from the system's point of view, statically indeterminant structures may have much redundancy and hence the failure of the structural system always requires that more than one component fails[13,14]. Especially for a continuous structure, such as a floating offshore structure or ship's structure, there is considerable statical indeterminancy and hence mathematical redundancy[8,15,16]. Hence, the concept of system reliability based design is desirable to give more uniform reliability and consistent safety within the overall structure, to achieve the optimal distribution of component strengths within a structure, and to take into account the structural redundancy in the design stage.

During the last decade the necessity for system reliability analysis has been emphasised, and many studies on this subject have been made for marine and civil structures. Some are concerned with sensitivity studies[17-19], some with application to optimal structural design[13,20-30] to minimise the structural weight and/or the total cost within reliability constraints, some to find the optimum strategy of inspection and maintenance[31-33] and some dealing with the gross error (blunder or human error) in the system reliability analysis[34-37]. Most of them, however, are concerned with discrete structures such as a truss work or a jacket platform for which the possible failure modes can be identified relatively easily. In the case of a continuous structure, such as a TLP, it is not so simple and easy to identify the possible failure modes and to define the re-distribution of load effects due to the failure of any component.

Offshore structures are complex redundant systems which are generally made of members, elements or components connected together in a particular way. This implies that estimation of the reliability of an offshore structure is a very complicated task. The detailed modelling of all parts of a large structural system is generally not feasible and the

strengthening effects of nominally non-structural components are neglected or considerably simplified. In the context of system reliability analysis, it is usually assumed that a structure can be idealised in such a way that there is only a finite number of possible locations or nodes at which local failure can occur[38].

Generally system failure is a series system of sub-parallel systems. A sub-parallel system consists of sub-series systems of component failure modes. The important tasks in the structural system reliability generally consists of three parts:

[1] Modelling the structure and defining the random variables

[2] Identification, description and enumeration of the failure modes of the structure

[3] Determination of failure probability or reliability indices of individual modes, and then evaluating the overall system reliability

Among these, the last two are probably more important in the system reliability analysis. Because there is a great number of possible failure modes in a practical structure, it is not practical to include all possible failure modes in evaluating the system reliability of complex structures. The modes which are expected to mainly contribute to the system failure must be taken into account in estimating the system reliability. These are often referred to as the most likely[39] or the most important or the most significant failure modes[11,40,41], or the stochastically dominant failure modes[42-44]. Hereafter these will be referred to as the most important failure modes. Identifying the most important failure modes usually takes a great portion of computational time in the system reliability analysis procedure. A major difficulty in the application of system reliability analysis to design is to find an efficient algorithm for identification of the most important failure modes in a complex structure[11,13,22]. Application of system reliability analysis is a relatively new area. Extensive research, however, has been performed during the last decade and several methods have been developed. Among them approximate methods have been employed for this subject rather than analytical methods. This will be described in Section 1.3.

It is necessary to make a number of simplifications and assumptions not only to

the structure itself, but also to the strength and loading properties of the structural elements. These may be thought to be major limitations of the application of structural system reliability theory to practical design procedure. In spite of these limitations it is believed that reliability analysis of structural systems is a useful tool in decision making in offshore engineering[32].

1.2 Literature Review

1.2.1 General Review

In the context of probability-based (or reliability-based) limit state structural design, three main features are developed: evaluation of the reliability and uncertainties, derivation of the strength formulae (or models), and incorporation of the two to produce the design code as a practical application to design.

The statistical nature of loading and strength was first recognised by the military aircraft industry. Pugsley and others pioneered the "hazard" approach to structural design for World War II aircraft in the U.K. Its practical application is attributed to Freudenthal who more than 40 years ago formulised a rational approach to the structural safety problem in the field of civil engineering. Since then an ever-increasing effort has been directed toward the application and development of the theory of probability and statistics in structural engineering. This has been greatly developed during the past two decades and a number of works have been reported and presented. References [5,13,14,45] are recently published as text books of the reliability method and its application.

As a review paper, the American Society of Civil Engineering Task Committee on Structural Safety [46] presented the state-of-the-art in this regard up to the early 1970's. In the Task Committee's final report on Safety, ASCE[47], Freudenthal et al presented the general idea of the probability-based design, and also the necessity of system reliability was described. They proposed the approximate bound of series system ("weakest-link" system). The elements relevant to the reliability analysis and its

applications to design of fixed jacket platforms have been integrated by the Committee on Reliability of Offshore Structures, ASCE[48]. The committee further discussed the benefits, advantages and difficulties of reliability-based design, and offered guidelines for future research.

Moses[49] reviewed recent developments of probabilistic characteristics of uncertainties and application of reliability theory in the selection and optimisation of safety factors in which component safety model, code calibration, system reliability and progress in the implementation of a reliability-based API RP2A guideline for platform design, etc was discussed. Recently Stiansen and Thayamballi[50] reviewed the past developments with emphasis on marine structures.

1.2.2 Reliability Index

o First-Order Reliability Index:

In evaluating the reliability of a single failure mode (component reliability analysis) several reliability indices (which are first traced back to a debate on structural safety in the Institution of Structural Engineers in 1955[51]) are proposed as a measure of structural safety. Cornell[52] first proposed the Mean Value First-Order Second Moment Reliability Method (MVFORM) in 1969, in which the reliability index is obtained as the ratio of mean safety margin to its standard deviation. Safety margin is defined as the difference between strength and load[2]. This reliability index has limitations. It is not invariant to different equivalent formulations of the same problem, errors are introduced with non-linear safety margin equations and the distributions of variables should be normal.

The first two limitations are avoided by using the, so called, Hasofer-Lind reliability index[53] (sometimes called geometric reliability index) which gives the reliability index which is invariant to different equivalent formulations and is defined as the shortest distance on the failure surface from its origin.

The last shortcoming has been removed by Rackwitz and Fiessler[54]. They presented an equivalent normal distribution for non-normal distributions and an iterative algorithm, called the "Rackwitz-Fiessler Algorithm", by incorporating the equivalent normal distribution concept, which is sometimes called the Advanced First-Order Second Moment Reliability Method (AFORM).

Hohenbicher and Rackwitz[55] developed a general probability distribution transformation with which a complex problem involving non-normal, correlated random variables can be reduced to the simpler problem of determining the failure probability or reliability index in the uncorrelated standard normal vector space.

Veneziano[56] proposed an alternative reliability index which is more general and flexible with regard to updating when new information is gained and also consistent. But its philosophy and application is not simple.

Ditlevsen[57] discussed some versions of the reliability index and further presented the generalised reliability index by which the problem of invariance in describing the limit state equation can be avoided. As an example, if g=0 is a safety margin , then g^3 and g^5 are also safety margins, but the three give different reliability indices. This problem of arbitrariness has been called the problem of dimension invariance.

These methods have been successfully applied to marine and civil structures. Detailed procedures are well presented in references [5,13,14,45]. Among them the Rackwitz-Fiessler algorithm is one of the most popular because of its efficiency and simplicity. More recently Chen and Lind[58] proposed an algorithm for evaluating more accurate reliability index by probability integration based on a three-parameter normal tail approximation to a non-normal distribution for each random variable. It was claimed that the algorithm was more efficient in that it was fast, gave smaller errors than the Rackwitz-Fiessler algorithm and did not require double precision computation.

Wu and Wirsching[59] proposed an alternative algorithm which was an extension of the Rackwitz-Fiessler[54] and Chen-Lind algorithms[58]. To find an "optimum" equivalent normal distribution a weighting function is selected and a least-squares method is employed to fit a high quality three-parameter normal cumulative distribution function to a non-normal distribution function.

White and Ayyub[60] introduced another approach called the "Reliability-Conditioned (RC) method" which found the most likely failure point on the failure surface and was intended to more consistently and accurately evaluate the required partial safety factors for a wide variety of limit state. It was claimed that the method overcame the shortcomings of the Mean Value and Advanced First-Order Reliability Method (MVFORM and AFORM) and extended the Level 3 method in a more useful form to handle general types of problems. They used their approach in the calibration of a design code format and in a fatigue problem in marine structures[61].

o Second-Order Reliability Index:

Higher approximations have been used to obtain a more accurate reliability index or failure probability, say, Second-Order Reliability Method, in which the limit state surface is approximated by a quadratic surface at the design point.

Gollwitzer and Rackwitz[62] proposed a procedure of searching for the reliability index by using first-order reliability concepts together with quadratic optimisation with multiple non-linear constraints.

Madsen[63] proposed an extension of the first-order reliability method to a more accurate second-order reliability method for better approximations of failure probability.

Kiureghian et al[64] proposed a comparatively simple method for a second-order reliability approximation based on a point-fitted paraboloid approximation, that is, an approach to fit paraboloid to the limit state surface around the design point (point-fitted paraboloid approximation).

Tvedt[65] proposed the derivation of a three term approximation to the probability content outside the approximating quadratic surface.

1.2.3 System Reliability Method

As mentioned before, system reliability has received much interest and its necessity has been well recognised since the mid-1960's because there are a number of possible failure modes, even in a simple structure. A major benefit of incorporating system strength is the additional structural reserve strength often found due to design symmetry, multiple load conditions, fabrication requirements and design approximations. The development of system reliability methods has mainly been concentrated in two parts: how to formulate the limit state equation of the failure mode, and how to evaluate the probability of system failure. Once the limit state is defined the reliability index and/or probability of failure for each mode can be evaluated by using the various methods described before.

Practical development of the method was initiated by Moses[21] who proposed the incremental load method for formulating the limit state equation (system safety margin equation) in which Mean Value First-Order Second Moment Reliability Concept was incorporated to evaluate the system safety level. He used the method in the system analysis of truss and framework structures. The basic idea behind this method is that a structure is progressively "unzipped" as successive members or components reach their strength capacity until overall failure occurs[21,40]. Later Moses extended the incremental load method to identify the most important or significant failure modes using the deterministic truncating criteria[11]. This method is attractive in that it can allow for the post-ultimate behaviour of a failed component and component strength formula can be used during formation of the limit state equation together with the concept of utilised strength at each load increment stage. Recently this method has been incorporated in the cost and/or cost optimisation studies[22,23].

After Moses presented the incremental load method, several useful system reliability method have been proposed in the past decade. Moses and Rashedi[66]

presented an approach for identifying the important failure modes using the linear programming technique. They presented the results for the structure under multiple loading and having a more realistic post-ultimate behaviour than previously.

Gorman[67] presented an automatic generating procedure of failure mode equations based on the rigid-plasticity concept.

Murotsu et al[68] proposed a heuristic procedure of automatically identifying the stochastically dominant failure modes with probabilistic truncating criteria. They extended their proposed method to the system reliability analysis of two dimensional framework structures under combined axial force, bending moment and shear force based on plastic failure criteria[69].

Thoft-Christensen and Søresen[70] presented two formulations of the so called "β-unzipping" method for frame structures in which yielding failure was considered. Later Thoft-Christensen[32] extended the method to take into account the various failure elements, such as failure due to yielding, buckling, fatigue, punching, etc, by which the system safety index at different failure levels was evaluated.

Ditlevsen and Bjerager[71] proposed another approach which was based on the lower and upper bound theorem of plasticity and an optimisation procedure was used in the identifying procedure. This method gave a reasonable upper bound of system failure probability.

Melchers and Tang[44,72] extended the incremental load method to truss structures with a more general member behaviour to derive the limit state expression and proposed an iterative approach, the so called "Truncated Enumeration Method (TEM)", to systematically determine the probabilistically most dominant failure modes through an exhaustive searching procedure. Chan and Melchers[73] applied the method to jacket platforms with realistic modelling of wave forces which takes account of their variation

with the incident wave location as it passed through the structure. Emphasis was placed on semi-brittle components behaviour.

More recently Lee and Faulkner[41] have presented the "extended incremental load method". This extends the conventional incremental load method by Moses[21] to include structures under multiple loading conditions which has been a major limitation of the incremental load method. Moreover it can more realistically allow for the post-ultimate behaviour of a failed component which can now be characterised by the post-ultimate slope and the residual strength. Also, strength formula can be used in the limit state equation based on the utilised strengths of components failed at each incremental stage. This method has been successfully used in the reliability analysis of TLP structural systems and for their sensitivity studies[19,74].

As a hybrid approach, Corotis et al[75,76] proposed the load space approach which was a combined form of the incremental load method to evaluate the system resistance and numerical integration techniques to estimate the system failure probability. Later they used this approach in cost optimisation problems of frame structure[27,29]. Edwards et al[12] presented a dual approach based on the Monte Carlo Importance Sampling procedure and failure mode analysis for offshore jacket platforms using the First-Order Second Moment Method.

All of the above mentioned methods look at the problem in terms of failure events. The complementary approach, or so called the "stable configuration or survival-set approach", was suggested by Bennett[77,78] and Bennett and Ang[79]. This was proposed as an alternative for system reliability analysis and it was claimed that it could predict upper bounds of system failure probabilities. But computational work is much more expensive than the methods mentioned earlier.

Since the exact evaluation of the system failure probability is difficult, several methods have been proposed to estimate the bounds of the probability. An early simple upper bound of a series system was given by Freudenthal et al[47]. Cornell[80]

presented the simple bounds when correlation was assumed to be positive or negative, in which the upper bound was the same as that proposed by Freudenthal[47] when correlation was assumed to be positive. If there are only a few dominant modes these bounds will give reasonable estimates.

For cases where failure modes are correlated with each other, narrow bounds were proposed by Ditlevsen[81]. Vanmarcke[82] and Murotsu et al[68,69] presented the corresponding upper bounds. More recently Guenard[39] presented the bounding technique with the dominant failure modes and the incomplete interim modes.

Ang and Ma[45] used the probabilistic network evaluation technique (PNET) to estimate the upper bound using a grouping technique. Chou et al[83] presented possible alternatives for a grouping technique by using the taxonomic analysis and Tichy and Vorlicek technique.

The concept of an equivalent safety margin of a single failure mode, which applies to a parallel system composing of failed components, was developed by Gollwitzer and Rackwitz[55] using first-order system reliability analysis. This is useful in calculating the probability of system failure of a large system.

These procedures have been successfully used in the system reliability analysis of marine and civil structures. Frangopol[84], Grimmelt and Schueller[85] and Schueller[86] compared the various system reliability analysis methods with regard to their accuracy, capability and efficiency.

Baker[38] described some of the recent developments in structural reliability theory, and discussed their benefits and applications to fixed offshore structures.

Hohenbichler and Rackwitz[87] reported the first-order concept in reliability methods in system reliability analysis. Ditlevsen and Bjerager[7] presented a review paper concerning development within the field of structural reliability theory with

particular attention to structural system reliability. An overall review of the system reliability methods in formulating a limit state equation and in evaluating the system failure probability is given in the report by Karamchandani[88]. He reviewed the current state-of-the-art in system reliability methods and their application to practical structures. The shortcomings and advantages of various methods were discussed with regard to their practical application and future potential.

1.2.4 Redundancy

For continuous structures, even discrete structures, it is difficult and practically impossible to quantify the degree of structural redundancy or indeterminancy. It is generally accepted that the structural redundancy for such structures can be expressed in terms of the reserve strength, which is defined as the strength (or resistance) beyond the design condition which the initial intact structure can sustain before progressive collapse develops as a structural system, and the residual strength, which is defined as the remaining strength of the structural system once a member (or component) has failed or been severely damaged as to be ineffective.

The concept of structural redundancy for offshore platforms was addressed by Marshall and Bea[89] and Marshall[90] in terms of reserve strength. Lloyd and Clawson[91] proposed the measures of structural redundancy, say reserve strength and residual strength, in terms of the reserve resistance factor (REF) and the residual resistance factor (RIF). They also introduced a member redundancy classification hierarchy for redundant structures. A member redundancy level ranges from zero for a member whose failure greatly affects the collapse of the structural system to five for a member whose failure has no effect on the collapse of the structural system. As a companion paper of reference [91], de Oliveira and Zimmer[15] also described the measures of structural redundancy termed as: redundancy index (RI), reserve strength index (RSI) and residual strength index (RDI), and a methodology for considering redundancy in the design stage for continuous structures. They proposed another index associated with serviceability termed as the allowable deflection index. The RSI and RDI have the same meanings as REF and RIF, respectively, of Lloyd and Clawson[91]. From

the studies if reference [89], [90] and [91], it was shown that typical jacket platforms should be able to resist about two times the design environmental load. More recently the probabilistic measure of redundancy has been proposed by Feng and Moses[22], Paliou et al[92] and Nodal et al[93]. The definitions of these measures are detailed in Chapter 2.

The reserve strength and the residual strength are closely interrelated through the concept of damage tolerance of the structural system. Mistree first put forward this concept of damage tolerance in 1982[94] and illustrated its application to offshore structures[95]. It has rapidly developed into a respectable reliability based discipline aimed at evaluating the importance of fatigue cracks in structural members and clearly can have considerable implications for inspection, repair and maintenance policies[96].

1.2.5 Applications

o Ship Structures:

The basic idea was discussed at the International Ship Structures Congress (ISSC) in 1967[97]. The application of the reliability methods to the field of marine structures can be first seen in an early paper by Mansour and Faulkner[98] who applied it to evaluating safety for longitudinal ship strength of a tanker and a naval frigate. Faulkner and Sadden[99] extended for five naval ships varying in length from 91-154 m. They compared the safety indices of their naval ships with those for pseudo-merchant ships designed by rule with the same length, and those for large merchant ships having a length range 158-328 m. Faulkner[100] proposed a semi-probabilistic approach using a global partial safety factor linked to any required safety index.

Stiansen et al[101] presented fundamental procedures for reliability analysis of ship structures and sample models in dealing with uncertainties in loading and strength of hull girders.

Aldwinckle and Pomeroy[102] presented the use of probabilistic approach in determining reliability and safety, and its application to design of ship's structure. They

also discussed the potential benefits to the socio-economic side.

Up to the present, the probabilistic approach or reliability methods have been consistently applied to ship's structures to achieve more consistent safety, etc. More recently Akita[103] presented a method of predicting the failure probability of ultimate collapse in deck structure under wave induced extreme longitudinal bending moments by considering the successive collapse of weaker panels between longitudinals, in which initial distortions of the welded plates were taken into account.

Guedes Soares and Moan[104] presented an uncertainty analysis of extreme still water and wave load effects in ships with emphasis on the modelling uncertainty of the wave load, and derived a consistent set of load partial safety factors for ship structural rules for the first time.

Mansour[105,106] compared the evaluated reliability indices for 18 ships by three methods: Direct Integration, Mean Value and Advanced First-Order Second Moment Reliability Method. He recommended that more attention be given to the direct integration approach.

Thayamballi et al[107] proposed a combined approach of a non-linear finite element technique with an Advanced First-Order Reliability Method using the Wu-Wirsching algorithm[59] in estimating the structural safety of three general cargo ship's hull girder under vertical bending, in which the ultimate longitudinal bending strength was calculated through a dynamic non-linear finite element technique. They also outlined both deterministic and probabilistic measurement of safety.

White and Ayyub[60] compared the partial safety factors of 18 ships[105] by their reliability conditioned algorithm with the first-order reliability method and the fully distribution method.

o Offshore Structures:

The reliability method has been more extensively and actively adopted in the offshore engineering field, from developing efficient methods to developing the probability-based limit state design code format. In the past decade various useful codes have been developed based on the probabilistic concept[9,10,108] and some are still being developed.

Moses introduced guidelines for calibrating the existing code, API RP2A, based on the reliability approach[109,110], and successively presented the Load and Resistance Factor Design (LRFD) code format for fixed offshore structures and reported its application to existing offshore structures. He also proposed that the system factor could be added in the design format[10,11].

Ellingwood and Galambos[1] presented a procedure for selecting the load and resistance factors in design format and described the probability-based loading and resistance criteria which were suitable for the development of a practical design code format for buildings and the principles developed have some relevance for offshore use.

Bea[112] presented a simplified reliability-based formulation procedure for fixed jacket platforms to determine environmental design parameters such as design wave height, design seabed acceleration, design return period and design safety factor. In the design formula the safety factor is based on the expected failure cost was included. A simple empirical relationship between reliability and the reliability index was also proposed to make derivation easy, which gave reasonable reliability values over the range of reliability index from 1.6 - 3.6.

A model code for the reliability based design for the continuous hull structure of TLPs was developed through the co-operative work of research, a classification society and industry[9]. The framework of strength formulae for stiffened cylinders has been well established in the aeronautical field. But it was not suitable for the principle components frequently appearing in a floating offshore structure, such as a semi-

submersible and a tension leg platform[113]. A special Conoco-ABS Rule Case Committee (RCC) was formed in 1982 to develop an appropriate non-mandatory design code for TLP structures. Tests for a realistic range of stiffened cylinders for fixed and floating offshore structure have been carried out at CBI industry and at the University of Glasgow. Useful strength formulae were reported, especially for the design of ring-stiffened and ring- and stringer-stiffened cylinders[113]. The TLP model code[9] recommended a component safety index of 3.0 for direct design using approved reliability algorithm, or 3.7 using tabulated partial safety factors.

Faulkner[3] , who was chairman of the committee, outlined the development of a state-of-the-art of the reliability based model code, the background of the RCC work and its main achievements, such as an interim loading model, greatly improved strength models, safety checking design code format, certain guiding principles for code calibration etc. He also emphasised that the inclusion of redundancy could have a significant effect on design saving and reliability-based inspection and repair policy and decisions and these studies should be continued to achieve more economic benefits. By using some of these advances for the design of the Jolliet field TLWP in the Green Canyon Block in the Gulf of Mexico, about 30% saving of steel weight has been achieved. Further weight saving can be achieved by using these reliability concepts with better loading models.

In the case of TLPs or semi-submersibles, the primary structural components are generally constructed of thin stiffened plated structure having very large cylindrical or other type cross-sections, stiffened by means of longitudinal stiffeners and ring frames or transverse frames. Das and Frieze[114] presented reliability studies of a stringer-stiffened cylinder using a modified DnV strength model[115]. Safety indices under different loading conditions were investigated and a sensitivity study was carried out to indicate the influential parameters. Das and Faulkner[116] presented a sensitivity study to investigate the influence of random variables such as the strength modelling parameter, yield stress, shell thickness and radius of cylinder on the safety indices of ring stiffened cylinders and ring- and stringer-stiffened cylinders.

Maes and Muir[117] investigated several design formats and examined the use of both partial load factors and specified exceedance probabilities for Canadian offshore use by varying the environmental loading conditions.

o Strength Modelling:

With regard to the strength formula reference [118] has compiled the various design codes and the relative accuracy of their predictions, when compared to available test results. It also reviewed the state-of-the-art knowledge in the field of buckling behaviour of offshore structure. More recently Warwick and Faulkner[119] reported a useful review paper for the strength formula of cylindrical components as used in fixed and floating offshore structures: unstiffened, ring-stiffened and ring- and stringer-stiffened cylinders. In their report, they discussed various strength models commonly used in design codes and compared these with reputable test data. They also recommended general and statistical requirements for a good strength models, and recommended strength formula for cylindrical components in offshore structure based on these criteria.

Strength formula for flat plated structure has been well established. For stiffened plates, Faulkner[120] presented the ultimate compressive strength of stiffened panels in a simple expression which was derived through an analytical methods conformed by test results. This has also been improved by using various numerical methods such as the finite element technique[121-124] and the finite difference method[125].

For the ultimate bending strength of a hull girder or of rectangular sections, Lin[125] presented a method for predicting the ultimate bending moment capacity of longitudinally stiffened hulls which was based on numerical analyses by the dynamic relaxation method, a kind of finite difference method, using the beam-column concept[126]. When bi-axial bending moments were coupled, Faulkner et al[127] proposed a circular interaction equation. When the structure was under combined axial compression and bi-axial bending moments, the present author[128] proposed an interaction equation for rectangular sections which was derived from a best fit numerical

analysis of results with non-linear analyses using the beam-column concept. These strength formulae have been used in the reliability analysis of TLP structural systems[19,41,74].

o System Reliability Analysis:

For the system reliability analysis of offshore structures a number of references concerned with fixed jacket platforms are available[12,38-40,43,69,73,92,93,129].

For floating offshore platforms, Murotsu et al[130] presented a system reliability assessment for the transverse strength of a semi-submersible platform subjected to extreme wave loads using the heuristic procedure together with the branch and bound method to select the probabilistically dominant failure modes. Their approach was based on plastic collapse analysis and the first-order reliability method was used to approximate the stochastic parameters of the wave induced loads.

Frieze[131] was concerned with the extension of the collapse analysis of a semi-submersible to approximately evaluate the load factor, and introduced the redundancy partial safety factor, which is equal to the inverse of the redundancy factor. Amdahl et al[132] presented the progressive collapse analysis of a semi-submersible, subjected to a no damaged and a damaged condition due to an accident using an idealised structural unit method based on a plastic hinge method, from which the reserve strength index and residual strength index were derived. This is discussed in Chapter 3.

Lee and Faulkner[19,41,74] presented an application of the "extended incremental load method" to TLP structural systems subjected to static, quasi-static and dynamic wave and motion induced hydrodynamic loads. TLP structures were modelled as three-dimensional frame structures and a modified safety margin equation was used to directly use the strength formulae developed for principle components.

The system reliability analysis of tendons in TLPs have been carried out by Pruce and Soong[133] and Guenard[39].

o Sensitivity Studies:

Sensitivity studies of component and system failure probability or reliability to changes in stochastic parameters and distribution types for design variables have also been done by several researchers to investigate the relative importance of design variables in the analysis with regard to their effects on safety. This type of study is of particular importance in reliability-based structural optimisation and in the calibration of design codes.

Baker and Ramachandran[134] presented the effects of mean and coefficient of variation of various parameters on the safety of a fixed jacket platform, such as wind speed, wave, current, yield stress, drag coefficient, added mass coefficient, marine growth and initial geometric imperfections.

Smith et al[135] showed the relative importance of strength modelling parameters, geometric properties, material properties and environmental loading variables on component reliability by varying their ratio of mean values and coefficients of variation to the characteristic values. They used the sensitivity results to obtain the optimum partial safety factors for the calibrations of various design codes.

For a frame structure Frangopol[17,18] carried out a sensitivity for the overall reliability of a structural system to changes in problem parameters such as correlation of resistance variables, that of loading variables, mean value of the load and the various methods of evaluating the system reliability.

Lee and Faulkner[19] presented a sensitivity study for TLPs to changes in resistance variables such as strength modelling error and the post-ultimate behaviour of failed components.

o System Reliability-Based Design:

One major aim of the system reliability analysis should be to relate the member or component strength with the system strength. Moses[11] and Faulkner[136] suggested

that the system factor (system partial safety factor), which represents the degree of redundancy of the structural system and is normally less than unity, could be added in the safety checking design format. Faulkner[136] suggested a simple procedure to predict the system factor as well as system reliability index given the first failed component reliability index and stochastic parameters associated with strength and loading. The basic idea of this procedure is to assume the probability density function of the system strength is achieved by shifting the probability density function of the component to the positive direction by multiplying its mean value by a reserve strength ratio, n (= mean system strength/mean component strength). Lee and Faulkner[19] then proposed a simple relationship for safe design:

$$\beta_{comp} + n \leq 5$$

to link acceptable component safety to the reserve strength of the system.

A number of works in which the reliability methods are incorporated with the deterministic optimisation theory (fixed safety factor concept) have been carried out to achieve greater economy and to provide a better basis for comparing different designs. Several formulations of linear or non-linear problems, constrained or unconstrained, are presented, in which the structural weight and the total cost, which includes the construction cost and cost of failure consequence, are usually taken as the objective function.

Moses and Stevensen[137] proposed the formulation of a reliability-based optimisation and procedure with total cost as an objective function. They used a gradient method with usable feasible directions. Moses[21] introduced the idea of reliability-based optimum design of a structure. Feng and Moses[22,23] addressed the system reliability-based design philosophy which minimises the structural cost and/or weight to satisfy a system reliability constraint. They used the incremental load method for identifying failure modes and computing the system reliability index by considering reserve and

residual strengths of the structure, and they introduced optimal criteria associated with an iterative procedure[23].

Frangopol[25,26] presented an overview of the major concepts and methods used in reliability-based structural optimisation and proposed formulations related to multi-criteria optimisation subject to reliability constraints imposed at both serviceability and ultimate limit states.

Murotsu et al[24,28] presented a component reliability-based optimisation for fixed offshore platforms to minimise the expected total cost which included the structural cost and the expected maintenance cost under constraints on the allowable failure probabilities of critical sections specified in the structure. They also recently presented the shape optimisation of truss structures to minimise the structural weight[30].

Soltani and Corotis[29] presented single and multi-objective formulations with objects such as cost of failure, initial cost, failure probability associated with collapse in various modes and failure probability associated with different levels of unserviceability, e.g., excessive deflection, inelastic behaviour, partial failure, using their load space system reliability approach.

Smith et al[135] reported the optimisation of partial safety factors in various design codes with the total cost as an objective function, and the average reliability of a structural component was taken as a constraint.

Generally, cost optimisation is preferred to weight optimisation in which the initial cost, failure cost and maintenance cost are included. Reference [13] by Thoft-Christensen and Murotsu and [138] by Murotsu introduced several recently developed formulations of optimisation problems coupled with reliability analysis, for the component and/or system.

o Fatigue:

Harbitz[139] presented a general procedure for accurate probability of fatigue failure calculations based on the rule of Det norske Veritas for offshore structures[115] using an importance sampling technique.

Wirsching and Chen[140] described the problem of fatigue damage under variable amplitude stresses using the characteristic S-N curve and fracture mechanics models. They also proposed models for reliability assessment relative to fatigue and their applications.

White and Ayyub[61] used the so called reliability conditioned method for the fatigue problem of marine structures, and they provided an example.

o In-Service Re-Assessment:

The reliability analysis methods have been applied to in-service re-assessment which is coupled with achieving an optimum strategy for inspection and repair.

Sørensen and Thoft-Christensen[31] presented the strategy for offshore structures by minimising the total cost including inspection, repair and also their qualities under the allowable reliability constraints of various failure elements, such as failure due to fatigue, etc.

Madsen[37] presented a developed numerical technique for computing updated reliabilities and updated distributions for the basic variables, which was intended for use in decision making for existing structures and required the evaluation of parametric sensitivity factors for parallel systems.

Bea and Smith[33] proposed an optimum strategy of inspection and maintenance for fixed offshore platforms in-service with consideration of reliability.

o Gross Errors:

Recently gross errors (blunders or human errors) is considered in evaluating reliability because most structural failures are due to human error[13,45]. Human errors have been more explicitly considered in the design and/or construction phases of a structure.

Lind[34] and Melchers and Harrington[35] introduced some models for human errors. Nowak and Carr[36] dealt with human errors in the selection of structural models and carried out their sensitivity analysis for various parameters of highway bridges, etc. They considered two types of errors in structural models: errors in realisation of the assumed model and incorrect selection of the model. Yamamoto and Ang[141] proposed a simple model for evaluating the significance of human errors on the reliability of the structure. They recommended that, in any case, data on human errors had to be continually accumulated. Nessiam and Jordan[142] proposed probabilistic models for the optimal level of human error control.

Melchers[143] briefly reviewed the principles by which human error information could be taken into account in reliability assessment, and described both empirical model and data for some types of human error which might arise in the design process.

Shiraishi[144] treated gross errors by using two-dimensional and fuzzy logic measures. Shiraishi and Furuta[145] presented an attempt to apply fuzzy set theory to the reliability analysis of damaged structures in which damaged states were represented in terms of fuzzy sets to define several linguistic variables. The probabilistic network evaluation technique was used and extended to treat the fuzzy quantities.

o Approach Coupled with Numerical Methods:

Numerical methods such as the finite element and boundary element methods have been coupled with system reliability analyses. The finite element method has been used to more explicitly consider the uncertainties in estimating the statistical parameters of load effects, such as stress, displacement and/or deformation, by taking into account

variations in load, dimensions and material properties for a reliability study[146-148]. Vanmarcke et al[148] presented a state-of-the-art review of stochastic finite element analysis and its formulations.

More recently Chryssanthopoulos et al[149] presented an approach for combining the Level 2 reliability method with non-linear finite element analysis for stringer-stiffened cylinders subjected to axial compression, in which uncertainties in the initial displacements of curved panels and stringers were explicitly modelled.

Vilmann and Bjerager[150] used the boundary element method in Mindlin plate analysis to investigate the effects of certain uncertainties in geometric parameters.

1.3 Review of the Methods for Structural System Reliability Analysis

System reliability analysis methods can generally be divided into three categories, i.e., analytical methods, approximate methods and hybrid methods, which are combined forms of analytical methods or analytical and approximate methods. Theoretically, the analytical method may give the exact probability of system failure, but it can be applied to only quite simple idealised problems and therefore not to real structures. Hence approximate methods are usually used for system reliability analysis. The recent review by Karamchandani[88] on the current state-of-the-art methods to evaluate limit state system failure probability is valuable.

1.3.1 Analytical Methods

There are several analytical methods for formulating the failure events and evaluating the system reliability. These include Numerical integration, Monte-Carlo simulation, Stratified sampling, Latin Hypercube, Importance sampling, Reduced space approach and Response surface based approach. But most of these are limited in application to only idealised simple structures and may be computationally inefficient. The last three methods, however, appear to be the most promising methods in use

today[88].

Among them, the importance sampling approach, which is a modified Monte-Carlo simulation, has been used by several researchers. For example, Edwards et al[12] applied the procedure to the system reliability analysis of a jacket platform. The important failure modes are obtained by Monte-Carlo simulation based on an importance sampling approach. The failure probabilities of these important modes are considered as decisive for the value of the system failure probability which is then evaluated by the Level 2 method.

For component reliability analysis for fatigue, Harbitz[139] presented a general procedure based on the importance sampling approach. However, these methods are practically difficult when individually used for practical structural systems. But when combined with approximate methods, as will be discussed in Section 1.3.3, they can be more easily used in reasonably complex structural systems.

1.3.2 Approximate Methods

In this method there are generally two types of approach depending on the type of formulation. One is the approach to principly get the failure probability rather than the reliability (probability of survival) and the other one is the complementary or vice versa approach.

After Moses suggested the incremental load method[21], various approximate methods have been rapidly developed which originally stemmed from this[11,41,42,70,71,77]. Approximate methods can be categorised into three: Failure Path Approach, Survival-Set Approach and Plasticity-Based Approach. These will be discussed in the following sections.

1.3.2.1 Failure Path Approach

The failure path approach generates the failure modes which are elements in the system failure event. There are generally two kinds of methods used to derive the failure

equation or safety margin equation: Element Replacement Method (ERM) [42,70] and Incremental Load Method (ILM)[11,21,40,41,74].

o Element Replacement Method:

The failure equation can be defined in terms of the forces in components and the strengths of the components. In order to obtain the failure equation for any particular failure mode, the basic idea behind this method is that failed components are removed from the structure and each is replaced by the equivalent load, i.e. the post-failure strength of failed components. The equivalent load replacing the failed component i is $\eta_i R_i$, where η_i is the post-failure strength factor which is the ratio between the post-failure strength and the resistance of the component, and R_i is the resistance. For ductile behaviour , $\eta_i = 1.0$, for brittle behaviour, $\eta_i = 0.0$ and for semi-brittle behaviour, $0.0 < \eta_i < 1.0$ [Fig. 1.1 (a)].

o Incremental Load Method:

This method is based on the mean values of random variables in strength and load. The basic idea behind this method is that the structure collapses progressively in a pre-defined failure sequence as the load increases, from which a set of these load increments is obtained. These load increments are defined in terms of the strengths of failed components. The total load at a particular component failure stage is the sum of the load increments to that stage and it represents the system resistance which consequently can be expressed in terms of the strengths of failed components.

This method is easy to understand and the existing structural analysis program can be used with slight modification. Since, after a component fails, the change of force in a survival component is the sum due to the next load increments and due to the unloading force in the most recently failed component (load shedding effect by the failed component), this procedure can also be applied to the structure with brittle and/or semi-brittle component behaviour.

1.3.2.2 Stable Configuration Approach

This approach[77] is based on looking at the problem in terms of sequences of which survival implies system survival, i.e., the complement of system failure. The survival modes (configurations) in which a structure may carry an applied load are examined to determine which survival modes are those which the structure is most likely to carry further applied load, i.e., which survival modes have the lowest probability of failure.The probability of system survival (reliability) is obtained from

$$(P_s)_{sys} = P[\, E(Z_1 > 0) \cap E(Z_2 > 0) \cap \ldots \cap E(Z_m > 0)\,] \qquad (1.1)$$

and the probability of system failure is obtained from Eq.(1.2) as a complimentary event of the survival event.

$$(P_f)_{sys} = 1 - (P_s)_{sys} \qquad (1.2)$$

The survival modes are found through a heuristic process, in which less important modes are neglected. Neglecting the potential survival modes (stable configurations) will be conservative and an upper bound will be obtained to the probability of system failure.

Bennett[78] applied this approach to the structure with brittle components, and Bennett and Ang[79] for evaluating the reliability of structures whose component behaviours are a non-linear based on the combination of the imposed deformation approach[152].

However, for a given system the number of survival modes is usually much larger than that of the failure modes, and so, in this sense, the magnitude of the problem in the stable configuration approach is larger and its procedure for finding the survival modes is more complicated than the failure path approach. Above all, the evaluation of the probabilities of survival modes (parallel system of element survival events) is difficult and there is no guarantee that the sequences identified are the most important ones.

1.3.2.3 Plasticity-Based Approach

This approach is based on the two plasticity theory with optimisation theory[71]: lower-bound theory and upper-bound theory of plasticity. Although this approach can be applied to a narrower class of structures than the failure path approach and the survival-set approach, i. e. only to the elasto-plastic structure, the advantage over other approximate methods is that it allows a more rigorous treatment of the probabilistic aspect of structural systems reliability. Results obtained for a simple structure showed that a lower bound was usually quite close to the true failure probability.

1.3.3 Hybrid Methods

Among the analytical methods, the reduced space approach and the response surface based approach have been combined with approximate methods to solve practical problems. In this thesis this type of approach is termed a hybrid method due to its combined nature of analytical methods and approximate methods.

References [29], [75], [76] and [153] used the incremental load method to obtain the system resistance in which non-linear structural analysis was employed and then the limit state is formed in the load space (or load effect space). The failure probability of this deterministic structure is then evaluated by integrating the joint distribution functions of loads over the failure region in the load space. This approach is usually called a load space approach or load effect approach.

In this method, since non-linear structural analysis is included in deriving the system resistance by varying the ratio of each loading, it seems to provide one possible way of more realistically taking into account the non-linearity for a reasonably complex structure. However, since in the system reliability analysis the structure analysis takes the main portion of computational time, even a simple structure may require considerable computational time. For this reason this method may be limited in its application to complex and large structures.

Another form of hybrid method can be the combined form of analytical methods.

However, this also has limitation when applied to practical structures[88].

1.3.4 Limitations of the Approximate Methods

The analytical method has the major shortcoming that up to the present it cannot be applied to practical problems. The hybrid method has the possibility of more realistically taking into account non-linear behaviour than the other methods. The approximate method is, therefore, usually used to solve practical problems, but it has several limitations. The major one is, first of all, it is applicable only to highly idealised structures and loads. Non-linearity of component (or element) behaviour is assumed as a two-state model [Fig. 1.1(a)]. It is not possible to consider the non-linear interaction failure surfaces. Above all, different paths and strain reversal of failed components cannot be allowed for.

1.3.5 Discussion on the System Reliability Analysis Methods

As mentioned in Section 1.3.4, in spite of their limitations approximate methods are usually used to solve the practical problems. Among the approximate methods, the failure path approach is most popular. In this, since the paths which are less important are neglected, the result will be unconservative. Also, it generates the failure modes, not the survival modes as in the stable configuration approach. Considering that the number of survival modes is much larger than that of the failure modes, it is computationally more efficient. Above all, this approach can be applied to the structure with ductile, brittle and semi-brittle component behaviour, and is therefore more general than the plasticity-based approach. Because of this most work on system reliability analysis has been done by the failure path approach, say using the incremental load method (ILM)[11,19,21-23,40,41,44,72-74,154] and the element replacement method (ERM)[13,39,42,69,70,93,129,155,156].

Table 1.1 shows the comparison between these two typical failure path approaches, ILM and ERM. First of all, regarding the behaviour of failed components, in the ILM the behaviour of the failed component can follow the post-ultimate behaviour and therefore, deformation of failed components can be allowed for. Since in this method the

load factor up to the particular failure stage can be obtained, post-ultimate behaviour of failed components can be considered more realistically by using the multi-state non-linear model [Fig. 1.1(b)]. One major limitation of this method is that it is applicable only to a single loading pattern. In the ERM the failed components are removed from the structure and their strength is replaced by the equivalent forces acting on the structure. Hence, their deformations are restricted and the post-ultimate behaviour of the failed components may not be considered realistically. But the idealised model of the two-state model [Fig.1.1(a)], say, ductile, semi-brittle and brittle behaviour, can be used to represent the post-ultimate behaviour in a simple way.

However, its merit over the ILM is that it is applicable to multiple loading cases. Recently, however, the limitation of the ILM has been removed by Lee[154] and Lee and Faulkner[41] by adopting the concept of a contribution factor which reflects the contribution from the utilised component strength for each loading case in the safety margin equation. This will be detailed in Section 2.4.1.

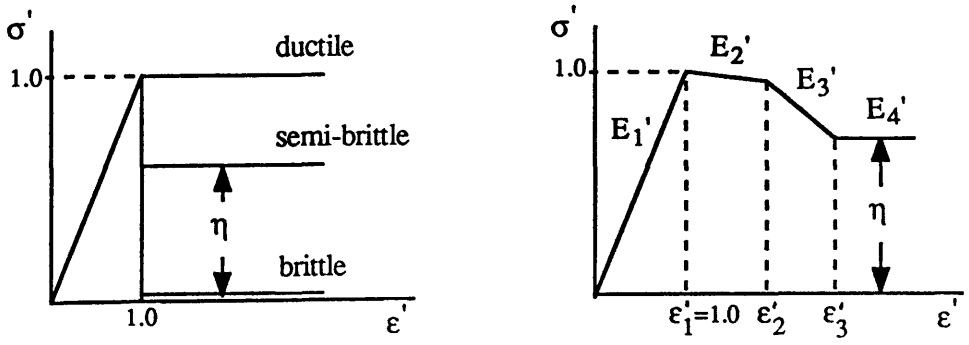

(a) Two-State Model

(b) Multi-State Model

Fig. 1.1 Typical Piecewise Simplified Models for Nonlinear Component Behaviour

Table 1.1 Comparison between Conventional ILM and ERM

	ILM	ERM
Behaviour of failed components	Deformation of failed components can be allowed to follow the post-ultimate behaviour	Deformation of failed components are restricted. Failed component are removed and their strength is replaced by the equivalent force acting on the structure
Merit	post-ultimate behaviour of failed components can be treated more realistically than the element replacement method	applicable to multi-loading cases
Limitation	applicable only to single loading case	post-ultimate behaviour of failed components is idealised as a two-state model: ductile, semi-brittle and brittle
Use of strength formula	strength formula can be directly used for the system reliability as well as component reliability analysis	strength formula may be used for component checks only

1.4 Aims of the Thesis

A major aim of the present study is to introduce a system reliability algorithm called the "Extended Incremental Load Method" which has been developed as an another approximate method. It takes the advantage of the conventional incremental load method over the element replacement method, and is applied to continuous structural systems, especially to floating offshore platforms, such as tension leg platforms or semi-submersibles.

The merits of the present method include:

[1] Although the method has been developed based on the conventional incremental load method, it has been extended so that it can be applied to structures under multiple loading conditions.

[2] The existing strength formulae for principle components in a structure are directly used and are incorporated into a modified safety margin equation which also include strength modelling parameters for components and these are treated as random variables. These strength formulae are used directly in the system reliability analysis procedure.

[3] The proposed algorithm can in principle be used to evaluate the structural system strength and reliability under multiple loading conditions with semi-brittle components by modelling the non-linear behaviour into the piecewise multi-state model.

The method, together with the procedure for identifying the most important failure modes, has been applied to simple structural systems to illustrate the validity of the method. The application to TLP structural systems, which are modelled into three dimensional frames, continuous structural components can also be used for systems having ductile and semi-brittle components.

A study of the sensitivity of system reliability index and component reliability index to changes in statistical parameters in loading and resistance variables is aimed at

showing the relative importance of variables with regard to their effects on the safety level. This provids certain useful information as an aid to decision-making in reliability-based design and re-assessment.

The study of the relation between safety and redundancy is aimed at helping to sensibly choose acceptable component and system safety levels in the design stage in the light of the reserve strength of the structural system.

1.5 Scope of the Thesis

The present work deals only with the time invariant reliability problem. The reliability with respect to failure throughout any anticipated lifetime of the structural system is evaluated. The effects of gross error in the design, fabrication and operational use of the structure are not considered.

Since failure may occur either in the actual members, as in trusses, or at localised high loaded zones, such as plastic hinges in rigid frames, the terminology of "components" will be used herein to refer to either.

Chapter 2 starts with introducing the basic definitions of the safety index and redundancy. The algorithms for evaluating the probability of failure and reliability index of a single failure mode and multiple failure modes is described. Details of the incremental load method and the element replacement method are presented. The developed present system reliability analysis method, the extended incremental load method, is detailed, together with the modified safety margin equation and the procedure for deriving the reduced element stiffness matrix. The existing procedure for identifying the most important failure modes is briefly reviewed and the present procedure is introduced. The application of the present method to simple structures is illustrated to show its validity for deriving the safety margin of a structure under multiple loading, and for identifying the important failure modes and the modified safety margin equation.

Strength models of principle components used in floating offshore platforms employed in this study are presented in Chapter 3. The strength model for the rectangular section is detailed to illustrate the basis of the proposed model.

Chapter 4 is concerned with the environmental loading of floating platforms for the reliability analysis. Hydrodynamic analysis using the Morison type approach is detailed.

The application of the present method to TLP structural systems, as examples of continuous structures, are presented in Chapter 5. The Hutton TLP is chosen for this study as an existing TLP and its two variants, TLP-A and TLP-B, are introduced to compare the results of system reliability analysis depending on the principle component types in these structures. The results are summarised in various tables for comparison of each model, together with three dimensional collapse mechanisms of identified important failure modes. The results of the three TLP models from an efficiency point of view is discussed. Redundancy analysis is also made.

Sensitivity studies of system and component reliability indices to changes in statistical parameters in loading and resistance variables are presented in Chapter 6. This is one of the major problems in system reliability. The influence of strength modelling parameters, certain geometric properties and yield stress, of load effects and post-ultimate behaviour on the system and component safety level, are investigated. For this study the Hutton TLP and a variant, TLP-B, are chosen as TLP models to compare the influence of variables depending on the type of principle component, say, ring stiffened cylinder and ring- and stringer-stiffened cylinder. For the system reliability of a structure with semi-brittle behaviour a simplified three-state model of non-linear behaviour is used and results are compared with the two-state model for which the procedure of deriving the equivalent nodal force vector is detailed. The results of discrete structures using semi-brittle and/or brittle components reported by others are also discussed to illustrate the comparison with results for continuous structural systems.

Chapter 7 deals with the correlation between structural safety and redundancy (reserve and residual strength). A simple procedure for predicting the relation of component and system safety to redundancy is introduced. From the study a couple of equations are suggested which may be helpful in selecting the allowable safety levels for economically efficiently design with adequate but not excessive safety. The basic concept of reliability-based optimal design is briefly described and one useful formulation is illustrated. System reliability-based design is discussed with the relevant terms and its anticipated difficulties. In-service re-assessment based on economic consideration is also discussed.

Chapter 8 reviews the present work in the context of the proposed method and system reliability analysis of discrete structures and of TLP structures and discusses the results for economically efficient design from the system's points of view. The results of sensitivity studies are summarised by placing emphasis on the economic importance of reducing the uncertainties associated with component strength modelling and with post-ultimate behaviour characteristics. The thesis ends by describing the main conclusions of the present work and recommendations for future research in the area of system reliability analysis and its application to design.

For easy understanding of the present approach four Appendices are added. Appendix A deals with an example illustrating the derivation of the safety margin for a portal frame under multiple loading by using the extended incremental load method with two type of equations. The calculation of the total load factor is illustrated in Appendix B. The procedure for identifying the most important failure modes in a simple truss structure is illustrated in Appendix C. Finally, in Appendix-D the derived flow vector of a finite element, when its one node has failed, is summarised for the principle components found in the TLP structure and for the beam element in the frame structure. They have been derived based on the strength formulae used in this study.

CHAPTER 2 SYSTEM STRENGTH

2.1 Basic Definitions

2.1.1 Reliability Index

As a simple situation where strength, R, and load (or load effect), Q, are given, the probability of failure, P_f, is defined as the probability that the load exceeds the strength, i.e.:

$$P_f = P[R < Q] = P[R - Q < 0] \tag{2.1}$$

and then the reliability, P_S, is defined as:

$$P_S = P[R > Q] = P[R - Q > 0] = 1 - P[R - Q < 0] = 1 - P_f \tag{2.2}$$

Such a simple situation is called the fundamental case and is illustrated in Fig. 2.1. The probability of failure can be easily calculated from:

$$P_f = \int_{-\infty}^{+\infty} F_R(x)\, f_Q(x)\, dx \tag{2.3.a}$$

or, alternatively,

$$P_f = \int_{-\infty}^{+\infty} (1 - F_Q(x))\, f_R(x)\, dx \tag{2.3.b}$$

Close-form solutions for the integral in Eq.(2.3) only exist for special cases. If R and Q are independent and normally distributed, $N(\underline{R}, \sigma_R)$ and $N(\underline{Q}, \sigma_Q)$, then the probability of failure can be exactly calculated. Let $Z = R - Q$. Then Z is also a normal variable with

mean and variance

$$\underline{Z} = \underline{R} - \underline{Q}$$
$$\sigma_Z 2 = \sigma_R 2 + \sigma_Q 2 \tag{2.4}$$

Therefore, the failure probability is given

$$P_f = P[R - Q < 0] = P[Z < 0]$$
$$= \Phi\left(\frac{0 - \underline{Z}}{\sigma_z}\right) = \Phi\left(-\frac{\underline{R} - \underline{Q}}{\sqrt{\sigma_R^2 + \sigma_Q^2}}\right) \tag{2.5}$$

The random variable, Z (= R – Q) is called the safety margin, of which distribution is illustrated in Fig. 2.2, and the relation of its mean $\underline{Z}$ to its standard deviation σ_Z is called reliability index or safety index, β. That is defined by:

$$\beta = \frac{\underline{Z}}{\sigma_Z} = \frac{\underline{R} - \underline{Q}}{\sqrt{\sigma_R^2 + \sigma_Q^2}} \tag{2.6}$$

Then it is seen from Eq.(2.5) that

$$P_f = \Phi(-\beta) \tag{2.7}$$

Its inverse form is

$$\beta = -\Phi^{-1}(P_f) \tag{2.8}$$

where $\Phi(\cdot)$ is the normal distribution function.

When coefficients of variation (COV) of random variables are given rather than standard deviations such that

$$V_R = \frac{\sigma_R}{\underline{R}}, \qquad V_Q = \frac{\sigma_Q}{\underline{Q}} \tag{2.9}$$

where V_R and V_Q are COV of R and Q. Additionally let $\theta = \underline{R} / \underline{Q}$, and then Eq.(2.8) becomes

$$\beta = \frac{\theta - 1}{\sqrt{(\theta V_R)^2 + V_Q^2}} \tag{2.10}$$

in which θ is referred to as the central safety factor.

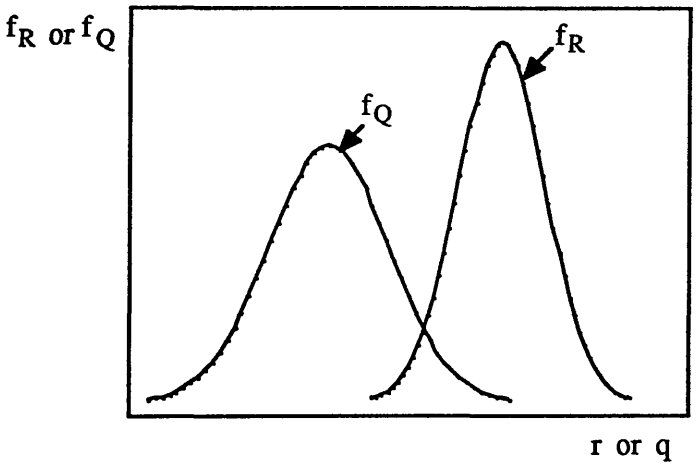

Fig. 2.1 Fundamental Case

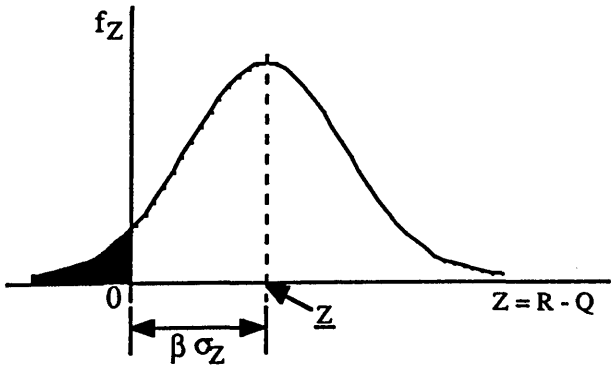

Fig. 2.2 Distribution of Safety Margin, Z and its Relation to Reliability Index β

2.1.2 Structural Redundancy

It has been much emphasised that the redundancy of a structure should be considered in design and system reliability analysis is important for verification of reserve and residual strength[8]. The classic definition of structural redundancy is the number of additional members or support reactions in excess of those required to calculate member forces by static equilibrium. However, even for discrete structures, such as portal frames and fixed jacket space frames, redundancy is more usefully measured by the role played by individual members in the structural system. This then identifies and allows for the existence of weak link (series) members in an otherwise highly redundant (and mainly parallel) system. In principle, each member should be systematically removed and the consequences on the residual strength of the system assessed in terms of the load at which progressive collapse occurs. A hierarchy of member importance can then be established.

Structural redundancy is usually characterised by reserve and residual strength. In general, the reserve strength is defined as the ultimate strength which the structure can sustain beyond the specified ultimate state, and the residual strength as the ultimate strength when structure is damaged. It is characterised by the importance of individual components to the structural system strength, i.e., whether their failure causes a small, significant or total loss of strength. Redundancy usually allows the structure to tolerate possible understrength of components due to accidental damage, corrosion, fatigue, fabrication flaws, etc[91].

Statically indeterminate structures (redundant structure) will in general have redundancy against overall system failure. Even components designed according to design code show redundancy against total component failure beyond local failure conditions by virtue of moment distribution type redundancy from two possible effects[136]:

[1] cross-section or internal redundancy analogous to the plastic shape factor in beam bending

[2] the need generally for a mechanism of hinges to develop along the component before final collapse can occur.

There may also be further reserve strength arising from simplifications often made even with comprehensive finite element modelling of the structure. Additional structural reserve strength can be found in design symmetry, multiple loading condition and fabrication requirements.

In general terms, and depending on the nature of the failure mechanism, a redundant structure offers a higher safety level than a non-redundant one, because there are a number of possible failure paths and failure of one of the components is not sufficient to trigger off the overall structural failure.

In the case of discrete structure the degree of redundancy can be known, but in the case of continuous structure it is practically impossible to think of the redundancy in terms of a degree of redundancy. The behaviour can then be largely described in terms of reserve strength and residual strength[15].

The concept of structural redundancy is not easy to define in simple ways since it takes multiple forms and various factors affect it. Generally structural redundancy depends on[14]:

[1] the number of members and the topology or the way the member are laid out

[2] the strength of each member

[3] the joint or connections between members

[4] the types of loads considered

[5] the member behaviour, especially the post-ultimate behaviour

Several measures of structural redundancy have been proposed[15,22,91,92]. The reserve strength is given in terms of the reserve strength index (RSI)[15] (the reserve resistance factor: REF[91]) and the residual strength in terms of the residual strength index (RDI)[15] (the residual resistance factor: RIF[91]). In this thesis the terms of RSI and RDI are used to express the reserve strength and the residual strength. They are defined as:

$$RSI = \frac{\text{Environmental Load at Collapse (undamaged)}}{\text{Design Environmental Load}}$$

$$RDI = \frac{\text{Environmental Load at Collapse (damaged)}}{\text{Environmental Load at Collapse (undamaged)}} \qquad (2.11)$$

The reserve strength index is a measure of the intact structure to carry load in excess of the design load. The residual strength index characterises the ultimate strength in damaged condition relative to the one in undamaged condition. The definitions above indicate that reserve strength and residual strength are obviously interrelated through the concept of damage tolerance. A damage tolerant structure must have both reserve strength (to avoid failure) and residual strength (to minimise the consequence of failure)[94]. The damaged structure can be safe if its design satisfies the relation between RSI and RDI that[15,91]:

$$RSI * RDI = \frac{\text{residual strength}}{\text{design strength}} > 1$$

For a consequence of member failure on the structural system, Lloyd and Clawson[91] have established a five point redundancy scale for structural members ranging from zero for members whose failure would lead to progressive collapse even for dead weight load conditions to four for a member whose failure has little effect on the design strength, but whose presence enhances the redundancy of nearby members, i.e., a normally lightly loaded member that provides an alternative load path when a nearby member fails. Categories 1 to 3 are for members whose failure leads to progressive collapse for a limited set of dead and live load conditions of increasing severity up to some (unspecified) multiple of the design environmental load. A sixth category (Level 5 on the scale) is reserved for non-structural members whose failure has no bearing on the design strength.

The above expressions for the structural redundancy are deterministic. As a probabilistic measure for the redundancy of the structural system, Feng and Moses[22]

proposed the following measure for a damaged structure based on the system reliability analysis.

$$\beta_{sys,R} = \text{Min}\,(\beta_{sys,R_i}) \tag{2.12}$$

where β_{sys,R_i} refers to the system reliability given that component i has failed. Hence, this quantity is defined as the system reliability given that any selected component has failed.

Nodal et al[93] proposed a β measure as a probabilistic measure of the redundancy for the structural system defined as:

$$RDI_{\beta} = \frac{\beta_{sys} - \beta_{comp}}{\beta_{sys}} \tag{2.13}$$

where β_{sys} is the reliability index of the system failure and β_{comp} is the reliability index of any first component failure. Eq.(2.13) is a β measure of the conditional reliability of the system given a first component failure. It may be related to the residual strength index, RDI in Eq.(2.11). For a statically determinate system, $\beta_{sys} \cong \beta_{comp}$ and the difference is always zero. In the opposite extreme, for a system with very high redundancy β_{sys} would be much larger than β_{comp} and the difference would be approximately equal to β_{sys} itself.

Frieze[131] introduced the redundancy factor based on the load factors associated with system failure (λ_{sys}) and component failure (λ_{comp}), respectively defined as:

$$RF = \frac{\lambda_{sys}}{\lambda_{comp}} \tag{2.14}$$

This may relate to the reserve strength index (RSI) in Eq.(2.11).

When using the incremental load method the load factor, λ_j, can be obtained, from which the mean load can be predicted up to the particular failure stage, j, i.e. when j components have failed. This can easily be extended to estimate the collapse load (in the mean sense)[41,154]. Then, the total load factor is defined as the ratio of the load when system collapse occurs to the mean applied load as:

$$[\text{ System Collapse Load }] = \lambda_T * [\text{ Mean Applied Load }] \qquad (2.15.a)$$

or, alternatively,

$$\lambda_T = \frac{\text{System Collapse Load}}{\text{Mean Applied Load}} \qquad (2.15.b)$$

where λ_T is referred to the total load factor [see Eq.(2.95)] when collapse occurs and is related to the reserve strength index (RSI) in Eq.(2.11)

For offshore platforms the well-designed jacket platforms in general can show the reserve strength index greater than 2.0[91]. The X-bracing jacket platform usually provides more reserve and residual strength than the K-bracing jacket platform. This arises from the more widely understood space frame type redundancy associated with the concepts of system stability and determinancy. This has been studied for fixed jacket platforms in a safety context by Marshall and Bea[89] and Nodal et al[93].

In the case of a TLP there may be inherent redundancy at the sufficiently large cross section and at the joint of a member. The diagonal bracing would provide further reserve strength before total collapse of the whole structural system could occur. A preliminary study for TLP[136] shows that the reserve strength indices are unlikely to be less than 1.5, and generally will be appreciably more than 2.0 in many practical designs. These are very large conservative biases so far ignored.

It is generally accepted that redundancy should be considered at the design stage

to achieve more economic benefit. Moses[11,110] and Faulkner[136] recommended that a system factor which relates the component strength to system strength could be added in the safety checking equation. This will be further described in Section 5.2.

2.2 Computation of Probability of Failure and Reliability Index

2.2.1 Reliability Index of Single Failure Mode

In this study the Rackwitz-Fiessler algorithm[54] is used to calculate the reliability index and/or the probability of failure of a single failure mode, which is an extension of Hasofer-Lind[53] and gives a reasonable estimate of the probability of failure. This algorithm is often called advanced first-order second reliability method (AFORM)

In general, the limit state equation (or safety margin or performance function or failure function) is of the form:

$$Z = g(y) = g(y_1, y_2, \ldots, y_n) \tag{2.16}$$

where y_i (i = 1,2, . . ., n) are n reduced variables of basic design variables, x_i (i = 1,2, . . ., n) as basic independent random variables defined as:

$$y_i = \frac{x_i - \underline{x}_i}{\sigma_{x_i}} \tag{2.17}$$

where $\underline{x}_i$ and σ_{x_i} are mean and standard deviation of variable x_i. Function, g, is some given non-linear function and describes the structural behaviour such that for $g > 0$ safe state is defined whereas $g < 0$ corresponding to failure, and failure state is given by $g = 0$. Expand Eq.(2.16) in linear Taylor series which should equal zero, if the limit state criterion is fulfilled:

$$g(y_1^*, y_2^*, \ldots, y_n^*) + \sum_{i=1}^{n} g_{,i} (y_i - y_i^*) = 0 \qquad (2.18)$$

where $g_{,i}$ is partial derivative of function g with respect to y_i evaluated at the unknown point, $y^* = \{ y_1^*, y_2^*, \ldots, y_n^* \}$. The problem is to find the point, y^*, where β becomes minimal. According to the first order reliability theory the limit state criterion is only fulfilled if the point lies on the failure surface. When such a point is found, the corresponding variable, x*, can be obtained from:

$$y_i^* = y_i - \alpha_i \beta \sigma_{y_i} \qquad (2.19)$$

where α_i is referred to as the sensitivity factor as defined in Eq.(2.21), which represent the relative importance of basic design variables. The point y* is usually obtained by the following iteration algorithm[54].

In general, at the (j+1)th iteration with the assumed point of $y^{(j)}$ obtained at the jth iteration.

Step 1: Evaluate the partial derivatives $g_{,i}^{(j)}$, i=1,2,. . . , n at the assumed point, $y^{(j)}$:

$$g_{,i}^{(j)} = \frac{dg(\{y^{(j)}\})}{dx_i} \qquad (2.20)$$

Step 2: Evaluate the sensitivity factor for all y_i, $\{\alpha^{(j)}\}$, given by:

$$\alpha_i^{(j)} = \frac{g_{,i}\, \sigma_{y_i}}{\sqrt{\sum_{i=1}^{n} (g_i^{(j)}.\sigma_{y_i})^2}} \qquad (2.21)$$

Step 3: Calculate the new point for the next iteration:

$$y^{(j+1)} = \left(\{y^{(j)}\}^T \{\alpha^{(j)}\} \right) \alpha^{(j)} - \frac{g(y^{(j)})}{\sqrt{\sum_{i=1}^{n} \left(g_i^{(j)} . \sigma_{y_i} \right)^2}} . \{\alpha^{(j)}\} \qquad (2.22)$$

Step 4: Calculate the reliability index:

$$\beta^{(j+1)} = | y^{(j+1)} | \qquad (2.23)$$

Step 5: Evaluate the design point:

$$x_i^{(j+1)} = y_i - \alpha_i^{(j)} \beta^{(j+1)} \sigma_{y_i} \qquad (2.24)$$

Step 6: Check the convergence:

$$\sqrt{\sum_{i=1}^{n} \left(\frac{y_i^{(j+1)} - y_i^{(j)}}{y_i^{(j)}} \right)^2} \leq \varepsilon$$

and

$$\frac{\beta^{(j+1)} - \beta^{(j)}}{\beta^{(j)}} \leq \varepsilon \qquad (2.25)$$

where ε is a small number as tolerance.

The above procedure will be continued until convergence criteria are satisfied. The failure probability is:

$$P_f = P(g < 0) = \Phi(-\beta) \qquad (2.26)$$

For the non-normal variable, its mean and standard deviation in Eq.(2.17) are replaced by the equivalent mean and standard deviation obtained from the following[54,157]:

$$\Phi\left(\frac{x_i^* - \underline{x}_i}{\sigma_{x_i}}\right) = F_{x_i}(x_i^*) \tag{2.27}$$

$$\frac{1}{\sigma_{x_i}}\phi\left(\frac{x_i^* - \underline{x}_i}{\sigma_{x_i}}\right) = f_{x_i}(x_i^*) \tag{2.28}$$

where x_i^* is the approximation point. $F(\cdot)$ and $f(\cdot)$ the distribution function and density function of the non-normal distribution, respectively, and $\Phi(\cdot)$ and $\phi(\cdot)$ the normal distribution function and normal density function, respectively, which has the effect of equating the cumulative probabilities of the probability densities of the actual and approximating normal distributions at the design point x_i^* . The solution of Eqs.(2.27) and (2.28) is:

$$\sigma_{x_i}^N = \frac{\phi\left[\Phi^{-1}\{F_{x_i}(x_i^*)\}\right]}{f_{x_i}(x_i)}$$

$$\underline{x}_i^N = x_i^* - \sigma_{x_i}\Phi^{-1}\{F_{x_i}(x_i^*)\} \tag{2.29}$$

$\underline{x}_i^N$ and $\sigma_{x_i}^N$ are the mean and standard deviation of the equivalent distribution. This approximation may become more and more inaccurate if the original distribution becomes increasingly skewed. After the design point is obtained from Eq.(2.19), the central safety factor (CSF) for each variable can be determined as the ratio of the design point value of a variable to its mean value:

$$\theta = \frac{x_i^*}{\underline{x}_i} \tag{2.30}$$

For design variables to which a strength model shows particular sensitivity, it is suggested that characteristic values rather than mean values should be used particularly in the design context. The partial safety factors appropriate for this thus relate the design and the characteristic values, and can be derived easily from the central factor since

$$x_{ik} = \underline{x}_i (1 \pm k_i V_{x_i}) \tag{2.31}$$

where x_{ik} is the characteristic value of the variable, k_i is a coefficient depending on the fractile represented by x_{ik} and V_{x_i} is COV of x_i. Minus sign is used for the resistance variable and plus sign for loading variable. From Eq.(2.30) the required partial safety factors, γ_i, is:

$$\gamma_i = \frac{x_i^*}{x_{ik}} = \frac{1 - \alpha_i \beta V_{x_i}}{1 \pm k_i V_{x_i}} \tag{2.32}$$

When k_i are zero, the partial safety factors equal to the central safety factors:

$$\gamma_i = 1 - \alpha_i \beta V_{x_i} \tag{2.33}$$

The above procedure computes the reliability index given the limit state equation and the associated statistical parameters of basic design variables. In code calibration the PSFs need to be determined for the target reliability index.The required PSFs on each of the basic design variables can also be computed following the above procedure by sustaining β as target reliability index, β^o.

2.2.2 Probability of Multiple Failure Mode

2.2.2.1 General Concept

In system reliability analysis there can be two typical models: Series system and Parallel system. The Series system is the weakest link chain type model [Fig.2.3(a)] in

which system failure occurs if any component fails, as in a statically determinate structure. The Parallel system is a fail-safe model [Fig.2.3(b)], as occurs in collapse of a statically indeterminate structure in which the system failure results only after several components reach their strength capacity. For practical application the reliability analysis is further complicated by the fact that most structures exhibit characteristics that are a combination of the Series systems and Parallel systems.

System failure is, in general, the union of each failure mode and a single failure mode is the intersection of the component failure of which the elements are possible failure modes. Any single failure mode is an interaction of the component failure. In more detail component failure is a union of component failure modes, for example, failure due to plasticity, local or global buckling, fatigue, etc, i.e. generally system failure is a series system of sub-parallel systems and each element consists of sub-series systems of component failure modes. The occurrence of any single mode results in the system failure[13,14].

In a large complex system, such as an offshore platform, there are a great number of possible failure events when component failure events and system failure modes are combined to result in the whole system failure. However, it is not practically possible to consider all possible failure events from the components side and/or from the systems side , and hence, for practical purposes, assumptions may inevitably be introduced.

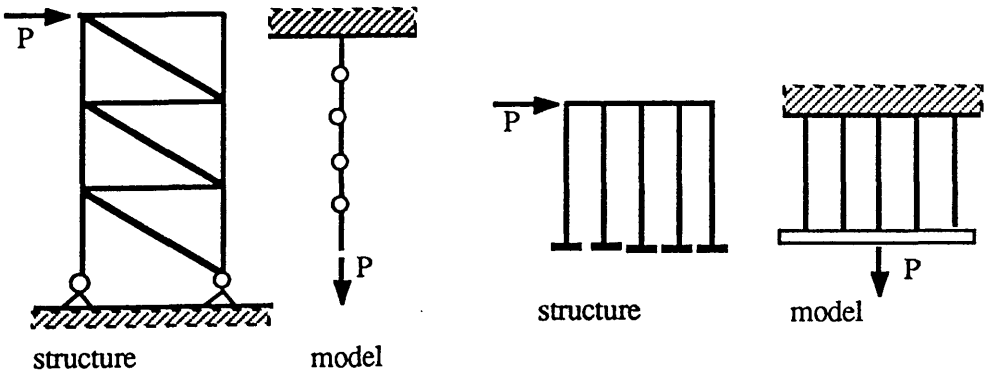

Fig. 2.3 System Modelling

When there are m possible modes, the different failure modes would have different limit state functions. The individual limit state function may be expressed as:

$$Z_i = g_i(x) = g(x_1, x_2, \ldots, x_n) \tag{2.34}$$

and then the event of the occurrence of failure mode i is:

$$E_i = [Z_i < 0] \tag{2.35}$$

Then the probability of system failure is the probability that any single mode occurs. That is:

$$(P_f)_{sys} = P(E_1 \cup E_2 \cup \ldots \cup E_m) = P\left(\bigcup_{i=1}^{m} E_i\right)$$

$$= \int \ldots \int_{[E_1 \cup \ldots \cup E_m]} f_{x_1, x_2, \ldots, x_n}(x_1, x_2, \ldots, x_n)\, dx_1 dx_2 \ldots dx_n \tag{2.36}$$

The safe event S_i is the complement of failure events, E_i. That is:

$$S_i = [Z_i > 0] \tag{2.37}$$

The survival of system is the complement event of the system failure and hence the probability of system survival or the reliability is that none of the m possible failure modes occur. That is given by:

$$(P_s)_{sys} = P(S_1 \cap S_2 \cap \ldots \cap S_m) = P\left(\bigcap_{i=1}^{m} S_i\right)$$

$$= \int \ldots \int_{[S_1 \cap \ldots \cap S_m]} f_{x_1, x_2, \ldots, x_n}(x_1, x_2, \ldots, x_n)\, dx_1 dx_2 \ldots dx_n$$

$$= 1 - (P_f)_{sys} \tag{2.38}$$

The basic numerical operation in general system reliability analysis is, therefore, the computation of probabilities of unions of interactions of componential failure domains in high-dimension random vector spaces. But the calculation of the probability of failure or safety of a system through Eq.(2.36) or (2.38) is generally difficult and approximate methods are almost always necessary. In this latter regard, bounds of the probability of system failure are useful.

2.2.2.2 Probability Bounds of Failure of Series System

As stated by Vanmarcke[82], one of the most difficult questions in structural system reliability analysis is how to deal with the statistical dependence between mode failure events. It is, therefore, not surprising that research workers in structural reliability have tried to develop bounding methods that include modal correlations.

Various authors have developed several methods for determining failure probability of a structural system based on different assumptions and techniques[84-86]. Frangopol[84] investigated the accuracy and reliability of various methods for the system reliability analysis of ductile systems with random independent strength acted on by random independent loads, i.e., to changes in strength and load correlations. Grimmeit and Schueller[85] compared various methods with respect to their results, capabilities and efficiencies through the benchmark study.

In this section simple bounds[47,80], narrow bounds[81], Vanmarcke's upper bound[82], Ang and Ma's upper bound[44] and the method by Guenard[39] for approximately determining the probability of failure of series system, Eq.(2.36), are described. For simplicity, the probability of system failure, $(P_f)_{sys}$ is denoted as P_f.

o Simple Bounds:

The simple upper bound can be seen in reference [47] and is given by:

$$P_f \leq \sum_{i=1}^{m} P_{f_i} \tag{2.39}$$

The simple bounds were proposed by Cornell[80]. His upper bound is obtained based on the assumption that all the m failure modes are perfectly correlated, and the lower bound based on the assumption that all failure modes are statistically independent.

When all modes are positively correlated:

$$\max [P_{f_i}, i = 1, m] \leq P_f \leq 1 - \prod_{i=1}^{m} (1 - P_{f_i}) \cong \sum_{i=1}^{m} P_{f_i} \qquad (2.40)$$

where $P_{f_i} = P(Z_i \leq 0)$, i.e., the probability of failure of i th mode.

And when all modes are negatively correlated:

$$P_f > 1 - \prod_{i=1}^{m} P_{s_i} \qquad (2.41)$$

where $P_{s_i} = P(Z_i > 0)$, i.e., the probability of survival of i th mode.

If there are only a few dominant modes, the bounds will be very close. However, if several modes fail with almost identical probabilities, modal correlation has to be taken into account. For this purpose some methods have been suggested, described as follows.

o Narrow Bounds:

In usual structural engineering the total failure probability is purposely made very small. This has the fortunate side-effect of making the bounds quite small in most cases. The bounds are given solely by the probability of the single-mode failure events $E_1, \ldots, E_m$ and their pairwise intersections $E_1 \cap E_2, \ldots, E_{m-1} \cap E_m$. In fact, the total failure event $\bigcup_{i=1}^{m} E_i$ has a probability which is bounded as follows[81]:

Upper bound:

$$P(\bigcup_{i=1}^{m} E_i) \leq \sum_{i=1}^{m} P(E_i) - \sum_{i=2}^{m} \max_{j<i} P(E_i \cap E_j) \qquad (2.42)$$

Lower bound:

$$P(\bigcup_{i=1}^{m} E_i) > P(E_1) + \sum_{i=2}^{m} \max [\, 0, P(E_i) - \sum_{j=1}^{i-1} P(E_i \cap E_j) \,] \qquad (2.43)$$

Since $0 \leq P(E_i \cap E_j) \leq \min [\, P(E_i), P(E_j) \,]$, it is always possible to determine a unique number ρ_{ij} such that

$$P(E_i \cap E_j) = P_{ij} = \Phi(-\beta_i, -\beta_j ; \rho_{ij}) \qquad (2.44)$$

where $\Phi(-\beta_i, -\beta_j ; \rho_{ij})$ is the bivariate normal distribution function corresponding to zero means, unit variances and correlation coefficient ρ_{ij}. The numbers β_i and β_j are the single-mode reliability indices of the i th and j th failure modes respectively, i.e., β_i is defined by the identity $P(E_i) = \Phi(-\beta_i)$, and correspondingly for β_j, $P(E_j) = \Phi(-\beta_j)$. The number ρ_{ij} in (2.44) is called the correlation coefficient between the i th and j th failure mode. The bounds (2.42) and (2.43) almost coincide for all of these correlation coefficients not larger than about 0.5 - 0.6 provided the total reliability index

$$\beta = -\Phi^{-1}[\, P(\bigcup_{i=1}^{m} E_i) \,] \qquad (2.45)$$

is larger than about 3.0. Without restrictions on the failure mode correlation coefficients very narrow bounds can be constructed on the basis of (2.42) and (2.43) through a particular method of conditional bounding. It requires no more than a single integration.

The bivariate normal distribution function, P_{ij} in Eq.(2.44) can be obtained from:

$$P_{ij} = \Phi(-\beta_i)\,\Phi(-\beta_j) + \int_0^{\rho_{ij}} \phi_2(-\beta_i, -\beta_j\,;\,r)\,dr \qquad (2.46)$$

where ϕ_2 is the two-dimensional normal density function given as:

$$\phi_2(x, y\,;\,r) = \frac{1}{2\pi\sqrt{1-r^2}}\,\exp\left[-\frac{1}{2(1-r^2)}\,(x^2+y^2-2rxy)\right] \qquad (2.47)$$

When given β_i, β_j and ρ_{ij}, direct calculation of $P(E_i \cap E_j)$ can be avoided by using the inequalities:

when $\rho_{ij} > 0$

$$\Phi(-\beta_i, -\beta_j\,;\,\rho_{ij}) \le \Phi(-\beta_i)\,\Phi(-\beta_{j\,|\,i}) + \Phi(-\beta_j)\,\Phi(-\beta_{i\,|\,j})$$

$$\Phi(-\beta_i, -\beta_j\,;\,\rho_{ij}) > \max\{\,\Phi(-\beta_i)\,\Phi(-\beta_{j\,|\,i}),\,\Phi(-\beta_j)\,\Phi(-\beta_{i\,|\,j})\,\} \qquad (2.48)$$

when $\rho_{ij} \le 0$

$$\Phi(-\beta_i, -\beta_j\,;\,\rho_{ij}) \le \min\{\,\Phi(-\beta_i)\,\Phi(-\beta_{j\,|\,i}),\,\Phi(-\beta_j)\,\Phi(-\beta_{i\,|\,j})\,\}$$

$$\Phi(-\beta_i, -\beta_j\,;\,\rho_{ij}) > 0 \qquad (2.49)$$

where

$$\beta_{i\,|\,j} = \frac{(\beta_i - \beta_j\,\rho_{ij})}{\sqrt{(1-\rho_{ij}^2)}} \qquad (2.50)$$

Narrow bounds are often referred to as Bi-modal bounds or Second-Order bounds.

o Vanmarcke's Upper Bound:

This upper bound is given by[82]:

$$P_f \leq P_{f_1} + \sum_{i=2}^{m} P_{f_i} \min_{j=1}^{i-1} P\left[(Z_j > 0) \mid (Z_i \leq 0) \right] \qquad (2.51)$$

in which the conditional probability that mode j survives given that mode i occurs is approximated in terms of the absolute value of the coefficient of correlation between the failure modes i and j, $|\rho_{ij}|$, of the safety indices β_i and β_j associated with these modes, and of the probability $P_{f_i} = \Phi(\beta_i)$ as :

$$P(Z_j > 0 \mid Z_i \leq 0) = 1 - \Phi\left(\frac{\max\left[\frac{\beta_j}{|\rho_{ij}|}, \beta_i \right]}{\Phi(\beta_i)} \right) \qquad (2.52)$$

This upper bound sometimes gives a better estimate than that given by the upper bound of narrow bounds.

o Ang and Ma's Upper Bound:

Probabilistic network evaluation technique (PNET)[45] is used to estimate the upper bound as follows:

$$P_f \leq 1 - \prod_{all} (1 - P_{f,group}) \equiv \sum_{groups}^{all} \max [P_{f,group}] \qquad (2.53)$$

in which $P_{f,group}$ is the probability of the "representative" event of a group of failure modes with high correlation. The probabilistic network evaluation technique (PNET) avoids calculating probabilities resulting from conditions leading to failure via a pair of failure modes. This method is based on the notion of demarcating correlation coefficient ρ_0 assuming those failure modes with high correlation ($\rho_{ij} > \rho_0$) to be statistically independent. The failure modes must be arranged in decreasing order of their probabilities of occurrence, and in each group the mode with the highest probability of

occurrence is chosen as the "representative" event of the group. Since the different groups are considered statistically independent, the overall probability of failure of the system is approximated by the right hand side of Eq.(2.53).

Recently Chou et al[83] presented possible alternatives for grouping technique by using the taxonomic (cluster) analysis [158] and Tichy and Vorlicek technique[159] . In the first alternative a complete linkage hierarchical clustering can be obtained on a given similarity matrix (the correlation matrix) and the most meaningful level of clustering can be obtained by comparing with a reference value, such as the demarcating correlation ρ_0 . Although this technique still requires an arbitrary ρ_0 value to define the dependency among failure modes, it embeds the consideration of mutual correlation during the formation of the cluster. In the second alternative, it eliminates using the arbitrary ρ_0 value, while the relationship among failure modes is embedded in the multi-variate correlation coefficient, which is the attractive point of the approach.

o Method by Guenard[39] :

If all possible failure modes are not included in the analysis then the result obtained is a lower bound on the probability of system failure, i.e. since some potential failure modes are ignored the true system failure probability will be larger. If, for any specific mode, all the component failures in the mode are not considered, i.e. an incomplete mode, then the probability of occurrence of the mode will be larger than the true value, and a system failure analysis including all such incomplete modes will result in an upper bound on the probability of system failure. Conceptually P_f is bounded as:

$$(P_f) \text{ from dominant modes} \leq P_f \leq (P_f) \text{ from incomplete modes} \qquad (2.54)$$

In the extreme case, the lower bound could be the probability of occurrence of any one particular complete sequence, and upper bound could be the probability that any component fails in the intact state, i.e. in each mode only the first component failure is considered and all further failures are ignored.

2.2.2.3 Concept of Equivalent Safety Margin of a Single Failure Mode

Any single failure mode is defined as a parallel system of component failures [Section 2.2.2.1]. When a safety margin equation is given in the form of linear combination of loading and resistance variables [see Eq.(2.62) in Section 2.3], the equivalent failure probability and the corresponding equivalent reliability index of a failure mode can be calculated using the concept of the equivalent linear safety margin suggested by Gollwitzer and Rackwitz[55].

When k components, r_1, r_2, . . . r_k have failed, let the j th failure mode be expressed as

$$Z_j = (Z_{j1} < 0 \cap Z_{j2} < 0 \cap \ldots \cap Z_{jn} < 0) \tag{2.55}$$

where Z_{ji} (i = 1, k) is the safety margin when component r_i has failed. Omitting the sub-index j for a moment, safety margin equations corresponding to failure modes can be written

$$Z_i = \alpha_{i1} X_1 + \alpha_{i2} X_2 + \ldots + \alpha_{ik} X_k + \beta_i$$

$$= \sum_{j=1}^{n} \alpha_{ij} X_j + \beta_i \tag{2.56}$$

where X_i (i = 1, 2, . . . , n) are n basic design variables. $\alpha_i = (\alpha_{i1} , \alpha_{i2} , \ldots , \alpha_{in})$ is a sensitivity vector for safety margin Z_i and β_i is the Hasofer-Lind reliability index[51].

A generalised reliability index β_p for the parallel system is then given by:

$$\beta_p = -\Phi^{-1}(\Phi_n (-\beta : [\rho])) \tag{2.57}$$

where,

$\beta = (\beta_1 , \beta_2 , \ldots , \beta_n)$

$[\rho] = [\rho_{ij}] = [\alpha_i^T \ \alpha_j]$ is a correlation matrix between each safety margin.

The equivalent linear safety margin Z^{eq} is now defined in such a way that the corresponding reliability index β^{eq} is equal to β_p and it has the same sensitivity as the parallel system against changes in the basic variables X_i, i = 1, 2, . . ., n.

Let the vector X of random variables be increased by a small vector $\varepsilon = (\varepsilon_1, \varepsilon_2, \ldots, \varepsilon_n)$. The corresponding reliability index $\beta_p(\varepsilon)$ for the parallel system is then

$$\beta_p(\varepsilon) = -\Phi^{-1}\left[P\left\{ \bigcap_{i=1}^{n} \left(\sum_{j=1}^{n} \alpha_{ij}(X_j + \varepsilon_j) + \beta_i \le 0 \right) \right\} \right]$$

$$= -\Phi^{-1}[\Phi_n(-\beta - [\alpha]\,\varepsilon \ ; [\rho])] \qquad (2.58)$$

where $[\alpha] = [\alpha_{ij}]$

Let the equivalent linear safety margin Z^{eq} be given by:

$$Z^{eq} = \alpha_1^{eq} Z_1 + \alpha_2^{eq} Z_2 + \ldots + \alpha_k^{eq} + \beta^{eq}$$

$$= \sum_{j=1}^{n} \alpha_j^{eq} Z_j + \beta^{eq} \qquad (2.59)$$

where $\alpha^{eq} = (\alpha_1{}^{eq}, \alpha_2{}^{eq}, \ldots, \alpha_n{}^{eq})$ is a sensitivity vector and $\beta^{eq} = \beta_p$. By the same increase ε of the basic design variables the reliability index $\beta^{eq}(\varepsilon)$ is:

$$\begin{aligned} \beta^{eq}(\varepsilon) &= \Phi^{-1}(\Phi (-\beta^{eq} - \alpha^{eq^T} \varepsilon)) \\ &= \beta^{eq} + \alpha^{eq^T} \varepsilon \\ &= \beta^{eq} + \alpha_1{}^{eq} + \alpha_2{}^{eq} + \ldots + \alpha_k{}^{eq} \end{aligned} \qquad (2.60)$$

It is seen from Eq.(2.60) and by putting $\beta_p(0) = \beta^{eq}(0)$ that the sensitivity vector is given by:

$$\alpha_i^{eq} = \frac{\left(\frac{d\beta_p}{d\varepsilon_i}\right)_{\varepsilon = 0}}{\sqrt{\sum_{j=1}^{n} \left\{ \left(\frac{d\beta_p}{d\varepsilon_j}\right)_{\varepsilon = 0} \right\}^2}} \quad , i = 1, 2, \ldots, n \qquad (2.61)$$

α_i^{eq} (i = 1, 2, . . ., n) is evaluated approximately by numerical differentiation.

2.3 Failure Path Approaches

For many redundant ductile and semi-brittle systems ultimate structural collapse occurs only after several components simultaneously reach their maximum capacity. In such a case a general expression for the safety margin of any failure mode can be expressed in the form of linear combination of resistance and loading variables[13,159]. For the m th failure mode:

$$Z_m = \sum_{k=1}^{j} C_{mk} R_k - \sum_{l=1}^{L} B_{ml} P_l \qquad (2.62)$$

where,

Z_m = safety margin of m th mode

R_k = resistance of the component k (deterministic)

P_l = the l th loading acting on the structure

C_{mk} = resistance coefficient

B_{ml} = load coefficient for P_l ,i.e. load effect due to unit value of load P_l (deterministic)

j = number of failed components

L = number of loading cases

The first part of Eq.(2.62) will be called the resistance term and the second part the loading term. When the failure of j th component leads to the collapse of the structure, $C_{mj} = 1.0$. The following two sections deal with deriving the safety margin by the two typical types of failure path approaches: Incremental Load Method and Element Replacement Method.

2.3.1 Incremental Load Method

This method is based on the mean resistances of components and mean load, and the load at which collapse occurs is approximately equal to the mean system resistance. The variance of system resistance may be computed by first-order reliability concept.

The method calls for progressive "unzipping" a structure as successive components reach their capacity until overall failure occurs. The incremental loading algorithm can utilise existing structure analysis algorithm and leads to simultaneous evaluation of mean and variance of strength. The result of a single unzippng analysis is a failure mode whose strength or resistance is expressed as a linear combination of the strength of components which fail during the load incrementing process.

Consider the m th failure mode. For single load pattern, when j components r_1, $r_2, \ldots, r_j$ have failed and between each incremental stage the load is increased by increments $P_1, P_2, \ldots, P_j$, then the utilisation equation is expressed as[11,21,40]

$$\begin{Bmatrix} R_1 \\ R_2 \\ \cdot \\ \cdot \\ R_j \end{Bmatrix} = \begin{bmatrix} a_{11} & & & & \\ a_{21} & a_{22} & & & \\ \cdot & \cdot & \cdot & & \\ \cdot & \cdot & & \cdot & \\ a_{j1} & a_{j2} & \cdot & \cdot & a_{jj} \end{bmatrix} \begin{Bmatrix} P_1 \\ P_2 \\ \cdot \\ \cdot \\ P_j \end{Bmatrix} \qquad (2.63)$$

where the element a_{ki} is referred to as the utilisation ratio and is defined as the proportion of strength of component k utilised in the i th load increment, which represents the relationship between component strength and load increment and may be a stress in some cases or even a more complex expression such as the interaction formula for combined loading. R_k is the strength of the failed component, r_k, and P_k is the load increment to fail the component r_k. In matrix form:

$$\{R_e\} = [a]\ \{P\} \tag{2.64}$$

where matrix [a] is the utilisation matrix and is a triangular matrix of which all elements in the upper triangle are zero, and $\{R_e\}$ and $\{P\}$ are the resistance vector of which elements are the strength of failed components and the load increment vector respectively.
The load increment vector is obtained by solving Eq.(2.64)

$$\{P\} = [P]^{-1}\ \{R_e\} \tag{2.65}$$

System resistance, R_{sys} is expressed as the sum of the load increments prior to failure:

$$\begin{aligned} R_{sys} &= P_1 + P_2 + \ldots + P_j \\ &= \sum_{k=1}^{j} C_k' R_k \end{aligned} \tag{2.66}$$

where C_k' is the sum of the k th column of $[a]^{-1}$

$$C_k' = \sum_{i=k}^{j} a_{ik}^{-1} \tag{2.67}$$

The system strength is then only a function of components which failed during the load incrementing process. The variance of the system resistance can be obtained by the first-order reliability concept with referring to Eq.(2.66). That is:

$$\sigma_{R_{sys}}^2 = \sum_{k=1}^{j} C_k'^2 \sigma_{R_k}^2 + \sum_{i=k} \sum C_i' C_k' \sigma_{R_i} \sigma_{R_k} \rho_{ki} \qquad (2.68)$$

where σ_{R_k} is the standard deviation of the strength of component r_k and ρ_{ki} is the correlation between component r_k and r_i.

The safety margin of the system is the difference between the system resistance and the loading.

$$Z_m = R_{sys} - P = \sum_{k=1}^{j} C_k' R_k - P \qquad (2.69)$$

Then, the reliability index β_m of the m th failure mode is evaluated simply as

$$\beta_m = -\Phi^{-1}\{ P(Z_m < 0) \} \qquad (2.70)$$

where Φ is the standard normal distribution function.

When Eq.(2.69) is rewritten normalising by the final resistance coefficient C_j', the coefficient of R_j becomes a unit, i.e.:

$$C_j = 1.0 \qquad (2.71.a)$$

and other coefficients become:

$$C_k = C_k'/C_j', \qquad k=1, 2, ...,j-1 \qquad (2.71.b)$$

The coefficient of load P is $1.0/C_j$. Since the utilisation matrix is a triangular matrix, $C_j = 1.0/a_{jj}$ and the coefficient of load P becomes a_{jj}, i.e. equal to the utilisation due to unit load of P. Hence, the loading term becomes:

$$Q = -a_{jj} \cdot P \tag{2.71.c}$$

where Q simply denotes the loading term. Referring to Eqs.(2.71.a) - (2.71.c), the equation of the safety margin, therefore, can be rewritten as:

$$Z_m = \sum_{k=1}^{j} C_k R_k - a_{jj} P \tag{2.72}$$

where $C_j = 1.0$

For the system with components of semi-brittle or brittle behaviour the utilisation equation can be expressed as[44]:

$$[B]\,[R_e] = [a]\,\{P\} \tag{2.73}$$

where [B] is referred to as the "unloading matrix", which represents the unloading effects that failed components have on the remaining unfailed components in a structure and is also a triangular matrix of which all elements in the upper triangle are zero. When a component r_k has failed in a semi-brittle manner, the element B_{ki} represents an increase in utilisation of an unfailed component r_i due to a unit reduction in strength of component r_k. Let the residual strength parameter of component r_k be η_k [see Fig. 1.1.(a)], and the increase in utilisation of unfailed component r_i due to the unloading of component r_k be S_{ki}, then the element B_{ki} becomes

$$B_{ki} = -(1 - \eta_k)\, S_{ki} \tag{2.74}$$

and the diagonal elements are unit, B_{ii} (i = 1, j). For ductile systems there is no unloading process, so [B] = [I].

The load increment vector is obtained from Eq.(2.73) as follows.

$$\{P\} = [a]^{-1} [B] \{R_e\} \tag{2.75}$$

The next procedures are the same as before.

2.3.2 Element Replacement Method

In this method after each componential failure, the structural stiffness is locally modified and the residual strength of failed components is accounted for by applying the artificial (or equivalent) nodal forces on the structure.

For illustration, consider a frame structure with n members and L loads applied to its nodes. Both ends of a member are expected to turn into hinges. Then, there are 2n possible hinges as components. The load effects of component k are written in the form:

$$S_k = \sum_{l=1}^{L} b_{kl} P_l \qquad (k = 1, 2, \ldots, 2n) \tag{2.76}$$

where P_l ($l = 1, L$) are the applied loads and b_{kl} the load effect coefficient of component k due to unit load of P_l. When a fully plastic moment capacity, R_k, is taken as the strength of component, k, the safety margin for this component is:

$$Z_k = R_k - S_k \tag{2.77}$$

When j components $r_1, r_2, \ldots, r_j$ have failed, the stiffness matrices of the associated members are replaced by the reduced ones and their residual strengths are applied to the nodes as artificial nodal forces. Then the load effects of unfailed component, k, can be obtained as the sum of those due to applied loads and those due to the artificial nodal forces.

$$S_{k\,(r_1, r_2, \ldots, r_j)} = \sum_{l=1}^{L} b_{kl}^{(j)} P_l - \sum_{i=1}^{j} a_{ki} R_i \tag{2.78}$$

where suffix $(r_1, r_2, \ldots, r_j)$ denotes a set of failed components arranged in the sequence of failure, and $b_{kl}^{(j)}$ represent the load effect coefficient due to applied loads when stiffness matrices of components, $r_1, r_2, \ldots, r_j$ are replaced by the reduced ones. Consequently the safety margin of the unfailed component, k, is given by:

$$Z_{k(r_1, r_2, \ldots, r_j)} = R_k - S_{k(r_1, r_2, \ldots, r_j)}$$

$$= R_k + \sum_{i=1}^{j} a_{ki} R_i - \sum_{l=1}^{L} b_{kl}^{(j)} P_l \qquad (2.79)$$

When failure of components, $r_1, r_2, \ldots, r_j$ results in the collapse of a structure, the reliability index of the mode is then given by:

$$\beta = -\Phi^{-1}\{ P(Z_{k(r_1, r_2, \ldots, r_j)} \leq 0) \} \qquad (2.80)$$

2.4 Present Approach

Up to the present, one of the important limitations of the approximate method which should be overcome is that the post-ultimate behaviour of a component might not be able to be considered realistically. As is well recognised, the post-ultimate behaviour of the failed components can greatly influence the system reliability.

In this section, the present system reliability analysis method, called the extended incremental load method, is introduced, which is an extended approach to the conventional incremental load method[11,21,40]. The basic idea of the present method is similar to the incremental load method. The present method primarily aims at extending the applicability of the conventional one to the multiple loading case, and also to more realistically taking into account the post-ultimate behaviour of the failed components, although not completely, using the concept of the load factor. The modified form of the safety margin equation is proposed to directly use the strength formulae in the system

analysis and to account for the randomness nature of the strength modelling parameter. The derivation of the reduced element stiffness matrix is described.

As described in Section 1.3.5 [see Table 1.1], the applicability of the conventional incremental load method is restricted to a single load pattern [scaled by a random load variable]. Moses and Rashedi[66] introduced its application to the multi-loading case for the ductile system, but the extension to the multi-loading case is based on incrementing one load and keeping the rest fixed to their final value. However, this is not consistent, i.e. all loads are incremented proportionally till failure, therefore, the validity of the formulation is not clear.

Since in the incremental load method the load factor up to any particular failure stage can be obtained, this factor may be used to predict the deformation of the failed component, in a general sense, based on the mean value of the load. Hence, it can be said that the incremental load method has potential to more realistically take into account the post-ultimate strength than other methods do to solve the limitation as mentioned above. If the incremental load method can be applied to the multiple loading case, it has the potential to evaluate the system reliability of a structure with complex components, such as floating offshore structures in which the post-ultimate behaviour of a component plays quite an important role. As will be discussed later, another shortcoming of the conventional incremental load method is that it usually cannot generate the most important failure modes.

In the incremental load method the utilisation ratio generally represents the relationship between component strength and load increments and may be a stress in some cases or even a more complex expression, such as the interaction formula for combined loading. The existing strength formula, developed for the principle components of offshore structure, such as column and pontoon, can be used for this purpose[9,113,118,119,128,160-162].

2.4.1 Extended Incremental Load Method

The procedure which derives the safety margin equation for the multi-loading case is similar to that of the single loading case in Section 2.3.1. In the present method the contribution factor defined below for each loading is introduced. Let L loading act on a structure in which j components $r_1, r_2, \ldots, r_j$ have failed. The utilisation equation for each loading may be expressed as Eq.(2.81) similar to the previous single loading case [see Eq.(2.63)]. For the l th loading:

$$\begin{Bmatrix} R_1 \\ R_2 \\ \cdot \\ \cdot \\ R_j \end{Bmatrix} = \begin{bmatrix} a_{11}^{(l)} & & & & \\ a_{21}^{(l)} & a_{22}^{(l)} & & & \\ \cdot & \cdot & \cdot & & \\ \cdot & \cdot & & \cdot & \\ a_{j1}^{(l)} & a_{j2}^{(l)} & \cdot & \cdot & a_{jj}^{(l)} \end{bmatrix} \begin{Bmatrix} P_1^{(l)} \\ P_2^{(l)} \\ \cdot \\ \cdot \\ P_j^{(l)} \end{Bmatrix} \qquad (2.81)$$

or simply

$$\{R_e\} = [a^{(l)}]\,\{P^{(l)}\} \qquad (2.82)$$

In this equation the superscript (l) represents the term related to the l th loading case. After solving Eq.(2.82) for the load increment vector, $\{P^{(l)}\}$, summing up each column of $[a^{(l)}]^{-1}$, and normalising the coefficient by the final one gives the resistance coefficients for l th loading case. The resistance coefficient $C_k^{(l)}$ corresponding to resistance R_k of component r_k for l th loading case is:

$$C_k^{(l)} = \sum_{i=1}^{j} \left(a_{ik}^{(l)^{-1}} / C_j^{\prime(l)} \right) \qquad , k = 1, 2, \ldots, j\text{-}1 \qquad (2.83.a)$$

and

$$C_j^{(l)} = 1.0 \qquad (2.83.b)$$

The index k (= 1, . . . , j) means the sequence of component failure.

The contribution of resistances of failed components for each loading case can be accounted for by introducing the contribution factor, CF. The contribution factor, $CF^{(l)}$ for the l th loading case is here defined as the relative proportion of utilisation of the j th component r_j (the last failed component) for all loading cases. Then, resultant resistance coefficients for all loadings are obtained by summing up the resistance coefficients for each loading multiplied by the corresponding contribution factor, i.e., the resultant resistance term is expressed as the sum of contributions of resistance for each loading case to the system resistance.

$$C_k = \sum_{l=1}^{L} C_k^{(l)} \cdot CF^{(l)} \qquad , k = 1, 2, \ldots, j\text{-}1 \tag{2.84.a}$$

with the contribution factor, $CF^{(l)}$ defined as:

$$CF^{(l)} = \frac{a_{jj}^{(l)}}{\sum_{l'=1}^{L} |a_{jj}^{(l')}|} \tag{2.84.b}$$

Hence, the resistance term in the equation of safety margin, i.e. system resistance, can be expressed as:

$$R_{sys} = C_1 R_1 + C_2 R_2 + \ldots + C_j R_j \tag{2.85.a}$$

where C_j is unity.

Referring to Eq.(2.71.c), the loading term can be easily obtained as the sum of the product of the utilisation ratio, $a_{jj}^{(l)}$ and load, $P^{(l)}$.

$$Q = -\left(a_{jj}^{(1)} P^{(1)} + a_{jj}^{(2)} P^{(2)} + \ldots + a_{jj}^{(l)} P^{(l)} \right) \qquad (2.85.b)$$

where Q simply denotes the loading term. With Eq.(2.85.a) and (2.85.b), the equation of safety margin for the m th failure mode becomes:

$$Z_m = R_{sys} - Q = \sum_{k=1}^{j} C_{mk} R_k - \sum_{l=1}^{L} B_{ml} P^{(l)} \qquad (2.86)$$

where C_{mk} and B_{ml} are resistance and loading coefficients for m th failure mode respectively, and $B_{ml} = a_{jj}^{(l)}$. This equation is the same as Eq.(2.1), except that the superscript appears in the loading term.

When using the incremental load method, summing up all elements of the inverse of utilisation matrix results in the load factor up to any particular failure stage. This concept can be extended to compute the load factor at any incremental stage and then to determine the strain of failed component in the mean sense under the multiple loading. In Eq.(2.81) an element of utilisation matrix is the utilised proportion of a component strength at a particular incremental stage due to unit load , $P^{(l)} = 1.0$. When the mean values of the applied loads are substituted the element of utilisation matrix represents the mean utilisation for each loading case. Hence, the total mean utilisation is simply the sum of the mean utilisation for each loading case.

Let $\lambda_1, \lambda_2, \ldots, \lambda_j$, be mean load factors corresponding to incremental stages. Then, the utilisation equation for the mean load may be expressed as

$$\begin{Bmatrix} R_1 \\ R_2 \\ \cdot \\ \cdot \\ R_j \end{Bmatrix} = \begin{bmatrix} A_{11} & & & & \\ A_{21} & A_{22} & & & \\ \cdot & \cdot & \cdot & & \\ \cdot & \cdot & & \cdot & \\ A_{j1} & A_{j2} & \cdot & \cdot & A_{jj} \end{bmatrix} \begin{Bmatrix} \lambda_1 \\ \lambda_2 \\ \cdot \\ \cdot \\ \lambda_j \end{Bmatrix} \qquad (2.87)$$

or simply:

$$\{R_e\} = [A]\{\Lambda\} \tag{2.88}$$

where A_{ki} is the total mean utilisation given as:

$$A_{ki} = \sum_{i=1}^{L} a_{ki}^{(l)} \underline{P}^{(l)} \tag{2.89}$$

and $\underline{P}^{(l)}$ is the mean value of load $P^{(l)}$. By inverting Eq.(2.88), the vector of the mean load factors for load increments can be obtained.

$$\{\lambda\} = [A]^{-1}\{R_e\} \tag{2.90}$$

The deformation of already failed component r_i (i = 1, 2, . . .,j-1) up to the previous stage are determined in the mean value sense. At the j th failure stage (the present failure stage) when component r_j has failed, the mean load factor, λ_j is calculated from Eq.(2.90). Let $\Delta\varepsilon_{r_i}^{(l)}$ be the strain increment due to unit value of load $P^{(l)}$ of component r_i , then the mean strain increment of the failed component r_i becomes:

$$\sum_{l=1}^{L} \Delta\varepsilon_{r_i}^{(l)} . \underline{P}^{(l)}, \qquad i = 1, 2, \ldots, j-1 \tag{2.91}$$

Since the load factor of the present stage is λ_j, the mean strain increment of component r_i at the present stage becomes:

$$(\Delta\varepsilon_{r_i})_j = \lambda_j \sum_{l=1}^{L} \Delta\varepsilon_{r_i}^{(l)} \underline{P}^{(l)} \tag{2.92}$$

Hence, the total strain up to the present stage is

$$(\varepsilon_{r_i})_j = (\varepsilon_{r_i})_{j-1} + (\Delta\varepsilon_{r_i})_j \qquad (2.93)$$

where $(\varepsilon_{r_i})_{j-1}$ is the strain state of component r_i up to the previous incremental stage. Strains of the components are normalised by the strain at the ultimate state, ε_u, i.e.:

$$(\varepsilon_{r_i}')_j = \frac{(\varepsilon_{r_i})_j}{\varepsilon_u} \qquad (2.94)$$

Referring to the normalised strain state calculated from Eq.(2.94), the strain state of each failed component up to the present incremental stage can be calculated and at this point the corresponding tangential stiffness (non-dimensional) of components can be obtained from the stress-strain curve. For example, in Fig.1.1(b) the tangential stiffness of component r_i is

E_2' when $\varepsilon_1 < (\varepsilon_{r_i})_j' < \varepsilon_2$

or

E_3' when $\varepsilon_2 < (\varepsilon_{r_i})_j' < \varepsilon_3$

or

E_4' when $\varepsilon_3 < (\varepsilon_{r_i})_j'$

The procedure described above may is one possible approach to more realistically consider the post-ultimate behaviour (post-failure behaviour) of a failed component even for the structure under multiple loading. Since the above procedure of determining the strain state of failed component is based on the mean load value and strain state of failed component is predicted at each incremental stage, i.e. at the failure stage of each component, when the tangential stiffness abruptly varies, e.g. from E_2' to E_3', or from E_3' to E_4' in Fig.1.1(b), its effect cannot be precisely taken into account because of the finite size of the strain increments. This is a small limitations of all piecewise linear procedure.

If collapse of a structure occurs when j components $r_1, r_2, \ldots, r_j$ have failed, the total load factor, λ_T is given as the sum of all load factors, i.e. :

$$\lambda_T = \sum_{i=1}^{j} \lambda_i \tag{2.95}$$

where elements of λ_i are calculated from Eq.(2.90). Since when using the interaction equation under the multiple load effects, the elements of utilisation matrix in Eq.(2.81) and the elements of total mean utilisation matrix in Eq.(2.87) are non-dimensional, λ_T represents the ratio of the load at collapse to the applied load.

2.4.2 Modified Safety Margin Equation

As described in the previous section, the utilisation ratio represents the utilised proportion of a component strength, and this can be obtained by using the complex strength formula. For a simple case, when there are only two random variables for component k, say, strength R_k as a resistance variable and load effect, Q_k, as a loading variable, the safety margin or limit state equation is given by [note: subscript k does not denote the characteristic value]:

$$Z_k(X_M, R, Q) = X_{M_k} R_k - Q_k \tag{2.96.a}$$

where X_{M_k} is commonly known as the modelling parameter (or modelling error) for the strength of component k and defined as[2]:

$$X_M = \frac{\text{actual behaviour}}{\text{predicted behaviour}} \tag{2.97}$$

which represents the subjective uncertainty of the strength model in the reliability analysis[8,13,163]. Mean of X_M is referred to as the bias, $\underline{X}_M$, and when there is sufficient data the random component of X_M is usually referred to as the modelling

uncertainty specified by its coefficient of variation, V_{X_M}, which should be no greater than 13% for a good strength model[163].

Faulkner et al[119,163] recommended the following statistical requirements related to the modelling error:

[1] The mean bias, $\underline{X}_M$, should be close to unity and should be within about +5% to -5%

[2] The modelling uncertainty, V_{X_M}, should be kept as low as possible and overall value of about 13% should be achievable for ultimate strength equations for most components.

[3] X_M should show low correlation with any basic design variables, that is, no skewness should be inherent in the strength model.

In Eq.(2.96.a), when a structure is under the multiple load effects, R_k can denote the reference strength of component k, e.g. ultimate axial compressive stress or ultimate radial pressure and Q_k the corresponding load effect, e.g. axial compressive stress or radial pressure. Dividing both sides of Eq.(2.96.a) by the component strength gives the alternative same safety margin without loss of any physical meaning. That is:

$$Z'_k(X_M, R, Q) = X_{M_k} - \frac{Q_k}{R_k} \tag{2.96.b}$$

in which Q_k/R_k implies the utilised proportion of component k as a loading variable in the safety margin. When using the Rackwitz-Fiessler algorithm[54], since the reliability index is invariant to the different limit state equations of the same problem, Eqs.(2.96.a) and (2.96.b) give the same reliability indices because of their same physical meanings.

In the case of multiple load effects, the safety margin for component k can be generally and conceptually expressed in the non-dimensional form as:

$$Z'_k(\{R\}, \{Q\}) = 1 - G(\{R\}_k, \{Q\}_l) \tag{2.98.a}$$

which is an interaction equation representing the failure surface [Fig. 2.4] and where $\{R\}_k$ denotes the resistance variable vector associated with the component strength, such as the geometric and material properties and $\{Q\}_l$ the loading variable vector associated with the load effects such as axial force and bending moments. As before, when the strength modelling parameter is introduced as another random variable, Eq.(2.98.a) can be rewritten as:

$$Z'_k(X_M,\{R\}, \{Q\}) = X_{M_k} - G(\{R\}_k, \{Q\}_l) \qquad (2.98.b)$$

The mean bias of X_{M_k} implies that the failure surface is to be shifted from the surface given by Eq.(2.98.a), and its COV the perturbation of the failure surface around the shifted one. For illustration, Fig. 2.4 shows two-dimensional failure surface. The strength modelling parameter may have to be treated as a random variable in strength. Because it differs, depending on the strength formula for a particular component type, and for the same type of strength formula it can be updated as experimental data are accumulated. These effects can be reflected by use of Eq.(2.98.b). Guenard et al[148] proposed the same idea with mean bias of X_M being hopefully close to unity and its probability density function representing the model uncertainty.

The reliability index is obtained from:

$$\beta = -\Phi^{-1}\{ F(X_M, \{R\}, \{Q\}) \leq 0 \} \qquad (2.99)$$

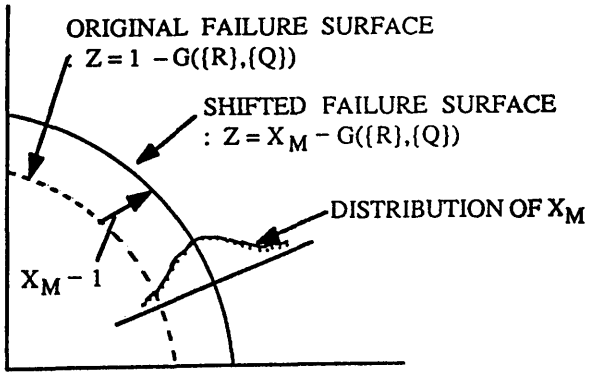

Fig. 2.4 Two-Dimensional Failure Surface

In order to use the strength formula for the present purpose, the safety margin equation given by Eq.(2.86), or Eq.(2.62) can be modified as follow to consider the effect of change in strength modelling parameter in system reliability analysis. Separating the resistance term of component r_j in Eq.(2.86), which is the last failed component, and considering that its coefficient is unity [see Eq.(2.71.a)]:

$$\begin{aligned} Z_m &= R_j + \sum_{k=1}^{j-1} C_{mk} R_k - \sum_{l=1}^{L} B_{ml} P^{(l)} \\ &= R_j - Q_j \end{aligned} \tag{2.100}$$

where Q_j is the load effect due to the already failed components, $r_1, r_2, \ldots, r_{j-1}$ and due to the loading acting on a structure:

$$Q_j = \sum_{l=1}^{L} B_{ml} P^{(l)} - \sum_{k=1}^{j-1} C_{mk} R_k \tag{2.101}$$

When introducing the strength modelling parameter of component r_j, X_{Mj}, Eq.(2.100) becomes [see Eq.(2.96.a)]:

$$Z_m = X_{M_j} R_j - Q_j$$

Dividing both sides of the above equation by R_j and re-substituting Eq.(2.101) can give the safety margin which has the same physical meaning as Eq.(2.86):

$$\begin{aligned} Z'_m &= X_{M_j} - \frac{Q_j}{R_j} \\ &= X_{M_j} + \sum_{k=1}^{j-1} C_{mk} \frac{R_k}{R_j} - \sum_{l=1}^{L} B_{ml} \frac{P^{(l)}}{R_j} \end{aligned} \tag{2.102}$$

Let $\{R\}_k$ and $\{Q\}_l$ be the resistance variable vector and the loading vector as before.

Then the first summation term in Eq.(2.102) can be regarded as a function of $\{R\}_k$, k=1, 2, . . . , j-1, and $\{R\}_j$, and the second term as a function of $\{Q\}_l$. Hence, with these the safety margin equation (2.86) can be conceptually modified in the non-dimensional form. That is, from Eq.(2.102):

$$Z'_m = X_{M_j} + \sum_{k=1}^{j-1} G_k(\{R\}_k, \{R\}_j) - \sum_{l=1}^{L} G_l(\{Q\}_l, \{R\}_j) \qquad (2.103)$$

where the first summation term is the contribution of the strength of the already failed components to the system safety margin and the second term is that of the loadings. The X_{M_j} denoted the strength modelling parameter of the j th component, r_j (last failed component) and $\{R\}_j$ the design variables of component, r_j , such as shell thickness, stiffener spacing, stiffener scantlings, yield stress, elastic modulus, etc. $\{R\}_k$ denote the design variables of already failed components, $r_1, r_2, \ldots, r_{j-1}$ and $\{Q\}_l$ the vector of load effects due to the l th loading. Function G_k and G_l show that they are associated with the strength of component r_k and with the l th loading case, respectively.

Since the function G is the interaction equation under multiple load effects, the elements of utilisation matrix in Eq.(2.81) represent the utilised proportion of the strengths of failed components when structural collapse occurs. Hence it can be said that expression of the safety margin equation as Eq.(2.103) is a feasible way to use the existing strength formula developed for the principle components in the system reliability analysis of a structure under multiple load effects and to take into account uncertainties of basic variables in strength and loading without loss of any physical meaning, and one possible way to flexibly evaluate the system reliability when the strength models are updated as more experimental data for components are accumulated. Each function G_k or G_l of Eq.(2.103) can be treated as a random variable and then its mean and variance can be easily obtained using the concept of the First-Order Second Moment Method. Doing this effectively represents the uncertainties in design variables to the safety margin. Let $\{X\}$ be a vector of the random variable representing the resistance and load effects, i.e.

$\{X\} = [X_M, \{R\}, \{Q\}]^T$, then the mean and the variance of function G_l (or G_k) are obtained from:

$$\underline{G_l} \cong G_l(\{\underline{X}\}) \tag{2.104.a}$$

$$\sigma^2_{G_l} \cong \sum_i \left\{\frac{dG_l}{dX_i}\right\}^2 \sigma^2_{X_i} + \sum_i \sum_j \left\{\frac{dG_l}{dX_i}\right\}\left\{\frac{dG_l}{dX_j}\right\}\sigma_{X_i}\sigma_{X_j}\rho_{ij} \tag{2.104.b}$$

where

$\{\underline{X}\}$ = the mean value vector of the random variable vector, $(\underline{X}_1, \underline{X}_2, \ldots, \underline{X}_i, \ldots)$

σ_{X_i} = the standard deviation of a random variable, X_i

ρ_{ij} = the correlation coefficient between X_i and X_j

and the terms in the brackets of Eq.(2.104.b) represent the partial derivatives of the function $G_l(\{X\})$ evaluated at the mean values of random variables. Due to the complex nature of the function $G_l(\{X\})$, its derivatives have to be determined numerically.

The detailed procedure of deriving the safety margin equation for a structure under multiple loading by the proposed method in this study is illustrated in Appendix-A for a portal frame model. The comparison of the results by safety margin equation (2.86) and its modified form, Eq.(2.103) is presented in Section 2.6.

2.4.3 Reduced Element Stiffness Matrix

For the structure analysis the structure is generally modelled as a finite element type space frame and the load effects such as axial force and bending moment, are calculated using the beam theory. A typical beam element is shown in Fig. 2.5. Both nodes of an element in Fig. 2.5 are expected to fail in the plastic hinge type when the load effects or their combined effect reach their capacities.

One of the problems in the system reliability analysis is to derive the reduced

stiffness matrix of an element after failure of its one or both nodes when the structure is under the multiple load effect. The strength formula Eq.(2.98.b) has usually the nonlinear interaction form, as described in section 1.3.4, and up to the present there is no way to consider the nonlinear interaction failure surface[88]. In this study, the concept of plasticity flow theory is used to derive the reduced stiffness matrix using the strength formula, generally given as Eq.(2.98.b).

When an element remains in an elastic state, i.e. no node fails, the relation between the nodal displacement and the nodal force vectors, {u} and {f} is given by

$$[k_0]\ \{u\} = \{f\} \tag{2.105}$$

where $[k_0]$ is the elastic stiffness matrix of an element.

Let $\{a_i\}$ and $\{a_j\}$ be the flow vectors for node i and j respectively, then the flow vector of an element is:

$$\{a\} = \begin{Bmatrix} \{a_i\} \\ \{a_j\} \end{Bmatrix} \tag{2.106}$$

and components of the flow vector of a failed element are given as the partial derivatives of the interaction equation (failure surface or limit surface equation, Fig. 2.4) with respect to nodal force vector:

$$a_k = \frac{dF}{df_k'} = \frac{dG}{df_k'} \tag{2.107}$$

where Z is the interaction equation, i.e. the strength formula and f_k' is the nodal force normalised by the ultimate strength corresponding to the associated load effects, e.g. the ultimate axial compressive stress or the ultimate bending moment when each load effect is

applied separately. The elements of flow vector are given as the partial derivatives of function G because the strength modelling parameter is not a function of nodal force.

The explicit form of the reduced stiffness matrix $[k_r]$, when one or both nodes of an element have failed, is given as follows:

[1] When one node, i, has failed:

$$[k_r] = [k_o] - \frac{[k_o]\{a_i\}\{a_i\}^T[k_o]}{\{a_i\}^T[k_o]\{a_i\}} \qquad (2.108)$$

[2] When both nodes, i and j, have failed:

$$[k_r] = [k_o] - [H]^T [G]^{-1} [H] \qquad (2.109)$$

where

$$[G_{ij}] = \{a_i\}^T [k_o] \{a_j\} \qquad [H_i] = \{a_i\}^T [k_o]$$

Using the above equations, the reduced stiffness matrix is obtained for each element and transformed with respect to the global co-ordinate system of structure. Then with this, the reduced total structural stiffness matrix is formed through the standard assembly procedure[164]. The required international forces or stresses are calculated with the reduced element stiffness matrix. Flow vectors are derived based on the strength formula and hence differ from the component types. These are illustrated in Appendix D.

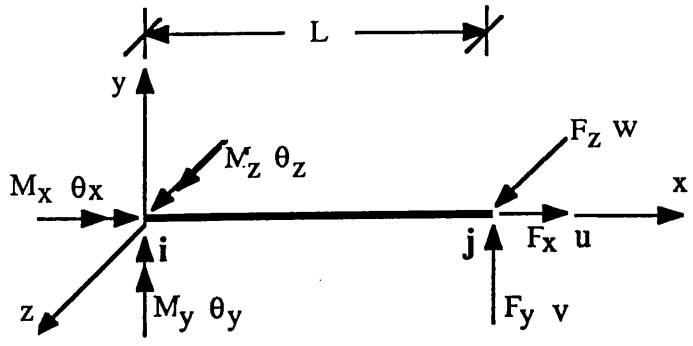

Fig. 2.5 Nodal Displacements and Nodal Forces of Beam Element

2.5 Procedures of Identifying the Most Important Failure Modes

When a structure is treated as a system, its failure should be seen as progressive collapse, or as a mechanism of successive failures of some of its components. Identification of the failure modes is selecting the failure modes and one of the most important parts of the failure path approach[11,13,88]. In a complex structure such as offshore platforms, the number of potential failure modes is usually very large. However, it is not practical to consider all possible failure modes to evaluate the probability of system failure. But, as is well recognised, only a few are important and dominant in evaluating the probability of system failure. Hence, a searching technique has to be used to identify the most important failure modes which have high probability of occurrence, i.e. low reliability indices.

The reason that the modes identified through searching techniques are termed as the "most important or most significant failure modes" is that, for a small structure, identifying the probabilistically (stochastically) most dominant failure modes may be possible but, for a large and complex structural system, it should be impossible to identify those that are "truly" probabilistically the most dominant ones due to the assumptions inevitably involved in a particular technique. Hence, they should possibly be termed as the "most important or most significant failure modes".

At present there are several procedures of identifying the most important failure modes[88]: Monte-Carlo simulation, Utilization ratio-based method, Marginal failure probability-based method, Truncated enumeration method and Branch and Bound method. These are described in this section.

2.5.1 Monte-Carlo Simulation[12]

Failure modes generated by this method may not be the most important ones, and this method usually requires much computational time. Because of this the method may be neither practical nor efficient for the practical problems.

2.5.2 Utilisation Ratio-Based Method

This procedure is based on the mean strengths of components and has been coupled with the incremental load method[11]. To identify the most important failure modes in this method the following deterministic criteria are used:

- component with the largest ratio of change of its utilisation is chosen as the best candidate for component failure.
- component for which the load factor is very large is ignored as a potential failure component.
- If two or more components have the same increase in utilisation ratio the one with the smallest load factor is a better candidate failure.

But the failure modes generated may not be the most important ones since, in identifying the failure modes, deterministic criteria mentioned above are used and the stochastic properties of random variables in resistance and load are not considered.

2.5.3 Marginal Failure Probability-Based method[13,42,43,165]

The idea of this method is that the candidate component chosen to fail is the one which has the highest marginal failure probability. A variation on this idea is that the candidate component chosen to fail is the one which is the last component of the failure path with the highest overall path failure probability rather than just the marginal probability of a component failure. Another variation of this method has been proposed in reference [165].

This procedure is divided into branching and bounding operations[42]. The branching operation is to select a component so that stochastically dominant failure modes may be obtained and based on the criterion that joint probability to fail is to be maximised. The bounding operation is to select the modes to be discarded and evaluate the contributions of the resulting failure modes.

This method and its variations probably generate important failure modes, but the order of failure probabilities of generated modes may not be obtained in decreasing order

of failure probabilities. It may be possible to overlook a mode in which the initial failure is less important but the latter failure is most important, i.e. more important failure modes may be ignored according to this procedure.

2.5.4 Truncated Enumeration Method[44]

This procedure has been proposed to iteratively determine the probabilistically dominant failure modes. By this procedure the probabilistically dominant failure modes can be derived from successive systematic curtailment of the results which would be obtained by complete enumeration within the accuracy of the criteria used for curtailment. But using this probably requires tremendous computational time since all potential sequences have to be exhausted.

2.5.5 Branch and Bounding Technique[39,156]

This method is a probabilistic search technique which has been used in the system reliability to obtain the most likely occurring sequences. Failure modes can be obtained in decreasing order of failure probability.

In this method the first step is to investigate the probability that a failure will occur in the intact structure. For each component r_j the probability, P_{f_j}, that component r_j fails in the intact structure is computed. Let component r_i be the component with the highest probability of failure. Hence, the damaged state associated with component r_i failed is the most likely to occur. Focus is now shifted to this damaged state. The next step is to investigate the probability of subsequent failures. The probability that a subsequent damaged state with component r_i and r_j ($r_i \neq r_j$) failed occurs is the probability of intersection of two events that component r_i fails in the intact structure and component r_j fails in a damaged structure with component r_i failed. Once this has been calculated for all surviving components, the focus shifts to the currently most likely damaged state. This could be either a damaged state with just one component failed (r_i) or a damaged state with two failed components (r_i and r_j). Subsequent failure in this most likely damaged state is investigated next. The procedure continues until the damaged state being focused

on results in collapse. The sequence of failures leading to this damaged state may be the most likely failure mode. This can be guaranteed because of the "look-back" feature in this algorithm. This procedure can be continued to generate other important failure modes.

2.5.6 Present Procedure

The identifying procedure in Sections 2.5.3.-2.5.5 are based on the purely stochastic criteria to generate the stochastically most important failure modes, whereas the procedure in Section 2.5.2 is based on the purely deterministic criteria, and hence, the results are the deterministically important ones. But one should not overlook the deterministically important modes although they are not always identical with the stochastically most important failure modes[166].

The present identifying procedure is primarily based on the stochastic criteria and aimed at reducing the computational time. The deterministic ones are also considered to identify the most important failure modes. The identifying procedure is composed of two procedures: Searching Procedure to select the most important failure modes and Discarding Procedure to discard the relatively less important modes in which similar deterministic criteria in reference [11] is employed [see Section 2.5.2].

[1] Searching Procedure

o Searching Procedure - 1:

At the first stage the failure probabilities of components failure are evaluated using the associated safety margins derived from results of structural analysis at the intact state. Then they are arranged in decreasing order of probability. As the first candidate component to fail, the component which has the highest probability of failure is chosen. When the component has failed, the stiffness matrix of the associated element is replaced by the reduced one [Section 2.4.3] and structural analysis is performed. Then the probabilities of failure of the remaining unfailed component are evaluated and arranged in the same way as before. Among these, the mode with the highest probability of failure is chosen (called PATH-A) as the best candidate interim mode. The last component of that

path is herein termed as the "focus component".

Among possible modes which are at the first failure stage, a searching procedure is performed to check if there is any mode which contains the focus component and which path probability is higher than that of PATH-A. The idea behind this is based on the fact that, as the number of failed components increases, the path failure probability usually decreases. If there is a mode of which failure probability is higher than that of PATH-A, the mode having the highest overall failure probability is selected (called PATH-B).

When these procedures are continued, the number of failed components contained in particular modes is different. During the searching procedure the focus component is selected in the modes which have the larger number of failed components, i.e. the modes to which structural failure is more progressed. At the current searching procedure PATH-A is generally the one which has the highest path failure probability among the modes having the largest number of failed components, which is denoted herein as N_{max}, i.e., N_{max} is the largest value of the numbers of failed components among all possible interim modes identified up to the current process. The value of N_{max} will be updated as the searching procedure is progressed.

PATH-B is the one which not only has the focus component as the last failed component, but also has the highest path failure probability among modes of which the number of failed components are less than N_{max}. If there is one or several modes, the one having the highest probability of failure among them is selected as the best candidate mode and focus is shifted to the mode. When there is no mode like that, PATH-A is selected.

o Searching Procedure - 2:

After passing through Searching Procedure-1, another procedure is introduced to check if there is any mode which is at the lower failure stage than PATH-A, i.e., of which the number of failed components is less than N_{max} has the higher path probability

than that of the mode selected before (PATH-A or PATH-B). If there are one or several modes to satisfy these condition, the one having the highest probability of failure among them is selected and focus is shifted to the mode. Otherwise PATH-A (or PATH-B) is selected as the most important interim mode (the best candidate mode) up to the present searching procedure. After then, probability of failure of the next component to fail is calculated for remaining survival components.

These procedure will be continued until collapse of structure occurs, which is defined as the occurence of singularity in the structural stiffness matrix, i.e.

$$\text{Det}\,[K] = 0 \tag{2.110}$$

where [K] is the total structural stiffness matrix at the current failure stage. Practically, the occurence of the structural collapse may be judged from

$$\frac{\text{Det}\,[K] \text{ of Current Failure State}}{\text{Det}\,[K] \text{ of Intact State}} \leq \varepsilon_{det} \tag{2.111}$$

where ε_{det} is the prescribed small number.

o Searching Procedure - 3:

In some cases the mode which is not selected as the best candidate interim mode can result in the structural collapse. Hence, one should check if such a mode exists among all the currently possible modes. But this causes a tremendous increase in computational time and a certain restriction may be necessary to save the computational time.

Let N_i be the number of failed components of mode i and N_{det} be the specified value to restrict the number of modes for determinant check. Then, the determinant check is restricted to the modes such that:

$$\frac{\text{Det}\,[K_i]}{\text{Det}\,[K_o]} \le \varepsilon_{det} \qquad \forall N_{max} > N_i \text{ and } (N_{det} < N_i) \tag{2.112}$$

where Det $[K_i]$ and Det $[K_o]$ are determinant of structural stiffness matrix for the i th failure mode and that of the intact structure. When $N_{det} = 1$, then the determinant check is carried out for all interim modes. While $N_{det} = N_{max}$, the determinant check is ignored.

From the author's experience, in the cases of simple structures as illustrated in the next section, the computational time for the above procedures is not a problem. But in the case of a large structure, the computational time is so great that it might not be practical to pass through all of the above procedures, especially Procedure - 3. In order to reduce computational time the following discarding procedures are introduced.

[2] Discarding Procedure

This procedure is to discard the relatively less important interim modes during the searching procedure from the deterministic and/or probabilistic sense.

o Discarding Procedure - 1:

Because the present method is based on the conventional incremental load method, deterministic discarding procedure can be carried out during formation of the utilisation matrix in such a way that the component having a very small utilisation or a very small change in the utilisation may be regarded as the less important one. Therefore, the associated mode may be discarded[11], i.e., at the first failure stage, when the utilisation of any component is less than a certain given value. The subsequent modes may be discarded or the interim mode of which the ratio of successive utilisation is very small, say, less than ε_{utr}, may be discarded because the mode can be regarded as a deterministically less important one.

o Discarding Procedure - 2:

When there are some interim modes progressed up to the specified failure stage (or level), searching procedure is restricted within the modes which satisfies the following conditions and others are discarded.

Let N_i be the number of failed components in mode i and N_{Limit} be an option variable which is used to discard the less important interim modes as below. During the searching procedure, when maximum of N_i for all interim modes is greater than N_{Limit}, the mode i of which N_i is less than N_{Limit} is discarded based on the assumption that the mode may be less important than the modes such that $N_{Limit} \leq N_i$. And so, the mode i such that $N_{Limit} \leq N_i$ is considered as a candidate mode in the searching procedure.

The above procedures, Searching Procedures and Discarding Procedures, are to be combined to generate the most important failure modes. Once a mode results in mechanism, the Discarding Procedure - 2 is applied and all procedures are to be continued to generate the next most important failure modes.

Every time the important failure mode is generated, the bounds of system failure probability (bounds of series system) are evaluated. According to the above identifying procedure failure modes are likely to be obtained in decreasing order of failure probability or, alternatively, in increasing order of corresponding reliability index, i.e.

$$P_{f_1} > P_{f_2} > \ldots > P_{f_m} > \ldots \tag{2.113.a}$$

or

$$\beta_1 < \beta_2 < \ldots. < \beta_m < \ldots \tag{2.113.b}$$

where P_{f_m} and β_m are the failure probability and the corresponding reliability index of the m th mode. As the number of failure modes identified increases the bounds of probability of the system failure $(P_f)_{sys}$ are expected to increase monotonically. In other words, the corresponding bounds of the system reliability index β_{sys} is expected to

monotonically decrease in such a way that:

$$(\beta_{sys,lower})1 > (\beta_{sys,lower})2 > \ldots > (\beta_{sys,lower})m > \ldots \qquad (2.114.a)$$

and

$$(\beta_{sys,upper})1 > (\beta_{sys,upper})2 > \ldots > (\beta_{sys,upper})m > \ldots \qquad (2.114.b)$$

Using this concept the searching procedure is terminated if the following criteria are satisfied, or if there is no more modes to be considered:

$$\frac{(\beta_{sys,lower})_{m-1} - (\beta_{sys,lower})_m}{(\beta_{sys,lower})_{m-1}} \leq \varepsilon_{sys} \qquad (2.115.a)$$

and

$$\frac{(\beta_{sys,upper})_{m-1} - (\beta_{sys,upper})_m}{(\beta_{sys,upper})_{m-1}} \leq \varepsilon_{sys} \qquad (2.115.b)$$

where

$(\beta_{sys,lower})m$, $(\beta_{sys,upper})m$ = lower and upper bound of system reliability index corresponding to bounds of system failure probability up to the present searching stage.

$(\beta_{sys,lower})m-1$, $(\beta_{sys,upper})m-1$ = lower and upper bound of system reliability index corresponding to bounds of system failure probability up to the previous searching stage.

ε_{sys} = prescribed small number for convergence checking of the system reliability

Sometimes it is possible for the identifying procedure to terminate just after

generating the first two modes, when the conditions of Eq.(2.115) are satisfied, even though the modes to be followed can possibly affect the bounds of β_{sys} such that Eq.(2.115) is not satisfied. For illustration, let β_1 and β_2 be the path reliability indices of the first two modes and be closely correlated positively such that $\rho_{12} \cong 1.0$. When the first mode (Mode 1) is generated, bounds of β_{sys} are equal to β_1, i.e.:

$$(\beta_{sys,lower})1 = (\beta_{sys,upper})1 = \beta_1 \tag{2.116}$$

When the second mode (Mode 2) is generated and $\beta_1 << \beta_2$, then the joint probability between Mode 1 and Mode 2 are approximated from Eq.(2.46):

$$P_{12} = \Phi(-\beta_1)\,\Phi(-\beta_2) + \int_0^{\rho_{12}} \phi_2(-\beta_1, -\beta_2 ; r)\, dr \cong \Phi(-\beta_2) \tag{2.117}$$

i.e. the joint probability is nearly the same as the probability of the second mode. For example, when ρ_{12} is 0.8 and 0.9, the reliability index β_{12} corresponding to the joint probability, P_{12} for several combinations of β_1 and β_2 are listed in Table 2.1.

Table 2.1 $\beta_{12} = -\Phi^{-1}(\Phi_2(-\beta_1, -\beta_2 ; \rho_{12})$

β_2 \ ρ_{12} / β_1	0.80		0.85		0.90		0.95	
	2.50	3.00	2.50	3.00	2.50	3.00	2.50	3.00
3.50	3.56	3.68	3.53	3.62	3.51	3.57	3.50	3.52
4.00	4.02	4.07	4.01	4.04	4.00	4.01	4.00	4.00
4.50	4.50	4.52	4.50	4.51	4.50	4.50	4.50	4.50
5.00	5.00	5.00	5.00	5.00	5.00	5.00	5.00	5.00
6.00	6.00	6.00	6.00	6.00	6.00	6.00	6.00	6.00

The upper and lower bounds may be approximated from the right hand side of Eqs.(2.42) and (2.43):

$$(P_f)_{sys,upper} = \sum_{i=1}^{2} P(E_i) - \sum_{i=2}^{2} \max_{j<i} P_{ij}$$

$$\cong \Phi(-\beta_1) - \Phi(-\beta_2)$$

$$\cong \Phi(-\beta_1) \qquad (2.118.a)$$

and

$$(P_f)_{sys,lower} = P(E_1) + \sum_{i=2}^{2} \max \left[0,\ P(E_i) - \sum_{j=1}^{i-1} P_{ij} \right]$$

$$= \Phi(-\beta_1) \qquad (2.118.b)$$

Hence, the bounds of system reliability index are:

$$(\beta_{sys,lower})_2 = (\beta_{sys,upper})_2 \cong -\Phi^{-1}\left(\Phi(-\beta_1)\right) = \beta_1 \qquad (2.119)$$

i.e. Eq.(2.115) can be satisfied just after the second mode is generated and the searching procedure is terminated at this stage. In order to avoid this phenomena and to check if the failure modes followed the second mode effect on the bounds of β_{sys}, the minimum number of required failure modes can be specified. Let this be M_{min}, then convergence check [Eq.(2.115)] is passed through when the number of identified failure modes, m, is greater than the minimum required number, i.e. when $M_{min} \leq m$.

The following summaries the parameters controlling the procedure of identifying the most important failure modes:

ε_{det} : Prescribed small number used to judge the singularity of the structural stiffness matrix from Eq.(2.111).

N_{max} : The maximum of the number of failed components for all possible interim modes.

N_{det} : The number to limit the number of interim modes of which determinants are to be checked from Eq.(2.112)]. The determinant check is restricted to the interim mode of which N_i are greater than N_{det} and less than N_{max}.
; when $N_{det} = 1$, check determinants of all possible interim modes
; when $N_{det} = N_{max}$, determinant check is not necessary.

ε_{utr} : Prescribed small number used to discard the mode when the ratio of two successively evaluated utilisations is less than given value for this.

N_{Limit} : The number to limit the number of interim modes to be considered as candidate ones in the searching procedure.
When number of failed components contained in any interim modes is less than the prescribed value for this parameter, the mode will be discarded, i.e. let N_i be the number of failed components in mode i. Then, when $N_i < N_{max}$, the mode will be discarded.
N_{max} is maximum of N_i for all interim modes.

ε_{sys} : Prescribed value used to check the convergence of bounds of system reliability indices [Eq.(2.115)]

M_{min} : The required minimum number of important failure modes to be identified

Theoretically, when $\varepsilon_{det} = 0.0$, $N_{det} = 1$, $\varepsilon_{utr} = 0.0$, $N_{Limit} = 1$, $\varepsilon_{sys} = 0.0$ and $M_{min} >> 1$, all possible failure modes can be identified.

In evaluating the bounds of a failure mode (bounds of a parallel system) and the bounds of the system failure probability (bounds of a series system), the narrow bounds are calculated[81].

The proposed identifying procedure may generate the most important failure from both the probabilistic and deterministic points of view. But, in fact, since specifying

certain values of parameters such as N_{det}, N_{Limit}, etc is inevitable for large and complex structural systems, the identified modes may not be the "truly" most important ones because the identified failure modes certainly depend on the parameters. Consequently, the system reliability must be dependent of the selected values of parameters. In spite of this the identified modes may be the "reasonably" most important ones. The present identifying procedure has a similar nature to the truncated enumeration method (TEM)[44] on one hand, and to the Branch and Bounding technique[39] on the other hand. The present procedure of identifying the important failure modes is detailed in Appendix C with the plane truss model in Section 2.6.1.

2.6 Applications to Discrete Structures

Two simple structures are selected to show the validity of the proposed method of deriving the safety margin equation of a structure under multiple loading and the procedure of identifying the most important failure modes to evaluate the structural system reliability.

2.6.1 Plane Truss Model

The plane truss model in Fig. 2.6[44] has 6 members as components and component failure is assumed to occur when the axial stress in a member reaches the yield stress. The same strength for compression and tension is assumed.

When both ε_{utr} used to discard the less important interim modes, ε_{sys} in Eq.(2.115) and $M_{min} >> 1$ in section 2.5.6 are small closing to zero, all possible failure modes can be generated. For a simple structure, like this model, prescribing the value of ε_{det}, N_{det} and N_{Limit} is meaningless. All possible failure modes of the truss example are illustrated in Table 2.2. The numbers in [ ] are path reliability indices (β_{path}) corresponding to their probabilities of failure. As seen in the table, failure modes are identified in decreasing order of failure probability and even in this simple structure we see the number of possible failure modes is not small. The upper bound of system

reliability index, β_{sys} does not vary after the second mode is generated. Among the possible modes when only the first four important failure modes are taken in evaluating the bounds of β_{sys}, neglecting the remaining 13 modes over-estimates the upper bound of β_{sys} by only 3.5%, which is the corresponding reliability index to the lower bound of the failure probability of system failure, $(P_f)_{sys,lower}$. This means that in practice only a few important failure modes are needed to estimate the bounds of the system reliability within reasonable level.

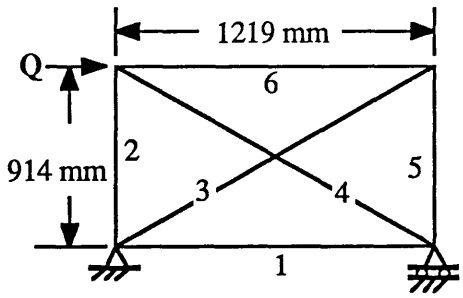

comp.	R_k	A_k
1, 2	36.708	133.0
3, 4	41.124	149.0
5, 6	36.708	133.0

A_k = Cross sectional area (m^2) $\quad$ $\underline{R}_k$ = Mean strength (= yielding axial force , kN)
E = 206,000 MPa $\quad$ COV of R_k = 0.1 $\quad$ COV of Q = 0.2

Fig. 2.6 Truss Model[44]

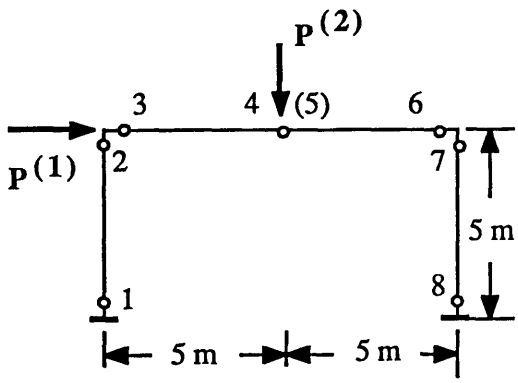

comp.	A_k	I_k	R_k
1, 2	4.0	3.58	0.075
3, 4	4.0	4.77	0.101
5, 6	4.0	4.77	0.101
7, 8	4.0	3.58	0.075

A_k = cross sectional area (m^2) $\quad$ I_k = moment of inertia (m^4)
mean yield stress = 276 MPa $\quad$ $\underline{R}_k$ = Mean strength (= plastic bending moment, MN)
$\underline{P}^{(1)}$ = 0.02 MN, $\underline{P}^{(2)}$ = 0.04 MN
COV of R_k = 0.05 $\quad$ COV of $P^{(1)}$ and $P^{(2)}$ = 0.3

Fig. 2.7 Frame Model[13]

Table 2.2 All Possible Failure Modes of Plane Truss Model

Mode No.	failed comp.	$(P_f)_{path}$ $[\beta_{path}]$	$(P_f)_{sys,upper}$ $[\beta_{sys,lower}]$	$(P_f)_{sys,lower}$ $[\beta_{sys,upper}]$
1	3, 4	0.122×10^{-1}[2.25]	0.122×10^{-1}[2.25]	0.122×10^{-1}[2.25]
2	4, 3	0.122×10^{-1}[2.25]	0.155×10^{-1}[2.16]	0.200×10^{-1}[2.06]
3	3, 1	0.580×10^{-2}[2.52]	0.155×10^{-1}[2.16]	0.223×10^{-1}[2.01]
4	4, 6	0.580×10^{-2}[2.52]	0.155×10^{-1}[2.16]	0.246×10^{-1}[1.97]
5	1, 3	0.334×10^{-2}[2.71]	0.155×10^{-1}[2.16]	0.260×10^{-1}[1.94]
6	6, 4	0.334×10^{-2}[2.71]	0.155×10^{-1}[2.16]	0.274×10^{-1}[1.92]
7	1, 6	0.170×10^{-2}[2.93]	0.155×10^{-1}[2.16]	0.281×10^{-1}[1.91]
8	6, 1	0.170×10^{-2}[2.93]	0.155×10^{-1}[2.16]	0.288×10^{-1}[1.90]
9	3, 2	0.225×10^{-3}[3.51]	0.155×10^{-1}[2.16]	0.288×10^{-1}[1.90]
10	4, 5	0.225×10^{-3}[3.51]	0.155×10^{-1}[2.16]	0.288×10^{-1}[1.90]
11	6, 2	0.641×10^{-4}[3.83]	0.155×10^{-1}[2.16]	0.288×10^{-1}[1.90]
12	1, 5	0.641×10^{-4}[3.83]	0.155×10^{-1}[2.16]	0.288×10^{-1}[1.90]
13	2, 3	0.199×10^{-4}[4.11]	0.155×10^{-1}[2.16]	0.288×10^{-1}[1.90]
14	5, 4	0.199×10^{-4}[4.11]	0.155×10^{-1}[2.16]	0.288×10^{-1}[1.90]
15	5, 1	0.125×10^{-4}[4.21]	0.155×10^{-1}[2.16]	0.288×10^{-1}[1.90]
16	2, 6	0.125×10^{-4}[4.21]	0.155×10^{-1}[2.16]	0.288×10^{-1}[1.90]
17	5, 2	0.644×10^{-6}[4.21]	0.155×10^{-1}[2.16]	0.288×10^{-1}[1.90]

2.6.2 Plane Frame Model

The plane frame model in Fig. 2.7[13] has 8 possible hinges as components. It is especially sensitive and has been frequently selected for evaluation of the system reliability and sensitivity analysis[17,42,76,165]. Component failure is assumed to occur when bending moment at a particular hinge reaches the plastic bending moment.

For this model the strength formula can be expressed in a simple form as

Eq.(2.120) [refer to Eq.(2.98.b)]. For component k:

$$Z'_k(X_M, \{R\}, \{Q\}) = X_{M_k} - \frac{Q_k}{R_k} \qquad (2.120)$$

where R_k is the plastic bending moment of component k as the strength and Q_k is the bending moment of component k due to loading as the load effect. X_{M_k} is its modelling error which is assumed to be deterministic having a mean value of 1.0 for all components, and all resistance and loading terms in the safety margin equation (2.103) are assumed to be normal.

For the parameters controlling the procedure of identifying the most important failure modes, $\varepsilon_{det} = 10^{-4}$, $N_{det} = N_{max}$, $\varepsilon_{utr} = 10^{-3}$, $\varepsilon_{sys} = 10^{-3}$ and $M_{min} = 8$ are given. The convergence condition is satisfied when 8 important modes are found. Fig.2.8 shows the failure states of the identified modes. Actually the number of all possible modes is very much larger. But, as seen in the figure, the reliability index of the 8th mode is 3.29, and so the remaining neglected failure modes are expected to be greater than this value and are unlikely to have much influence on the evaluation of the system reliability.

The first mode for path 4-7-8-2 is considered to illustrate the safety margin in the form of Eq.(2.103). In the proposed identifying procedure when a mode of failure has the close correlation (correlation coefficient between two modes $\cong 1.0$) as another mode already identified, this new mode is not presented. For example the modes for path 7-4-8-2, 7-4-2, 7-8-4-2 and 4-7-2 have close correlations as the first mode for path 4-7-8-2 and the safety margin equation of these five modes is the same as given by, in the form of the modified safety margin equation (2.103):

$$\begin{aligned} Z'_{4\text{-}7\text{-}8\text{-}2} &= X_{M_2} + 2.693\, R'_4 + 1.0\, R'_7 + 0.795 \times 10^{-6}\, R'_8 \\ &\quad - (0.715 \times 10^{-5}\, P^{(1)'} + 2.667\, P^{(2)'}) \\ &\cong X_{M_2} + 2.693\, R'_4 + 1.0\, R'_7 - 2.667\, P^{(2)'} \end{aligned} \qquad (2.121)$$

where X_{M_2} is the strength modelling parameter of component 2 with mean of unity and COV of 0.0 as assumed. R'_7 and R'_4 effectively represent the strength of components 7 and 4 with mean of unity and COV of 0.071. $P^{(1)'}$ and $P^{(2)'}$ effectively represent the loading $P^{(1)}$ and $P^{(2)}$ with mean of unity and COV of 0.304. These COVs are obtained by using the first-order reliability concept.

Details of deriving the safety margin equation are presented in Appendix-A. As seen in Eq.(2.121), for this failure mode the horizontal load $P^{(1)}$ and component 8 theoretically do not move or participate in the failure when the associated mechanism forms. But due to computational truncation errors very small coefficients do appear in Eq.(2.121). However, their effects on the safety margin and the safety level can be seen to be negligible. From Eq.(2.121) component 8 does not contribute to the safety margin, i.e. without it a collapse mechanism can be formed which is path 4-7-2. This is one of the failure modes having the same correlation as the mode for path 4-7-8-2. This component 8 at collapse is referred to as a non-active hinge, but before collapse it was being considered in the particular failure path being examined.

The results of the frame model are summarised in Table 2.3. The first three modes seem to be dominant in evaluating the bounds of β_{sys}. As described in Section 2.4.1, the total load factor, λ_T , defined as Eq.(2.95), may represent the reserve strength. The λ_T's , of the modes in Fig. 2.8 are also listed in Table 2.3. From the table it can be seen that within the identified modes the probabilistically most important mode is that for path 4-7-8-2, while the deterministically most important modes are the modes for path 4-8-7-1 and 8-4-7-1 although their path reliability indices (β_{path}) are about 18 % greater than that of the mode for path 4-7-8-2 and λ_T's of the modes for path 4-8-7-1 and 8-4-7-1 are about 5 % less than that of the mode for path 4-7-8-2. Whereas the mode for path 4-6-8-3 which has the highest β_{path} has λ_T of about 15% greater than that of the mode for path 4-7-8-2. The first three modes result in the same mechanisms, but although their λ_T's are same, they have different levels of β_{path}. This can be also applied for the 5th and the 6th modes and may be due to the different redistribution of load effects according to the different failure sequences. From this point it can said that the deterministically

important mode is not identical with the probabilistically important mode, i.e. the mode having the smallest λ_T does not give the lowest β_{path}.

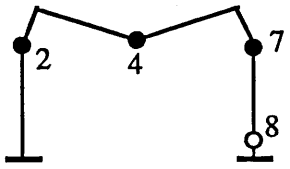

(1) $\beta_{4\text{-}7\text{-}8\text{-}2} = 2.46$
($P_f = 0.703 \times 10^{-2}$)

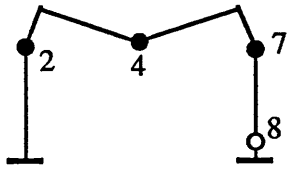

(2) $\beta_{8\text{-}4\text{-}7\text{-}2} = 2.49$
($P_f = 0.635 \times 10^{-2}$)

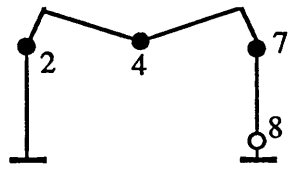

(3) $\beta_{4\text{-}8\text{-}7\text{-}2} = 2.56$
($P_f = 0.526 \times 10^{-2}$)

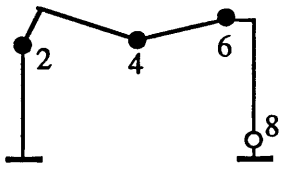

(4) $\beta_{4\text{-}6\text{-}8\text{-}2} = 2.87$
($P_f = 0.207 \times 10^{-2}$)

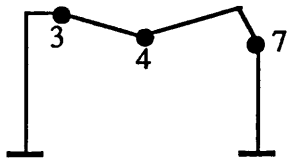

(5) $\beta_{7\text{-}4\text{-}3} = 2.88$
($P_f = 0.201 \times 10^{-2}$)

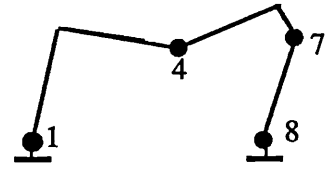

(6) $\beta_{4\text{-}8\text{-}7\text{-}1} = 2.88$
($P_f = 0197 \times 10^{-2}$)

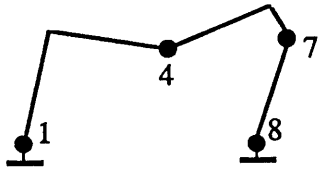

(7) $\beta_{8\text{-}4\text{-}7\text{-}1} = 2.90$
($P_f = 0.185 \times 10^{-2}$)

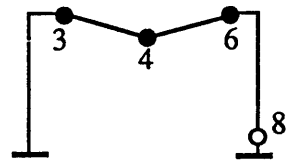

(8) $\beta_{4\text{-}6\text{-}8\text{-}3} = 3.29$
($P_f = 0.507 \times 10^{-3}$)

● : active hinge
o : non-active hinge

Fig. 2.8 Failure States of Important Failure Modes for Plane Frame Model

Table 2.3 Summary of Results for Frame Model

Mode No.	failure path	β_{path} $[(P_f)_{path}]$	total load factor, λ_T	$\beta_{sys,lower}$ $[(P_f)_{sys,upper}]$	$\beta_{sys,upper}$ $[(P_f)_{sys,lower}]$
1	4-7-8-2	2.46 $[0.703 \times 10^{-2}]$	1.76	2.46 $[0.703 \times 10^{-2}]$	2.46 $[0.703 \times 10^{-2}]$
2	8-4-7-2	2.49 $[0.635 \times 10^{-2}]$	1.76	2.22 $[0.134 \times 10^{-1}]$	2.22 $[0.134 \times 10^{-1}]$
3	4-8-7-2	2.56 $[0.526 \times 10^{-2}]$	1.76	2.12 $[0.171 \times 10^{-1}]$	2.15 $[0.157 \times 10^{-1}]$
4	4-6-8-2	2.87 $[0.207 \times 10^{-2}]$	1.89	2.12 $[0.171 \times 10^{-1}]$	2.15 $[0.157 \times 10^{-1}]$
5	7-4-3	2.88 $[0.201 \times 10^{-2}]$	1.89	2.12 $[0.171 \times 10^{-1}]$	2.15 $[0.157 \times 10^{-1}]$
6	4-8-7-1	2.88 $[0.197 \times 10^{-2}]$	1.67	2.10 $[0.178 \times 10^{-1}]$	2.15 $[0.157 \times 10^{-1}]$
7	8-4-7-1	2.90 $[0.185 \times 10^{-2}]$	1.67	2.10 $[0.178 \times 10^{-1}]$	2.15 $[0.157 \times 10^{-1}]$
8	4-6-8-3	3.29 $[0.507 \times 10^{-3}]$	2.02	2.10 $[0.178 \times 10^{-1}]$	2.15 $[0.157 \times 10^{-1}]$

Table 2.4 shows comparison of the results when using safety margin equations (2.86) and (2.103). The proposed equation (2.103) usually gives a lower reliability index than Eq.(2.86), but the difference is less than 1% and can be ignored.

Table 2.4 Comparison between Two Safety Margin Equations for the Frame Model

Failure Modes	7-4-2	7-4-8-2	7-4-3	7-4-8-3	7-4-8-1
by Eq. (2.86)	2.48	2.48	2.88	2.88	2.91
by Eq. (2.103)	2.46	2.46	2.88	2.88	2.90

2.6.3 Discussion

The results of two simple structural models justify the validity and the applicability of the present system reliability method of deriving the safety margin equation and the procedure of identifying the most important failure modes to evaluate the structural system reliability to a structure under multiple loading.

It was shown that identifying a small number of the most important failure modes could give reasonable and acceptable bounds of β_{SYS} from a practical point of view. In general using Eq.(2.103) as the safety margin equation may give a different path reliability index (or path failure probability), and consequently give a different system reliability index. But it can be said that using Eq.(2.103) is one possible way of directly using the strength formula in system reliability analysis. In addition, referring to the relation between the path reliability index and the total load factor, it was found that the deterministically important mode was not identical with the probabilistically important mode. Further discussion of this point will be made in Section 5.4.4.

CHAPTER 3 STRENGTH OF CONTINUOUS STRUCTURES

3.1 General

The principle components found in TLP or semi-submersible structures are ring-stiffened cylinders, ring- and stringer-stiffened cylinders and the rectangular box-girders as shown in Figs. 3.1 to 3.3. The experiences found in the structures indicated that, in general, under the given environmental condition the components were subjected to the combined action of axial force, bending moments, shear force and radial pressure due to hydrostatic and hydrodynamic actions and the primary load was axial compression.

In probability-based limit state design, it is necessary to use the strength models derived based on the limit state analysis. In this study strength models of cylindrical components, as in references [9] and [113], are used. The ultimate strength of axial compression and radial pressure is given. Interaction equations under the combined action of axial compression and radial pressure used in this study are presented. For rectangular box-girder the models proposed by the author[128] are used for the ultimate strength of axial compression, bending and their combined action and have been derived based on numerical analysis. Details of numerical results and derivation of strength models are presented.

3.2 Ring-Stiffened Cylinder

3.2.1 Axial Compression

Since shell element is very sensitive to initial imperfection, such as initial deflection (shape imperfection), adopting the notion of "knock-down" factor is inevitable.

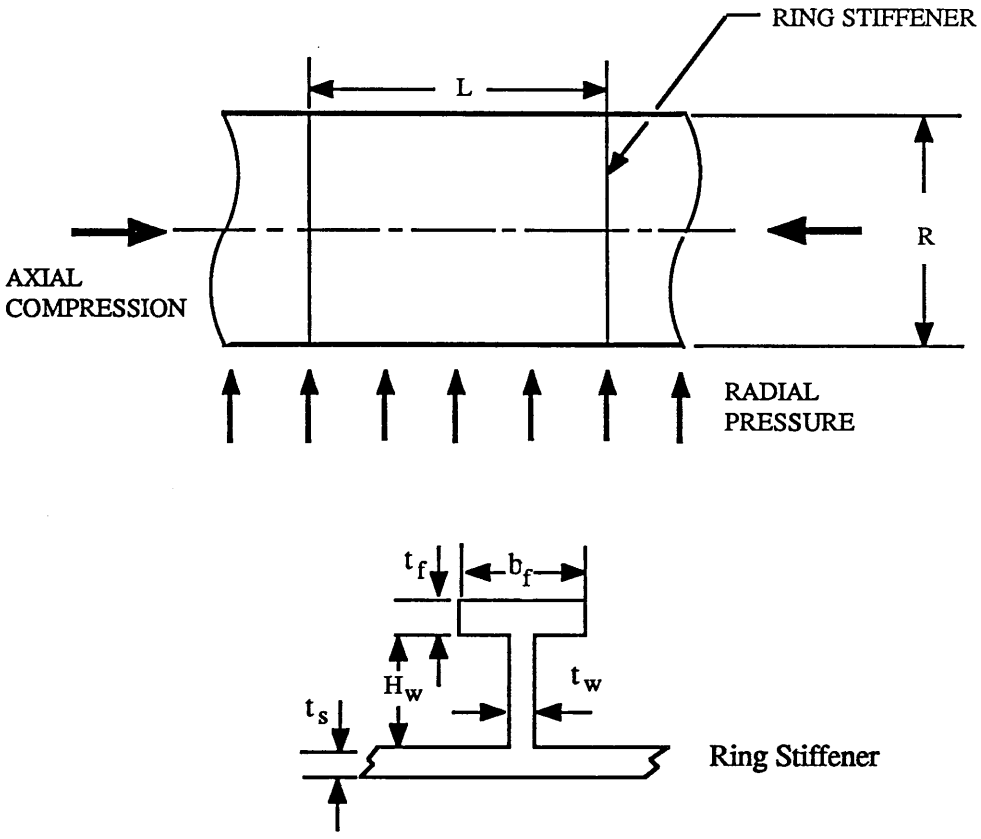

Fig. 3.1 Ring-Stiffened Cylinder

The mean ultimate compressive stress of ring-stiffened cylinder [Fig. 3.1], σ_{xu} is given in the form of DnV type[115].

$$\sigma_{xu} = \phi \sigma_Y \tag{3.1}$$

where

$$\phi = \sqrt{1 + \lambda_e^4}$$

$$\lambda_e = \sqrt{\frac{\sigma_Y}{\sigma_e}} \quad : \quad \text{slenderness parameter for the imperfect shell}$$

$$\sigma_e = \rho \sigma_i \quad : \quad \text{elastic buckling stress for the imperfect shell}$$

and σ_e is the expected (mean) elastic buckling stress given by:

$$\sigma_e = B\,\rho_n\,\sigma_i \qquad (3.2)$$

where B is a mean bias factor assessed from elastic test data which compensates for the lower bound nature of ρ_n.given by:

$$B = 1.2 \qquad \text{for } \lambda_n > 1.0$$

$$= 1.0 + 0.2\,\lambda_n \qquad \text{for } \lambda_n \le 1.0$$

$$\lambda_n = \sqrt{\frac{\sigma_Y}{\rho_n\,\sigma_i}}$$

ρ_n is the nominal or lower bound knock-down factor to allow for shape imperfections given by:

$$\rho_n = 0.75 - 0.46\left(\frac{Z-1}{19}\right)^{0.4} + 0.001\,Z\left(3 - \frac{\frac{R}{t}}{100}\right) \qquad \text{for } Z \le 20$$

$$= 0.35 - 0.0002\left(\frac{R}{t}\right) \qquad \text{for } Z > 20$$

σ_i is the elastic buckling stress for a perfect shell given by:

$$\sigma_i = C\,\sigma_{cr} \qquad (3.3)$$

where C is the length dependent elastic shell buckling coefficient given as:

$$C = 1.0 \qquad \text{for } Z > 2.85$$

$$C = \frac{\pi^2}{4\sqrt{3}}\frac{1}{Z} + \frac{\sqrt{3}}{\pi^2}Z \cong \frac{1.425}{Z} + 0.175\,Z \qquad \text{for } Z \le 2.85$$

and Z is the Batdorf length parameter given by

$$Z = \frac{L^2}{Rt}\sqrt{1-\nu^2} \qquad , L = \text{distance between ring frames}$$

The value of Z of 2.85 divides the short and moderate length cylinder. σ_{cr} is the classical buckling stress for a perfect thin cylinder from Donell's shell equation[167,168].

$$\sigma_{cr} = K_c \frac{\pi^2 E}{12(1-\nu^2)} \left(\frac{t}{L}\right)^2 \tag{3.4}$$

where K_c is a buckling coefficient given by:

$$K_c = \frac{4\sqrt{3}}{\pi^2} Z \cong 0.702\, Z \tag{3.5}$$

By substituting Eq.(3.5) in Eq.(3.4) with Poissons ratio ν of 0.3, σ_{cr} becomes:

$$\sigma_{cr} = 0.605 \frac{Et}{R} \tag{3.6}$$

3.2.2 Radial Pressure

The mean ultimate radial pressure, P_u, is approximately given by:

$$P_u = B\, P_Y \left(1 - 0.5 \frac{P_Y}{p_{rm}}\right) \qquad \text{for } \frac{p_{rm}}{P_Y} > 1.0$$

$$= B\, 0.5\, p_{rm} \qquad \text{for } \frac{p_{rm}}{P_Y} \leq 1.0 \tag{3.7}$$

where B is the mean bias factor of 1.17 to approximate the mean value of P_u and p_{rm} is

given by:

$$p_{rm} = \frac{p_m}{\sqrt{1 - 0.5\frac{p_m R}{t\sigma_e}}} \tag{3.8}$$

where p_m is the von Mises hydrostatic elastic buckling pressure given by:

$$p_m = \frac{0.919\,E\left(\frac{t}{R}\right)^2}{\frac{L}{\sqrt{Rt}} - 0.636} \tag{3.9}$$

and σ_e is given as Eq.(3.3). P_Y is the pressure when hoop stress reaches yield:

$$P_Y = \frac{\sigma_Y\left(\frac{t}{R}\right)}{1 - \gamma G} \tag{3.10}$$

where

$$\gamma = \frac{A\,(1 - 0.5\,v)}{(A + t_w t)\left[1 + \frac{2\,t\,N}{\alpha(A + t_w t)}\right]}$$

A is the effective area given by: as a function of stiffener area, A_{st}, and radius to centre of stiffener, R_{st}:

$$A = A_{st}\left[\frac{R}{R_{st}}\right]^2$$

and G is given by:

$$G = \frac{2\,(\sinh \alpha L/2 \cos \alpha L/2 + \cosh \alpha L/2 \sin \alpha L/2)}{\sinh \alpha L + \sin \alpha L}$$

$$\cong 1.0 \qquad \text{for } \alpha L \leq 1.6$$

$$= 1.60 - 0.37\,\alpha L \qquad \text{for } 1.6 < \alpha L \leq 4.4$$

$$= 0 \qquad \text{for } \alpha L > 4.4$$

$$\alpha L = \frac{1.285\,L}{\sqrt{R\,t}}$$

$$N = \frac{\cosh \alpha L - \cos \alpha L}{\sinh \alpha L + \sin \alpha L}$$

$$\cong 0.5\,\alpha L \qquad \text{for } \alpha L \leq 2.0$$

$$= 1.0 \qquad \text{for } \alpha L > 2.0$$

3.2.3 Combined Loading

The loading system of combined axial compression and radial pressure is most likely to occur in offshore structures. The interaction equation of the ring stiffened cylinder is given in a simple form[113]:

$$\left[\frac{P}{P_u}\right]^m + \left[\frac{\sigma_x}{\sigma_{xu}}\right]^n = 1 \qquad (3.11)$$

where P is the radial pressure, P_u is the ultimate radial pressure given as Eq.(3.7) and σ_x is the total axial stress resulting from both axial load, pressure and bending moments. This can be conservatively assessed by multiplying the resultant term by (2/R) to convert them to equivalent axial compression at the appropriate part of the section. The total axial stress is , therefore, given by:

$$\sigma_x = \sigma_{xa} + \frac{1}{A_T}\frac{2}{R}\sqrt{M_y^2 + M_z^2} \qquad (3.12)$$

where A_T is the total sectional area ($= 2\pi Rt$), and M_y and M_z are bending moments about y- and z-axis, respectively. σ_{xu} is the ultimate axial compressive stress given as Eq.(3.1). In the above equation, m = 2 and n = 1 are used in this study.

When a cylinder is generally subjected to the combined action of axial compression, radial pressure and torsion, an alternative form of the interaction equation has been derived by Odland and Faulkner[160] which was based on the Odland approach[169], and has the following quadratic form:

$$\left[\frac{\sigma_{xo}}{\sigma_{Ex}} + \frac{\sigma_{\theta o}}{\sigma_{E\theta}} + \frac{\tau}{\tau_E}\right]^2 + \left[\frac{\sigma_{eff}}{\sigma_Y}\right]^2 = 1 \qquad (3.13.a)$$

where σ_{Ex}, $\sigma_{E\theta}$ and τ_E are the elastic buckling stress of imperfect shell for single actions given by:

$$\sigma_{Ex} = \rho_x \sigma_{xcr} \qquad \sigma_{E\theta} = \rho_\theta \sigma_{\theta cr} \qquad \tau_E = \rho_\tau \tau_{cr} \qquad (3.13.b)$$

and ρ's are shape knock-down factors. The corresponding reduced slenderness is defined by:

$$\lambda_x^2 = \frac{\sigma_y}{\sigma_{Ex}} \quad , \quad \lambda_\theta^2 = \frac{\sigma_y}{\sigma_{E\theta}} \quad , \quad \lambda_{x\theta}^2 = \frac{\sigma_y}{\sqrt{3}\,\tau_E} \qquad (3.13.c)$$

σ_{eff} is the actual value of the effective stress according to the von Mises yield criterion defined as:

$$\sigma_{eff} = \sqrt{\sigma_x^2 + \sigma_\theta^2 - \sigma_x\sigma_\theta + 3\tau^2} \qquad (3.14)$$

and σ_{Ex}, $\sigma_{E\theta}$ and τ_E are the elastic buckling stresses for each individual action. τ is the shear stress due to torsion, σ_{xo} is axial stress given by:

$$\begin{aligned} \sigma_{xo} &= -\sigma_x && \text{for } \sigma_x \le 0 \\ &= 0 && \text{for } \sigma_x \le 0 \end{aligned} \qquad (3.15)$$

and $\sigma_{\theta o}$ is hoop stress due to radial pressure, P, given by:

$$\begin{aligned} \sigma_{\theta o} &= -\sigma_\theta && \text{for } \sigma_\theta \le 0 \\ &= 0 && \text{for } \sigma_\theta \le 0 \end{aligned} \qquad (3.16)$$

and

$$\sigma_\theta = \frac{P R}{t}$$

Later Frieze et al[170,171] proposed a modified form of Eq.(3.13) excluding the torsion term and adopting the knock-down factor for each action to account for the inelastic behaviour. That is:

$$\left[\frac{\sigma_{xo}}{\rho_x \sigma_{xcr}} + \frac{\sigma_{\theta o}}{\rho_\theta \sigma_{\theta cr}}\right]^2 + \left[\frac{\sigma_{eff}}{\sigma_Y}\right]^2 = 1 \qquad (3.17)$$

where σ_{eff}, σ_{xo} and $\sigma_{\theta o}$ are defined as Eqs.(3.14) - (3.16). σ_{xcr} is the critical elastic axial stress given as Eq.(3.4) and $\sigma_{\theta cr}$ the critical elastic hoop stress given by:

$$\sigma_{\theta cr} = K_c \frac{\pi^2 E}{12(1-\nu^2)} \left(\frac{t}{L}\right)^2 \qquad (3.18)$$

where K_c is the buckling coefficient given by:

$$K_c = 1.038\sqrt{Z} \qquad \text{for } Z \leq 100 : \text{moderate length cylinder}$$

$$= \frac{4}{\pi^2\sqrt{1-\nu^2}} Z\left(\frac{t}{R}\right) \qquad \text{for } Z > 100 : \text{long cylinder}$$

ρ_x and ρ_θ are the elasto-plastic knock-down factors derived to best fit the test data. These are:

$$\rho_x = 0.281 + 19.2\left[\sqrt{Z}\,\frac{E}{\sigma_Y}\right]^{-0.518}$$

$$= 0.833 + 3510\left[\sqrt{Z}\,\frac{E}{\sigma_Y}\right]^{-1.13} \qquad (3.19)$$

The quadratic interaction between yielding and elastic buckling may not always be applicable throughout the complete interaction range and it does not explicitly account for residual stress. However, Eq.(3.13) or (3.17) has a simple form with three advantages:

[1] The failure criterion approaches linear interaction for very slender structures

[2] It approaches the von Mises yield criterion for extremely stocky structure

[3] It can account for the effect of tensile stresses.

3.3 Ring- and Stringer-Stiffened Cylinder

3.3.1 Axial Compression

When ring- and stringer-stiffened cylinders [Fig. 3.2] are subjected to axial compression, the main collapse modes which may occur singly or in combination are:

[1] Local shell element buckling

[2] Interframe column buckling which is the stringer-shell buckling batween ring frames

[3] General instability, in which both stringers and ring frames buckle together

[4] local torsional buckling of stringers and/or ring frames

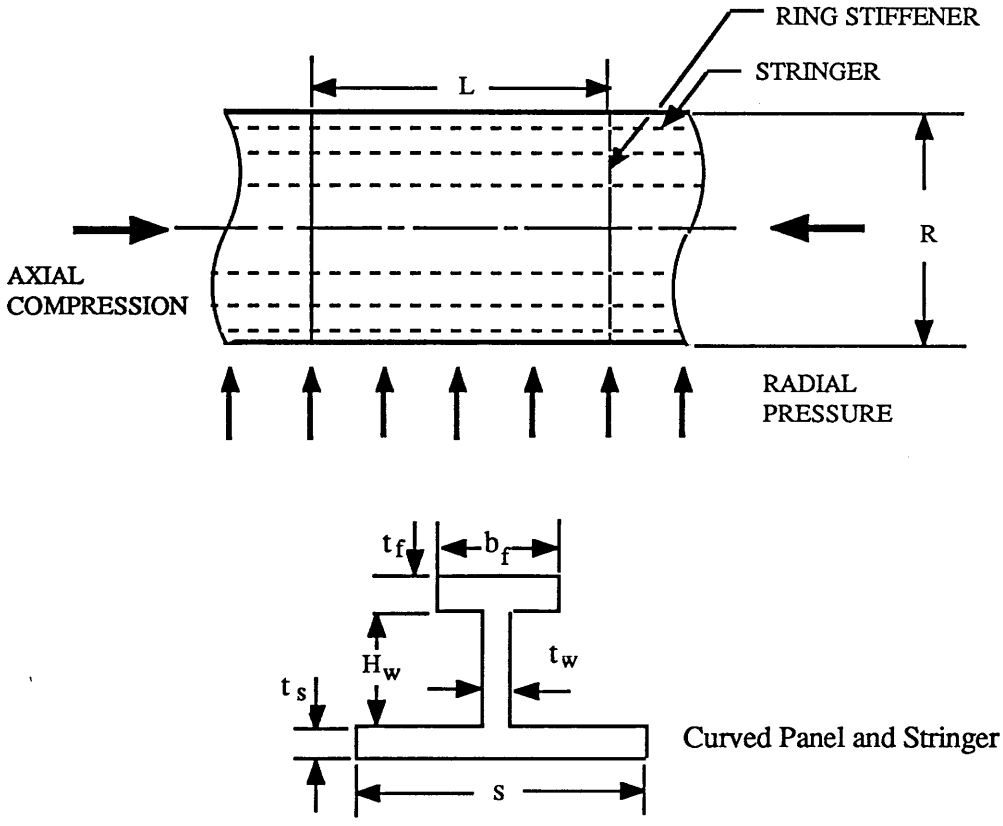

Fig. 3.2 Ring- and Stringer-Stiffened Cylinder

Local shell element buckling is excluded from collapse because generally for the cylinder with low slenderness ratio, s/t, in which s is the spacing of stringers, the initial post-buckling behaviour is stable as for rectangular plates as long as the stringers provide the straight boundaries. For the cylinder with higher slenderness ratios the post-buckling behaviour becomes very sensitive to geometric imperfection. However, this is essentially allowed for by the much lower knock-down factors which then apply.

In design the general instability is precluded by conservative proportioning of the ring frames, i.e. they are assumed to provide rigid pin supports. This assumption implies that the ring frames have sufficient in-plane bending rigidity so that they do not participate

in the collapse process. Local buckling of stringer, i.e. tripping, can also be excluded by appropriately proportioning the stiffener size. Consequently the formulation recommended for a stringer-stiffened cylinder is equally applicable to ring- and stringer-stiffened cylinders.

There are generally three approaches in design formulation of stringer-stiffened cylinders subjected to axial compression: Column analysis ignoring curvature effect (DnV, 1977), Orthotropic curved shell and Discrete stiffener shell analysis allowing curvature (ECCS). The orthotropic shell approach works well for a shell with a densely spaced stringer, such as those found in aerospace structures, but may not be so suitable for marine structures in which stringers are less densely spaced. Model test data indicate that the discrete stiffener-shell analysis offers great promise and yet is much simpler than the orthotropic shell approach. The effective width type approach used to define the behaviour of a flat panel can, therefore, be adopted for stringer-stiffened curved panels[9,113,162].

Ultimate axial compressive stress σ_{xu} is given by:

$$\sigma_{xu} = \sigma_{ic} \frac{N (A_{st} + s_e t)}{A_T} \qquad (3.20.a)$$

where N is the number of stringers, A_{st} denotes the actual sectional area of one stringer [Fig. 3.2]:

$$A_{st} = h_w t_w + b_f t_f$$

s_e is the effective width defined below, t is shell thickness and A_T is the total sectional area including shell and stringers:

$$A_T = 2\pi Rt + NA_{st} = N A_s (1 + \gamma) \qquad (3.21)$$

where $A_S = st$: shell area between stringers and $\gamma = A_{st} / A_S$: area ratio of stringer to shell. s is the curved panel width between stringers :

$$s = \frac{2\pi R}{N} \tag{3.22}$$

Using notation γ, Eq.(3.20.a) is rewritten as:

$$\sigma_{xu} = \sigma_{ic} \frac{(\gamma + \frac{s_e}{s})}{(1+\gamma)} \tag{3.20.b}$$

σ_{ic} is the inelastic collapse stress derived using the Ostenfield-Bleich expression for tangent modulus and given by:

$$\sigma_{ic} = \sigma_Y \left[1 - \frac{p_s (1-p_s)}{\psi} \right] \qquad \text{for } \psi > p_s$$

$$= \psi \qquad \text{for } \psi \le p_s \tag{3.23}$$

in which p_S is the ratio of the structural proportional limit to yield stress and a value of 0.75 is recommended for stress-relieved structure, i.e. $\eta = 0.0$ in which η is the welding tension block parameter [see Fig. 2.4]. Otherwise $p_S = 0.5$. ψ is the imperfect elastic buckling parameter defined by:

$$\psi = \frac{\sigma_{ie}}{\sigma_Y} \tag{3.24}$$

where σ_{ie} is the elastic collapse stress composed of two parts as:

$$\sigma_{ie} = \sigma_C + \sigma_S \tag{3.25}$$

where σ_c and σ_s are simply the column (Euler) buckling stress of stringer and that of the thin shell buckling stress, which can be calculated separately as follow:

o Shell Buckling Stress:

The shell buckling stress, σ_s is given by:

$$\sigma_s = \rho_s \left[0.605 \frac{Et}{R} \left(\frac{1}{1+\gamma} \right) \right] \tag{3.26}$$

in which the term in [ ] is the elastic critical stress of perfect shell, and ρ_s the mean shell knock-down factor due to shape imperfection and a value of 0.75 is recommended[9,113]. Reference [119] recommends p_s value of 0.5 which provides the best fit to test data when considering the inelastic model.

o Column Buckling Stress of Stringer:

The column buckling stress of stringer, σ_c is defined as:

$$\sigma_c = \frac{\pi^2 E I_e'}{\left[(A_s + s_e t) L^2 \right]} \tag{3.27}$$

where I_e' is the moment of inertia including the reduced effective width, s_e' defined by:

$$s_e' = s \left(\frac{0.53}{\lambda} \right) R_r \qquad \text{for } \lambda > 0.53$$

$$= s \qquad \text{for } \lambda \leq 0.53 \tag{3.28}$$

with λ defined by:

$$\lambda = \sqrt{\frac{\sigma_Y}{\sigma_e}} \tag{3.29}$$

which denotes the curved shell slenderness parameter. σ_e is the mean elastic buckling stress for imperfect curved panel given by:

$$\sigma_e = B\,\rho_n\,\sigma_{cr} \tag{3.30}$$

where σ_{cr} is the elastic buckling stress of a perfect shell defined as:

$$\sigma_{cr} = 0.904\,E\left[\frac{t}{s}\right]^2\left[4+\frac{3\,Z_s^2}{\pi^4}\right] \qquad \text{for } Z_s \le 11.4$$

$$= 0.605\,E\left[\frac{t}{R}\right] \qquad \text{for } Z_s > 11.4 \tag{3.31}$$

ρ_n is the nominal or lower bound knock-down factor given by:

$$\rho_n = 1 - 0.019\,Z_s^{1.25} + 0.0024\,Z_s\left[1-\frac{R}{300\,t}\right] \qquad \text{for } Z_s \le 11.4$$

$$= 0.27 + \frac{1.5}{Z_s} + \frac{27}{Z_s^2} + 0.008\sqrt{Z_s}\left[1-\frac{R}{300\,t}\right] \qquad \text{for } 11.4 < Z_s \le 70 \tag{3.32}$$

where Z_S is the Batdorf width parameter defined by:

$$Z_s = \frac{s^2}{Rt}\sqrt{1-\nu^2}$$

$$\cong 0.954\,\frac{s^2}{Rt} \quad \text{when } \nu = 0.3 \tag{3.33}$$

and B is the mean bias factor assessed from elastic test data and given as:

$$B = 1.15 \qquad \text{for } \lambda_n = \sqrt{\frac{\sigma_Y}{\rho_n \sigma_{cr}}} > 1$$

$$= 1 + 0.15\lambda_n \qquad \text{for } \lambda_n \leq 1 \tag{3.34}$$

In Eqs.(3.31) and (3.32) the Z_S value of 11.4 is taken to approximately represent the division between "narrow" and "wide" panels. The presence of R_r in Eq.(3.18) affects the reduced effective width by a factor of R_r. The reduction factor for stringer-stiffened cylinders can be derived from that of flat panels. For flat panels with width, b, and thickness, t, R_r is given as:

$$R_r = 1 - \left[\frac{\sigma_r}{\sigma_Y}\right]\left[\frac{b}{b_e}\right]\left[\frac{E_t}{E}\right] \qquad \text{for } \beta > 1.0$$

$$= 1 \qquad \text{for } \beta \leq 1.0 \tag{3.35}$$

where

$$\frac{\sigma_r}{\sigma_Y} = \frac{2\eta}{\frac{b}{t} - 2\eta} \qquad : \text{mean compressive residual stress}$$

η is the welding tension block parameter, b_e/b is the ratio of the reduced effective width to plate width given by:

$$\frac{b_e}{b} = \frac{2}{\beta} - \frac{1}{\beta^2} \tag{3.36}$$

E_T/E is the plate tangent modulus ratio given by:

$$\frac{E_T}{E} = \frac{\lambda^4}{(1+0.25\lambda^4)^2} \qquad \text{for } \lambda \le \sqrt{2}$$

$$= 1 \qquad \text{for } \lambda > \sqrt{2} \tag{3.37}$$

and β and λ are the slenderness parameters of plate and plate-stiffener combined column:

$$\beta = \frac{b}{t}\sqrt{\frac{\sigma_Y}{E}} \tag{3.38}$$

$$\lambda = \sqrt{\frac{\sigma_Y}{\sigma_{cr}}} \tag{3.39}$$

Since, for the simply supported plates, σ_{cr} is given as:

$$\sigma_{cr} = 4\frac{\pi^2 E}{12(1-\nu^2)}\left[\frac{t}{b}\right]^2 \tag{3.40}$$

From Eqs.(3.38) - (3.40) the relation between β and λ is derived as:

$$\beta = \frac{\lambda}{C} \tag{3.41}$$

where:

$$C = \sqrt{\frac{3(1-\nu^2)}{\pi^2}}$$

$$\cong 0.53 \qquad \text{when } \nu = 0.3 \tag{3.42}$$

Substituting Eq.(3.41) into Eq.(3.36):

$$\frac{b_e}{b} = \frac{2C}{\lambda} - \frac{C}{\lambda^2} \cong \frac{1.05}{\lambda} - \frac{0.28}{\lambda^2} \tag{3.43}$$

Hence:

$$\frac{b}{b_e} = \frac{\lambda^2}{1.05\,\lambda - 0.28} \tag{3.44}$$

The inequality $\beta > 1.0$ leads to:

$$\beta = \frac{\lambda}{C} > 1.0, \quad \text{hence equivalently } \lambda > 0.53 \tag{3.45}$$

Therefore, replacing b and b_e by s and s_e', the reduction factor for the stringer-stiffened shell can be obtained as:

$$R_r = 1 - \left[\frac{2\eta}{\frac{s}{t} - 2\eta}\right]\left[\frac{\lambda^2}{1 + 0.25\,\lambda^4}\right]^2\left[\frac{\lambda^2}{1.05\,\lambda - 0.28}\right] \quad \text{for } \lambda > 0.53$$

$$= 1 \quad \text{for } \lambda \le 0.53 \tag{3.46}$$

in which λ is defined as Eq.(3.29) and η defined as:

η = 4.5 : for continuous structural fillet welding.

= 3.0 : for light fillet weld welding s or where shakeout is significant.

= 4.5 : for stress-relieved structure.

From the above equations the inelastic collapse stress σ_{ic} can be calculated in Eq.(3.23).

Finally, the effective width, s_e in Eq.(3.20) (not the reduced effective width, s_e') can be obtained from Eq.(3.43) by replacing b and b_e by s and s_e respectively, and given by:

$$s_e = s\left[\frac{1.05}{\lambda_e} - \frac{0.28}{\lambda_e^2}\right] R_r \qquad \text{for } \lambda_e > 0.53$$

$$= s \qquad \text{for } \lambda_e \le 0.53 \qquad (3.47)$$

where the reduced slenderness parameter, λ_e is:

$$\lambda_e = \sqrt{\frac{\sigma_{ic}}{\sigma_e}} = \lambda\sqrt{\frac{\sigma_{ic}}{\sigma_Y}} \qquad (3.48)$$

The presence of R_r in Eq.(3.47) affects the behaviour of the stiffened shell in two ways, namely, the reduction of the proportional limit by σ_r, and the effective width by a factor of R_r in Eq.(3.46) with replacing λ by λ_e given as Eq.(3.48). Therefore, substituting σ_{ic} and s_e in Eq.(3.20.b) gives the ultimate axial compressive strength of stringer-stiffened cylinder.

3.3.2 Radial Pressure

The ultimate hoop stress due to radial pressure, $\sigma_{\theta u}$ is given by:

$$\sigma_{\theta u} = \frac{P_u R}{t} \qquad (3.49)$$

P_u is the collapse pressure defined below:

$$P_u = \sigma_Y\left[9.728\frac{f_1 Z_p}{s L^2} + 1.368\, t^2 f_2 f_3\left(\frac{2}{L^2} + \frac{1}{s^2}\right)\right] \qquad (3.50)$$

where s is the curved panel width between stringers given as Eq.(3.22), Z_p is the plastic section modulus given by:

$$Z_p = \frac{1}{4} t_w \left[(h_w+t)^2 - \left(\frac{b_f t_f}{t_w}\right)^2 + \frac{2 (h_w+t) b_f t_f}{t_w} \right] \tag{3.51}$$

and f_1, f_2 and f_3 are constants derived as:

$$f_1 = 1 + \left[\frac{1}{35.06} \frac{s^2}{Rt} \right]^{1.75}$$

$$f_2 = 1 + \left[\frac{1}{30.55} \frac{s^2}{Rt} \right]^{3.50}$$

$$f_3 = 1 + 2.65 \left[\frac{t}{L}\right] \left[\frac{E}{\sigma_Y}\right] \sqrt{\frac{t}{2R}} \tag{3.52}$$

The constants f_1, f_2 and f_3 are derived to give the best fit with test data which covered the following ranges:

$190 < R/t < 500$ $\qquad$ $0.2 < L/R < 1.0$

$4 < Z_S < 34$ $\qquad$ $45 < Z_L < 300$

where Z_L is the Batdorf length parameter calculated from Eq.(3.33) with s = L.

3.3.3 Combined Loading

The same interaction equation (3.11) was proposed for the stringer-stiffened cylinder under the combined axial compression and radial pressure[113]. It can be rewritten in terms of hoop stress instead of radial pressure:

$$\left[\frac{\sigma_\theta}{\sigma_{\theta u}}\right]^m + \left[\frac{\sigma_x}{\sigma_{xu}}\right]^n = 1 \tag{3.53}$$

where the hoop stress is calculated from

$$\sigma_\theta = \frac{P R}{t}$$

and the ultimate hoop stress can be calculated from Eq.(3.49) with the ultimate pressure calculated from Eqs.(3.50) - (3.52). DnV[115] uses m = n = 2, and the TLP RCC[113] initially favoured m = 2 and n = 1 as for the ring-stiffened cylinder. The model code of TLP RCC[9] presently uses a different form as follows expressed in terms of axial stress and hoop stress:

$$\left[\frac{\sigma_\theta}{\sigma_{\theta u}}\right] + 1.5\left[\frac{\sigma_x}{\sigma_{xu}}\right] - 0.5\left[\frac{\sigma_x}{\sigma_{xu}}\right]^2 - \left[\frac{\sigma_\theta}{\sigma_{\theta u}}\right]\left[\frac{\sigma_x}{\sigma_{xu}}\right] = 1 \qquad (3.54)$$

A more general form of interaction equation which can cover a wide range of load combinations has been proposed by Faulkner[161], which is an extension based on the Odland approach[169] and by which a more convenient ϕ-parameter can be used for each individual load component instead of the DnV type[115] slenderness parameters. Recently Faulkner and Warwick[162] published the correlation of the interaction model with test data. The derived procedure is illustrated as follows:

When σ_{xo} and $\sigma_{\theta o}$ are both compressive stress components the Odland interaction equation (3.13.a) becomes:

$$\left[\frac{\sigma_x}{\sigma_{Ex}} + \frac{\sigma_\theta}{\sigma_{E\theta}}\right]^2 + \left[\frac{\sqrt{\sigma_x^2 + \sigma_\theta^2 - \sigma_x \sigma_\theta}}{\sigma_Y}\right]^2 = 1 \qquad (3.55)$$

Expanding and putting

$$\sigma_{Ex} = \frac{\sigma_Y}{\lambda_x^2} \quad , \quad \sigma_{E\theta} = \frac{\sigma_Y}{\lambda_\theta^2}$$

$$\left[\frac{\sigma_x}{\sigma_Y}\right]^2 [\lambda_x^4 + 1] + \left[\frac{\sigma_\theta}{\sigma_Y}\right]^2 [\lambda_\theta^2 + 1] + \left[\frac{\sigma_x}{\sigma_Y}\right]\left[\frac{\sigma_\theta}{\sigma_Y}\right] [2\,\lambda_x^2 \lambda_\theta^2 - 1] = 1 \qquad (3.56)$$

Define the ϕ-parameters for individual loading:

$$\phi_x = \frac{\sigma_{xu}}{\sigma_Y} = \frac{1}{\sqrt{1+\lambda_x^4}} \quad , \quad \phi_\theta = \frac{\sigma_{\theta u}}{\sigma_Y} = \frac{1}{\sqrt{1+\lambda_\theta^4}} \qquad (3.57)$$

Substituting Eq.(3.56) into Eq.(3.55), we have:

$$\left[\frac{R_x}{\phi_x}\right]^2 + R_x R_\theta \left[\frac{2\sqrt{(1-\phi_x^2)(1-\phi_\theta^2)}}{\phi_x \phi_\theta} - 1\right] + \left[\frac{R_\theta}{\phi_\theta}\right]^2 = 1 \qquad (3.58)$$

where

$$R_x = \frac{\sigma_x}{\sigma_Y} \quad , \quad R_\theta = \frac{\sigma_\theta}{\sigma_Y}$$

The terms ϕ_x and ϕ_θ can easily be evaluated from the single load action models. This equation gives better correlation with test data than other models presently in use.

Comparisons and discussions for various strength models of ring-stiffened cylinders and ring- and stringer-stiffened cylinders presently used in various design codes are presented in reference [119].

3.4 Rectangular Box-Girder

Longitudinal frame systems are frequently found in the structural system of a rectangular box-girder such as a ship's hull girder and a TLP's pontoon (Fig. 3.3) because of its adequate way to resist compressive loads. As is well recognised, the performance of this type of structure, as that of other redundant structures, may be strongly affected by pre-ultimate loss of stiffness and post-ultimate load carrying capacity of structural components.

The present approach is based on the beam-column concept[126] in which the rectangular cross-section is modelled as the combination of structural members such as plates, stiffened panels and "hard corners". The stiffness of a member at any point in the strain range can be obtained from the results derived from a separate study. This is based on the assumption that failure of a member is not directly influenced by other members of the cross-section considering that except for the overall grillage collapse the ductile collapse of the girder is most probable due to progressive failure rather than a coincidence of failures of the structural members.

The ultimate strength of box-girder under axial, bending and their combined loading has close correlation with the compressive strength of stiffened panels. To derive the strength formula, a parametric study has been carried out within a wide range of several important parameters.

In the following sections, the pre- and post-ultimate behaviour of the rectangular box-girder will be presented. Strength formulae for stiffened panels and for axial compressive strength and bending strength of rectangular box-girders have been derived based on the numerical results of a parametric study. Finally, an interaction equation, when the structure is under combined axial compression and bi-axial bending, is proposed. They have also been derived based on the numerical results of a parametric study.

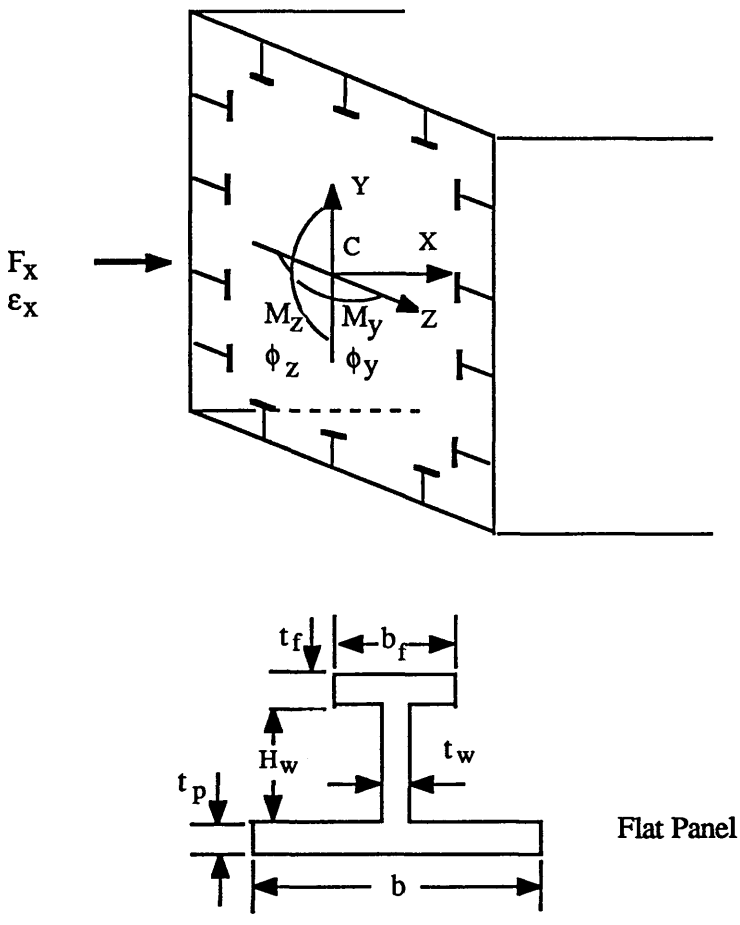

Fig. 3.3 Rectangular Box-Girder

3.4.1 Behaviour of a Rectangular Box-Girder

3.4.1.1 Beam-Column Concept

The main feature of the beam-column approach is that one isolated stiffener with an associated width of plate is considered to be representative of the whole panel behaviour using stress-strain curves to describe the plate contribution. This concept is much simpler than the well known rigorous numerical method, such as the finite element method.

o Plate Elements:

Much of a typical rectangular cross-section is formed by plate and it plays an important role in strength, particularly under compression. Loss of stiffness in the

plating, which may be caused by buckling or premature yielding, leads to loss of performance of the cross-section.

Many parameters have an effect on the compressive strength of plate: aspect ratio, boundary condition, initial deflection, lateral pressure, weld induced residual stress and welding procedure. The influence of these parameters is discussed in reference [172]. Among them initial deflection and weld induced residual stress generally reduce the strength of plates with that same slenderness and hence affect the shape of their stress-strain curves.

Long plate buckling occurs in approximately a square half-wave. Various numerical and experimental work has shown that it is reasonable to assume the boundary condition in such a way that boundary condition of simply supported at loaded edges constrained to remain straight but free to move bodily in the plane of plate. The effect of lateral pressure can be approximated by introducing an equivalent initial deflection which may not be valid for slender plates due to membrane stress set up by the lateral load[173]. However, the effect of membrane stress in comparatively stocky plates , frequently found in a TLP structure, may be small and can therefore be neglected. This approximation is used in this study without much loss of accuracy.

The effect of weld induced residual stress on the shape of a stress-strain curve can be considered by using the simplified procedure as in reference [125]. It is assumed that the residual stress takes the idealised pattern, as shown in Fig. 3.4, where the uniformly distributed tension stress centered at the stiffener-plate weld with a width of $2\eta t$ is equilibrated by a zone of uniformly distributed compressive residual stress with a width of $(b - 2\eta t)$. η is the welding tension block parameter as for the stringer-stiffened cylinder. From this assumed distribution the value of residual stress results from equilibrium as:

$$\sigma_r' = \frac{\sigma_r}{\sigma_Y} = \frac{2\eta t}{b - 2\eta t} \tag{3.59}$$

Therefore, in this study, slenderness and initial deflection of a plate are taken as fundamental parameters to derive the stress-strain curve of the particular residual stress free plate. The slenderness of the plate takes the form of that defined by Eq.(3.38) and the initial deflection the form of:

$$\frac{\delta_o'}{\beta^2} \tag{3.60}$$

as proposed by Faulkner[174]. The values of fundamental parameters of residual stress free standard plates in this study are listed in Table 3.1 and their stress-strain curves are shown in Fig. 3.5, which were derived by using the Ritz type approach[175]. Actually all curves are numerically given in the non-dimensional form, i.e. as a relation between non-dimensional stress, σ' ($= \sigma_{av} / \sigma_Y$) and non-dimensional strain, ε' ($= \varepsilon_{av} / \varepsilon_Y$). The Aitken-Lagrangian interpolation method is used to obtain the stress-strain curves of the non-standard plates.

When the plate is subjected to tension, the behaviour is assumed to follow the material stress-strain curve and, to take into account the effect of residual stress, the following parabola equation is used:

$$\begin{aligned}
\sigma' &= \frac{\varepsilon'}{1+\sigma_r'} && \text{for } 0 \le \varepsilon' < 1 \\
&= \frac{-\varepsilon + (2+4\sigma_r')\,\varepsilon' - 1}{4\sigma_r'(1+\sigma_r')} && \text{for } 1 \le \varepsilon' < 1+2\sigma_r' \\
&= 1 && \text{for } 1+2\sigma_r \le \varepsilon'
\end{aligned} \tag{3.61}$$

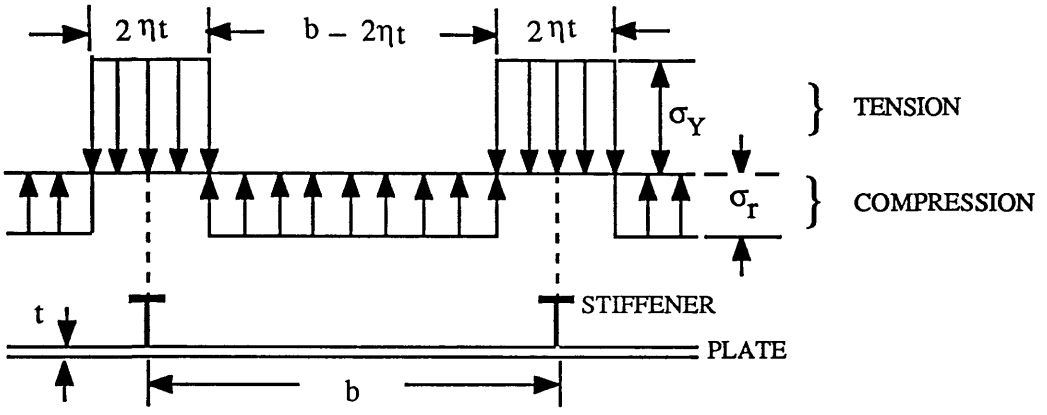

Fig. 3.4 Idealised Residual Stress Distribution in Plate

Table 3.1 Slendernesses and Initial Deflection Parameters of Standard Plates

β	0.816	1.021	1.225	1.632	2.041
b/t	20	25	30	40	50

δ_o'/β^2	0.05	0.10	0.15	0.20	0.25	0.30

$\delta_o' = \frac{\delta_o}{t}$: δ_o = maximum deflection of plate, t = plate thickness

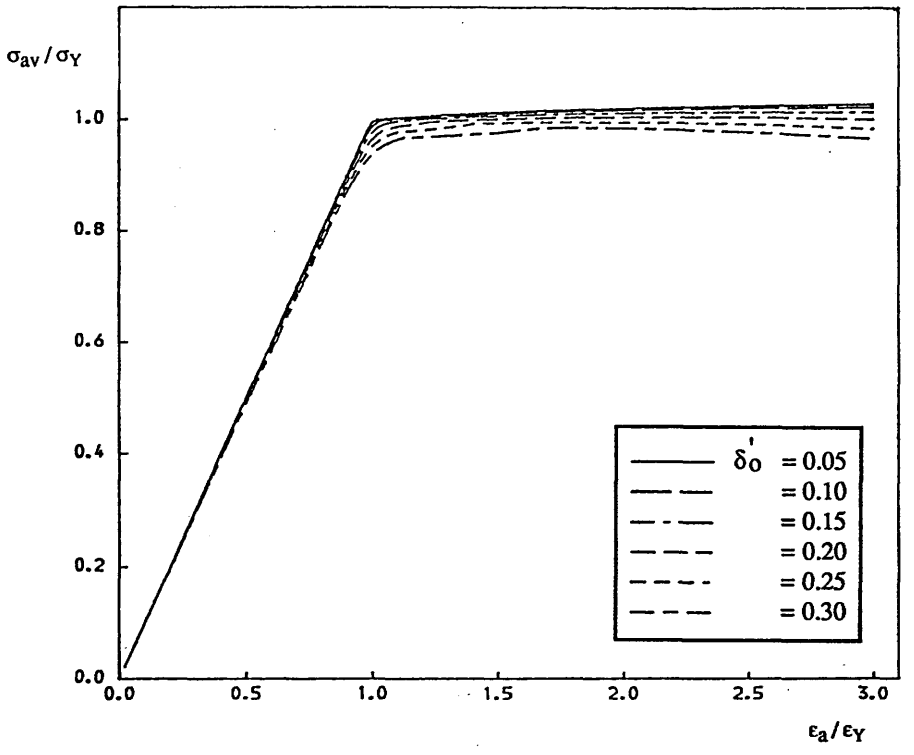

(a) $\beta = 0.816$

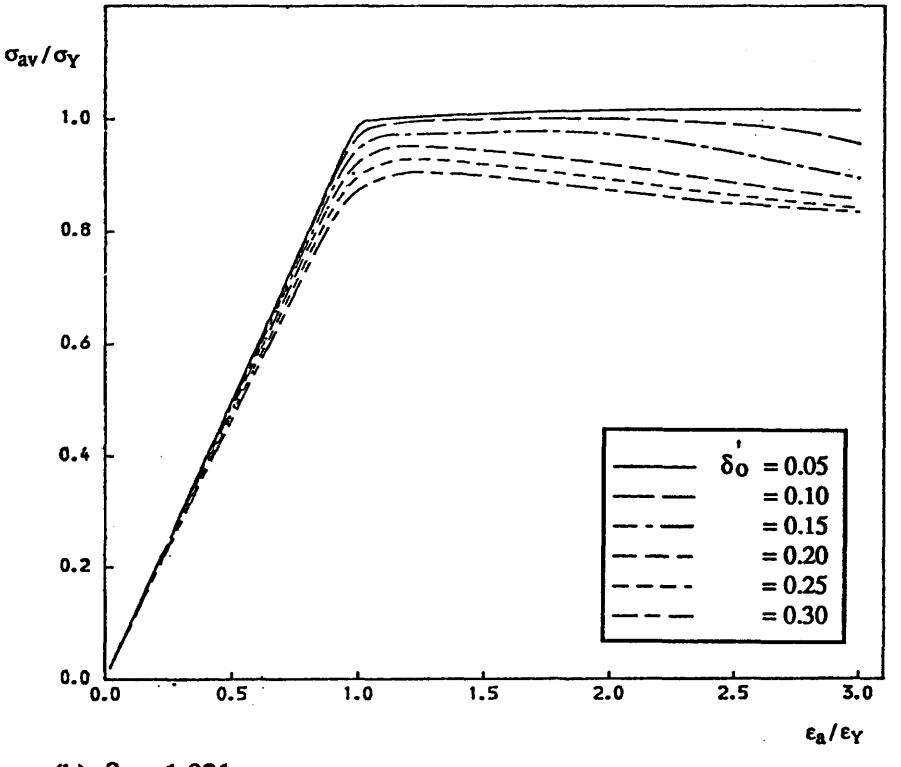

(b) $\beta = 1.021$

Fig. 3.5 Stress-Strain Curves of Standard Plates

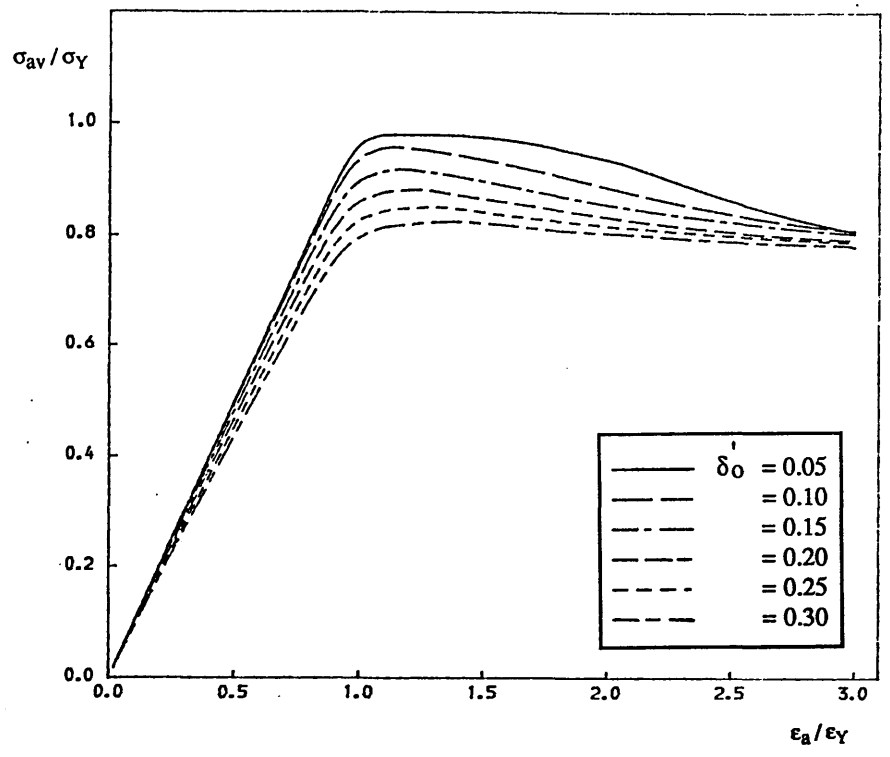

(c) $\beta = 1.225$

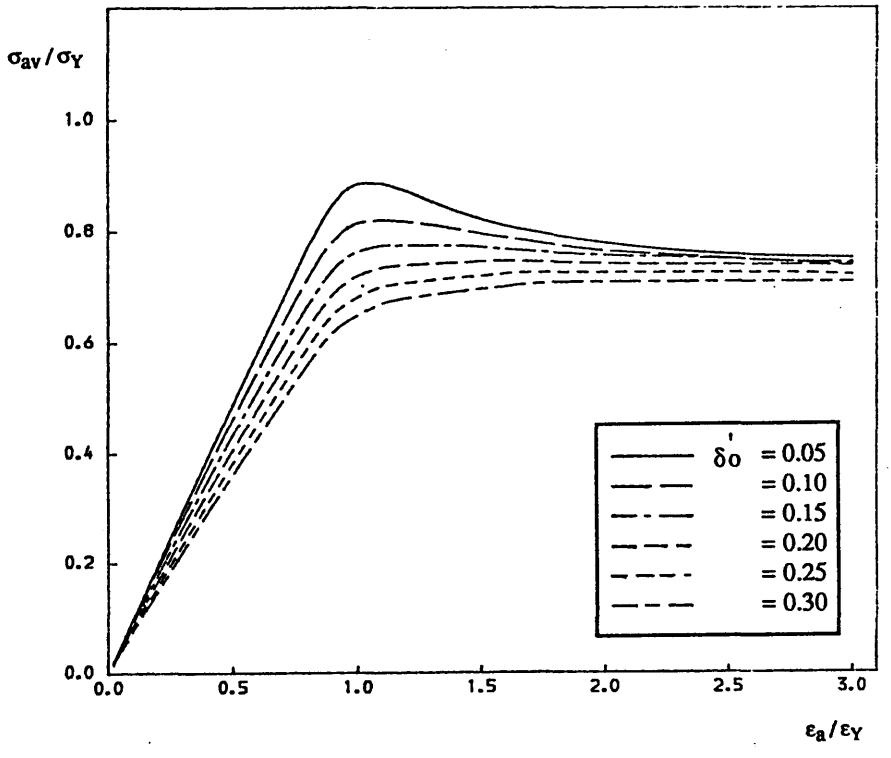

(d) $\beta = 1.632$

Fig. 3.5 (continued)

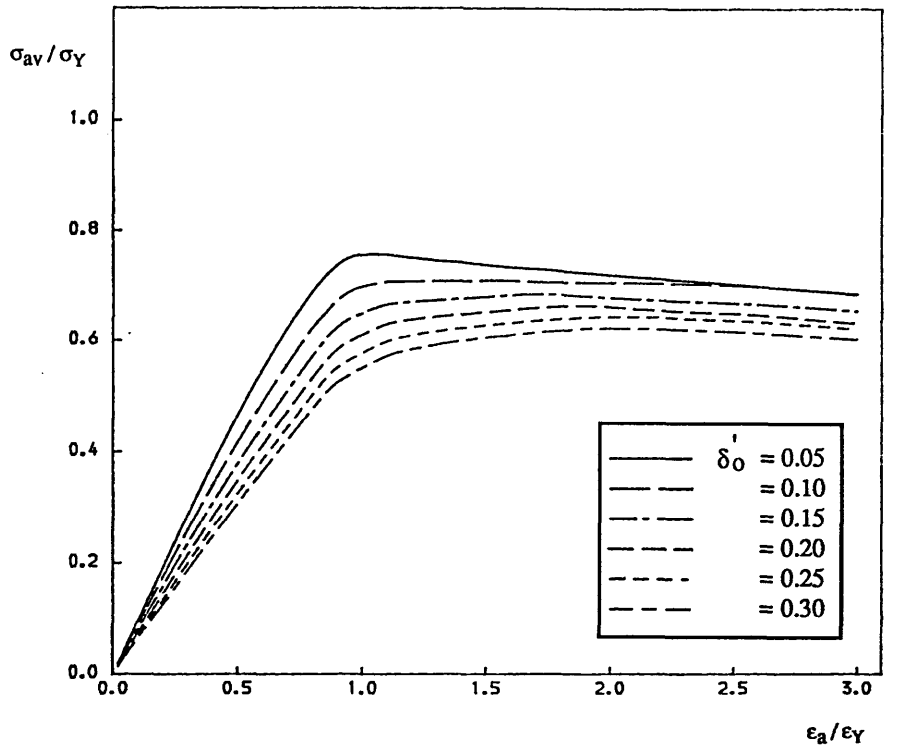

(e) $\beta = 2.041$

Fig. 3.5 (continued)

o Stiffened Panels:

As described before, the ultimate axial compression and bi-axial bending moment are primarily governed by the compressive strength of stiffened panels[120]. The behaviour of stiffened panels under compressive loads is relatively complicated due to a large number of possible combinations of plate and stiffener geometry, boundary conditions and loading types. Therefore, it is very difficult to take account of all possible failure modes. The most probable failure modes of stiffened panels under compression are categorised as follows:

[1] Column-like failure of stiffener-plate combination

[2] Sideways tripping of the stiffener about its line of attachment to plate

[3] Overall grillage buckling involving bending of transversals

In practical structures the longitudinal stiffeners and associated plating between

transversals are frequently involved in collapse. The first two are primary modes of failure, and stiffener sections are normally proportioned so that tripping does not occur until after collapse.

In the present study, in order to produce the load-end shortening curves of stiffened panels, an associated width of plate is assumed to be equal to the longitudinal stiffener spacing. The matrix displacement method is employed to solve the non-linear equilibrium equation for the elasto-plastic large deflection analysis of stiffened panels, for which the finite element used has a cubic displacement function for bending deformation in accordance with the Euler beam theory and a linear displacement function for in-plane deformation, respectively. The modelling of a stiffened panel is illustrated in Fig. 3.6. The model is double span to take into account the interaction effect between adjacent spans and the simply supported boundary condition is imposed at the position of transversal. The stiffener section is subdivided into several layers to allow the plastification of the section in the direction of depth as load increases. The plate is treated as a single layer and its stiffness at any point in the strain range can be obtained from the stress-strain curve derived from a separate study. This can consider the loss of stiffness due to plate buckling and plastification and can be applied to any element of beam-column. The stress-strain relation of each layer of stiffener follows the material behaviour. This modelling can allow in a simple way the analysis of stiffened panels with different material properties. For the sake of simplicity, the following assumptions are adopted in this study:

[1] Since the web depth of stiffener model is comparatively small, effect of shear deformation is neglected. But for the case of a deep girder it should probably be considered.

[2] Since most design stiffener sections are proportioned to limit the possibility of local instability, sideways tripping is assumed not to occur.

[3] Welding induced residual stresses in the stiffener are usually smaller than those in plates, and therefore, its effect can be neglected.

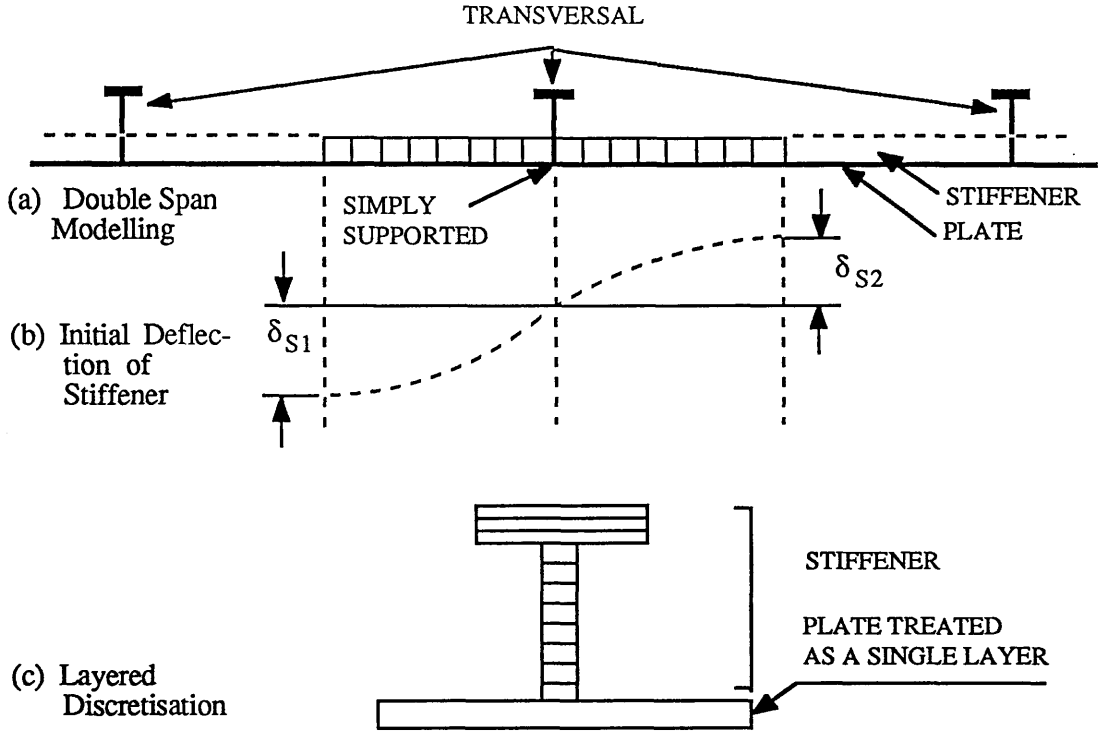

Fig. 3.6 Beam-Column Model

3.4.1.2 Formulation of Behaviour Under Combined Loading

When a rectangular section is subjected to combined loading of axial compression and bi-axial bending, as shown in Fig. 3.3, with the assumption that the effect of shear deformation is neglected, strain increment, $\Delta\varepsilon$ at any point (y,z) in the section is:

$$\Delta\varepsilon = \Delta\varepsilon_x + y\Delta\phi_z + z\Delta\phi_y \tag{3.62}$$

where $\Delta\varepsilon_x$ is increment of axial strain, and $\Delta\phi_z$ and $\Delta\phi_y$ are increments of curvatures due to bending about y- and z-axis, respectively. y and z are y- and z-co-ordinates relative to the instantaneous centroidal axis changes progressively as a result of local buckling and yielding parts of the cross-section. In Fig. 3.3 the direction of compressive force and bending moments is positive. According to Hooke's law the stress increment, $\Delta\sigma$, at any point (y,z) in the section is:

$$\Delta\sigma = E^*\Delta\varepsilon_x + yE^*\Delta\phi_z + zE^*\Delta\phi_y \tag{3.63}$$

where E^* is the effective tangential modulus at (y, z) in the section, which is the slope of stress-strain curve of stiffened panel and can be easily obtained from the curve for a given strain point. Increments of axial compression, ΔF_x and bending moments about y- and z-axis, ΔM_y and ΔM_z are given as stress resultants by integrating the stress increment, Eq.(3.63) over the sectional area:

$$\begin{aligned}\Delta F_x &= \int_A \Delta\sigma \, dA \\ &= \int_A E^* dA \, \Delta\varepsilon_x + \int_A yE^* dA \, \Delta\phi_z + \int_A zE^* dA \, \Delta\phi_y\end{aligned} \tag{3.64.a}$$

$$\begin{aligned}\Delta M_z &= \int_A y \, \Delta\sigma \, dA \\ &= \int_A yE^* dA \, \Delta\varepsilon_x + \int_A y^2E^* dA \, \Delta\phi_z + \int_A yzE^* dA \, \Delta\phi_y\end{aligned} \tag{3.64.b}$$

$$\begin{aligned}\Delta M_y &= \int_A z \, \Delta\sigma \, dA \\ &= \int_A zE^* dA \, \Delta\varepsilon_x + \int_A yzE^* dA \, \Delta\phi_z + \int_A z^2E^* dA \, \Delta\phi_y\end{aligned} \tag{3.64.c}$$

Rewriting Eq.(3.64) in matrix form, the relation between increments of strain and stress resultants is obtained as:

$$\begin{Bmatrix} \Delta F_x \\ \Delta M_z \\ \Delta M_y \end{Bmatrix} = \begin{bmatrix} a & m_z & m_y \\ m_z & I_z & I_{yz} \\ m_y & I_{yz} & I_y \end{bmatrix} \begin{Bmatrix} \Delta\varepsilon_x \\ \Delta\phi_z \\ \Delta\phi_y \end{Bmatrix} \tag{3.65.a}$$

or:

$$\{\sigma\} = [K]\{\varepsilon\} \tag{3.65.b}$$

where:

$$a = \int_A E^* dA \qquad m_z = \int_A yE^* dA \qquad m_y = \int_A zE^* dA$$

$$I_z = \int_A y^2E^* dA \qquad I_y = \int_A z^2E^* dA \qquad I_{yz} = \int_A yzE^* dA$$

From Eq.(3.65) pre- and post-ultimate solution can be obtained by incrementing the strain terms, or the stress resultant term. In the latter case, solutions are obtained from:

$$\{\varepsilon\} = [K]^{-1}\{\sigma\} \tag{3.66}$$

3.4.1.3 Comparison of Numerical Results

Since there is no available test data under the combined loading, only the ultimate uni-axial bending moment by the present approach is compared with some test results. Three test models close to marine structure are selected: Model 2 and Model 4 by Dowling et al[176], and Model 23 by Reckling[177]. All models were tested under pure bending. Details of material and geometric properties, and initial imperfections are listed in Table 3.2. They are modelled into plates, stiffened panels and "hard corners", as illustrated in Fig. 3.7.

A case study for each model is listed in Table 3.3. Table 3.4 summaries the present numerical results in the form of ratio of numerically calculated ultimate bending moment to that by test. Numerical results by Dow et al[178] and Lin[125] are also included for comparison. The agreement with test results is satisfactory, and the present numerical results show good agreement with others, as seen in Table 3.4. Dow et al's

results are slightly lower than the present ones, while the present predictions are closer to the test data than Lin's results. Non-dimensional bending moment-curvature curves for Model 4 and 23 are plotted in Fig. 3.8.

Table 3.2 Details of Test Models

(a) Model 2 by Dowling et al[176]

breadth (B) : 1219.2 mm height (H) : 914.4 mm tranverse spacing (L) : 787.4 mm							
properties / component	plate			stiffener			
	t mm	E N/mm^2	σ_Y N/mm^2	scantling mm	E N/mm^2	σ_Y N/mm^2	spacing mm
compression flange	4.86	208500	297	46 x 4.76 x 15.87 x 4.76L	191500	276.2	243.8
tension flange	4.86	208500	297	46 x 4.76 x 15.87 x 4.76L	191500	276.2	243.8
web	3.37	216200	219	46 x 4.76 x 15.87 x 4.76L	191500	276.2	243.8

total sectional area	21551.6 mm^2
elastic neutral axis from midplan of bottom plate	462.5 mm
plastic neutral axis from midplan of bottom plate	495.3 mm
moment of inertia I_z	3346.8 m^2- mm^2
plastic bending moment M_{zp}	2228.7 KN-m
compressive residual stress σ_r'	0.176
initial plate deflection	b/400
initial stiffener deflection	-L/1450 +L/2280

Table 3.2 (continued)

(b) Model 4 by Dowling et al[176]

breadth (B) : 1219.2 mm height (H) : 914.4 mm tranverse spacing (L) : 787.4 mm							
properties / component	plate			stiffener			
	t mm	E N/mm^2	σ_Y N/mm^2	scantling mm	E N/mm^2	σ_Y N/mm^2	spacing mm
compression flange	5.01	207000	221.0	46 x 4.76 x 15.87 x 4.76L	199200	287.9	121.9
tension flange	4.94	208700	215	50.8 x 6.35 FLAT	206200	303.8	121.9
web	4.94	214100	280	46 x 4.76 x 15.87 x 4.76L	199200	287.9	98.4 114.3

total sectional area	29078.9 mm^2
elastic neutral axis from midplan of bottom plate	465.3 mm
plastic neutral axis from midplan of bottom plate	505.7 mm
moment of inertia I_z	4237.6 m^2-mm^2
plastic bending moment M_{zp}	2597.0 KN-m
compressive residual stress σ_r'	0.562
initial plate deflection	b/800
initial stiffener deflection	-L/510 +L/510

Table 3.2 (continued)

(c) Model 23 by Reckling[177]

breadth (B) : 600.0 mm height (H) : 400.0 mm tranverse spacing(L) : 500.0 mm							
properties / component	plate			stiffener			
	t mm	E N/mm^2	σ_Y N/mm^2	scantling mm	E N/mm^2	σ_Y N/mm^2	spacing mm
compression flange	2.5	210000	246.0	27.5 x 2.5 x 20 x 2.5L	210000	246.0	85.7
tension flange	2.5	210000	246.0	27.5 x 2.5 x 20 x 2.5L	210000	246.0	85.7
web	2.5	210000	246.0	30 x 2.5 FLAT	210000	256.0	100.0

total sectional area	6875.0 mm^2
elastic neutral axis from midplan of bottom plate	198.75 mm
plastic neutral axis from midplan of bottom plate	198.75 mm
moment of inertia I_z	193.1 m^2- mm^2
plastic bending moment M_{zp}	266.3 KN-m
compressive residual stress σ_r'	0.2
initial plate deflection	0.25 t
initial stiffener deflection	-L/1000 +L/1000

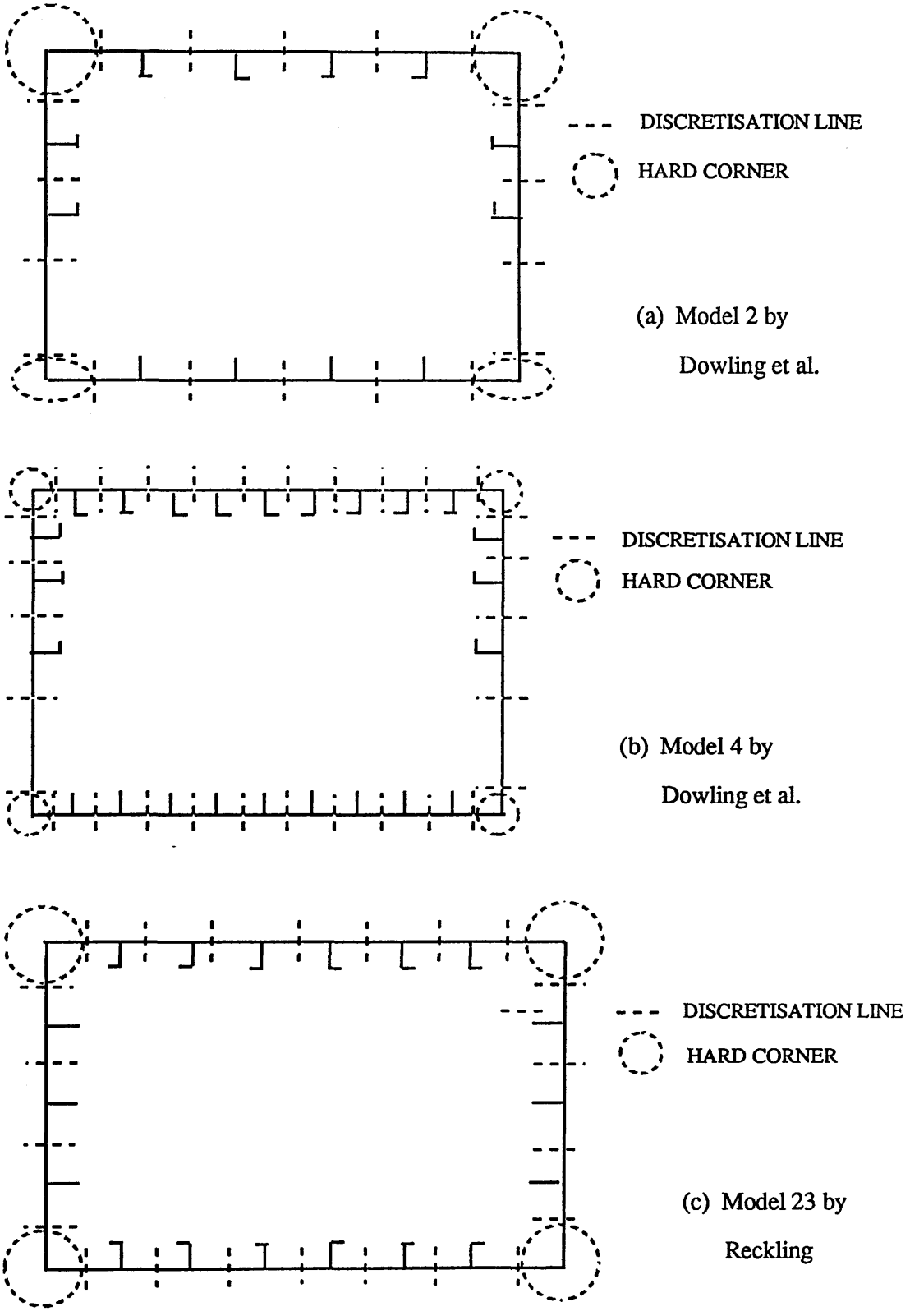

Fig. 3.7 Discretisation of Test Models[176,177]

Table 3.3 Case Study for Three Test Models

(a) Model 2 by Dowling et al.

Case	1	2	3	4
residual stresses in tension flange are included ?	NO	YES	NO	YES
"hard corner" is fully effective ?	YES	YES	half effective	half effective

(b) Model 4 by Dowling et al.

Case	1	2	3	4	5	6
residual stresses in tension flange are included ?	NO	NO	NO	YES	YES	YES
number of stiffened panels included in "hard corner"	0	1	2	0	1	2

note: "hard corners" are assumed to be fully effective in all cases

(c) Model 23 by Reckling

Case	1	2	3	4	5	6
residual stresses in tension flange are included ?	YES	YES	YES	NO	NO	NO
number of stiffened panels included in "hard corner"	0	1	2	0	1	2

note: "hard corners" are assumed to be fully effective in all cases

Table 3.4 Comparison of Present Results with Test and Other Numerical Results

(a) Model 2 by Dowling et al.

Case	Ultimate Bending Moment Ratio (Numerical Result / Test Result)		
	Author	Dow et al.	Lin
1	1.073	1.057	1.050
2	1.058	—	—
3	0.982	1.003	—
4	0.966	—	—

(b) Model 4 by Dowling et al.

Case	Ultimate Bending Moment Ratio (Numerical Result / Test Result)		
	Author	Dow et al.	Lin
1	1.013	—	1.059
2	1.038	0.942	—
3	1.061	1.003	—
4	0.981	—	1.047
5	1.015	—	—
6	1.040	—	—

(c) Model 23 by Reckling

Case	Ultimate Bending Moment Ratio (Numerical Result / Test Result)		
	Author	Dow et al.	Lin
1	0.886	—	—
2	0.940	0.953	0.935
3	0.972	0.993	0.942
4	0.899	—	—
5	0.948	—	0.934
6	0.974	—	0.941

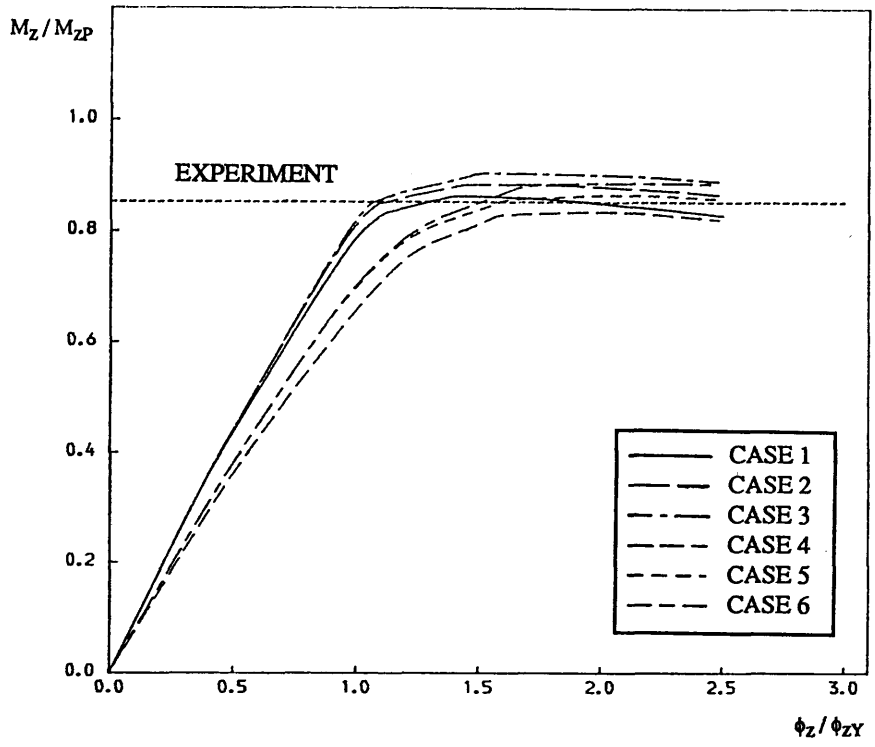

(a) Model 4 by Dowling et al.

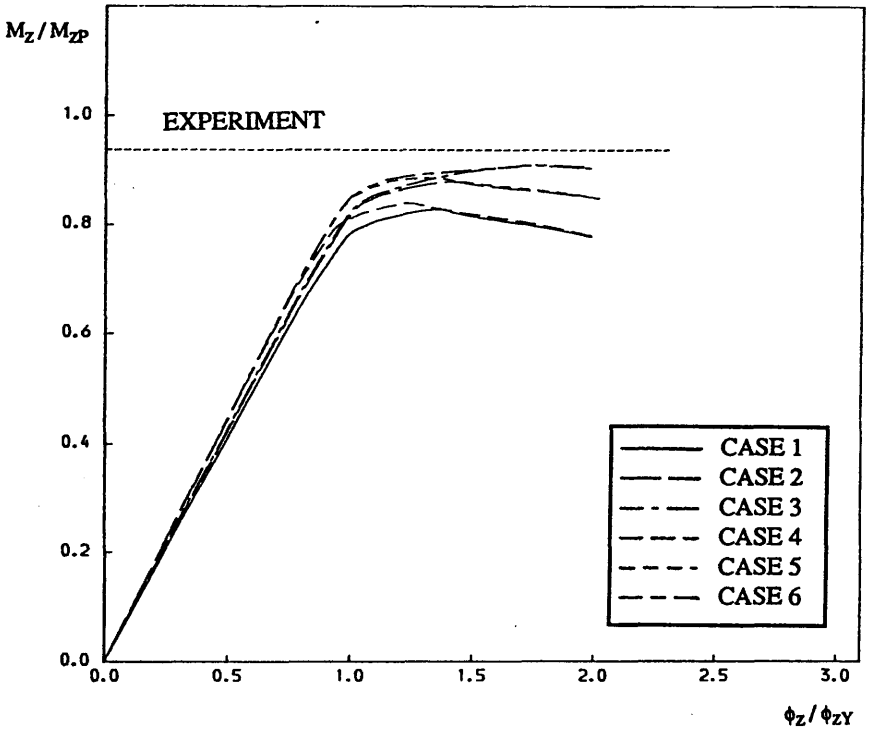

(b) Model 23 by Reckling

Fig. 3.8 Bending Moment-Curvature Curves

3.4.2 Parametric Study

To derive the strength formula for rectangular box-girder a parametric study has been carried out by varying geometric properties. Fig 3.9 shows the typical rectangular section found in a TLP's pontoon. For simplicity, the round corners are replaced by straight lines. There are many parameters affecting the ultimate behaviour of the box-girder. Values of geometric properties for the parametric study are summarised in Table 3.5. As is well recognised, the ultimate behaviour of a box-girder under axial compression, bending moments, or their combined loading, has close correlation with the compressive strength of stiffened panels from the experience of a ship's hull girder. The compressive strength of a stiffened panel is much affected by the slenderness of the stiffener-plate combination in the column sense and by the slenderness of associated plates which can represent the effects of buckling and plastification of a plate on the strength of a stiffened panel.

This study, therefore, mainly concentrated on varying geometric parameters, as seen in Table 3.5. Material properties were chosen suitable for a TLP's pontoon as practical values. The range of stiffener scantling was determined so that tripping did not occur and initial imperfections of plate and stiffener were given uniquely to be suitable for practical structures with reference to the tolerance recommended in various design codes[115,179,180]. Results from 180 cases of stiffened panels and 240 cases of rectangular box-girder have been obtained.

Table 3.5 Values of Parameters in the Parametric Study

aspect ratio of section	B/H	= 0.857, 0.75, 0.67, 0.60
longitudinal stiffener spacing	b	= 700, 800, 900, 1000 mm
aspect ratio of plate	L/b	= 2.0, 2.5, 3.0, 3.5, 4.0

scantling (mm)

case	component	plate thickness t	stiffener $h_w \times t_w \times b_f \times t_f$
case 1	deck	26	325 x 13 x 150 x 25 T
	side shell	28	350 x 14 x 150 x 25 T
	bottom	30	375 x 15 x 150 x 25 T
case 2	deck	26	350 x 13 x 150 x 25 T
	side shell	28	375 x 14 x 150 x 25 T
	bottom	30	400 x 15 x 150 x 25 T
case 3	deck	26	375 x 13 x 150 x 25 T
	side shell	28	400 x 14 x 150 x 25 T
	bottom	30	425 x 15 x 150 x 25 T

lateral pressure	0.30 MPa at deck plating	0.35 MPa at side shell plating
	0.40 MPa at bottom plating	

compressive residual stress ratio	$\sigma_r' = 0.2$
initial deflection of plate	$\delta_0 = b / 200$
initial deflection of stiffener	$\delta_{S1}, \delta_{S2} = \pm 0.015\ L$
elastic modulus	$E = 210000\ N / mm^2$
yield stress	$\sigma_Y = 350\ N / mm^2$

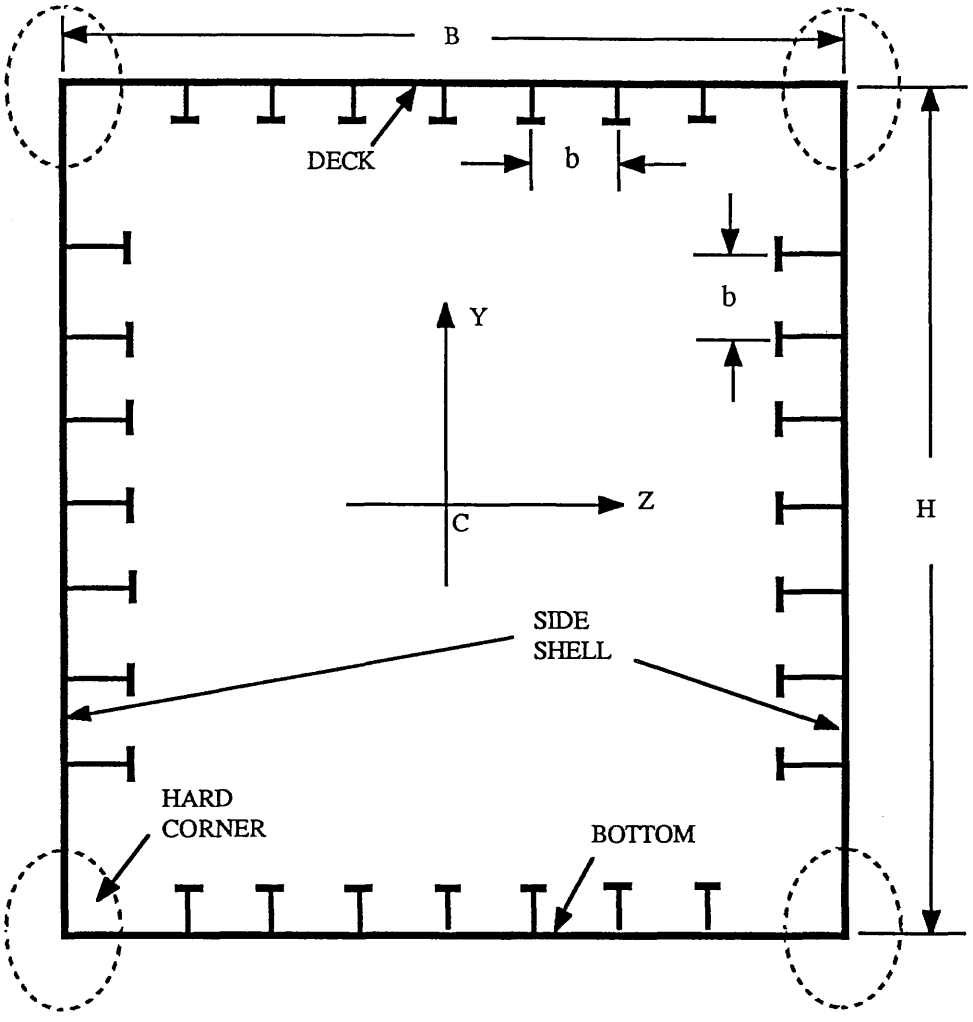

Fig. 3.9 Typical Rectangular Box-Girder Section

3.4.3 Compressive Strength of Stiffened Panels

As described previously, the ultimate behaviour of a box-girder is closely correlated with the compressive strength of stiffened panels. From the results of parametric study, the compressive strength parameter, ϕ, which is given by σ_u / σ_Y where σ_u is the average stress when collapse occurs, was derived through regression analysis as a function of slenderness of plate-stiffener combined column, λ, and plate slenderness, β, by considering the effect of lateral pressure. β is given as Eq.(3.38) and λ is given alternative of Eq.(3.39) as:

$$\lambda = \frac{L}{\pi r}\sqrt{\frac{\sigma_Y}{E}} \tag{3.67}$$

where r is radius of gyration of stiffener-plate combined section given by:

$$r = \sqrt{\frac{I}{A}}$$

In all calculations the width of plate was assumed to be fully effective. The parameter, ϕ, was assumed to be:

$$\phi = f_1(w')\, f_2(\lambda)\, f_3(\beta) \tag{3.68}$$

f_1 is a function of non-dimensional lateral pressure, w' defined as:

$$w' = \frac{w}{\sigma_Y \left[\frac{t}{b}\right]^2} \tag{3.69}$$

where w is a uniformly distributed lateral pressure (MPa). The function $f_2(\lambda)$ was determined so that it had to satisfy:

[1] $f_2(\lambda) = 1.0$ for $\lambda = 0$, and $\beta = w' = 0$

[2] $f_2(\lambda) =$ Euler curve $= 1 / \lambda^2$ for $\lambda > \lambda_0$, and $\beta = w' = 0$

The value of λ_0 was approximately determined so that it fitted best to test data when applying the regression analysis, i.e., minimise the COV of ratio, ϕ_e / ϕ_p, where ϕ_e is the ϕ value by test and ϕ_p by formula, and their mean was close to unity. The result is given by:

$$\phi = \frac{\sigma_u}{\sigma_Y}$$

$$= \left(\frac{1}{1 + 0.04\ w'}\right) \frac{1}{f(\lambda)\sqrt{1 + 0.15\ \beta^2}} \qquad (3.70.a)$$

with function $f(\lambda)$ ($= 1 / f_2(\lambda)$) given:

$$f(\lambda) = 1 + 0.209\ \lambda^2 + 0.156\ \lambda^4 \qquad \text{for } 0 \le \lambda \le 1.59$$
$$= \lambda^2 \qquad \text{for } 1.59 \le \lambda \qquad (3.70.b)$$

Table 3.6 compares the predicted compressive strength parameters by Eq.(3.70), ϕ_p with the numerically calculated ones, ϕ_N. Fig. 3.10 illustrates the comparison between ϕ_N and, ϕ_p . Mean and COV of ratio, ϕ_N / ϕ_p are 0.961 and 3.3%, respectively.

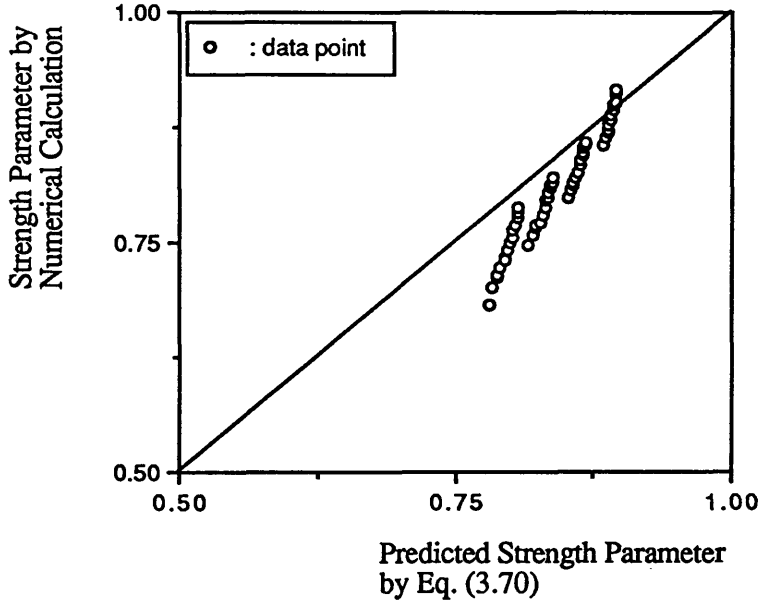

Fig. 3.10 Comparison between ϕ_N and ϕ_p

Table 3.6 Comparison of Compressive Strength Parameters: Prediction by Eq.(3.70), ϕ_p and Numerical Prediction, ϕ_N

L/b	b	λ	β	w'	ϕ_N	ϕ_p	ϕ_N/ϕ_p
2.0	700.0	0.136	1.099	0.621	0.910	0.894	1.018
2.0	700.0	0.127	1.099	0.621	0.913	0.895	1.020
2.0	700.0	0.119	1.099	0.621	0.915	0.895	1.022
2.5	700.0	0.170	1.099	0.621	0.896	0.892	1.004
2.5	700.0	0.159	1.099	0.621	0.900	0.893	1.008
2.5	700.0	0.149	1.099	0.621	0.903	0.894	1.011
3.0	700.0	0.204	1.099	0.621	0.883	0.890	0.992
3.0	700.0	0.190	1.099	0.621	0.889	0.891	0.998
3.0	700.0	0.179	1.099	0.621	0.893	0.892	1.001
3.5	700.0	0.238	1.099	0.621	0.869	0.887	0.980
3.5	700.0	0.222	1.099	0.621	0.877	0.888	0.987
3.5	700.0	0.208	1.099	0.621	0.883	0.890	0.993
4.0	700.0	0.272	1.099	0.621	0.856	0.883	0.969
4.0	700.0	0.254	1.099	0.621	0.863	0.885	0.975
4.0	700.0	0.238	1.099	0.621	0.871	0.887	0.982
2.0	800.0	0.161	1.256	0.811	0.853	0.866	0.985
2.0	800.0	0.150	1.256	0.811	0.856	0.867	0.987
2.0	800.0	0.140	1.256	0.811	0.860	0.867	0.991
2.5	800.0	0.201	1.256	0.811	0.840	0.863	0.973
2.5	800.0	0.187	1.256	0.811	0.845	0.865	0.977
2.5	800.0	0.175	1.256	0.811	0.849	0.865	0.981
3.0	800.0	0.241	1.256	0.811	0.827	0.860	0.962
3.0	800.0	0.225	1.256	0.811	0.834	0.862	0.968
3.0	800.0	0.210	1.256	0.811	0.839	0.863	0.972
3.5	800.0	0.281	1.256	0.811	0.813	0.856	0.950
3.5	800.0	0.262	1.256	0.811	0.820	0.858	0.956
3.5	800.0	0.245	1.256	0.811	0.827	0.860	0.962
4.0	800.0	0.321	1.256	0.811	0.800	0.851	0.940
4.0	800.0	0.299	1.256	0.811	0.807	0.854	0.945
4.0	800.0	0.280	1.256	0.811	0.815	0.856	0.952

Table 3.6 (continued)

L/b	b	λ	β	w'	ϕ_N	ϕ_p	ϕ_N / ϕ_p
2.0	900.0	0.186	1.413	1.027	0.812	0.836	0.971
2.0	900.0	0.174	1.413	1.027	0.816	0.837	0.975
2.0	900.0	0.162	1.413	1.027	0.820	0.838	0.979
2.5	900.0	0.233	1.413	1.027	0.798	0.833	0.958
2.5	900.0	0.217	1.413	1.027	0.804	0.834	0.964
2.5	900.0	0.203	1.413	1.027	0.809	0.835	0.969
3.0	900.0	0.279	1.413	1.027	0.781	0.828	0.943
3.0	900.0	0.260	1.413	1.027	0.789	0.830	0.950
3.0	900.0	0.244	1.413	1.027	0.796	0.832	0.957
3.5	900.0	0.326	1.413	1.027	0.765	0.823	0.930
3.5	900.0	0.304	1.413	1.027	0.773	0.826	0.936
3.5	900.0	0.284	1.413	1.027	0.781	0.828	0.943
4.0	900.0	0.373	1.413	1.027	0.747	0.816	0.915
4.0	900.0	0.347	1.413	1.027	0.758	0.820	0.924
4.0	900.0	0.325	1.413	1.027	0.768	0.823	0.933
2.0	1000.0	0.213	1.570	1.268	0.777	0.805	0.965
2.0	1000.0	0.198	1.570	1.268	0.783	0.806	0.971
2.0	1000.0	0.186	1.570	1.268	0.787	0.807	0.975
2.5	1000.0	0.266	1.570	1.268	0.755	0.801	0.943
2.5	1000.0	0.248	1.570	1.268	0.764	0.802	0.952
2.5	1000.0	0.232	1.570	1.268	0.770	0.804	0.958
3.0	1000.0	0.320	1.570	1.268	0.732	0.795	0.921
3.0	1000.0	0.298	1.570	1.268	0.743	0.797	0.932
3.0	1000.0	0.278	1.570	1.268	0.751	0.800	0.939
3.5	1000.0	0.373	1.570	1.268	0.711	0.788	0.902
3.5	1000.0	0.347	1.570	1.268	0.723	0.791	0.913
3.5	1000.0	0.325	1.570	1.268	0.734	0.794	0.924
4.0	1000.0	0.426	1.570	1.268	0.683	0.780	0.876
4.0	1000.0	0.397	1.570	1.268	0.700	0.784	0.892
4.0	1000.0	0.371	1.570	1.268	0.715	0.788	0.907
						mean	0.961
						COV	3.3%

Several methods and formulae to predict the compressive strength parameter of stiffened panel have been proposed, which can be divided into three categories:

[1] Effective width approach : by Faulkner[120] and Carlsen[180]

[2] Single parameter, λ formula : by Bjorhovde and Rondal and Maquoi (see reference [181])

[3] Two parameter, λ and β, formula: by Lin[125]

The proposed formula, Eq.(3.70) belongs to category 3. The methods and formulae by others are briefly described as follows:

o Method by Faulkner:

This method is based on the Johnson-Ostenfeld type formulation together with the effective width approach for plate behaviour, in which the effects of initial deflection and residual stress can be considered. Since the strength formula of axial compression for the stringer-stiffened cylinder, described in Section 3.3.1, has been derived based on the same approach adopted for the stiffened flat panel, the situation is similar, except that the curvature effect of the curved panel is to be removed. The compressive strength parameter is given by:

$$\phi = \frac{\sigma_u}{\sigma_Y} = \frac{\sigma_e}{\sigma_Y} = \left[\frac{A_{st} + b_e t}{A_{st} + b t}\right] \tag{3.71}$$

where A_{st} is the sectional area of stiffener, and the edge stress σ_e (or effective stress) is governed by the compression collapse of the stiffener and its associated plating. Thus, for column collapse from Johnson's parabola replacing σ_e by σ_c gives:

$$\sigma_e = \sigma_c \cong \sigma_Y \left(1 - 0.25\,\lambda_{ce}^2\right) \qquad \text{for } \lambda_{ce} \le \sqrt{2}$$

$$= \sigma_{cr} \qquad \text{for } \lambda_{ce} < \sqrt{2} \tag{3.72}$$

where σ_{cr} is the Euler buckling stress and the reduced slenderness parameter, λ_{ce}, is given by:

$$\lambda_{ce} = \frac{L_e}{\pi r_{ce}} \sqrt{\frac{\sigma_Y}{E}} \tag{3.73}$$

and

$$r_{ce} = \sqrt{\frac{I_e'}{A_{st} + b_e t}} \tag{3.74}$$

where L_e is the reduced effective length and I_e' the moment of inertia associated with the reduced effective width given by:

$$\frac{b_e'}{b} = \frac{1}{\beta} \sqrt{\frac{\sigma_Y}{\sigma_e}} \tag{3.75}$$

The effective width b_e of the plate relates to the slenderness as in Eq.(3.36). Due to the weld induced residual stress, the effective widths, b_e' and b_e , should be reduced by the factor R_r given by:

$$R_r = 1 - \frac{2\eta}{\frac{b}{t} - 2\eta} \left[\frac{\beta^2}{2\beta - 1} \right] \left[\frac{\beta - 1}{1.5} \right] \tag{3.76}$$

o Method by Carlsen:

This is based on the Perry-Robertson formulation, together with the effective width approach for the plate strength through parametric study by using the finite difference method. The compressive strength parameter, ϕ, is given by:

$$\phi = \frac{\sigma_u}{\sigma_y} = \frac{A_e}{A}\frac{(1+\gamma+\xi)-\sqrt{(1+\gamma+\xi)^2-4\gamma}}{2\gamma} \qquad (3.77)$$

where

$$\gamma = \frac{\sigma_Y}{\sigma_{cr}}$$

$$\xi = \frac{A\,\delta_S}{Z}$$

A = sectional area of stiffener-plate combined section

Z = section modulus $\qquad \delta_S$ = stiffener initial deflection

When calculating σ_{cr} and Z, the plate is considered to be fully effective due to its small influence on the strength of the stiffened panel.

The stiffener initial deflection, δ_S is always assumed to be δ_S = 0.0015 L. But for plate induced collapse, account is taken for the shift of neutral axis due to loss of effectiveness of plate by modifying δ_S as follows:

$$\delta_S = 0.0015\,L + Z_p\left[\frac{A}{A_e} - 1\right] \qquad (3.78)$$

in which A_e is the effective sectional area calculated with the effective width, b_e. In the case of plate induced collapse, b_e, is given, similar to Eq.(3.36), by:

$$\frac{b_e}{b} = \frac{1.8}{\beta} - \frac{0.8}{\beta^2} \le 1.0 \qquad (3.79.a)$$

In the case of stiffener induced collapse:

$$\frac{b_e}{b} = 1.1 - 0.1\,\beta \leq 1.0 \qquad (3.79.b)$$

o Single Parameter Formula:

Bjorhovde derived the following set of equation for the mean value of collapse strength based on test data and based on three assumptions: (1) the initial imperfection is the same as the buckled shape of a pinned end elastic column (2) the maximum value of the initial imperfection, i.e. L/1000, is approximately equal to the maximum permissible tolerance and (3) there is no-end restraint. The formulae is given by:

$$\begin{aligned}
\phi = \frac{\sigma_{cr}}{\sigma_y} &= 1.0 && \text{for } \lambda \leq 0.15 \\
&= 1.035 - 0.202\,\lambda - 0.222\,\lambda^2 && \text{for } 0.15 < \lambda \leq 1.0 \\
&= -0.111 + \frac{0.636}{\lambda} + \frac{0.087}{\lambda^2} && \text{for } 1.0 < \lambda \leq 2.0 \\
&= 0.009 + \frac{0.877}{\lambda^2} && \text{for } 2.0 < \lambda \leq 3.6 \\
&= \frac{1}{\lambda^2} && \text{for } \lambda > 3.6
\end{aligned} \qquad (3.80)$$

in which λ is the slenderness parameter associated with plate width and is calculated from Eq.(3.67). To avoid the operational complications arising from five different cases, Rondal and Maquoi (see reference [181]) suggested the following single equation to replace the last five equations for $\lambda > 0.15$:

$$\phi = \frac{Y - \sqrt{Y^2 - 4\lambda^2}}{2\lambda^2} \qquad (3.81)$$

where $Y = 0.956 + 0.293\,\lambda + \lambda^2$

o Two parameter formula:

Lin[125] derived the ϕ equation based on the parametric study by using the dynamic relaxation method in terms of the two slenderness parameters, λ and β, such that it fitted best to numerical results. The plate width was considered to be fully effective when calculating the slenderness parameters as for the present proposed equation (3.70). The formula was assumed to have the form of:

$$\phi = \frac{1}{\sqrt{C_1 + C_2\lambda^2 + C_3\beta^2 + C_4\lambda^2\beta^2 + C_5\lambda^4}} \qquad (3.82.a)$$

Through a curve fitting method with numerical data for the stiffened panels, the coefficients, C_1 to C_5, were determined as follows:

$$C_1 = 0.960 \qquad C_2 = 0.765 \qquad C_3 = 0.176$$
$$C_4 = 0.131 \qquad C_5 = 1.046 \qquad (3.82.b)$$

The predictions of ϕ by the proposed equation (3.70) are compared with test data by Faulkner[182] and by Horne et al[181,184]. Table 3.7 shows the comparisons with test data by Faulkner, and Tables 3.8 - 3.10 with test data by Horne et al, in which ϕ_e's denotes the compressive strength parameters by test and ϕ_p's predicted values by the proposed equation. Figures in the tables are ratio of two ϕ values, i.e., ϕ_e/ϕ_p.The predicted value of ϕ_p's by other methods and formulae are also included to compare the results by the present formula [Eq.(3.70)] with their results. Table 3.11 summaries the results of Tables 3.7 to 3.10.

The method by Faulkner, Eqs.(3.71) to (3.77), and the proposed equation (3.70) show good agreement with test data, and gives the mean value of the ratio (ϕ_e/ϕ_p) close to unity and low COV such that they are always less than 10% for all cases of test models. For all test models both methods give COVs of 7.2% and 7.8%, respectively. This implies that the two methods well satisfy the recommended requirements for

strength formula as mentioned in Section 2.4.2[119,163]. The prediction by Carlsen's method almost always much underestimates the ϕ values and shows higher COVs, except for stiffener induced collapse test models by Horne et al., such that mean of the ratio (ϕ_e/ϕ_p) is underestimated by 10 to 28% and COV's are around 10%, but less than 13% [see Section 2.4.2]. For all test models it gives a mean of the ratio, ϕ_e/ϕ_p , of 1.16 and COV about 12%. The prediction by Lin's formula, Eq.(3.82), shows a similar tendency to Carlsen's. While Rondal and Maquoi's formula, Eq.(3.81), [Bjorhovde's formula, Eq.(3.80) is similar to this] usually much over-estimates the strength and shows much fluctuation such that the mean of the ratio, ϕ_e/ϕ_p in some cases is lower by about 10 or 18% and COVs usually greater than other prediction methods and formulae.

Comparisons of the predicted value, ϕ_p, with test results, ϕ_e, are plotted in Figs. 3.11 to 3.15 for the above prediction methods and formula, except for Bjorhovde's because of its similar nature to Rondal and Maquoi's.

Comparison should be done with test data under the combined axial compression and lateral pressure. However, since there is only a very limited number of available test results, comparison cannot be done within a wide range. In this study a test series carried out by Smith[185] is selected. Comparison between ϕ_p by the proposed equation (3.70) with test results, ϕ_e, is listed in Table 3.12 and plotted in Fig. 3.16. The COV of the ratio, ϕ_e/ϕ_p, is relatively higher than those of the previous cases, but comparatively good agreements are obtained by the proposed equation.

In conclusion, the present formula, Eq.(3.70), in spite of its simplified nature, generally gives a satisfactory prediction of the compressive strengths of stiffened panels compared with the test results and those of other prediction methods and formulae. One shortcoming of the formula is that it cannot reflect the change in magnitudes of imperfections, such as residual stress and the initial deflection of plate and stiffener, because, in the present parametric study, the imperfections have been uniquely imposed. However, since the imperfection levels were appropriately selected to be suitable for the practical structures with reference to the tolerance recommended in various design codes,

it can be said that the proposed formula has validity in the practical sense. Further comparisons should probably be carried out for the combined loading case of axial compression and lateral pressure.

The proposed formula, Eq.(3.70) is plotted in the form of ϕ_p - λ curves when β = 0.0, 1.0, 1.5, 2.0, 2.5 and 3.0 in Fig. 3.17.

Table 3.7 Comparison of Predicted Compressive Parameter (ϕ_p) with Test Results (ϕ_e) Tested by Faulkner[182]

Test Model	λ	β	ϕ_e	Prediction Method (ϕ_e / ϕ_p)				
				Faulkner	Carlsen	Rondal	Lin	Present
P1	0.276	1.04	0.976	1.024	1.074	0.962	1.080	0.935
P2	0.303	2.01	0.733	0.978	1.031	0.953	0.983	1.055
P4	0.304	3.99	0.567	0.986	1.179	0.953	1.139	0.939
P5	0.534	0.99	0.824	0.923	1.032	0.870	1.000	1.057
P6	0.599	1.98	0.750	1.001	1.135	0.841	1.123	0.966
P8	0.622	4.16	0.515	0.984	1.224	0.831	1.190	0.927
P9	0.822	1.02	0.716	0.922	1.136	0.722	1.069	1.071
P10	0.897	1.97	0.660	1.031	1.218	0.676	1.207	0.949
P11	0.973	3.03	0.494	1.018	1.226	0.727	1.145	0.982
P12	0.939	4.19	0.448	1.032	1.333	0.649	1.232	0.897
P13	0.411	1.02	0.988	1.063	1.201	0.917	1.137	0.905
P14	0.298	2.04	0.764	0.993	1.116	0.955	1.030	1.007
P15	0.335	2.96	0.569	1.016	1.067	0.943	0.940	1.127
P16	0.341	4.05	0.506	1.040	1.185	0.941	1.037	1.035
P17	0.796	0.98	0.822	0.991	1.314	0.738	1.195	0.952
P18	0.580	1.98	0.656	0.919	1.014	0.850	0.973	1.112
P19	0.691	3.09	0.563	1.149	1.242	0.796	1.103	1.003
P20	0.687	4.12	0.455	1.036	1.236	0.798	1.076	1.030
P21	1.242	1.03	0.696	1.121	1.715	0.467	1.561	0.788
P22	0.893	2.04	0.515	0.885	1.120	0.678	0.950	1.204
P23	1.024	3.04	0.491	1.178	1.454	0.595	1.183	0.948
P24	1.017	4.02	0.384	1.024	1.366	0.599	1.080	1.018

Table 3.8 Comparison of Predicted Compressive Parameter (ϕ_p) with Test Results (ϕ_e) Tested by Horne et al[183,184] : Plate Induced Collapse

Test Model	λ	β	ϕ_e	Prediction Method (ϕ_e / ϕ_p)				
				Faulkner	Carlsen	Rondal	Lin	Present
7	0.44	1.70	0.79	0.950	1.041	0.871	1.039	1.010
8	0.43	1.72	0.85	1.023	1.115	0.934	1.118	0.938
11	0.45	1.70	0.79	0.962	1.045	0.875	1.043	1.008
12	0.44	1.70	0.79	0.950	1.041	0.871	1.039	1.010
13	0.45	1.69	0.75	0.912	0.991	0.831	0.988	1.063
14	0.44	1.70	0.83	0.996	1.092	0.915	1.091	0.962
A11	0.53	2.84	0.55	0.969	1.007	0.631	0.948	1.142
A21	0.52	2.88	0.64	1.124	1.170	0.731	1.108	0.977
A12	0.53	2.86	0.56	1.000	1.048	0.643	0.970	1.117
A23	0.52	2.91	0.62	1.068	1.105	0.708	1.080	1.002
A22	0.51	2.83	0.56	0.990	1.007	0.637	0.956	1.130
PF2	0.73	0.87	0.78	0.931	1.023	1.006	1.061	1.051
PF5	0.79	0.90	0.79	1.002	1.114	1.066	1.132	1.003
PF11	0.79	0.88	0.72	0.948	1.050	0.971	1.029	1.104
SW1	0.85	1.70	0.71	1.083	1.253	1.007	1.197	0.955
SW3	0.85	1.70	0.71	1.081	1.245	1.007	1.197	0.955
SW5	0.85	1.70	0.64	0.976	1.104	0.908	1.079	1.059
SW7	0.85	1.70	0.69	1.076	1.235	0.978	1.163	0.982

Table 3.9 Comparison of Predicted Compressive Parameter (ϕ_p) with Test Results (ϕ_e) Tested by Horne et al[183,184] : Stiffener Induced Collapse

Test Model	λ	β	ϕ_e	Prediction Method (ϕ_e / ϕ_p)				
				Faulkner	Carlsen	Rondal	Lin	Present
3	0.24	1.73	0.85	1.004	1.094	0.874	1.061	0.965
9	0.48	1.72	0.78	0.969	1.053	0.875	1.047	1.010
FS4	0.86	0.84	0.67	0.833	0.985	0.969	1.025	1.145
FS9	0.84	0.83	0.75	0.929	1.097	1.054	1.114	1.036
AS2	0.66	0.82	0.81	0.936	0.993	0.997	1.040	1.050
AF2	0.65	0.81	0.89	1.007	1.037	1.089	1.133	0.961

Table 3.10 Comparison of Predicted Compressive Parameter (ϕ_p) with Test Results (ϕ_e) Tested by Horne et al[183,184] : Overall Collapse

Test Model	λ	β	ϕ_e	Prediction Method (ϕ_e / ϕ_p)				
				Faulkner	Carlsen	Rondal	Lin	Present
D11	1.11	1.73	0.63	1.024	1.482	1.163	1.336	0.882
D21	1.04	1.62	0.57	0.858	1.264	0.975	1.118	1.055
D12	1.02	1.59	0.65	0.962	1.425	1.088	1.247	0.945
D22	1.07	1.67	0.60	0.911	1.366	1.060	1.217	0.969
E11	1.17	2.92	0.47	1.111	1.205	0.928	1.243	0.893
E21	1.15	2.87	0.44	1.034	1.131	0.849	1.137	0.981
E12	1.17	2.92	0.48	1.134	1.230	0.948	1.270	0.874
E23	1.16	2.90	0.45	1.053	1.146	0.878	1.177	0.945

Table 3.11 Summary of Comparison of Predicted Compressive Parameter (ϕ_p) with Test Results (ϕ_e) Tested by Faulkner[182] and by Horne et al[183,184]
: mean and COV of ratio, ϕ_e/ϕ_p

Test Model	Prediction Method (ϕ_e / ϕ_p)				
	Faulkner	Carlsen	Rondal	Lin	Present
all models tested by Faulkner (22 models)	1.014 [6.9%]	1.120 [12.9%]	0.826 [26.7%]	1.111 [11.6%]	0.996 [8.8%]
plate induced collapse models tested by Horne et al. : Case 1 (18 models)	1.002 [5.9%]	1.094 [7.4 %]	0.866 [15.7%]	1.069 [6.9%]	1.026 [6.1%]
stiffener induced collapse models tested by Horne et al. : Case 2 (6 models)	0.946 [6.2%]	1.043 [4.2%]	0.976 [8.4%]	1.070 [3.7%]	1.028 [6.2%]
overall collapse models tested by Horne et al. : Case 3 (8 models)	1.011 [8.8%]	1.281 [9.5%]	0.986 [10.3%]	1.218 [5.5%]	0.943 [6.0%]
all models tested by Horne et al. (32 models)	0.994 [7.2%]	1.131 [11.0%]	0.917 [14.5%]	1.106 [8.4%]	1.005 [6.9%]
all models tested by Faulkner and by Horne et al. (54 models)	1.002 [7.2 %]	1.163 [12.4%]	0.880 [20.4%]	1.108 [9.9%]	1.001 [7.8%]

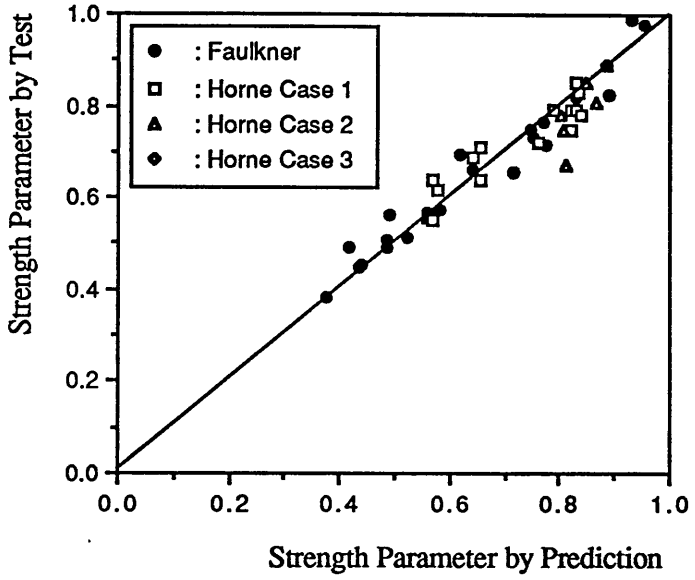

Fig. 3.11 Comparison between ϕ_e and ϕ_p by Faulkner

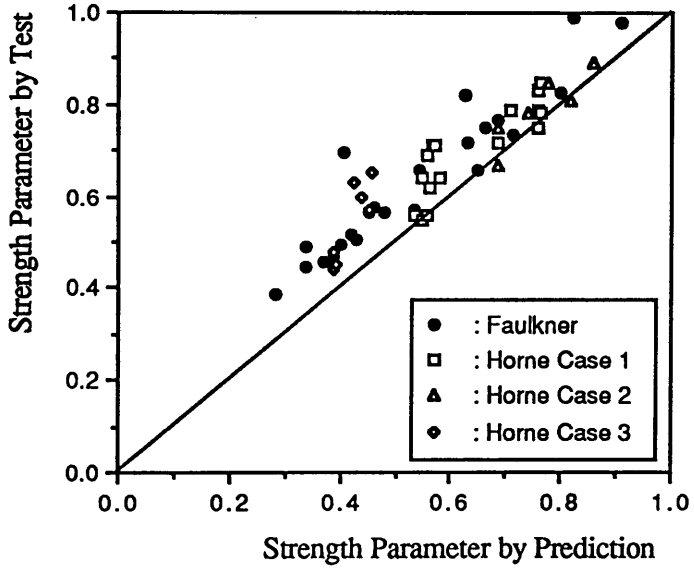

Fig. 3.12 Comparison between ϕ_e and ϕ_p by Carlsen

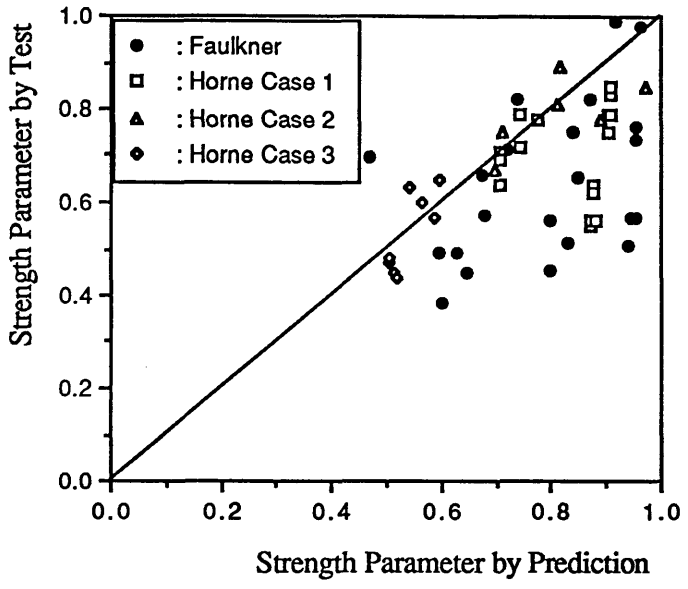

Fig. 3.13 Comparison between ϕ_e and ϕ_p by Rondal and Maquoi

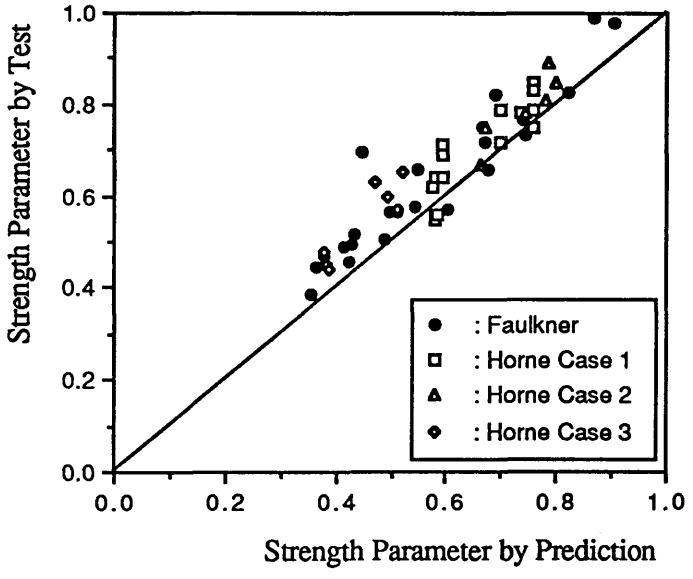

Fig. 3.14 Comparison between ϕ_e and ϕ_p by Lin

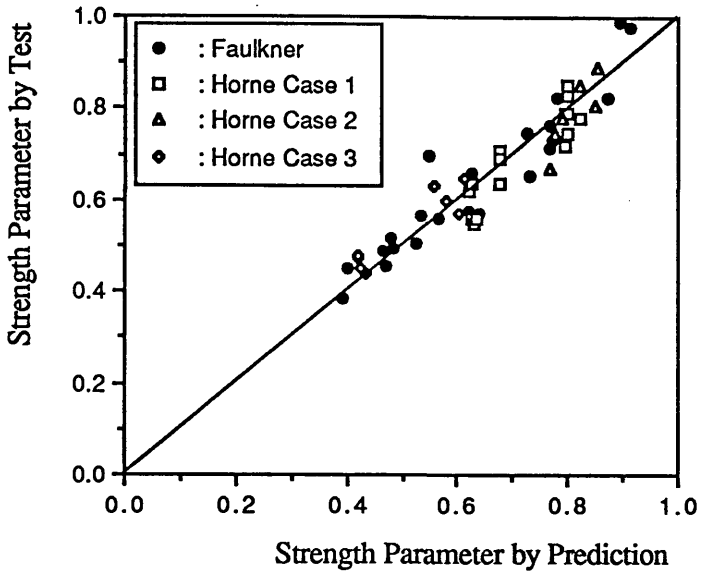

Fig. 3.15 Comparison between ϕ_e and ϕ_p by Proposed Formula

Table 3.12 Comparison of Predicted Compressive Parameter (ϕ_p) by the Proposed Formula with Test Results (ϕ_e) Tested by Smith[185]
: under the Combined Axial Compression and Lateral Pressure

Test Model	λ	β	w' (psi)	ϕ_e	ϕ_e / ϕ_p
1B	0.23	2.72	15	0.73	1.177
2A	0.42	1.42	7	0.91	1.094
3A	0.70	1.68	3	0.69	0.945
4A	0.53	1.43	8	0.83	1.030
				mean	1.062
				COV	8.0%

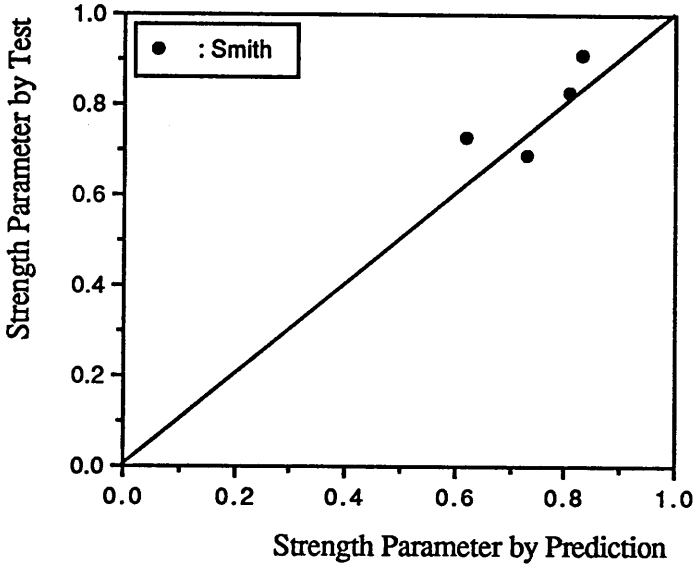

Fig. 3.16 Comparison between ϕ_e by Smith and ϕ_p by Proposed Formula

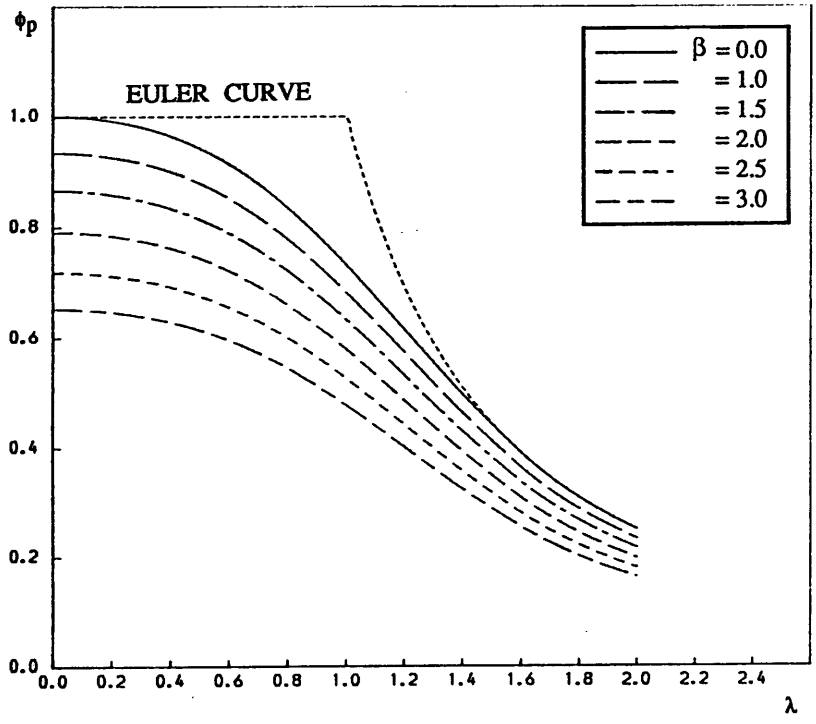

Fig. 3.17 Compressive Strength Curves of Stiffened Panels (lateral pressure = 0)

In the following three sections strength formulae for ultimate compressive force, F_{xu} and for ultimate bending moment, M_u, are separately derived in terms of the compressive strength parameter, ϕ, of the stiffened panel through regression based on numerical results of the parametric study for the rectangular sections, as mentioned in Section 3.4.2. The interaction equation under the combined axial compression and bi-axial bending moments will be introduced which has also been derived based on the numerical results of different levels of each loading.

3.4.4 Ultimate Compressive Strength

Taking into account the effect of "hard corner" the equilibrium concept gives the equation predicting the ultimate axial compressive strength, F_{xu}. That is derived as:

$$F_{xu} = F_Y (\gamma_B \phi_B + \gamma_S \phi_S + \gamma_D \phi_D) \tag{3.83}$$

where F_Y is the fully plastic axial compression given by:

$$F_Y = \int_A \sigma_Y \, dA$$

and ϕ_B, ϕ_S and ϕ_D are the compressive strength parameters, given as Eq.(3.70), of the stiffened panels in bottom, side shell and deck, respectively. γs are the relative area ratio defined as:

$$\begin{aligned} \gamma_B &= A_B / A_T && \text{for bottom} \\ \gamma_S &= A_S / A_T && \text{for one-side shell} \\ \gamma_D &= A_D / A_T && \text{for deck} \\ \gamma_{HC} &= A_{HC} / A_T && \text{for " hard corner "} \end{aligned} \tag{3.84}$$

where A_T is the total sectional area, and A_B, A_S and A_D are areas of stiffener-plate combination in the bottom, one-side shell, and deck, respectively. The area of hard corner, A_{HC}, is:

$$A_{HC} = A_T - (A_B + 2A_S + A_D) \tag{3.85}$$

Eq.(3.83) implies that at the ultimate state the load allocated on the components in bottom, side shell, deck and hard corner are proportional to their load carrying capacities. In this study, "hard corner" is regarded as the portion of the section of which stress-strain relation was expected to follow the material behaviour.

Comparison of the ultimate compressive strengths predicted by Eq.(3.83) with numerically predicted ones are listed in Table 3.13 for 20 cases. They are plotted in Fig. 3.18. Eq.(3.83) shows very close correlation with the numerical results.

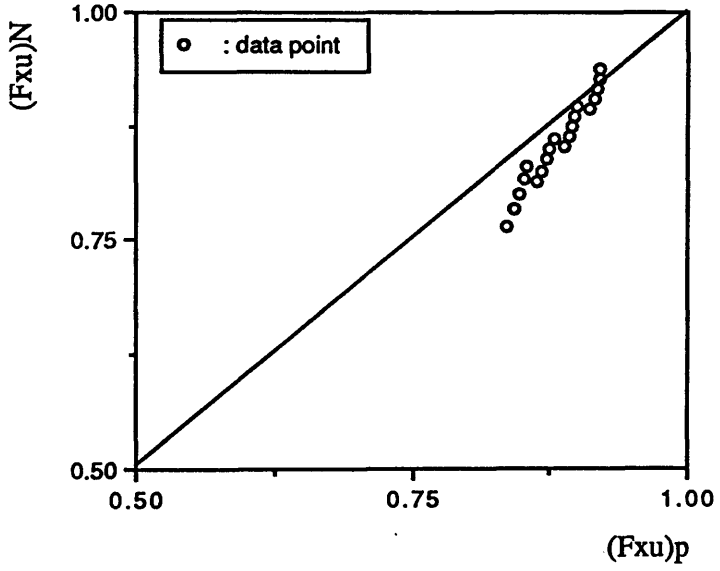

Fig. 3.18 Comparison between Numerical and Predicted Ultimate Compressive Strength

Table 3.13 Comparison of Ultimate Compressive Strengths:
by Eq.(3.83), $(F_{xu})_p$, and Numerically Calculated Ones, $(F_{xu})_N$
(B/H = 0.857, stiffener case 1)

L/b	b	$(F_{xu})_N$	$(F_{xu})_p$	$(F_{xu})_N / (F_{xu})_p$
2.0	700.0	0.936	0.921	1.017
2.5	700.0	0.927	0.919	1.008
3.0	700.0	0.916	0.917	0.999
3.5	700.0	0.905	0.915	0.989
4.0	700.0	0.893	0.912	0.979
2.0	800.0	0.897	0.900	0.997
2.5	800.0	0.886	0.898	0.987
3.0	800.0	0.875	0.895	0.978
3.5	800.0	0.863	0.892	0.967
4.0	800.0	0.852	0.889	0.959
2.0	900.0	0.861	0.878	0.981
2.5	900.0	0.851	0.875	0.972
3.0	900.0	0.839	0.872	0.962
3.5	900.0	0.826	0.868	0.952
4.0	900.0	0.813	0.863	0.942
2.0	1000.0	0.831	0.855	0.972
2.5	1000.0	0.817	0.851	0.959
3.0	1000.0	0.800	0.847	0.944
3.5	1000.0	0.783	0.842	0.930
4.0	1000.0	0.765	0.836	0.916
			mean	0.971
			COV	2.6%

3.4.5 Ultimate Bending Moment

Several strength formula estimating the ultimate bending moment for a ship's hull girder, including buckling, have been proposed[98,99,125,186-188]. In the present study the strength formula for the ultimate bending moment has been derived based on the concept proposed by Faulkner and Sadden[99] and the equation of systematic error was derived through the regression analysis to best fit its prediction to results of the parametric study.

As in reference [99], the ultimate bending moment, M_u (M_{yu} or M_{zu}), is given by:

$$M_u = Z\sigma_u(1+\zeta_s) = Z\sigma_{Y,av}\phi(1+\zeta_s) \tag{3.86}$$

where Z is the section modulus of the section associated with the bending about y- or z-axis [Fig. 3.3], ζ_s is a systematic error to consider the margin between the moments at which compression collapse occurs in the weakest portion of the section, and the ultimate bending moment, ϕ, is the compressive strength parameter defined as Eq.(3.70), and $\sigma_{Y,av}$ is the average yield stress of stiffener-plate combination. A systematic error was derived as a function of slendernesses, i.e. λ and β, the slenderness of the stiffened panel and that of the associated plate at the weakest portion, and the area ratio between the compressive part and the web part of the section. It was assumed to have a form of:

$$\zeta_s = C_1 + \frac{C_2}{\sqrt{\frac{A_1}{A_2}}} \tag{3.87.a}$$

where A_1 and A_2 are areas of compression flange and web. C_1 and C_2 are coefficients, which have been derived through regression analysis as follows:

$$\begin{aligned} C_1 &= -0.329 + 2.160\,\lambda\beta - 4.041\,\lambda^2\beta \\ C_2 &= 0.423 - 1.657\,\lambda\beta + 3.687\,\lambda^2\beta \end{aligned} \tag{3.87.b}$$

Tables 3.14(a) and (b) illustrate the numerical results under the ultimate bending moment about z-axis and y-axis respectively (16 cases for each direction), and also the systematic error calculated from the results. Comparison of the predicted systematic errors by Eq.(3.87) and the predicted ultimate bending moment predicted by Eq.(3.86) with numerically predicted ones are listed in Table 3.14(c), and plotted in Fig. 3.19(a) and (b), respectively. The predicted systematic error by Eq.(3.87) shows very close correlation with the numerical results such that mean of the ratio, $(\zeta_s)_N/(\zeta_s)_p$ is close to unity and its COV is 3.3 %. The predicted ultimate bending moments also show the same correlation except slightly lower mean of the ratio, $(M_{zu})_N/(M_{zu})_p$.

With Eqs.(3.83) and (3.86) the ultimate strength, when each loading is applied separately, can be obtained. The estimated ultimate bending moment by Eq.(3.86) is compared with the test results by Dowling et al[176] and by Reckling[177], and also with the numerically estimated ones discussed in Section 3.4.1.3. These are listed in Table 3.15. The ultimate bending moment by Eq.(3.86) seems to be reasonably satisfactory.

Table 3.15 Comparison of Ultimate Bending Moments (Test / Prediction)

Model	λ^{*1}	β^{*1}	$\phi_p{}^{*2}$	A_1/A_2	ζ_s	Eq.(3.86)	Ratio*3
Model 2	0.646	1.893	0.723	1.938	0.060	0.989	1.019
Model 4	0.491	0.794	0.902	1.539	0.129	0.938	1.020
Model 23	0.465	1.173	0.865	1.806	0.162	0.963	1.055

*1 : slenderness of stiffened panel and plate for weakest portion of section

*2 : compressive strength parameter predicted by Eq.(3.70)

*3 : ratio of the ultimate bending moment by test to that by Eq.(3.86)

Table 3.14 Comparison of Ultimate Bending Moments: by Proposed Equation, $(M_u)_p$ and Numerically Calculated Ones, $(M_u)_N$ when L/b = 4.0

(a) Numerical results of ζ_s and M_{zu}

Case	B/H	b	λ	β	ϕ_N	A_1 / A_2	$(\zeta_s)_N$	$(M_{zu})_N$
1	0.857	700	0.238	1.099	0.871	0.761	0.251	0.904
2	0.857	800	0.280	1.256	0.815	0.761	0.283	0.870
3	0.857	900	0.325	1.413	0.768	0.762	0.316	0.842
4	0.857	1000	0.371	1.570	0.715	0.762	0.370	0.818
5	0.75	700	0.238	1.099	0.871	0.646	0.263	0.904
6	0.75	800	0.280	1.256	0.815	0.646	0.294	0.869
7	0.75	900	0.325	1.413	0.768	0.646	0.328	0.841
8	0.75	1000	0.371	1.570	0.715	0.647	0.381	0.816
9	0.67	700	0.238	1.099	0.871	0.561	0.273	0.903
10	0.67	800	0.280	1.256	0.815	0.561	0.305	0.868
11	0.67	900	0.325	1.413	0.768	0.562	0.338	0.840
12	0.67	1000	0.371	1.570	0.715	0.562	0.392	0.815
13	0.60	700	0.238	1.099	0.871	0.496	0.283	0.903
14	0.60	800	0.280	1.256	0.815	0.496	0.314	0.867
15	0.60	900	0.325	1.413	0.768	0.496	0.348	0.839
16	0.60	1000	0.371	1.570	0.715	0.497	0.401	0.813

Table 3.14 (continued)

(b) Numerical results of ζ_s and M_{yu}

Case	B/H	b	λ	β	ϕ_N	A_1 / A_2	$(\zeta_s)_N$	$(M_{yu})_N$
17	0.857	700	0.227	1.021	0.892	1.216	0.167	0.922
18	0.857	800	0.267	1.166	0.836	1.216	0.199	0.891
19	0.857	900	0.310	1.312	0.788	1.216	0.227	0.862
20	0.857	1000	0.354	1.458	0.738	1.216	0.269	0.838
21	0.75	700	0.227	1.021	0.892	1.433	0.154	0.922
22	0.75	800	0.267	1.166	0.836	1.433	0.183	0.889
23	0.75	900	0.310	1.312	0.788	1.433	0.209	0.859
24	0.75	1000	0.354	1.458	0.738	1.433	0.252	0.835
25	0.67	700	0.227	1.021	0.892	1.650	0.143	0.921
26	0.67	800	0.267	1.166	0.836	1.650	0.170	0.887
27	0.67	900	0.310	1.312	0.788	1.650	0.196	0.857
28	0.67	1000	0.354	1.458	0.738	1.649	0.236	0.831
29	0.60	700	0.227	1.021	0.892	1.868	0.135	0.921
30	0.60	800	0.267	1.166	0.836	1.867	0.162	0.886
31	0.60	900	0.310	1.312	0.788	1.866	0.185	0.855
32	0.60	1000	0.354	1.458	0.738	1.866	0.220	0.827

Table 3.14 (continued)

(c) Comparison

Case	ϕ_c	$(\zeta_s)_N$	$(\zeta_s)_c$	$(\zeta_s)_N / (\zeta_s)_c$	$(M_u)_N$	$(M_u)_c$	$(M_u)_N/(M_u)_c$
1	0.887	0.251	0.236	1.065	0.904	0.909	0.994
2	0.856	0.283	0.266	1.064	0.870	0.902	0.965
3	0.823	0.316	0.303	1.044	0.842	0.894	0.943
4	0.788	0.370	0.348	1.065	0.818	0.887	0.922
5	0.887	0.263	0.257	1.023	0.904	0.916	0.987
6	0.856	0.294	0.286	1.030	0.869	0.907	0.958
7	0.823	0.328	0.324	1.012	0.841	0.899	0.936
8	0.788	0.381	0.372	1.024	0.816	0.894	0.913
9	0.887	0.273	0.277	0.987	0.903	0.922	0.979
10	0.856	0.305	0.304	1.001	0.868	0.912	0.952
11	0.823	0.338	0.343	0.984	0.840	0.904	0.929
12	0.788	0.392	0.396	0.991	0.815	0.901	0.905
13	0.887	0.283	0.296	0.956	0.903	0.928	0.972
14	0.856	0.314	0.321	0.977	0.867	0.916	0.947
15	0.823	0.348	0.361	0.963	0.839	0.908	0.924
16	0.788	0.401	0.417	0.960	0.813	0.907	0.897
17	0.897	0.167	0.170	0.981	0.922	0.930	0.991
18	0.869	0.199	0.201	0.987	0.891	0.928	0.960
19	0.838	0.227	0.234	0.968	0.862	0.922	0.935
20	0.805	0.269	0.266	1.011	0.838	0.912	0.918
21	0.897	0.154	0.154	1.004	0.922	0.927	0.995
22	0.869	0.183	0.186	0.984	0.889	0.926	0.960
23	0.838	0.209	0.219	0.955	0.859	0.921	0.933
24	0.805	0.252	0.249	1.012	0.835	0.909	0.918
25	0.897	0.143	0.140	1.022	0.921	0.924	0.997
26	0.869	0.170	0.174	0.981	0.887	0.924	0.959
27	0.838	0.196	0.207	0.951	0.857	0.919	0.932
28	0.805	0.236	0.235	1.002	0.831	0.907	0.917
29	0.897	0.135	0.129	1.045	0.921	0.922	0.999
30	0.869	0.162	0.164	0.986	0.886	0.923	0.960
31	0.838	0.185	0.197	0.940	0.855	0.918	0.931
32	0.805	0.220	0.224	0.982	0.827	0.905	0.913
				mean : 0.999			mean : 0.948
				COV : 3.3%			COV : 3.1%

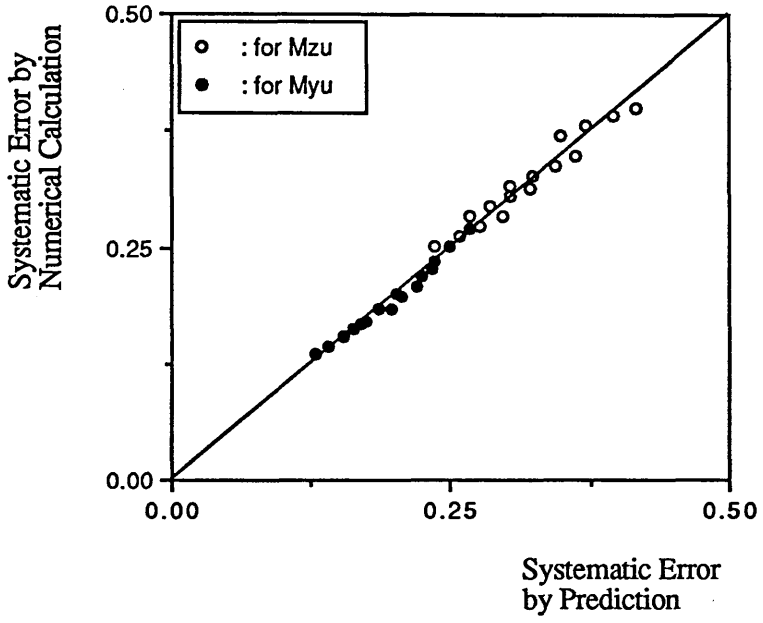

(a) Systematic Error : $(\zeta_s)_N$ and $(\zeta_s)_p$

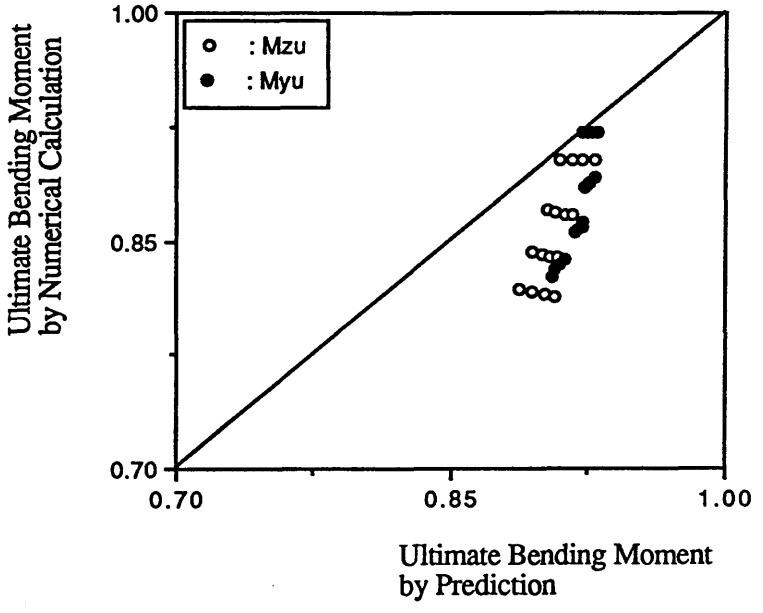

(b) Ultimate Bending Moment : $(M_u)_N$ and $(M_u)_p$

Fig. 3.19 Comparison of Systematic Error and Ultimate Bending Moments

Table 3.16 Details of a Typical Numerical Model

B = 9600.0 mm		H= 12800.0 mm			L = 2800.0 mm			B/H = 0.75
properties / component	lateral pressure MPa	plate t mm	plate E N/mm^2	plate σ_y N/mm^2	stiffener scantling mm	stiffener E N/mm^2	stiffener σ_Y N/mm^2	stiffener spacing mm
DECK	0.30	26	210000	350.0	350 x 13 x 150 x 25 T	210000	350	800
BOTTOM	0.40	30	210000	350.0	400 x 15 x 150 x 25 T	210000	350	800
SIDE SHELL	0.35	28	210000	350.0	375 x 14 x 150 x 25 T	210000	350	800

total sectional area		1.6561 m^2
elastic neutral axis from midplan of bottom plate		6.17 m
plastic neutral axis from midplan of bottom plate		6.01 m
moment of inertia about z-axis	z	39.87 m^4
about y-axis	Iy	26.13 m^4
fully plastic axial compression	F_y	577.79 MN
plastic bending moment about z-axis	Mzp	2563.47 MN-m
y-axis	Myp	2123.58 MN-m
nondimensional ultimate strength	Fxu / Fy	0.867
when applied separately	Mzu (+) / Mzp	0.877
	Mzu (-) / Mzp	0.905
	Myu / Myp	0.896

3.4.6 Combined Loading

In order to investigate the form of the interaction equation under the combined axial compression and bi-axial bending moments, numerical analysis has been carried out selecting a typical rectangular section [see Fig. 3.9]. Table 3.16 illustrates details of geometric and material parameters, initial deflections, etc. and the ultimate strengths, F_{xu}, M_{zu} and M_{yu} for the typical numerical model. The data are similar to those found in the Hutton TLP. Since the section is not symmetric about z-axis, there is a difference between the ultimate bending moment for sagging condition (positive M_z) and for hogging condition (negative M_z).

Using Eq.(3.65) and by varying the relative incremental rate of $\Delta\varepsilon_x$, $\Delta\phi_z$ and $\Delta\phi_y$ in the equation, two cases of numerical study have been performed to determine the form of the expected interaction equation.

Case 1 : Numerical analysis to investigate the relation between M_z and M_y
i.e the relation of bi-axial bending

Case 2 : Numerical analysis to investigate the relation between F_x
and bending moment, M_z and/or M_y
i.e. combined axial compression and bending moment

The numerical results for Case 1 are listed in Table 3.17, and based on these data an interaction equation under bi-axial bending moments has been derived as:

$$\left[\left(\frac{M_y}{M_{yu}}\right)^{1.8} + \left(\frac{M_z}{M_{zu}}\right)^{1.8} \right]^2 = 1 \qquad (3.88.a)$$

And, for Case 2 numerical results are listed in Table 3.18 when $M_y = 0$ and Table 3.19 when $M_z = 0$. Based on these data the relation between axial compression and bending moment has been derived as:

$$\frac{F_x}{F_{xu}} + \left[\frac{M}{M_u}\right]^{3.6} = 1 \qquad (3.88.b)$$

where M is M_Z or M_y. Combining Eqs.(3.88.a) and (3.88.b), the interaction equation under the combined axial compression and bi-axial bending moments is given by:

$$\frac{F_x}{F_{xu}} + \left[\left(\frac{M_y}{M_{yu}}\right)^{1.8} + \left(\frac{M_z}{M_{zu}}\right)^{1.8}\right]^2 = 1.0 \qquad (3.89)$$

When hull girder is under the bi-axial bending moments, circular formula was proposed by Faulkner et al[127].

$$\left[\frac{M_z}{M_{zu}}\right]^2 + \left[\frac{M_y}{M_{yu}}\right]^2 = 1 \qquad (3.90)$$

The predicted ultimate strength by proposed Eq.(3.89) and by the circular formula Eq.(3.90) are compared with the numerical results of Case 1, as illustrated in Table 3.17 and Fig. 3.20. As far as the present numerical results are concerned, Eq.(3.89) gives a mean value closer to unity and a lower COV than Eq.(3.90). As can be seen in Fig. 3.20, the circular formula slightly over-estimates the limit state. Hence, it can be said that Eq.(3.89) better represents the limit state than Eq.(3.90). Comparison between the predictions by Eq.(3.92) and the numerical results of Case 2 are summarised in Tables 3.18 and 3.19 and shown in Figs. 3.21 and 3.22. The agreement with numerical results is satisfactory.

Further calculations have been carried out when the rectangular box-girder is under the combined axial compression and bi-axial bending loading condition. The numerical results can be seen in Table 3.20 with the predictions by Eq.(3.89). It can be seen that the proposed strength formula well represents the limit state close to numerical results as for the previous cases.

Since there is no available test data for a rectangular box-girder under the combined loading condition, the proposed strength formula can not be compared. The interaction equation, Eq.(3.89), under the combined axial compression and bi-axial bending moments is plotted to demonstrate the shape changes of limit surface to various different loading levels. Fig 3.23(a) shows the relation between M_Z/M_{Zu} and M_y/M_{yu} when F_X/F_{Xu} are 0.0, 0.25, 0.50, 0.75, and Fig. 3.23(b) the relation between F_X/F_{Xu} and M_Z/M_{Zu} when M_y/M_{yu} are 0.0, 0.25, 0.50, 0.75. In Fig. 3.23(a) there seems to be no shape change of the failure surface for bi-axial bending and it is shown that, as axial compression increases, the interaction effect between axial compression and bending on the limit state becomes more and more apparent, although axial compression was increased at the same rate. In Fig. 3.23(b) it can be seen that as the bending moment, M_y, increases, the shape change of the failure surface between axial compression, F_X, and bending moment, M_Z, becomes apparent and the interaction effect is more significant than in Fig. 3.23(a). The shapes of failure surface between F_X and M_y are the same as Fig. 3.23 (b).

Table 3.17 Comparison of Eqs.(3.89) and (3.90) with Numerical Results of Case 1 Under Bi-Axial Bending : M_z/M_{zu} vs M_y/M_{yu} when $F_x/F_{xu} = 0$

No.	M_z/M_{zu}	M_y/M_{yu}	Eq.(3.89)	Eq.(3.90)
1	1.000	0.000	1.000	1.000
2	0.969	0.202	1.002	0.959
3	0.883	0.397	0.978	0.879
4	0.743	0.576	0.914	0.781
5	0.607	0.714	0.907	0.771
6	0.479	0.828	0.959	0.837
7	0.332	0.925	1.012	0.932
8	0.177	0.982	1.022	0.989
9	0.000	1.000	1.000	1.000
10	– 0.174	0.985	1.032	1.000
11	– 0.329	0.937	1.052	0.975
12	– 0.476	0.844	0.999	0.881
13	– 0.609	0.726	0.944	0.807
14	– 0.750	0.582	0.948	0.813
15	– 0.888	0.400	0.999	0.899
16	– 0.970	0.204	1.007	0.965
17	– 1.000	0.000	1.000	1.000
		Mean	0.987	0.911
		COV	3.9%	8.9%

Table 3.18 Comparison of Eq.(3.89) with Numerical Results of Case 2 Under the Combined Axial Compression and Bending Moment : F_x/F_{xu} vs M_z/M_{zu} when $M_y/M_{yu} = 0$

No	F_x/F_{xu}	M_z/M_{zu}	Eq.(3.89)	No	F_x/F_{xu}	M_z/M_{zu}	Eq.(3.89)
1	0.000	1.000	1.000	16	0.991	– 0.179	0.993
2	0.068	0.976	0.986	17	0.979	– 0.310	0.994
3	0.150	0.957	1.003	18	0.937	– 0.487	1.012
4	0.272	0.908	0.978	18	0.819	– 0.671	1.057
5	0.437	0.859	1.015	20	0.626	– 0.808	1.090
6	0.570	0.814	1.047	21	0.398	– 0.899	1.079
7	0.651	0.774	1.049	22	0.200	– 0.944	1.053
8	0.763	0.704	1.046	23	0.154	– 0.961	1.021
9	0.826	0.647	1.035	24	0.000	– 1.000	1.000
10	0.901	0.540	1.010				
11	0.934	0.475	1.003				
12	0.956	0.401	0.993				
13	0.974	0.306	0.988				
14	0.986	0.178	0.988				
15	1.000	0.000	1.000				
						Mean	1.018
						COV	3.0%

Table 3.19 Comparison of Eq.(3.89) with Numerical Results Under the Combined Axial Compression and Bending Moment: F_x/F_{xu} vs M_y/M_{yu} when $M_z/M_{zu} = 0$

No	F_x/F_{xu}	M_z/M_{zu}	Eq.(3.89)	No	F_x/F_{xu}	M_z/M_{zu}	Eq.(3.89)
1	0.000	1.000	1.000	6	0.823	0.660	0.955
2	0.130	0.941	1.071	7	0.930	0.494	0.991
3	0.239	0.895	1.099	8	0.962	0.308	1.024
4	0.432	0.848	1.016	9	0.978	0.178	1.020
5	0.645	0.771	0.964	10	1.000	0.000	1.000
						Mean	1.014
						COV	4.1%

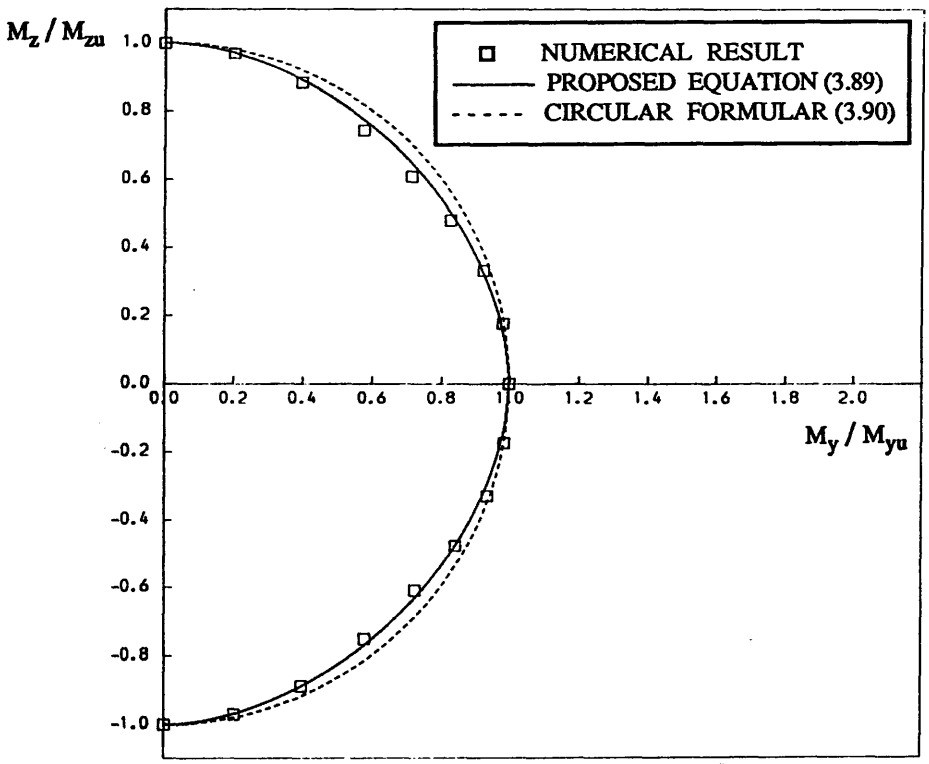

Fig. 3.20 Interaction Curves Between Bi-Axial Bending : M_z/M_{zu} vs M_y/M_{yu}

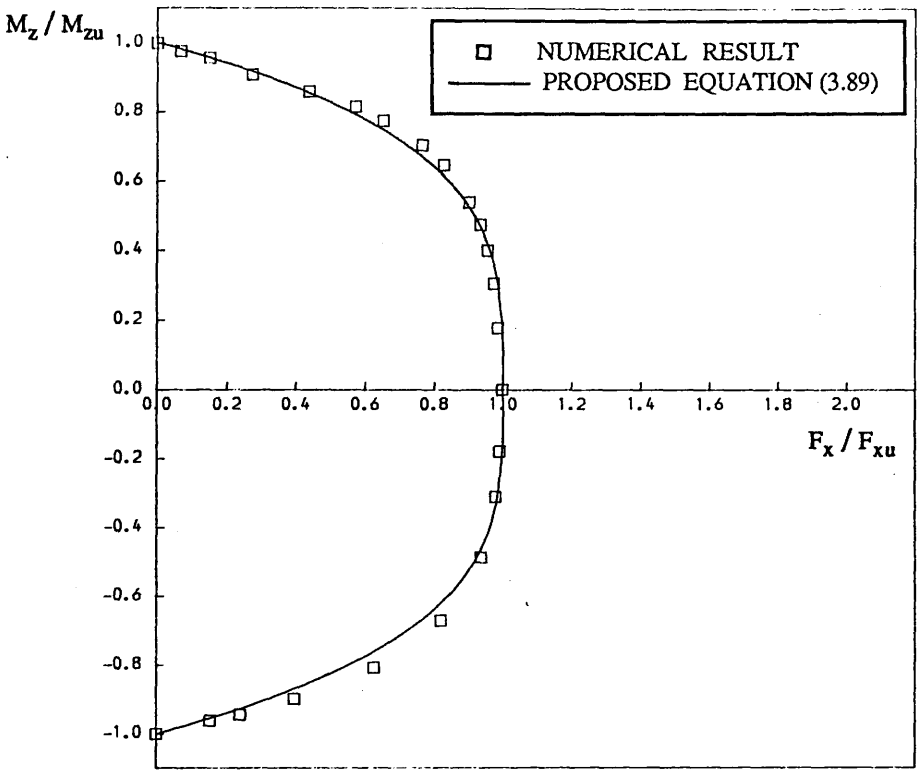

Fig. 3.21 Interaction Curves Between Axial Compression and Bending about z-axis : F_x/F_{xu} vs M_z/M_{zu}

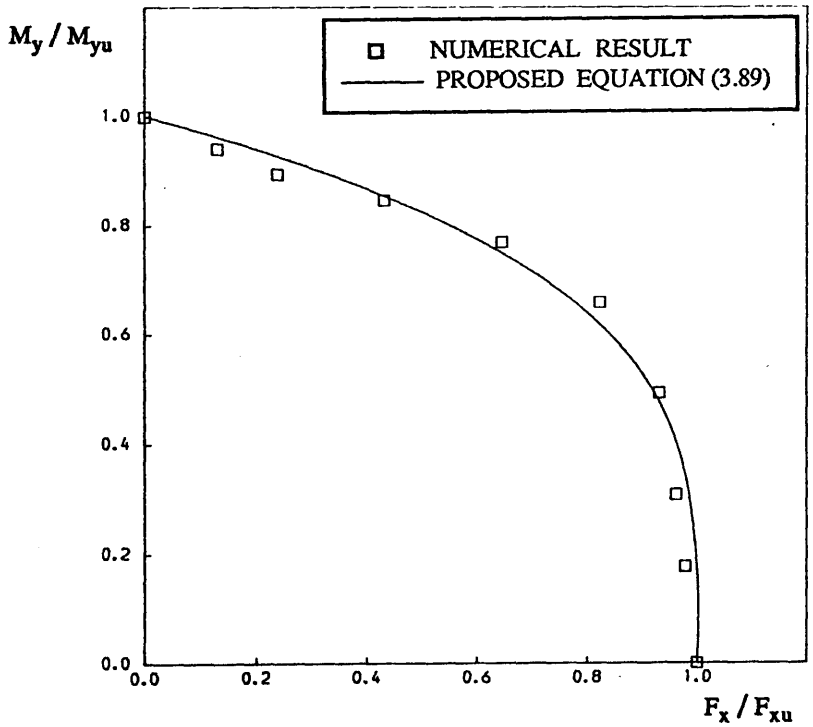

Fig. 3.22 Interaction Curves Between Axial Compression and Bending about y-axis : F_x/F_{xu} vs M_y/M_{yu}

Table 3.20 Comparison of Eq.(3.89) with Numerical Results Under the Combined Axial Compression and Bi-Axial Bending Moment

No	F_x/F_{xu}	M_z/M_{zu}	M_y/M_{yu}	Eq.(3.89)
1	0.914	0.105	0.482	0.996
2	0.864	0.305	0.445	0.987
3	0.836	0.386	0.420	0.988
4	0.720	0.603	0.336	1.024
5	0.633	0.552	0.454	0.975
6	0.579	0.508	0.553	0.988
7	0.458	0.788	0.221	0.965
8	0.385	0.730	0.380	0.937
9	0.287	0.568	0.637	0.936
10	0.129	0.822	0.390	0.915
			Mean	0.970
			COV	3.0%

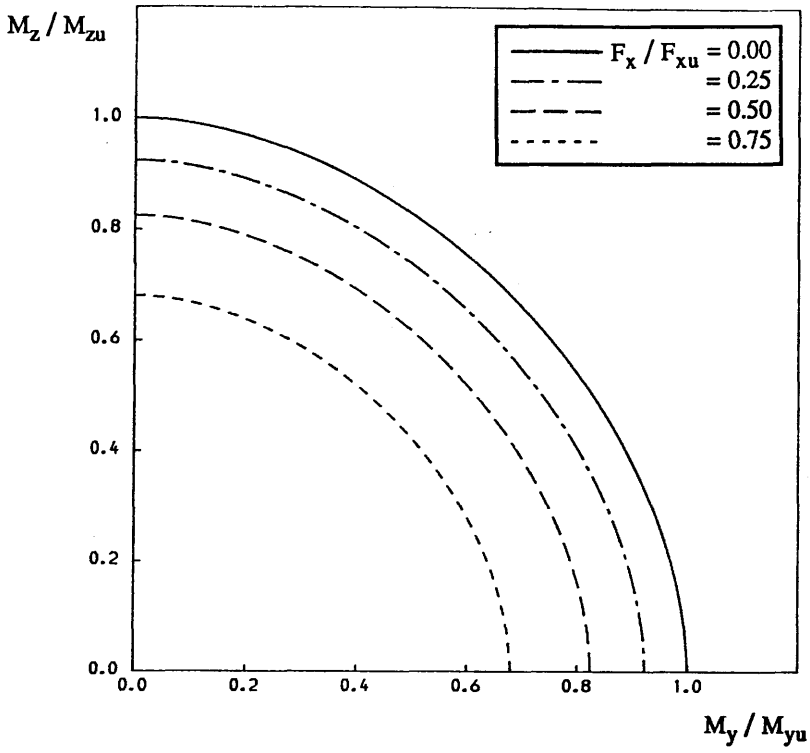

(a) M_z/M_{zu} vs M_y/M_{yu}

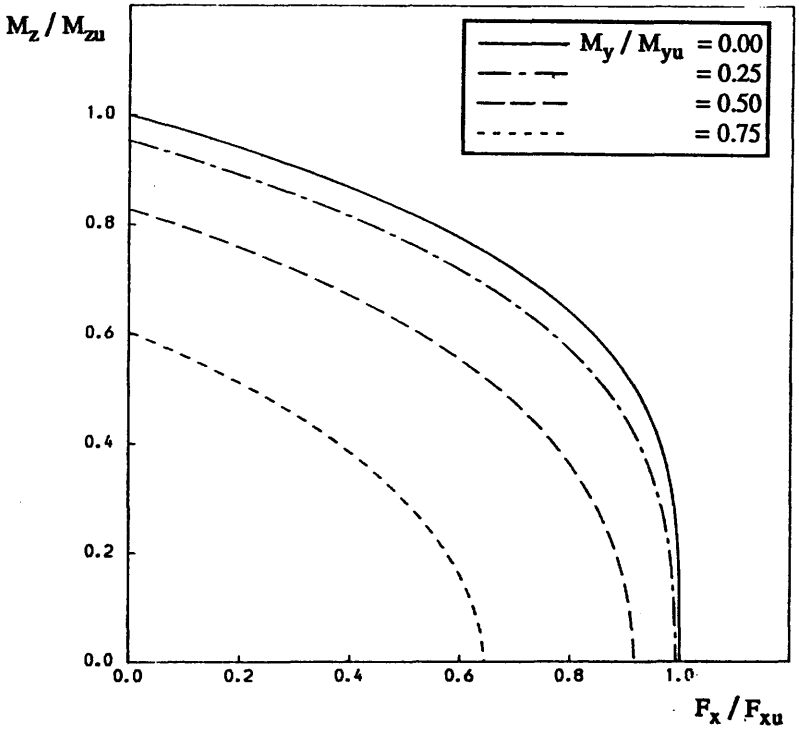

(b) F_x/F_{xu} vs M_z/M_{zu}

Fig.3.23 Interaction Curves

CHAPTER 4 LOADING FOR TLP STRUCTURES

4.1 Definitions

The system reliability analysis of a floating offshore structure generally consists of two main parts. The first one is estimating the environmental loadings acting on the structure during its life time and load effects and the second one is the reliability analysis, component and/or system reliability, using the appropriate algorithm.

In the context of structural design, estimating the environmental loads and their effects should be most important. For a TLP structure, when it is exposed to environmental conditions, external forces arise from various environmental phenomena, such as wave, wind, current, water pressure, gravity and interactions between structure and environmental phenomena. Since there are a number of uncertainties in environmental loading, loading model and load effects should be treated stochastically, and there should be more degree of uncertainty with loading than with strength because of more unknown factors affecting loads. Because of this in most design, the higher uncertainties associated with loading are usually reflected by imposing a higher value of COV. But in some cases this may lie somewhat more on the conservative side.

In the aspect of platform response to environmental influences, a TLP structure as a semi-submersible is distinctively different from other platforms in that the platform is free to move with waves in the horizontal direction but restrained to a great extent in the vertical direction. Because of these characteristics a TLP's response generally shows dominance in a frequency range away from the equilibrium state of a typical wave spectrum and significant response at the low frequency range of wave spectrum.

As seen in Fig. 4.1, a TLP structure resembles a semi-submersible except in its mooring system and foundation structure. The mooring systems in a semi-submersible

are the conventional catenary system which offers the restoring forces in a horizontal direction, but their stiffness in the vertical direction is negligible. The mooring systems for a TLP are usually vertical and often referred to as "tendons" (or tethers). These tendons are pre-tensioned by the excess buoyancy provided by the platform and have such high stiffness in the vertical direction that natural periods of heave, roll and pitch are limited to 2 to 4 sec. The restoring forces in the horizontal direction are provided by the horizontal component of pre-tension in tendons in the offset position. These components are usually small, and thus the natural periods for sway, surge and yaw are in the order of 100 sec. Comparison of natural periods for a TLP structure with those for a semi-submersible are shown in Fig. 4.2. It can be seen that a good TLP design attempts to keep natural periods for heave and pitch on the low side.

Environmental loading can be divided into 3 categories[9,189]: static , quasi-static and dynamic component. They are simultaneously acting on the structure as external forces and then their load effects are calculated by modelling the overall TLP structure into a space frame type finite element model. Fig. 4.1 also shows the environmental loading acting on a TLP structure.

4.2 Load Components

4.2.1 Static Loading

Static load, which is expected not to vary significantly in time, includes weight of structure, weight of permanent ballast and permanently installed equipment, machinery with liquids at operating levels and external hydrostatic pressure effects in calm sea conditions, calculated on the basis of a datum reference level such as the mean sea level. Additionally water level should be considered. TLP responses are strongly dependent upon water level which also determines the pre-tension in tendon systems (initial tension). The pre-tension affects horizontal restoring forces and thus determines the horizontal offset of the platform. Further, the pre-tension influences the dynamic response characteristics of the platform. These loads usually have the form of the

distributed load or of the concentrated load.

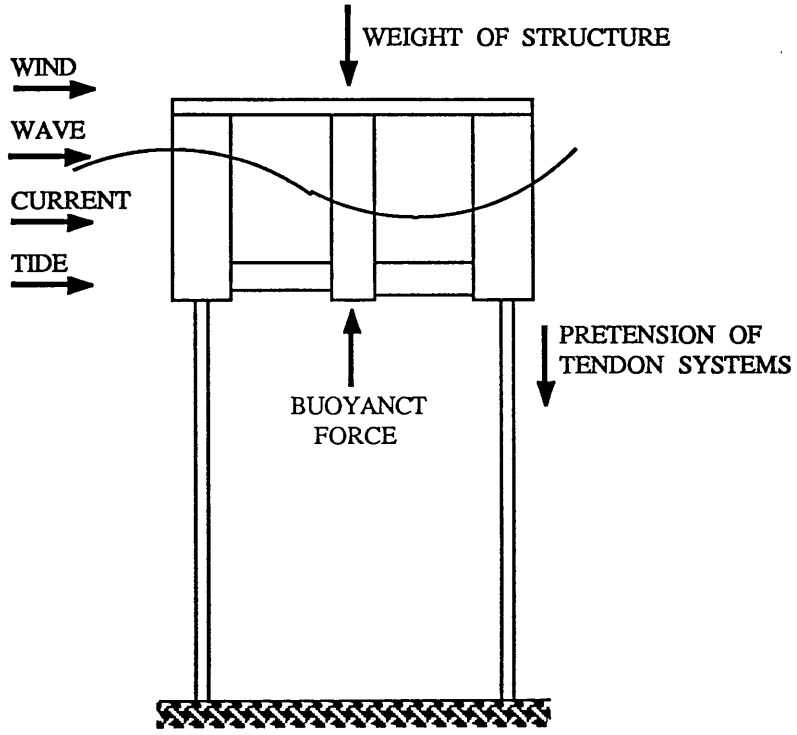

Fig. 4.1 TLP and Environmental Loading

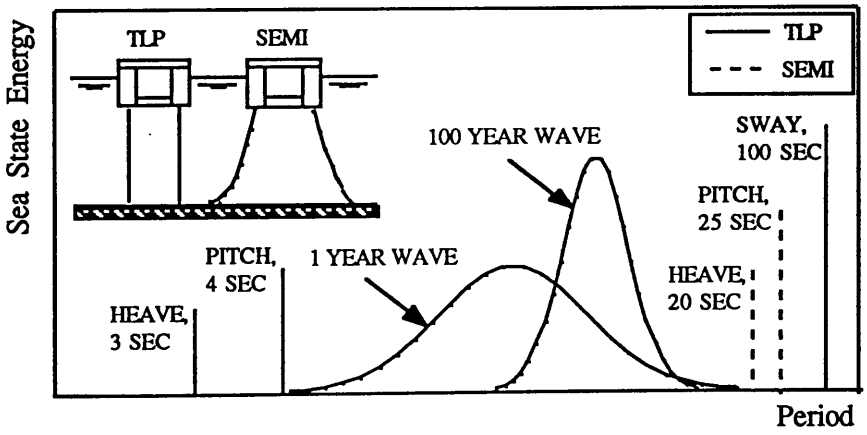

Fig. 4.2 System Natural Periods Comparison of TLP and Semi-Submersible

4.2.2 Quasi-Static Loading

Load that is non-oscillatory in nature yet not purely static is termed as a quasi-static load. Quasi-static load includes the load due to wind, current, wave drift and quasi-static motion. In this study wave drift force is not considered, but it can be estimated by using the Maruo's formula[190]. For the worst condition, directions of wind and current are assumed to be always the same as wave direction. Estimating wind and current induced load is followed to reference [9].

o Wind Load:

Wind load acts normal to flat surface or normal to the axis of members not having flat surface exposed to air and can be calculated from Eq.(4.1) [Fig. 4.3]:

$$F_w = \frac{1}{2} \rho_a C_s V_z^2 A \sin \alpha \qquad (4.1)$$

where

F_W = wind load (N) ρ_a = density of air (= 1.203 kg/m^3)

C_S = shape coefficient

=1.5 for beam

= 1.5 for sides of deck structure

= 0.6 for cylindrical sections

= 1.0 for overall projected area of platform

V_{10} = wind velocity at 10 m above sea level (m/sec)

V_Z = wind velocity at z above sea level (m/sec) given by:

$$= V_{10} \left[\frac{z - 2.2}{7.8}\right]^{0.1128}$$

A = projected area on a plane normal to the direction of the considered force

α = angle between wind direction and the axis coincident with the center line of the member (radian)

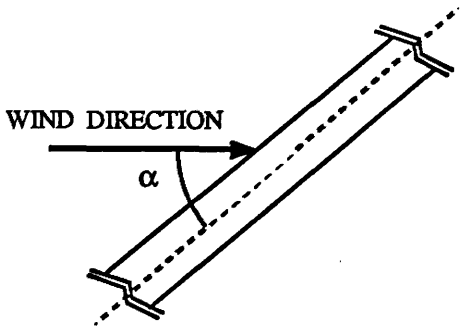

Fig. 4.3 Wind Load

o Current Load:

For the force on submerged parts of the structure due to current alone, only the wind induced component is considered and the direction is assumed to be coincident with the wind direction. This is reasonable to do since the overall current loads and the platform response due to the forces are insigificant compared to the first order wave induced forces. The current profile is assumed to be linear between the waterline and the baseline of the platform. The following equation may be used for calculating the current force, F_C, per unit length:

$$F_C = \frac{1}{2} C_D \rho V^2 A_c \qquad (4.2)$$

where:

F_C = current load per unit length (N/m) ρ = water density

C_D = drag coefficient [see Table 4.1] V = current velocity (m/sec)

A_C = projected area (m^2)

Another important load for TLP is that due to the quasi-static motion which represents an offset and setdown from the initial position due to the action of quasi-static loads. The quasi-static offset from the initial vertical position of the platform [Fig. 4.3] may be determined approximately by solving the following equation when wave drift force is included[9,189]:

$$([H] + [T]) \{X_i\} = (F_W + F_C + F_D) \quad (4.3)$$

where X_i is the motion in the i th mode and [H] and [T] denote the restoring matrix defined in the next section due to the hydrostatic force and the elastic force of the tendon system, respectively. F_W , F_C and F_D are force vectors due to wind, current and wave drift, respectively.

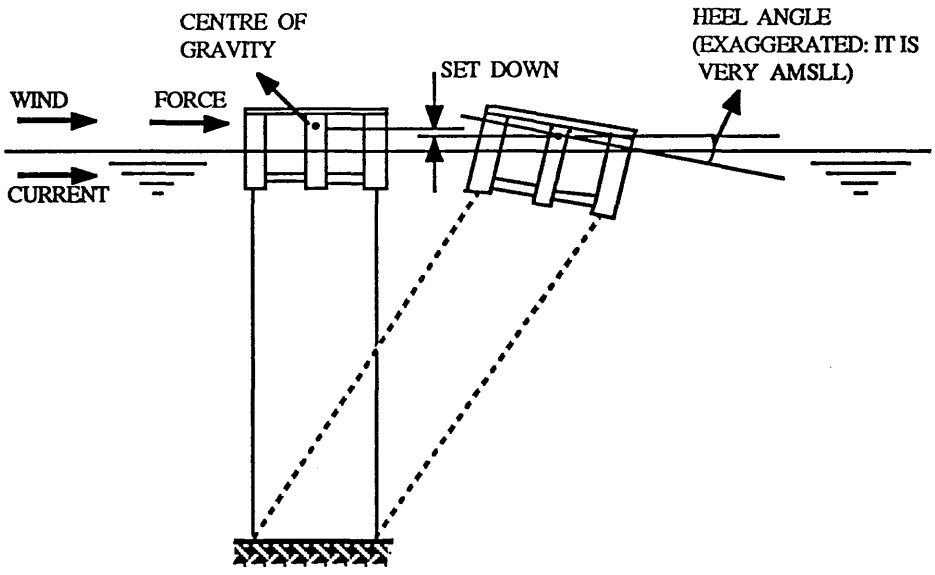

Fig. 4.4 Quasi-Static Offset

4.2.3 Hydrodynamic Loading

Possible methods for estimating the hydrodynamic load due to wave and motion of the structure are the Morison type approach, 2- or 3-dimensional diffraction theory and methods combining the different methods[189,191-201]. The last two methods are computationally more expensive than the Morison type approach, which is adequate for the present study. As a modified approach of the Morison's is averaging the wave gradient, velocity and acceleration across the member cross-section and the results are closer to those by the 3-dimensional diffraction theory. The combining method is computing the fluid properties by 2- or 3-dimensional diffraction theory and adding a

term which represents the viscous drag force[198]. TLP RCC[9] recommends that hydrodynamic loading should be estimated by 2- or 3-dimensional diffraction theory. However, when the important wave lengths are large compared to the typical cross-sectional dimension of members of the structure, the Morison type approach may lead to results of acceptable accuracy.

Various non-linear phenomena are generally involved in motion analysis of the TLP. The typical non-linear effects are viscous drag force which are non-linear functions of the fluid velocity, large platform motion and wave amplitude effects, and non-linear forces of the mooring system[189,196]. In the case of a TLP, it appears that the system is only weakly non-linear insofar as the global response is concerned. The hydrodynamic loading can be estimated by using the hydro-elasticity concept[199,202], but here the structure is assumed to be sufficiently rigid. In this study the Morison type approach is adopted to estimate the hydrodynamic loading in which the drag, inertia, Froud-Krylov and appropriately distributed diffraction forces are included. The non-linear drag force term is replaced by the equivalent linear drag force term[193,194] and Airy's linear wave theory is employed. The linear equation of motion is derived for a floating platform according to the Morison approach.

4.2.3.1 Linear Equation of Motion

The force action on an infinitesimal element of length, dl, due to wave is given by[191] :

$$dp(t) = (\frac{1}{2} C_D \rho D u_p u_p + C_M \rho A u_p) dl \qquad (4.4)$$

where ρ = water density

u_p, u_p = velocity and acceleration of water particle

A, D = cross sectional area and diameter of the element

C_M, C_D = inertia and drag coefficient

To distinguish between the contributions of the actual displaced mass per unit length, ρA, and the added mass, $(C_M - 1)\,\rho A$, Eq.(4.4) can be rewritten as:

$$dp(t) = \{\frac{1}{2} C_D \rho D u_p u_p + (C_M - 1)\rho A u_p + \rho A u_p \}\, dl \qquad (4.5)$$

Following the discussion by Chakrabarti[204] on a paper by Malhotra and Penzien[203] it can be shown that the revised form of Morison's equation to allow for structural motion is:

$$dp(t) = \{ \frac{1}{2} C_D \rho D\, |u_p - u_s|\, (u_p - u_s) + (C_M - 1)\rho A\, (u_p - u_s) + \rho A u_p \}\, dl \qquad (4.6)$$

where u_S and u_S are velocity and acceleration of structural element. The total force acting on an element of length L is given by:

$$p(t) = \int_0^L \{\frac{1}{2} C_D \rho D\, |u_p - u_s|\, (u_p - u_s) + (C_M - 1)\rho A\, (u_p - u_s) + \rho A u_p\}\, dl \qquad (4.7)$$

By the Newton's second law:

$$\begin{aligned} m u_s &= p(t) \\ &= \int_0^L \frac{1}{2} C_D \rho D\, |u_p - u_s|\, (u_p - u_s)\, dl + \int_0^L (C_M - 1)\rho A\, (u_p - u_s)\, dl + \int_0^L \rho A u_p\, dl \\ &= \int_0^L \frac{1}{2} C_D \rho D\, |u_p - u_s|\, (u_p - u_s)\, dl + \int_0^L (C_M - 1)\rho A u_p\, dl + \int_0^L (C_M - 1)\rho A u_s\, dl \\ &= \int_0^L \rho A u_p\, dl \end{aligned} \qquad (4.8)$$

where m is the mass of an element. If velocities and accelerations of water particle and

structural element are uniform over an element having values at mass centre, Eq.(4.8) becomes:

$$mu_s = \frac{1}{2} C_D \rho D l \, |u_p - u_s| (u_p - u_s) + (C_M - 1)\rho A l u_p - (C_M - 1)\rho A l u_s + \rho A l u_p \tag{4.9}$$

This can be rewritten as:

$$mu_s = \frac{1}{2} C_D \rho A_n \, |u_p - u_s| (u_p - u_s) + C_a \rho V u_p - C_a \rho V u_s + \rho V u_p \tag{4.10}$$

where

C_a = added mass coefficient ($= C_M - 1$)

A_n = projected area of an element normal to the direction of water particle

V = volume of displacement of an element (= Al)

The quadratic drag force term may be replaced by an equivalent linear drag force:

$$\frac{1}{2} \rho A_n \, |u_p - u_s| (u_p - u_s) \cong C_{DL} (u_p - u_s) \tag{4.11}$$

where C_{DL} is an equivalent linear drag coefficient. Replacing the quadratic drag force term by an equivalent linear drag force term, Eq.(4.10) becomes:

$$mu_s = \frac{1}{2} \rho C_{DL} A_n u_r (u_p - u_s) + C_a \rho V u_p - C_a \rho V u_s + \rho V u_p \tag{4.12}$$

or, rewriting

$$(m + m_a) u_s + \frac{1}{2} \rho C_{DL} A_n u_r u_s = \frac{1}{2} \rho C_{DL} A_n u_r u_p + (m_a + \rho V) u_p \tag{4.13}$$

where m_a (= $C_a \rho V$) is the added mass and u_r (= $u_p - u_s$) is the relative velocity between water particle and structural element. By inserting the restoring force term the equation of motion is given by:

$$(m+m_a)u_s + \frac{1}{2}\rho C_{DL} A_n u_r u_s + k u_s = f(t) \tag{4.14}$$

where f(t) is the exciting force defined as the right hand side of Eq.(4.13). Hence, the total external force acting on an element due to wave and structural motion is given by:

$$f_e = -(m+m_a)u_s + m_a u_p + \frac{1}{2}\rho C_{DL} A_n u_r (u_p - u_s) \tag{4.15}$$

By transforming the equation of motion (4.14) to the global co-ordinate of which origin is located at the centre of gravity [Fig. 4.4] and assembling it for all elements, the equation of motion is given by:

$$[M]\{u_S\} + [B]\{u_S\} + [K]\{u_S\} = \{F(t)\} \tag{4.16}$$

where {F(t)} is the exciting force vector., and [M] , [B] and [K] are mass, damping and restoring matrices respectively given as follows. Mass matrix is composed of the structural mass matrix and the added mass matrix. That is:

$$[M] = [M_S] + [M_a] \tag{4.17}$$

The structural mass matrix is given by:

$$[M_s] = \begin{bmatrix} M & 0 & 0 & 0 & 0 & 0 \\ & M & 0 & 0 & 0 & 0 \\ & & M & 0 & 0 & 0 \\ & \text{sym} & & I_{44} & I_{45} & I_{46} \\ & & & & I_{55} & I_{56} \\ & & & & & I_{66} \end{bmatrix} \tag{4.18}$$

where M is the mass of the structure, I_{jj} is the mass moment of inertia in the j th mode, and I_{jk} is the product of inertia between the j and k th modes.

The added mass matrix is given by:

$$[M_a] = \begin{bmatrix} A_{11} & 0 & 0 & 0 & A_{15} & A_{16} \\ & A_{22} & 0 & A_{24} & 0 & A_{26} \\ & & A_{33} & A_{34} & A_{35} & 0 \\ & \text{sym} & & A_{44} & 0 & A_{46} \\ & & & & A_{55} & A_{56} \\ & & & & & A_{66} \end{bmatrix} \tag{4.19}$$

Note that A_{jk} (for $j \neq k$) are the added mass cross-coupling coefficients for th k th mode coupled into the j th mode of motion, so that, for example, A_{15} is the added mass coefficient for pitch coupled into surge.

The linear damping matrix is given by:

$$[B] = \begin{bmatrix} B_{11} & 0 & 0 & 0 & B_{15} & B_{16} \\ & B_{22} & 0 & B_{24} & 0 & B_{26} \\ & & B_{33} & B_{34} & B_{35} & 0 \\ & \text{sym} & & B_{44} & 0 & B_{46} \\ & & & & B_{55} & B_{56} \\ & & & & & B_{66} \end{bmatrix} \tag{4.20}$$

The stiffness matrix [K] can be obtained by summing up the hydrostatic restoring coefficients, [H] and the stiffness matrix due to the tendon system, [T] in the case of TLP, i.e.:

$$[K] = [H] + [T] \tag{4.21}$$

while in the case of a semi-submersible, only the hydrostatic restoring coefficients are included. The hydrostatic stiffness matrix [H] is given by:

$$[H] = \begin{bmatrix} 0 & 0 & 0 & 0 & 0 & 0 \\ & 0 & 0 & 0 & 0 & 0 \\ & & H_{33} & H_{34} & H_{35} & 0 \\ & \text{sym} & & H_{44} & H_{45} & 0 \\ & & & & H_{55} & 0 \\ & & & & & 0 \end{bmatrix} \tag{4.22}$$

For the elements on the waterline with cross sectional area A_i each element of the matrix in Eq.(4.22) is given as follow:

$$H_{33} = \sum_{i=1}^{n} \rho g A_i$$

$$H_{34} = \sum_{i=1}^{n} \rho g A_i Y_i = H_{43}$$

$$H_{35} = \sum_{i=1}^{n} \rho g A_i X_i = H_{53}$$

$$H_{45} = \sum_{i=1}^{n} \rho g A_i X_i Y_i = H_{54}$$

$$H_{44} = \sum_{i=1}^{n} \left[\rho g A_i Y_i^2 + I_A \right]$$

$$H_{55} = \sum_{i=1}^{n} \left[\rho g A_i X_i^2 + I_A \right] \tag{4.23}$$

where

X_i, Y_i = co-ordinate of centre of area element i

I_A = moment of inertia of area element about its axis through its own centre.

n = number of area elements on the water line

In the case of a TLP, the pre-tension of the tendon system plays an important role in restoring force in all motions. The tendon stiffness matrix with respect to the centre of gravity of the structure is given by[205] :

$$[T] = \begin{bmatrix} T_{11} & 0 & 0 & 0 & T_{15} & T_{16} \\ & T_{22} & 0 & T_{24} & 0 & T_{26} \\ & & T_{33} & T_{34} & T_{35} & 0 \\ \text{sym} & & & T_{44} & 0 & 0 \\ & & & & T_{55} & 0 \\ & & & & & T_{66} \end{bmatrix} \qquad (4.24)$$

The elements of [T] are:

$$T_{11} = T_i / L \qquad T_{34} = K_T \times (Y_T - Y_G)$$

$$T_{15} = T_i / L \times (Z_T - Z_G) \qquad T_{35} = K_T \times (X_T - X_G)$$

$$T_{16} = - T_i / L \times (Y_T - Y_G) \qquad T_{44} = K_T \times (Y_T - Y_G)^2 + T_i/L\,(Z_T - Z_G)^2$$

$$T_{24} = - T_i / L \times (Z_T - Z_G) \qquad T_{55} = K_T \times (X_T - X_G)^2 + T_i/L\,(Z_T - Z_G)^2$$

$$T_{26} = - T_i / L \times (X_T - X_G) \qquad T_{66} = K_T \times (X_T - X_G)^2 + T_i/L\,(Y_T - Y_G)^2$$

$$T_{33} = K_T \qquad (4.25)$$

where:

T_i = initial tension of unit tendon system

K_T = tendon stiffness

X_G, Y_G, Z_G = co-ordinate of the centre of gravity

X_T, Y_T, Z_T = tendon top co-ordinate

The equivalent linear drag coefficient C_{DL} may be related to the exact quadratic coefficient by an optimisation procedure in which C_{DL} is selected in such a way that the mean square error between the linear and quadratic estimates of the drag force is minimised. For regular wave and platform motion:

$$C_{DL} \cong C_D \times \frac{8}{3\pi} U_r \tag{4.26}$$

where U_r is the amplitude of the oscillatory resultant normal velocity, and for random wave and platform motion:

$$C_{DL} \cong C_D \times \sqrt{\frac{8}{\pi}}\, \underline{U}_r \tag{4.27}$$

where $\underline{U}_r$ is the root mean square (RMS) value of the randomly varying resultant normal velocity or the square root of the relative velocity variance.

In both cases, C_{DL} is seen to depend upon the relative velocity between the water particle velocity and the structural element velocity. The solution, in this case, must therefore involve an iterative procedure which is repeated until the error is within an acceptable bound. For most realistic platform configuration, the convergence is quite rapid since the viscous force is only a small part of the total force system on the platform. Convergence check is based on:

$$u_p - u_s \leq \varepsilon \tag{4.28}$$

for regular wave and platform motion, and

$$\text{Var}\,[\, u_p - u_s \,] = \sigma_r^2 \leq \varepsilon \tag{4.29}$$

for random wave and platform motion.

The main difficulty with the application of Morison's equation lies in the proper choice of C_D and C_M from a wide range of published data. Although these coefficients can be shown to vary systematically with other parameters, such as Reynold's number, Keulegan-Carpenter number and relative roughness[193,194], there is still considerable residual uncertainty. In this study, C_D and C_M are given as Table 4.1[206].

4.2.3.2 Equivalent Spring System

Restoring forces due to hydrostatic stiffness and due to the tendon system are replaced by equivalent spring constants at the appropriate position as shown in Fig. 4.6. The equivalent spring constants, $K_1, \ldots, K_5$ in Fig. 4.6 are obtained from the following equilibrium equations:

$$\sum_{j=1}^{4} Z_j K_4 = K_{15}$$

$$\sum_{j=1} Z_j K_5 = -K_{24}$$

$$4(K_2 + K_3) + n(K_1 + K_3) = K_{33}$$

$$\sum_{i=1}^{n} Y_i^2 K_1 + \sum_{j=1}^{4} Y_j^2 K_2 + \sum_{j=1}^{4} Z_j^2 K_5 = K_{44}$$

$$\sum_{i=1}^{n} X_i^2 K_1 + \sum_{j=1}^{4} X_j^2 K_2 + \sum_{j=1}^{4} Z_j^2 K_4 = K_{55} \qquad (4.30)$$

where

K_{15} etc : the restoring coefficient

$j = 1 \sim 4$: for corner column $i = 1 \sim n$: for mid-column

n = number of mid-column X_i, Y_i, Z_i : co-ordinate of spring

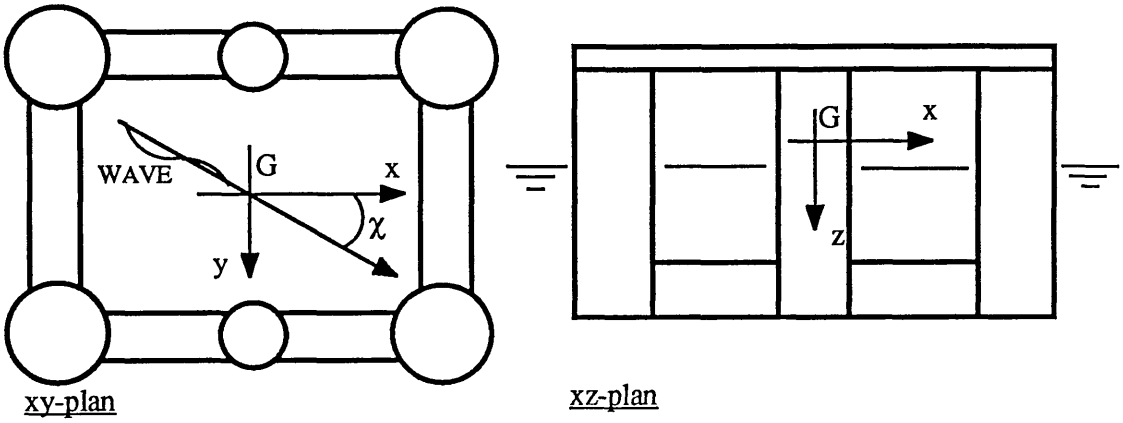

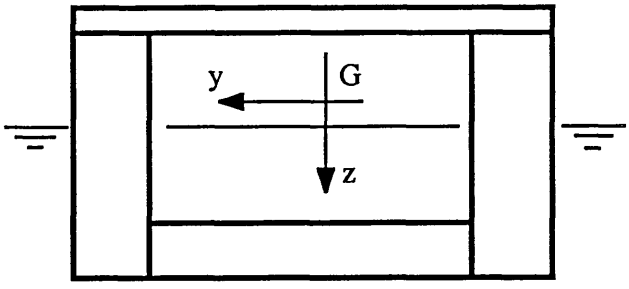

G : centre of gravity

Fig. 4.5 Coordinate System

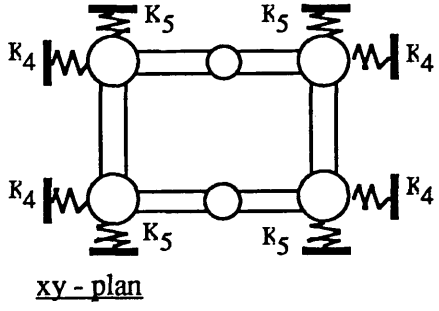

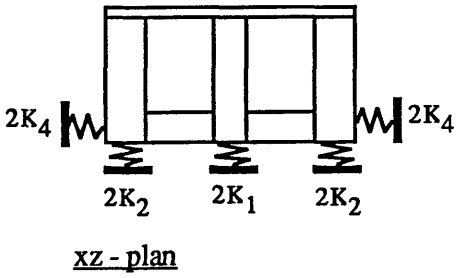

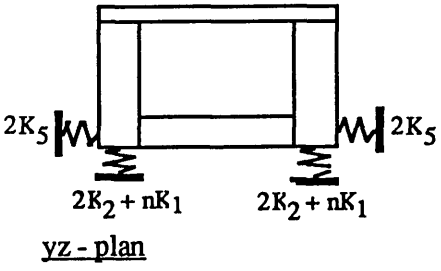

n : number of mid-columns

Fig. 4.5 Equivalent Spring System

Table 4.1 Added Mass and Drag Coefficient[206]

(1) Added Mass Coefficient

Cylindrical member : $C_a = 1.0$

Rectangular box, sides b and d, b parallel to flow

$C_a = \pi/4 \, K_L \, (d/b)$ and K_L is given by

$K_L = 1 / \{1 + (d/L)^2\}$ with L = length of member ($L > d$)

(2) Drag Coefficient

Cylindrical member : $C_D = 0.7 \, K_L$

Rectangular box, sides b and d, side d facing flow

with corner radius r ($0 < r \, d/2$) :

$$C_D = 2.0 \, K_L \, K_r \, K_b$$

Axis of a member is normal to flow, and K_L, K_r and K_b are given by:

$$K_L = 0.5 + 0.1 \, L/d \qquad \text{for } L/d \leq 5$$
$$= 1.0 \qquad \text{for } L/d > 5$$

$$K_b = 1.0 \qquad \text{for } b/d \leq 2$$
$$= (8 - b/d) / 6 \qquad \text{for } 2 < b/d \leq 5$$
$$= 0.5 \qquad \text{for } b/d > 5$$

$$K_r = 1.0 \qquad \text{for } r/d \leq 0.10$$
$$= (4.3 - 13 \, r/d) / 3 \qquad \text{for } 0.10 < b/d \leq 0.25$$
$$= 0.35 \qquad \text{for } r/d > 0.25$$

CHAPTER 5 RELIABILITY STUDIES FOR TLP STRUCTURES

5.1 General

During the last two decades the concept of a tension leg platform (TLP) attracted attention as a platform for use in deepwater production. Today it is considered to be one of the most promising deepwater platforms of the offshore industry. For water depths beyond 1500 m, this concept is especially desirable because of its economical feasibility in that, due to tendons and less deck/hull area, the TLP is not at all cost-sensitive to the increasing water depth and, in addition, the floating part of the structure can be transferred to another site after depletion. The TLP can also be used in earthquake zones since the tendon system is flexible since the transmission of motion to the main structure can be avoided. The TLP concept is relatively new and possesses many complex and challenging deepwater design features. To design an economically viable and safe TLP requires extensive pre-engineering work to study various tasks specific to the structure[205,207].

The basic concept of a TLP is to impose excessive buoyancy and hence, in still water weights of structure itself, equipment installed, etc. and the pre-tension of tendons are balanced with buoyancy. Because of this, as described in the previous chapter, the characteristics of the platform response to environmental influences is distinctively different from other compliant ones, such as semi-submersibles and articulated towers, as well as fixed ones in that the platform is free to move with wave, wind or current in the horizontal direction. Its motion in the vertical direction is restrained to a great extent and is likely to be that of an inverted vertical column.

There are two examples. One is operated in the Hutton field in the North sea (the Hutton TLP in Fig. 5.1) which is the first TLP in the world, and the other is under construction and will be installed in the Jolliet Field Green Canyon block in the Gulf of

Mexico (the Jolliet TLP in Fig. 5.2). Even though the TLP is developed for deep water, there is a natural trend to try deep water concepts in shallow waters, of which the Hutton TLP is an example.

The structural system of a TLP is one of the typical continuous structures and its main structural components, such as columns, bracing, pontoons and decks, have high redundancy, especially around their joints which are designed to adequately transfer load effects between principle structural components. Since like other compliant platforms it is very sensitive to weight, the development of the TLP may depend on reducing its weight while still retaining the appropriate, efficient strength[207,208].

The Hutton TLP has 6 columns of ring stiffened cylinder and pontoons of rectangular box girder. The Jolliet TLP has 4 columns and pontoons of ring- and stringer-stiffened cylinder (orthogonally stiffened cylinder). The structural test result verified that orthogonally stiffened cylinders were more efficient than ring-stiffened cylinders for loadings similar to those found in TLPs. Similar experience could be found in ship design and therefore much reduction of structural weight can be achieved. In the design of the Jolliet TLP about 30% reduction of structural weight was achieved using orthogonally stiffened cylinders[8,9,207,209]. Table 5.1 shows the comparison of these two TLPs, Hutton and Jolliet[209].

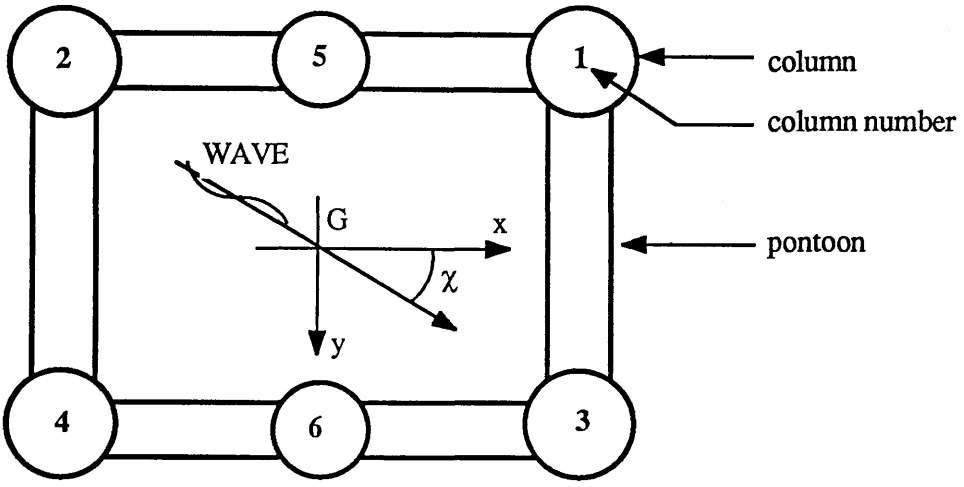

xy - plan

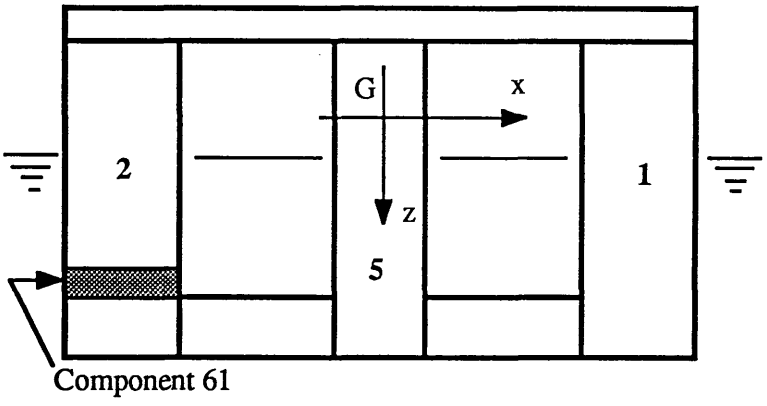

xz - plan

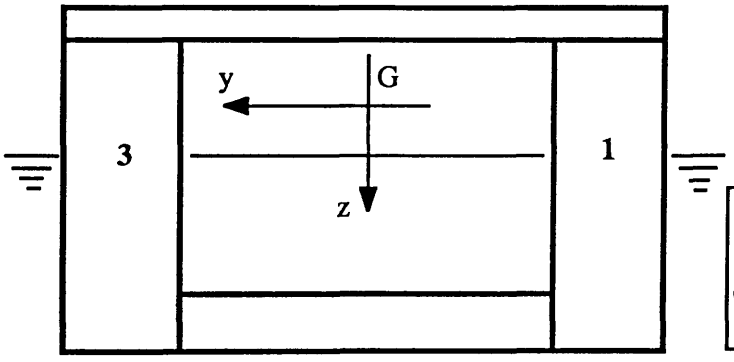

yz - plan

o All columns : ring-stiffened cylinders

o All pontoons : rectangular box-girders

Fig. 5.1 Hutton TLP

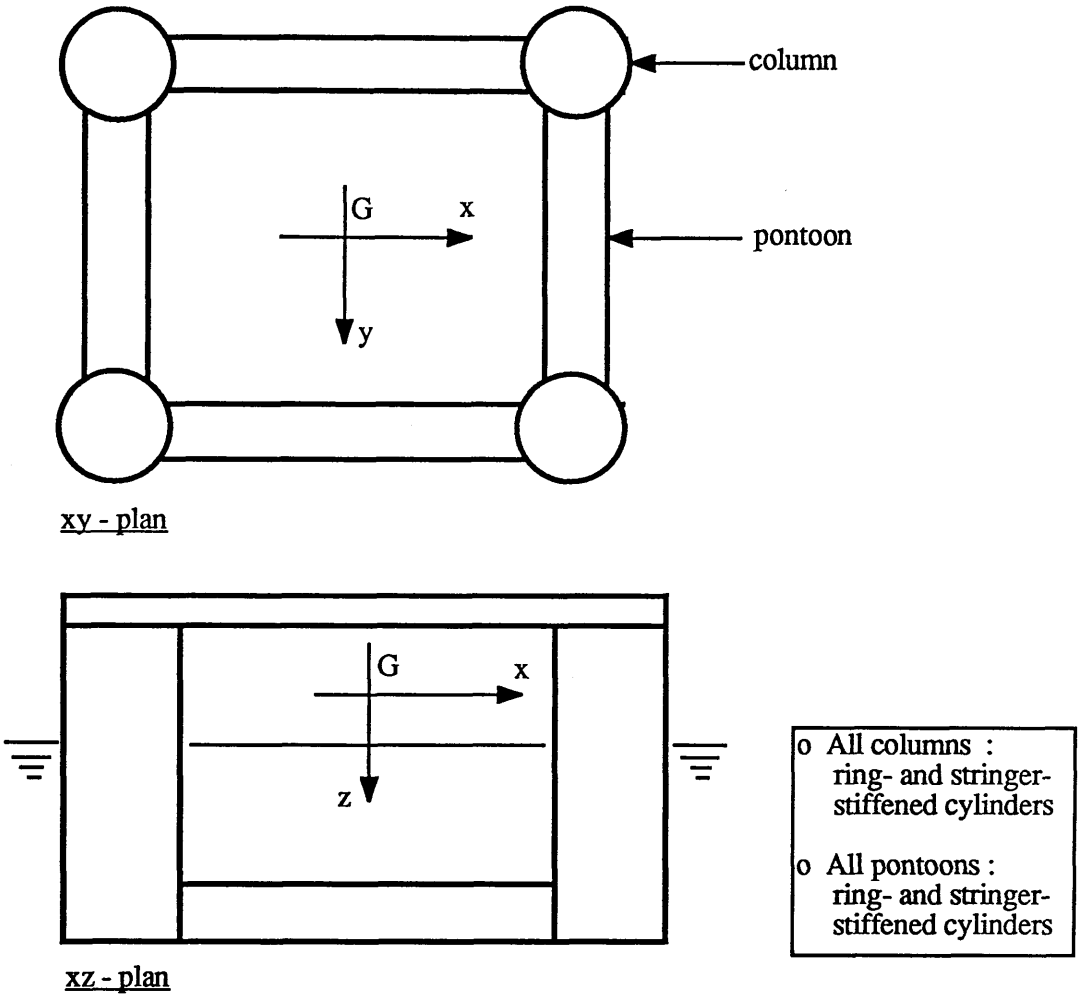

Fig. 5.2 Jolliet TLP

Table 5.1 Comparison between the Hutton TLP and the Jolliet TLP[209]

	Hutton TLP	Jolliet TLP
Field		
Recovered reserves : oil	190 mn bbls	40 mn bbls
: gas	—	2.1 bn m^3
Peak capacity : oil	110,000 b/day	35,000 b/day
: gas	—	1.4 mn m^3 /day
No. of wells	21	16
On stream date	Aug. 1984	Sept. 1989
Location		
Water depth	147 m	536 m
Design wave height	30.4 m	22.0 m
Platform configurations		
Operating displacement	61,536 tons	16,700 tons
Operating draft	32 m	24 m
No. of tendons	16	12
Initial tension of tendon	11,330 tons	4,900 tons
Riser pre-tension	1,350 tons	1100 tons
Weight of structure	48,035 tons	10,700 tons
Columns : corner column	4 x ring stiffened cylinder	4 x ring- and stringer-stiffened cylinder
: mid column	2 x ring stiffened cylinder	—
Pontoons	rectangular box girder	ring- and stringer-stiffened cylinder

For structural analysis, TLP structures are modelled into the finite element type space frame, as illustrated in Figs. 5.7 and 5.10. The boundary conditions are imposed to minimise restraining of the structures. The load effects, such as axial forces and bending moments, are calculated based on the Euler beam theory. In the system reliability analysis, the following assumptions are made:

[1] Failure is assumed to occur under combined actions of axial loads and bending moment, therefore, the effects of shear and torsion are ignored.

[2] Failure is restricted to the main structural system and hence failure of the tendon system is not considered.

[3] Component failure is restricted to the components of columns and pontoons. Deck structure is not included

[4] Joints are assumed to be sufficiently stiff so that they can transfer forces to each other, therefore, the components around the joints do not fail.

[5] Three categories of loading, namely, static, quasi-static and dynamic, give the same load effects.

[6] All random variables are assumed to be statistically independent.

[7] Gross error is not explicitly considered.

[8] Problem is time invariant.

A computer program has been developed based on the present approach described in Section 2.4 for the system reliability analysis of structure under the multiple loading condition, especially for the floating offshore structures such as TLPs and semi-submersibles. The program can cover from estimation of the environmental loading to the reliability assessment. Fig. 5.3 briefly shows the general flow of the developed computer program which is composed of 3 major parts:

[1] Estimating the three categories of environmental loading and transferring loads into equivalent nodal forces

[2] Structural analysis

[3] Reliability analysis

Reliability analysis consists of evaluating the reliability indices (and probabilities

of failure) of components and systems level. For the system reliability analysis, the safety margin is derived according to the present method described in Section 2.4. The procedure of identifying the most important failure modes is followed as illustrated in Section 2.5.6, through which the probabilistically most important ones may be found which may also be the deterministically important ones When generating the failure mode, the bounds of the probability of system failure are calculated, and finally, will be averaged to give the system reliability level of the structure.

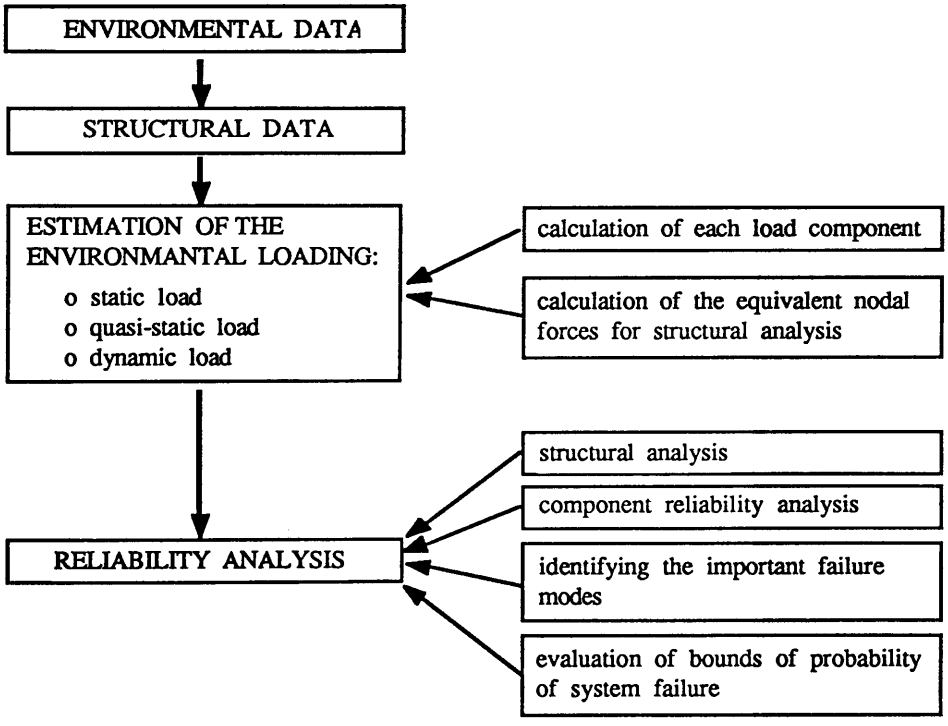

Fig. 5.3 General Flow of the Computer Program

5.2 Uncertainty Modelling

Treating uncertainties in strengths and loads is the major merit and advantage of the reliability-based limit state design process over the conventional working stress-based design process. Uncertainties arise from various reasons and can be divided into two categories, say, objective and subjective uncertainty. Objective uncertainty is due to inherent variability concerned with the random nature of physical phenomena. This uncertainty can be described by representing the physical quantities as random variables, e.g. thickness and radius of cylinder, yield stress, elastic modulus, etc., or random processes wherever time variations are important. This uncertainty can be assessed by applying classical statistical methods. Typical coefficients of variation are usually less than 10 %.

Subjective uncertainty is mainly due to limitations of mathematical models for strength and load in use for design, the analysis estimating loads and their effects, neglect of certain physical variables, human error (gross error) etc. This uncertainty usually has more effect on the safety level of a structure than the objective one has. It can also be statistically treated by using a certain type of model but the uncertainty will be included in doing that itself.

5.2.1 Uncertainties in Design Variables

The design variables are usually taken as geometric and material properties of a structural component associated with its strength, e.g. for the ring- and stringer-stiffened cylinders, shell thickness and radius of cylinder, spacing of ring frames and scantlings of stringer and ring frame, and elastic modulus and yield stress. Imperfection will normally show significant variability, especially for cylindrical members. Chryssanthopoulos et al[149] included geometric imperfections in their reliability study but the statistical data for imperfections are not yet well established. Therefore, one would usually assume imperfection equal to the tolerance specified in design codes and therefore, they can be treated as deterministic variables.

Uncertainties of design variables are inherent and therefore objective. They arise from the fabrication process of material and can be characterised by their means, coefficients of variation (COVs) and distribution types.

In design yield stress must be the most important and influential basic variable in strength. COV for yield stress reportedly ranges between 5% and 10%. An extensive study by Baker found it to vary between 6% and %[114]. COV for elastic modulus is smaller than that for yield stress and sensitivity to this was negligible and hence this parameter is sometimes treated as a constant. In the present study COVs of 8% for yield stress and 4% for elastic modulus are taken[9,113]. Uncertainties of geometric parameters are usually smaller than that for yield stress. For this study COVs are taken as 4% but the height and breadth of the rectangular section [Fig. 3.3] are treated as constants. It is generally accepted that distributions of variables in strength should be log-normal and most geometric parameters can be represented by normal distributions. Uncertainty modelling for design variables of principle components in a TLP structure are listed in Table 5.2. They are used in this study. Strength modelling should be an important strength variable. This will be shown in the next section.

Table 5.3 Uncertainties of Design Variables

Cylindrical Component

design variable	COV (%)	distribution type
radius of cylinder	4.0	normal
thickness of shell	4.0	normal
scantlings of stringer and ring frame	4.0	normal
spacing of ring frame	4.0	normal
yield stress	8.0	log-normal
elastic modulus	4.0	log-normal

Table 5.2 (continued)

Rectangular Section

design variable	COV (%)	distribution type
breadth and height of section	0.0	—
thickness of plate	4.0	normal
scantlings of stiffener	4.0	normal
spacing of transverse frame	4.0	normal
yield stress	8.0	log-normal
elastic modulus	4.0	log-normal

5.3.2 Modelling Uncertainties

So that the reliability analysis can serve as a decision-making tool in the practice of structural design, it is necessary to include elements for subjective assessment of modelling uncertainty information in the reliability model itself. This type of uncertainty is concerned with the way of describing loads and then evaluating their effects and describing strength capacity. It principly arises from the fact that the predicted values of loads and strength will be different from those realised in practice. The difference will show a random and, perhaps, systematic variation.

The uncertainty introduced into the process of predicting loads and strength as a result of this is usually termed as the modelling uncertainty and is due to two main sources:

[1] The number of basic physical variables has been limited to a finite number leaving out a possible infinite set of parameters that in the model idealisation process have been judged to be of secondary or negligible importance for the problem in hand. The neglected certain physical variables can act as generators of

a background noise.

[2] The limitations of mathematical functions predicting load and strength, apart from the inherent uncertainty of themselves in their own evaluations, may incorrectly model the behaviour of a structure. This is due to simplification of the functions in use and to lack of knowledge about the detailed interplay between the considered variables.

Structural analysis itself may have an effect upon the actual value of load effects but uncertainty due to this is negligible in comparison to the other two.

Although modelling uncertainties can be and should be assessed by using classical statistical methods, their final resolution requires appreciable engineering judgement. Modelling uncertainty is, therefore, essentially a subjective one and in principle can be reduced by improved modelling[163].

Modelling uncertainty should be quantified using data from model tests and/or full scale tests wherever possible. The most convenient way to quantify this uncertainty is introducing the modelling parameter (or modelling error) defined as Eq.(2.97) which is the ratio of actual or experienced behaviour to predicted behaviour by mathematical model. This parameter was first proposed by Ang and Cornell[2].

o Strength Model:

In the present reliability study, the modelling parameter for strength has been incorporated in the safety margin equation (limit state function) as by the modified safety margin equation [Eq.(2.103)]. The uncertainty of strength modelling parameter is characterised by its mean bias, $\underline{X}_M$, coefficient of variation, V_{X_M} and distribution type. $\underline{X}_M$ and V_{X_M} can vary depending on the form of strength formula which implies that the evaluated safety level can be much affected by the strength formula itself and differ from the strength model used in the analysis. They also depend on the situation since, as more test data are accumulated, they can be updated. This implies that it can be easily expected that the mean and COV of safety margin and, consequently, the evaluated safety level,

will be very sensitive to change in the mean bias and especially to change in the COV of strength modelling parameter due to its position within the safety margin Eq.(2.103).

In this study the distribution of strength modelling parameter is assumed to be log-normal rather than normal as taken by TLP RCC[9]. This is based on the fact that among the design variables in Section 5.2.1 yield stress may be supposed to mainly contribute to strength and, hence, on the strength model in use. Table 5.3 shows the mean biases ($\underline{X}_M$) and COVs (V_{X_M}) of strength models for the principle components of a TLP structure under combined loading[119] used in the present study.

The values of $\underline{X}_M$ and V_{X_M} for ring-stiffened cylinders may be acceptable levels. For ring- and stringer-stiffened cylinder, when Eq.(3.53) is used, V_{X_M} is taken as the maximum required level as recommended by Faulkner et al[119,163]. When Eq.(3.58) is used for ring- and stringer-stiffened cylinder, the values of $\underline{X}_M$ and V_{X_M} are taken as the recently revised ones[119]. In this study Eq.(3.11) for ring-stiffened cylinders and Eq.(3.53) for ring- and stringer-stiffened cylinders have been consistently used to compare the evaluated system safety levels of structures having different types of principle components. Eq.(3.58) has also been used to show the results when using the different strength models for the same component type.

As described in Section 3.4.6, there is no available test data for rectangular box-girder under the combined loading condition of axial compression and bi-axial bending. Since its failure is very closely correlated with the failure of a stiffened panel in the weakest portion in the section[128], mean bias and COV of the strength modelling parameter is postulated, based on this fact, but its COV is raised to 10% to account for the uncertainty in this fact itself.

o Loading Model:

It is usually expected that the degree of uncertainty with load model is higher than that with strength model. This arises from the fact that there must be more unknown factors affecting loads and their effects. In practice, it is generally not possible to obtain

the parameters of the probability distribution of the actual load. Instead design environmental loads are directly derived from specified design environmental conditions such as design wave height, design wind speed, etc. and then, mean bias, COVs and distribution type are imposed on it.

When each type of loading has been calculated it will be transferred into the equivalent nodal force vector acting on nodes for structural analysis and then load effects such as axial forces and bending moments will be calculated. Static load effect is usually modelled as normal distribution with relatively small COV. Quasi-static component is modelled as normal distribution but with higher COV. Static and quasi-static load effects are sometimes modelled as log-normal distributions[43].

Referring to the uncertainties in dynamic load effect, when using the extreme value analysis with significant wave heights as proposed by Chen et al[189], the inherent uncertainties stemming from the extreme value probability density function resulting from the order statistic analysis is found to be less than 10%. However, such uncertainties are likely overwhelmed by the largely subjective uncertainties, the quantification of which relies mostly on design experience. The best estimation indicates that such uncertainties may contribute about 25% to COV of the dynamic load effect[189]. Thus COV of dynamic component was chosen to be 30%. When estimating the dynamic load effect it is based on a single design wave with 100 years return period wave height, the uncertainty will be reduced, say 10%, but the magnitude of load effects is much greater than those estimated by the extreme value analysis [see Fig. 5.4]. Regarding the distribution type, various approaches for defining the different extreme load types and Gumbel (Type I), Weibull have been suggested[194,210].

In this study, the dynamic load effects are estimated based on a single design wave and the distribution of all types of load effects is assumed to be log-normal. Their COVs are chosen to be 10%, 20% and 10% for static, quasi-static and dynamic component, respectively. Table 5.4 shows uncertainty modelling of load effects chosen for the present reliability study.

From the discussions in this section the distribution types of the resistance and loading coefficients in the safety margin equation Eq.(2.103) are given to be log-normal.

Table 5.3 Strength Modelling Uncertainties: Mean Bias ($\underline{X}_M$) and COV (V_{X_M})

principle component	interaction equation	$\underline{X}_M$	V_{X_M}
ring stiffened cylinder	Eq.(3.11)	0.99	10 %
ring- and stringer-stiffened cylinder	Eq.(3.53)	0.99	13 %
	Eq.(3.58)	1.052	11.9 %
Rectangular Box Girder	Eq.(3.89)	1.00	10 %

Table 5.4 Uncertainty Modelling for Load Effects

load effect component	mean bias	COV	distribution type
static	1.0	10 %	log-normal
quasi-static*	1.0	20 %	log-normal
dynamic	1.0 for axial load effect 1.2 for other load effects	10 %	log-normal

* : load effect due to wave drift force is not considered

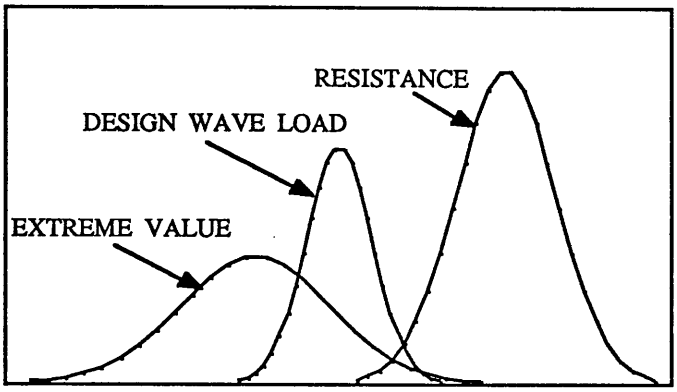

Fig. 5.4 Two Types of Distribution of Dynamic Load Effect

5.3 TLP Models for Reliability Studies

In this study, three TLP models are selected for the system reliability analysis of continuous structures. One of the TLP models is the Hutton TLP[211]. Fig. 5.1 shows the co-ordinate system for motion analysis. Principle characteristics are listed in Table 5.5. The space frame model of the Hutton TLP for structure analysis is illustrated in Fig. 5.5, in which the structural system is composed of 55 nodal points and 62 beam elements. In system reliability analysis, since structure analysis is to be repeated many times and requires much computational time, the number of nodal points and elements are reduced in this study. Geometric and material data for the structure analysis are listed in Table 5.6.

Two variants of the Hutton TLP are chosen for comparison of the reliability of structures having different component types, i.e. the ring stiffened cylinder and the ring- and stringer-stiffened cylinder. One is called herein, 'TLP-A', shown in Fig.5.6, which is the variant TLP model by replacing the corner columns of the Hutton TLP by ring- and stringer-stiffened cylinders designed according to TLP RCC model code[9]. Weight of one corner column has been reduced by 25% compared to that of the Hutton TLP. The space frame model is the same as that of the Hutton TLP [Fig. 5.5]. Its geometric and

material data for structure analysis are listed in Table 5.7.

The other TLP model, called here 'TLP-B', is chosen as shown in Fig. 5.7, which is the variant model by simply removing the mid-columns from TLP-A and hence has 4 corner columns of ring- and stringer-stiffened cylinders of which geometric and material properties are the same as those of TLP-A. This model is similar to the Jolliet TLP [Fig. 5.2] except for structural types of pontoons (Pontoons of Jolliet TLP are ring- and stringer-stiffened cylinders). Adjusted principle characteristics of TLP-B is listed in Table 5.8. For the mooring system the initial tension of a tendon unit has been reduced by about 356 tons on the assumption that tendon weight and riser tension retain the same level as those of the Hutton TLP. Its space frame model is illustrated in Fig. 5.8 and geometric and material data are listed in Table 5.9.

Two variants are chosen to compare the efficiency of the structure, one having a ring stiffened cylinder and the other having a ring- and stringer-stiffened cylinder from the system's side. The two variants have the same overall structural dimension as the Hutton TLP. Table 5.10 summaries the three TLP models.

In the space frame models both nodes of each beam element can fail in the form of plastic hinges. The hinges are herein termed as components. When there are N elements in a structure the number of possible components is 2N. Component numbers are imposed in such a way that for element i the numbers are 2i-1 and 2i for node i and j, respectively [Fig. 2.5]. From assumptions in Section 5.1 it can be supposed that the components of elements representing joint part and elements of deck structure will not turn into hinges. When any node is shared by more than two elements and they are co-linear, only one component is considered as a candidate hinge and the others are not considered. This way the actual number of possible components (hinges) is 36 for the Hutton TLP and TLP-A [Fig. 5.5] and 24 for TLP-B [Fig. 5.8].

Table 5.5 Principal Characteristics of the Hutton TLP[211]

Water Depth		: 147.0 m
LENGTH	Between column centers	: 78.00 m
	Overall	: 95.76 m
BREADTH	Between column centers	: 74.00 m
	Overall	: 91.76 m
HEIGHT	Keel to main deck	: 57.70 m
	Main deck to weather deck	: 11.25 m
DRAFT	Operating	: 32.00 m at L.A.T.
COLUMN	4 Corner Columns	: 17.76 m Dia.
	2 Mid-Columns	: 14.50 m Dia
PONTOON	Height	: 10.86 m
	Width	: 8.06 m
	Corner radius	: 1.50 m
WEIGHT	TLP Weight	: 48,035 tons
	Tendon Weight	: 850 tons
INITIAL TENSION	Riser	: 1,321 tons
	Tendon (at L.A.T.)	: 11,330 tons
Displacement (at L.A.T.)		: 61,536 tons

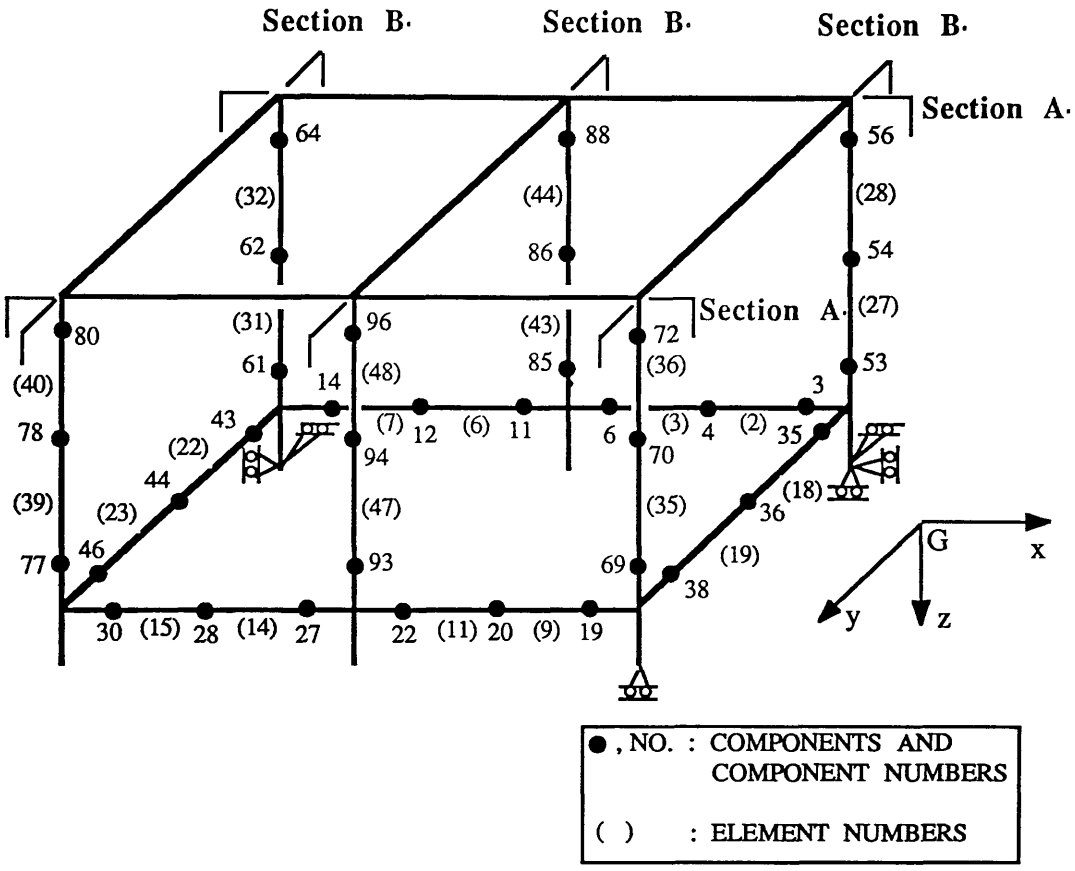

Fig. 5.5 Space Frame Model for the Hutton TLP (and TLP-A)

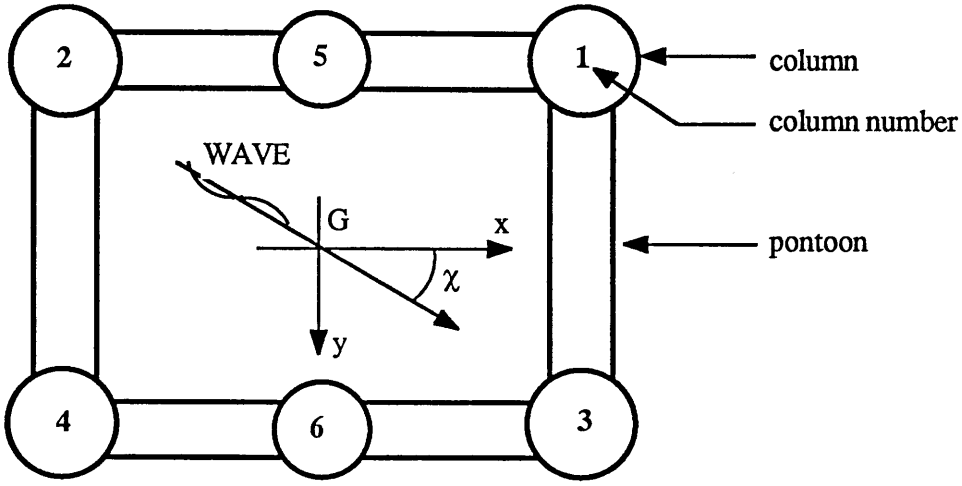

xy - plan

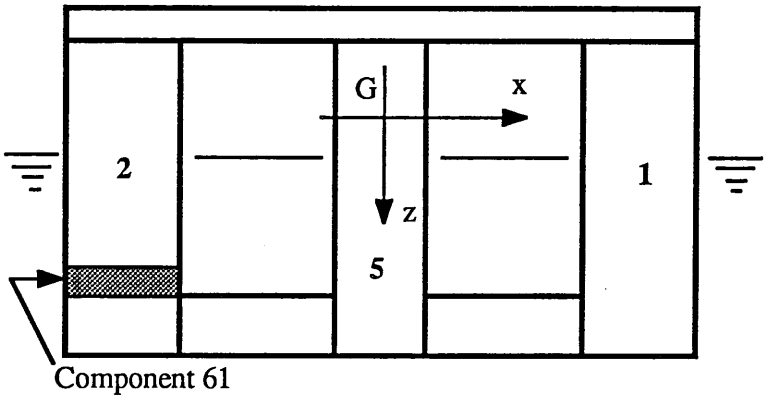

xz - plan

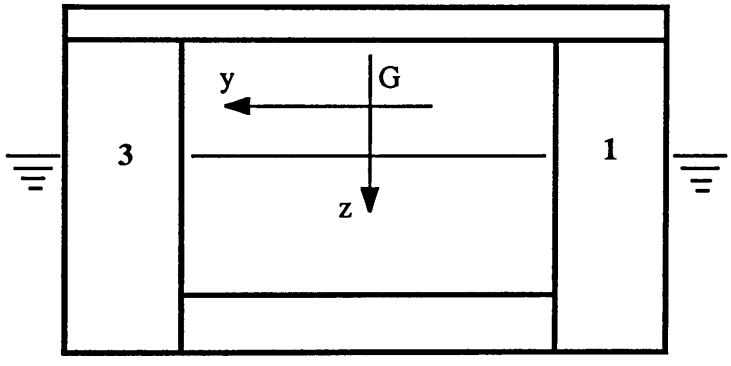

yz - plan

- o Corner columns : ring- and stringer-stiffened cylinders
- o Mid-columns : ring-stiffened cylinders
- o All pontoons : rectangular box-girders

Fig. 5.6 TLP-A

Table 5.6 Geometric and Material Data of the Hutton TLP

Geometric Data

Component		Scantlings (m)
Pontoons	bottom	: thickness = 0.030 frame spacing = 0.750
		stiffener = 0.425 x 0.015 x 0.150 x 0.025 T
	side shell	: thickness = 0.028 frame spacing = 0.750
		stiffener = 0.400 x 0.014 x 0.150 x 0.025 T
	deck	: thickness = 0.026 frame spacing = 0.750
		stiffener = 0.375 x 0.013 x 0.150 x 0.025 T
Corner Column	upper part	: thickness of shell = 0.030
		ring frame spacing = 1.035
		ring stiffener = 0.525 x 0.022 x 0.225 x 0.025 T
	lower part	: thickness of shell = 0.0365
		ring frame spacing = 1.035
		ring stiffener = 0.525 x 0.025 x 0.250 x 0.030 T
Mid-Column	upper part	: thickness of shell = 0.029
		ring frame spacing = 1.035
		ring stiffener = 0.400 x 0.020 x 0.225 x 0.020 T
	lower part	: thickness of shell = 0.029
		ring frame spacing = 1.035
		ring stiffener = 0.450 x 0.022 x 0.225 x 0.025 T

Material Data

Mean of Elastic Modulus : 200,000 MN/m^2

Mean of Yield Stress : 391 MN/m^2

Table 5.7 Geometric and Material Data of TLP-A

Geometric Data

Component		Scantlings (m)	
Pontoons	same as for the Hutton TLP [Table 5.7]		
Corner Column	upper part :	no. of stringers	= 60
		thickness of shell	= 0.020
		stringers	= 0.250 x 0.013 x 0.190 x 0.019 T
		ring frame spacing	= 2.200
		ring stiffener	= 0.425 x 0.022 x 0.225 x 0.025 T
	lower part :	no. of stringers	= 60
		thickness of shell	= 0.025
		stringers	= 0.300 x 0.015 x 0.190 x 0.019 T
		ring frame spacing	= 2.200
		ring stiffener	= 0.525 x 0.025 x 0.250 x 0.030 T
Mid-Column	upper part :	thickness of shell	= 0.029
		ring frame spacing	= 1.035
		ring stiffener	= 0.400 x 0.020 x 0.225 x 0.020 T
	lower part :	thickness of shell	= 0.029
		ring frame spacing	= 1.035
		ring stiffener	= 0.450 x 0.022 x 0.225 x 0.025 T

Material Data

Mean of Elastic Modulus : 200,000 MN/m^2

Mean of Yield Stress : 391 MN/m^2

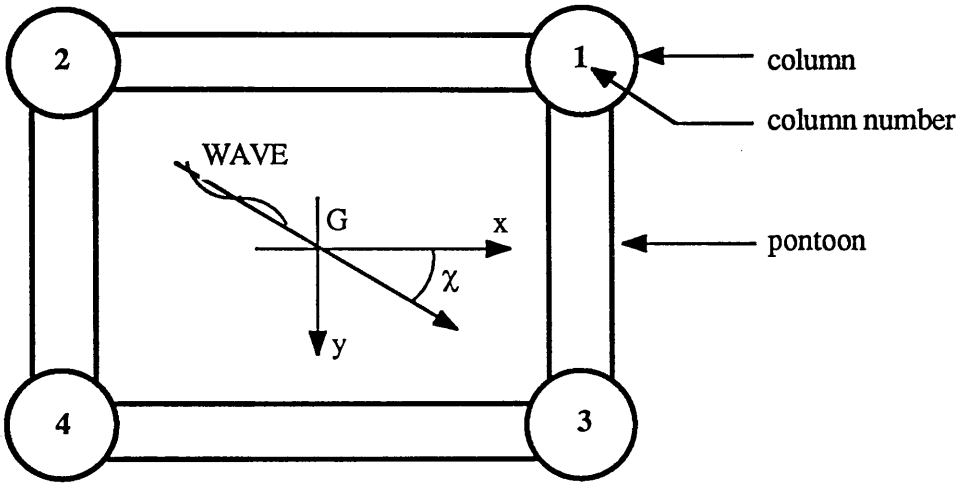

xy - plan

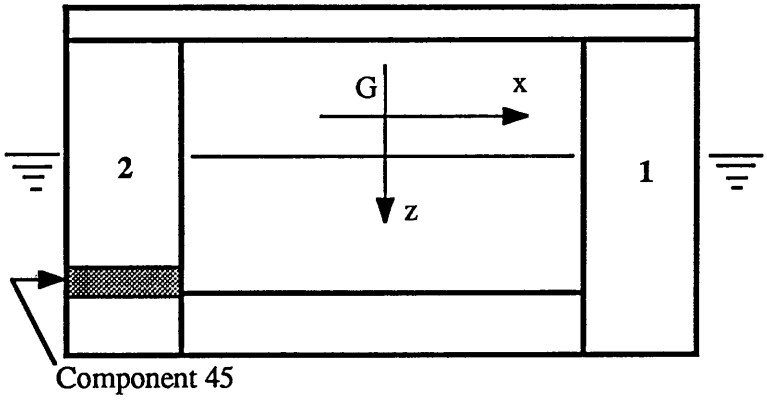

xz - plan

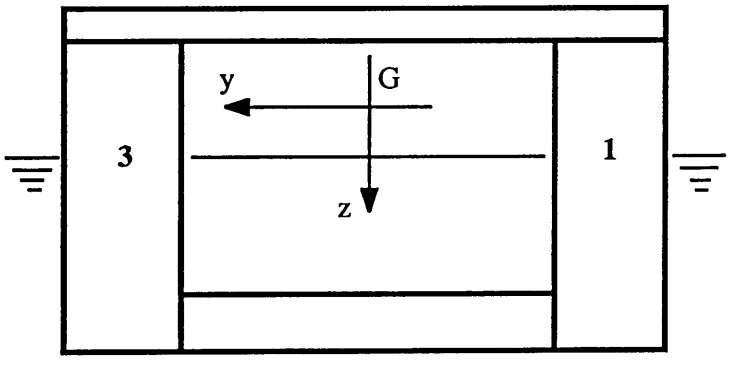

yz - plan

- All columns : ring- and stringer-stiffened cylinders
- All pontoons : rectangular box-girders

Fig. 5.7 TLP-B

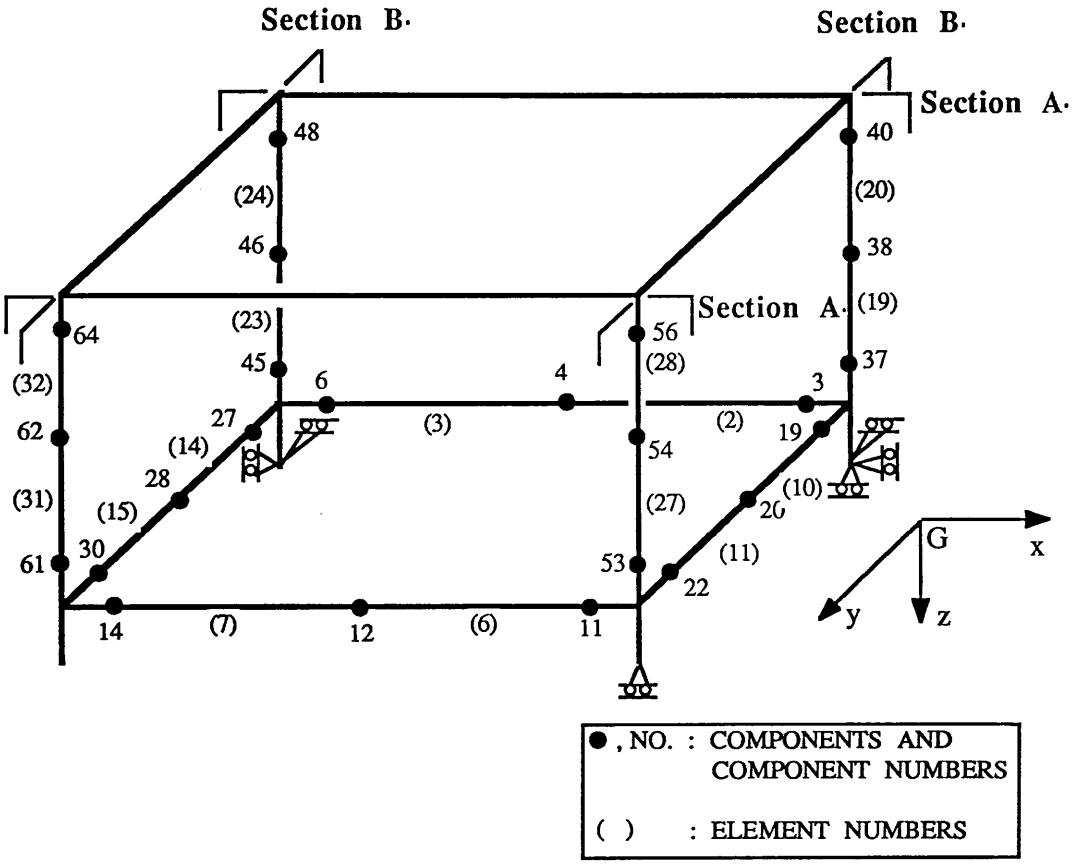

Fig. 5.8 Space Frame Model for TLP-B

Table 5.8 Principal Characteristics of TLP-B

Water Depth		: 147.0 m
LENGTH	Between column centers	: 78.00 m
	Overall	: 95.76 m
BREADTH	Between column centers	: 74.00 m
	Overall	: 91.76 m
HEIGHT	Keel to main deck	: 57.70 m
	Main deck to weather deck	: 11.25 m
DRAFT	Operating	: 32.00 m at L.A.T.
COLUMN	4 Corners	: 17.76 m Dia.
PONTOON	Height	: 10.86 m
	Width	: 8.06 m
	Corner radius	: 1.50 m
WEIGHT	TLP Weight	: 40,259 tons
	Tendon Weight	: 850 tons
INITIAL TENSION	Riser	: 1,321 tons
	Tendon (at L.A.T.)	: 10,974 tons
Displacement (at L.A.T.)		: 53,403 tons

Table 5.9 Geometric and Material Data of TLP-B

Geometric Data

Component	Scantlings (m)		
Pontoons	same as for the Hutton TLP [Table 5.7]		
Corner Column	upper part :	no. of stringers	= 60
		thickness of shell	= 0.020
		stringers	= 0.250 x 0.013 x 0.190 x 0.019 T
		ring frame spacing	= 2.200
		ring stiffener	= 0.425 x 0.022 x 0.225 x 0.025 T
	lower part :	no. of stringers	= 60
		thickness of shell	= 0.025
		stringers	= 0.300 x 0.015 x 0.190 x 0.019 T
		ring frame spacing	= 2.200
		ring stiffener	= 0.525 x 0.025 x 0.250 x 0.030 T

Material Data

Mean of Elastic Modulus : 200,000 MN/m^2

Mean of Yield Stress : 391 MN/m^2

Table 5.10 Three TLP Models

model	descriptions of structural configuration
Hutton TLP	- 6 columns : 4 x corner column of ring stiffened cylinder 2 x mid-column of ring stiffened cylinder
TLP-A	- 6 columns : 4 x corner column of ring- and stringer-stiffened cylinder 2 x mid-column of ring stiffened cylinder - 4 corner columns of ring stiffened cylinder in Hutton TLP are replaced by ring- and stringer-stiffened cylinders*
TLP-B	- 4 corner columns of ring- and stringer-stiffened cylinder - 2 mid-columns of ring stiffened cylinder in TLP-A are removed, or 4 corner columns of ring stiffened cylinders in Hutton TLP are replaced by ring- and stringer-stiffened cylinders* and 2 mid-columns are removed.

* : Structural weight ratio of one ring- and stringer-stiffened cylinder to the original ring stiffened cylinder is about 0.75.

note : All models have the same overall dimensions

5.4 Reliability Analysis of TLP Models

System reliability analysis of the three TLP models has been carried out under the same design environmental condition for the Hutton TLP as seen in Table 5.11[212] by using the developed computer program [Section 5.1]. Ductile behaviour is assumed for the post-ultimate behaviour of failed components. Three wave directions, χ, are considered throughout the analysis, say χ = 0, 45 and 90 deg[9,189].

5.4.1 The Hutton TLP

Fig. 5.9 illustrates RAOs of surge and heave motions by using the Morison type approach described in Section 4.2.3, when wave directions are 0^o, 45^o and 90^o, and comparisons with those by the diffraction theory[189]. As can be seen in the figure the Morison type approach offers reasonable results compared to those by the diffraction theory. Surge and heave force RAOs for three wave directions are plotted in Fig. 5.10.

System reliability analysis of the Hutton TLP has been performed when the structure is under design environmental loading condition [Table 5.11]. Values of parameters controlling the procedure of identifying the important failure modes mentioned in Section 2.5.6 are given in Table 5.12.

With the values of control parameters of Table 5.12, four failure modes have been generated for all wave directions. Reliability indices, probability of failure of the identified important failure modes and bounds of system reliability ($\beta_{sys,lower}$ and $\beta_{sys,upper}$) and probability of system failure ($(P_f)_{sys,lower}$ and $(P_f)_{sys,upper}$), as the results of system analysis, are listed in Tables 5.13, 5.14 and 5.15 for $\chi = 0^o$, 45^o and 90^o, respectively. Figures in [ ] are the probabilities of failure. In general, the failure modes have been identified in increasing order of path reliability indices, β_{path} (or in decreasing order of path probability of failure, P_f) except for the case of $\chi = 90^o$. There seems to be no difference between the upper and lower bound of system reliability indices (and of the probabilities of system failure) and the first identified mode seems to dominate the bounds for all wave direction.

The results are summarised in Table 5.16. The average system reliability index is the value corresponding to the average of lower and upper bounds of probability of system failure. As far as the present computational results are concerned, when $\chi = 45^o$, i.e., under quartering sea, the system reliability is lowest followed by that for following sea. The system reliability indices for $\chi = 0^o$ and $\chi = 90^o$ are about 4% and by 8.4% greater than that for $\chi = 45^o$, respectively. The total average reliability index is calculated

according to the total average probability of system failure given that the same probability of occurrence is imposed for each wave direction. The total average of system failure probability is 0.602×10^{-10} and the corresponding average reliability index is 6.44.

Table 5.17 illustrates the reliability index and probability of failure of the first failed component in any identified mode and those of the component of Column 2 located just above pontoon, i.e. bottom bay of Column 2 which is designated here Component 61 [shaded part in Fig. 5.1 and see also Fig. 5.5].

Location of failed components and collapse modes of the identified failure modes is shown in Figs. 5.11 and 5.12 for $\chi = 0^o$, in Figs. 5.13 and 5.14 for $\chi = 45^o$ and in Figs. 5.16 and 5.17 for $\chi = 90^o$. As can be seen in the figures, the critical components are those of columns located around joints rather than those of pontoons, especially for $\chi = 0^o$. For the case of $\chi = 0^o$, many components in Section A-1 of Fig. 5.5 have failed. This may be due to the re-distribution of load effects arising from failure of the first failed component. That is, Component 64 and subsequently failed components have more influence on the components in Section A-1 rather than on the components in other sections. Similar distribution of failed components can be applied for the case of $\chi = 90^o$ in Section B-3, whereas for the case of $\chi = 45^o$ failed components are more scattered. Generally, it can be found that failed components gather in the section where the first failed component is.

In Figs. 5.11, 5.13 and 5.15, β_{path} represents the path reliability index and λ_T the total load factor calculated from Eq.(2.95) when structural failure occurs [Section 2.4.1]. λ_T is the ratio of the load at collapse to the applied mean load (design load) as can be seen in Eqs.(2.15.a) and (2.15.b) and may be related to the reserve strength index in Eq.(2.11) [Section 2.1.2]. From the figures of collapse modes λ_T varies from 1.87 for Mode-2 when $\chi = 0^o$, to 4.13 for Mode-3 when $\chi = 45^o$, and their average is 2.63, i.e. the Hutton TLP can sustain about 2.6 times the design load in the average sense.

From the above results, the values of λ_T shows that the Hutton TLP seems to

possess high reserve strength, and considering that because structural collapse is approximately judged from Eq.(2.111) rather than from Eq.(2.110), the failure states are not the complete collapse ones, λ_T's of the actual structure may be greater than the calculated values. The values of path reliability indices and system ones compared to those of components also imply considerable residual strength of the structure in the probabilistic sense. Further discussion about this will be given in Section 5.4.4.

Table 5.11 Design Environmental Condition for the Hutton TLP[212]

Wind		
1 minute mean wind velocity at 10 m elevation wind gradient variation with elevation according to the equation in section 4.2.2		V_{10} = 44.0 m/sec
Waves		
(1) Regular design waves:	wave height	H_W = 30.3 m
	period	T_W = 14.6 - 18.5 sec
(2) Irregular waves:	significant wave height	H_Z = 16.6 m
	average zero-crossing period	T_Z = 13.9 sec
Current		
5 minute mean velocity at 10 m depth		V_C = 0.85 m/sec
Water Level		
Range between HDWL and LDWL		2.9 m

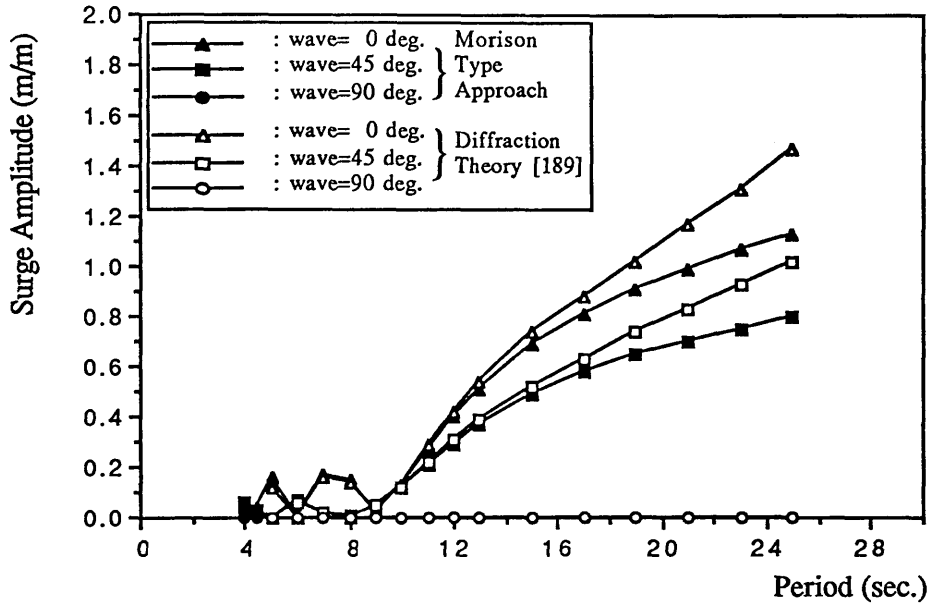

(a) Surge

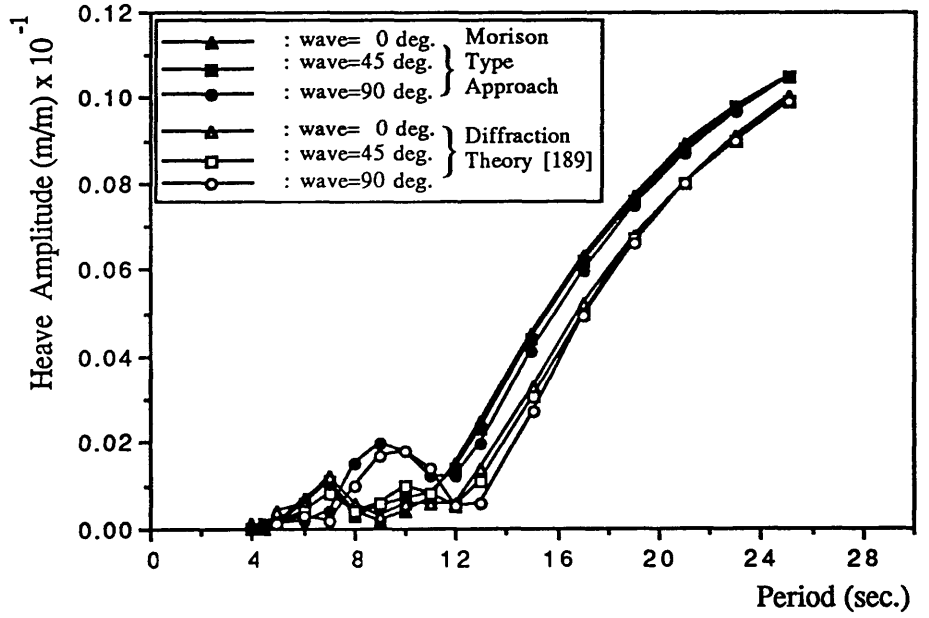

(b) Heave

Fig. 5.9 Motion RAOs of the Hutton TLP at 32 m Draft

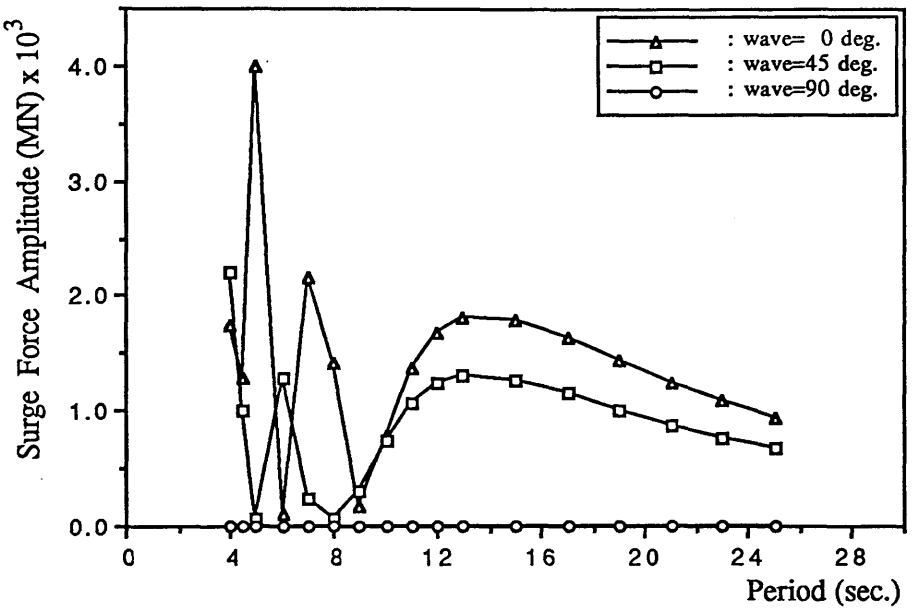

(a) Surge

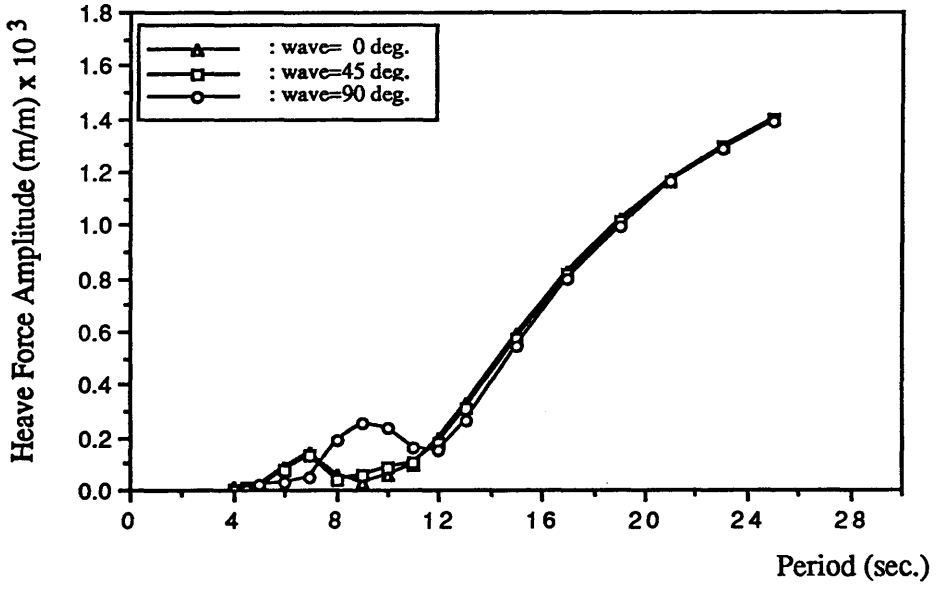

(b) Heave

Fig. 5.10 Force RAOs of the Hutton TLP at 32 m Draft

Table 5.12 Values of Control Parameters in the Identifying Procedure

parameter	value	description
ε_{det}	1.0×10^{-8}	used to judge the singularity of the structural stiffness matrix [Eq.(2.111)]
N_{det}	N_{max}	used to check the determinants of interim modes, and N_{max} is maximum of the number of failed components contained in any mode for all possible interim modes [Eq.(2.112)]
ε_{utr}	1.0×10^{-4}	used to discard the mode when the ratio of two successively evaluated utilisations is less than this given value
N_{Limit}	6	used to limit the number of candidate interim modes
ε_{sys}	1.0×10^{-2}	used to check the convergence of bounds of system reliability indices [Eq.(2.115)]
M_{min}	4	the required minimum number of failure modes to be identified

Table 5.13 Identified Important Failure Modes of the Hutton TLP for $\chi = 0^o$

mode no.	failed components	β_{path} [$(P_f)_{path}$]
Mode-1	64, 85, 61, 72, 56, 80, 88, 77, 69, 93	6.55 [0.288×10^{-10}]
Mode-2	64, 85, 61, 72, 56, 80, 88, 77, 69, 53	7.12 [0.563×10^{-12}]
Mode-3	64, 85, 61, 72, 56, 80, 88, 77, 69, 46	7.66 [0.971×10^{-14}]
Mode-4	64, 85, 61, 72, 56, 80, 88, 77, 69, 86	7.82 [0.272×10^{-14}]

Bounds of β_{sys} and $(P_f)_{sys}$:

$\beta_{sys,lower}$ and $(P_f)_{sys,upper}$ = 6.55 and 0.294×10^{-10}

$\beta_{sys,upper}$ and $(P_f)_{sys,lower}$ = 6.55 and 0.294×10^{-10}

Table 5.14 Identified Important Failure Modes of the Hutton TLP for $\chi = 45^o$

mode no.	failed components	β_{path} $[(P_f)_{path}]$
Mode-1	61, 93, 85, 69, 64, 53, 72, 3, 14	6.31 [0.137×10^{-9}]
Mode-2	61, 93, 85, 69, 64, 53, 72, 3, 38, 77	6.71 [0.984×10^{-11}]
Mode-3	61, 93, 85, 69, 64, 53, 72, 3, 38, 4	7.24 [0.225×10^{-12}]
Mode-4	61, 93, 85, 69, 64, 53, 72, 3, 38, 88	7.31 [0.137×10^{-12}]

Bounds of β_{sys} and $(P_f)_{sys}$:

$\beta_{sys,lower}$ and $(P_f)_{sys,upper}$ = 6.30 and 0.147×10^{-9}

$\beta_{sys,upper}$ and $(P_f)_{sys,lower}$ = 6.30 and 0.147×10^{-9}

Table 5.15 Identified Important Failure Modes of the Hutton TLP for $\chi = 90^o$

mode no.	failed components	β_{path} $[(P_f)_{path}]$
Mode-1	64, 77, 56, 69, 38, 61, 43, 46, 53	6.84 [0.411×10^{-11}]
Mode-2	64, 77, 56, 69, 38, 61, 43, 46, 85	8.28 [0.603×10^{-16}]
Mode-3	64, 77, 56, 69, 38, 61, 43, 46, 93	8.51 [0.819×10^{-17}]
Mode-4	64, 77, 56, 69, 38, 61, 43, 53, 35	6.98 [0.151×10^{-11}]

Bounds of β_{sys} and $(P_f)_{sys}$:

$\beta_{sys,lower}$ and $(P_f)_{sys,upper}$ = 6.83 and 0.411×10^{-11}

$\beta_{sys,upper}$ and $(P_f)_{sys,lower}$ = 6.83 and 0.411×10^{-11}

Table 5.16 Summary of System Reliability Analysis of the Hutton TLP

χ	$\beta_{sys,lower}$ [$(P_f)_{sys,upper}$]	$\beta_{sys,upper}$ [$(P_f)_{sys,lower}$]	average β_{sys} [average $(P_f)_{sys}$]
0	6.55 [0.294×10^{-10}]	6.55 [0.294×10^{-10}]	6.55 [0.294×10^{-10}]
45	6.30 [0.147×10^{-9}]	6.30 [0.147×10^{-9}]	6.30 [0.147×10^{-9}]
90	6.83 [0.411×10^{-11}]	6.83 [0.411×10^{-11}]	6.83 [0.411×10^{-11}]

Total Average of $\beta_{sys} = 6.44$

$(P_f)_{sys} = 0.602 \times 10^{-10}$

Table 5.17 Component Reliability Index and Probability of Failure for the Hutton TLP

χ	first failed component	Component 61
0	2.14 [0.163×10^{-1}]	3.78 [0.790×10^{-4}]
45	5.31 [0.549×10^{-7}]	5.31 [0.549×10^{-7}]
90	5.36 [0.415×10^{-7}]	6.39 [0.810×10^{-10}]

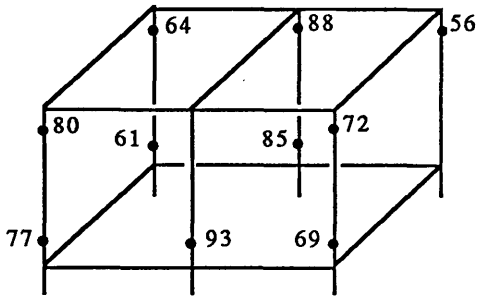

(1) Mode-1

failed components

: 64, 85, 61, 72, 56, 80, 77, 69, 93

β_{path} = 6.55 λ_T = 2.13

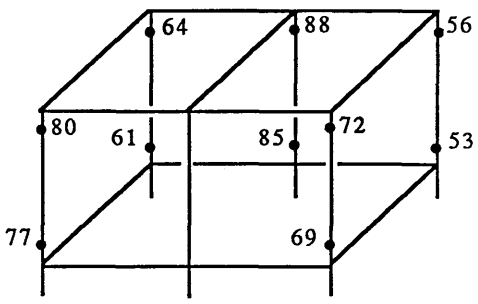

(2) Mode-2

failed components

: 64, 85, 61, 72, 56, 80, 77, 69, 53

β_{path} = 7.12 λ_T = 1.87

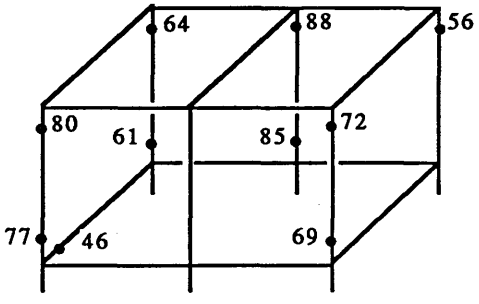

(3) Mode-3

failed components

: 64, 85, 61, 72, 56, 80, 77, 69, 46

β_{path} = 7.66 λ_T = 2.29

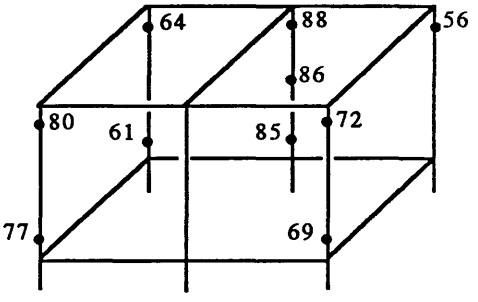

(4) Mode-4

failed components

: 64, 85, 61, 72, 56, 80, 77, 69, 86

β_{path} = 7.82 λ_T = 2.15

Fig. 5.11 Structural Failure States of the Hutton TLP for $\chi = 0^o$

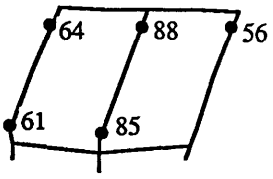

Section A-1

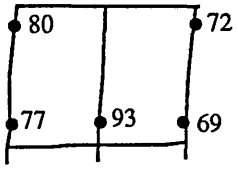

Section A-2

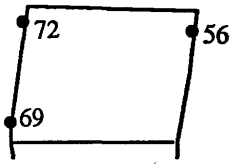

Section B-1

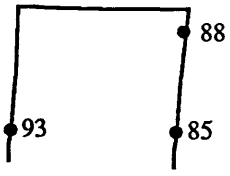

Section B-2

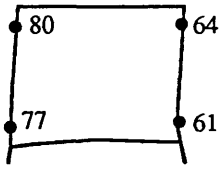

Section B-3

(1) Mode-1

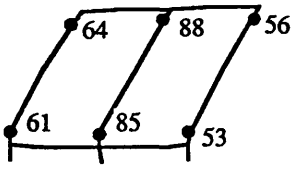

Section A-1

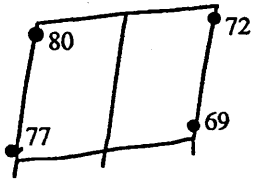

Section A-2

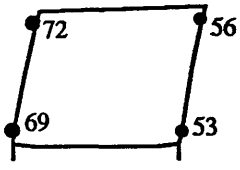

Section B-1

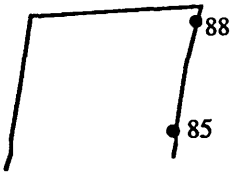

Section B-2

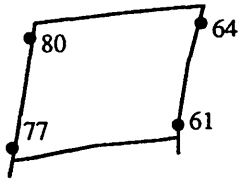

Section B-3

(2) Mode-2

Fig. 5.12 Collapse Modes of the Hutton TLP for $\chi = 0^{o}$

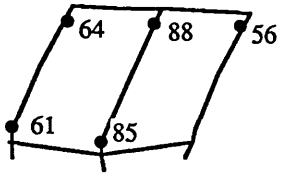

Section A-1

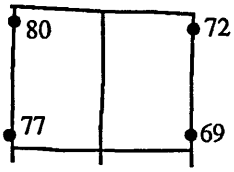

Section A-2

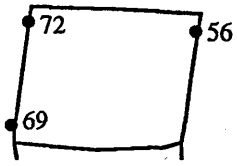

Section B-1

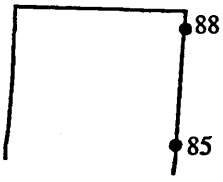

Section B-2

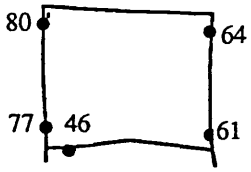

Section B-3

(3) Mode-3

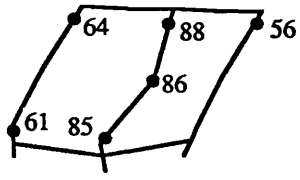

Section A-1

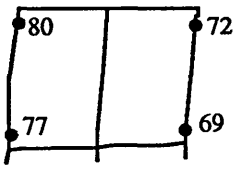

Section A-2

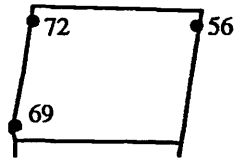

Section B-1

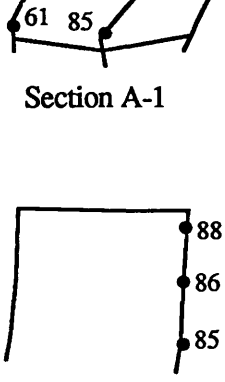

Section B-2

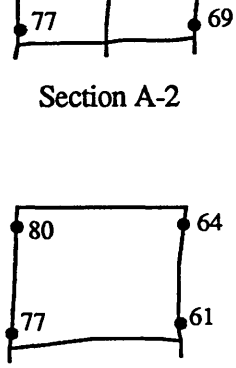

Section B-3

(4) Mode-4

Fig. 5.12 Collapse Modes of the Hutton TLP for $\chi = 0^{o}$ (continued)

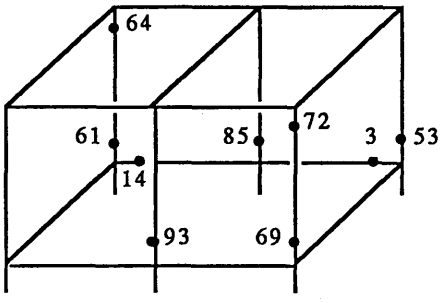

(1) Mode-1

failed components

: 61, 93, 85, 69,64, 53, 72, 3, 14

β_{path} = 6.31 λ_T = 3.07

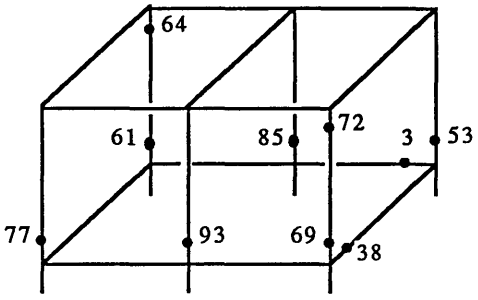

(2) Mode-2

failed components

: 61, 93, 85, 69,64, 53, 72, 38, 77

β_{path} = 6.71 λ_T = 2.53

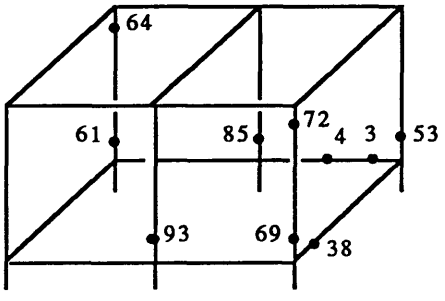

(3) Mode-3

failed components

: 61, 93, 85, 69,64, 53, 72, 3, 38, 4

β_{path} = 7.24 λ_T = 4.13

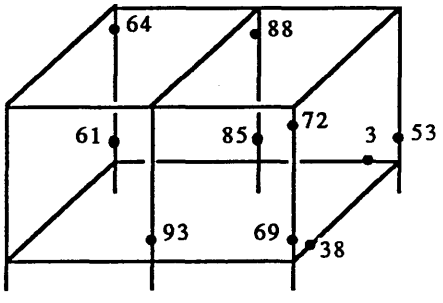

(4) Mode-4

failed components

: 61, 93, 85, 69,64, 53, 72, 3, 38, 88

β_{path} = 7.31 λ_T = 2.48

Fig. 5.13 Structural Failure States of the Hutton TLP for $\chi = 45^o$

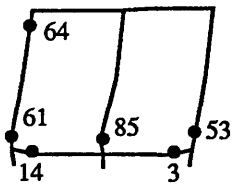

Section A-1

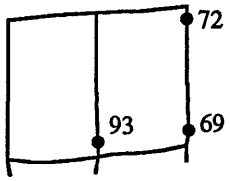

Section A-2

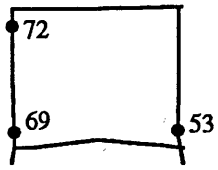

Section B-1

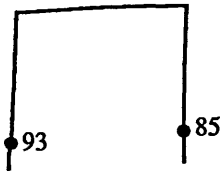

Section B-2

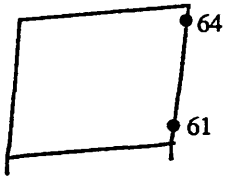

Section B-3

(1) Mode-1

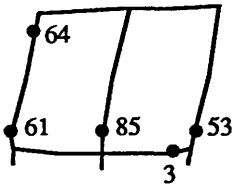

Section A-1

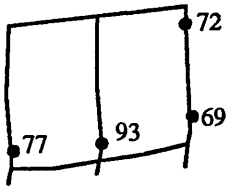

Section A-2

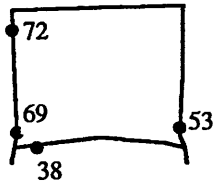

Section B-1

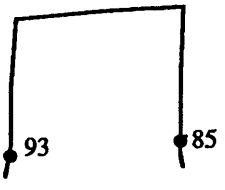

Section B-2

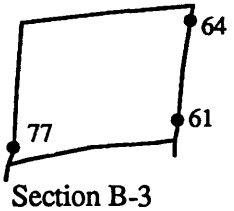

Section B-3

(2) Mode-2

Fig. 5.14 Collapse Modes of the Hutton TLP for $\chi = 45^{o}$

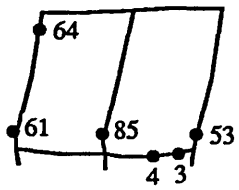

Section A-1

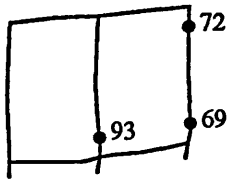

Section A-2

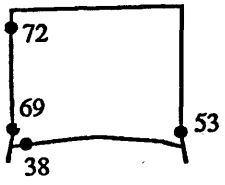

Section B-1

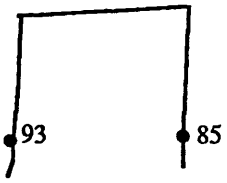

Section B-2

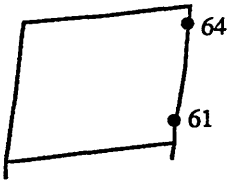

Section B-3

(3) Mode-3

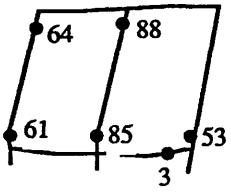

Section A-1

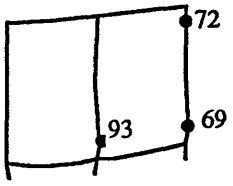

Section A-2

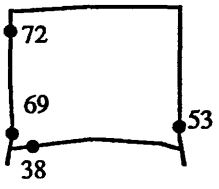

Section B-1

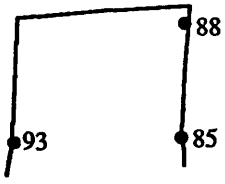

Section B-2

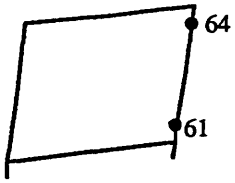

Section B-3

(4) Mode-4

Fig. 5.14 Collapse Modes of the Hutton TLP for $\chi = 45^{o}$ (continued)

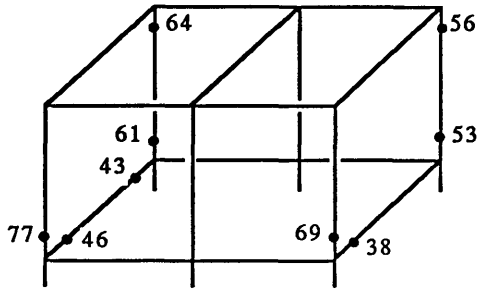

(1) Mode-1

failed components

: 64, 77, 56, 69, 38, 61, 43, 46, 53

β_{path} = 6.85 λ_T = 2.63

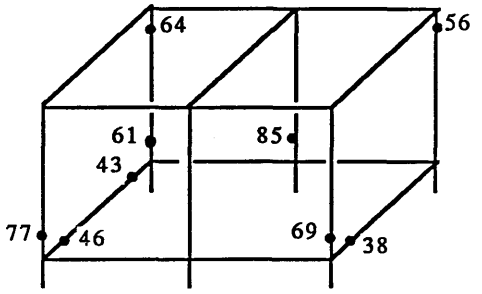

(2) Mode-2

failed components

: 64, 77, 56, 69, 38, 61, 43, 46, 85

β_{path} = 8.24 λ_T = 3.82

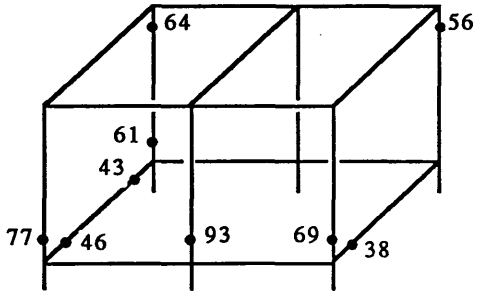

(3) Mode-3

failed components

: 64, 77, 56, 69, 38, 61, 43, 46, 93

β_{path} = 8.52 λ_T = 2.48

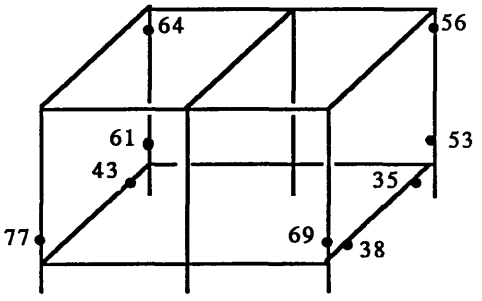

(4) Mode-4

failed components

: 64, 77, 56, 69, 38, 61, 43, 53, 35

β_{path} = 6.98 λ_T = 3.48

Fig. 5.15 Structural Failure States of the Hutton TLP for $\chi = 90^o$

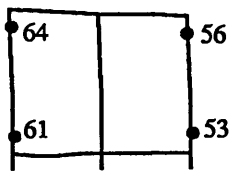

Section A-1

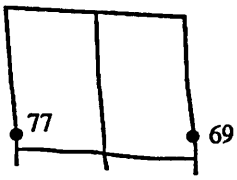

Section A-2

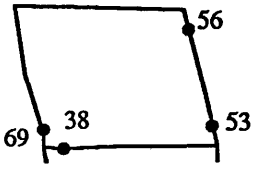

Section B-1

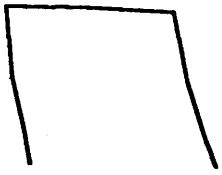

Section B-2

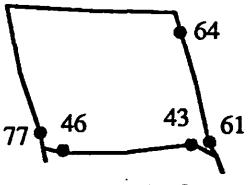

Section B-3

(1) Mode-1

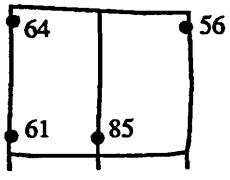

Section A-1

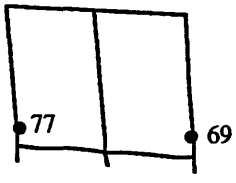

Section A-2

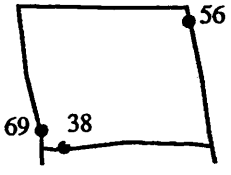

Section B-1

Section B-2

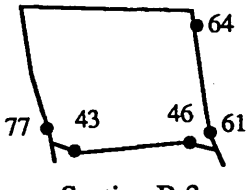

Section B-3

(2) Mode-2

Fig. 5.16 Collapse Modes of the Hutton TLP for $\chi = 90^{o}$

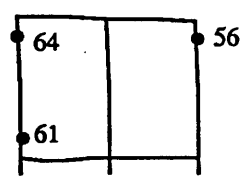

Section A-1

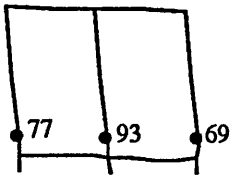

Section A-2

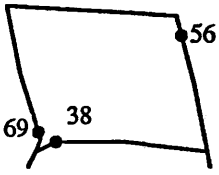

Section B-1

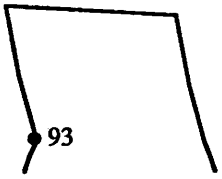

Section B-2

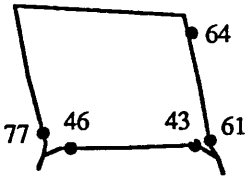

Section B-3

(3) Mode-3

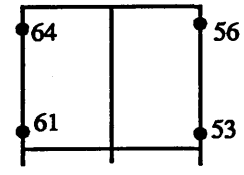

Section A-1

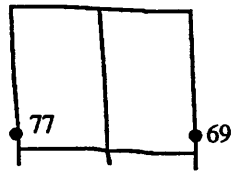

Section A-2

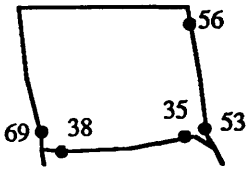

Section B-1

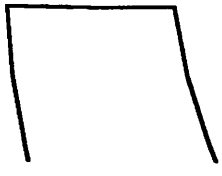

Section B-2

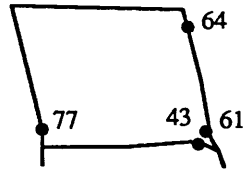

Section B-3

(4) Mode-4

Fig. 5.16 Collapse Modes of the Hutton TLP for $\chi = 90^{o}$ (continued)

5.4.2. TLP-A

A system reliability analysis of TLP-A has been performed under the same design environmental condition as that for the Hutton TLP as in Table 5.11. From geometric data for the Hutton TLP in Table 5.6 and for TLP-A in Table 5.7 the structural weight ratio of one corner column of TLP-A to that of the Hutton TLP is about 0.75, for which ring frames are included. The structural weight and its distribution of corner column for this model differ from those for the Hutton TLP but their influence on the loading can be neglected, i.e. three categories of the environmental loading are supposed to be the same as those of the Hutton TLP for system reliability analysis of this model.

The interaction equation given as Eq.(3.53) has been used for the components of corner columns and Eq.(3.11) for the components of mid-columns as for the Hutton TLP. The same values of parameters controlling the procedure of identifying the important failure modes as for the Hutton TLP as in Table 5.12. Four failure modes have been generated for each wave direction as the case of the Hutton TLP. The analysis results are presented in Tables 5.18, 5.19 and 5.20 for each wave direction in the same manner as for the Hutton TLP: path reliability indices, probabilities of failure and bounds of system reliability index and/or bounds of system failure probability. The failure modes have generally been found in increasing order of path reliability index (in decreasing order of failure probability), except for the case of $\chi = 90^{o}$. There seems to be no difference between bounds of β_{sys} and $(P_f)_{sys}$ for all wave directions as for the Hutton TLP.

The results are re-summarised in Table 5.21 with the total average of probability of system failure and corresponding average system reliability index calculated under the same assumption as described in the previous section. From Table 5.21, when $\chi = 0^{o}$, i.e., under following sea, β_{sys} is lower than other two cases of wave directions differently from the case of the Hutton TLP of which β_{sys} for $\chi = 45^{o}$ was lowest. The average value of β_{sys} of 6.26 is about 2.8% lower than that of the Hutton TLP. This is due to the comparatively high value of $(P_f)_{sys}$ (lower β_{sys}) when $\chi = 0^{o}$. But the difference between β_{sys}'s of TLP-A and the Hutton TLP is negligibly small in spite of

there being less structural material. The average β_{sys} for $\chi = 45^o$ and 90^o are about 8.2% and 10% greater than that for $\chi = 0^o$, respectively. Table 5.22 illustrates the reliability indices of the first failed components in the failure modes and of Component 61, shaded part in Fig. 5.6 [see also Fig. 5.5].

Fig. 5.17 shows the structural failure states and Fig. 5.18 the collapse modes when $\chi = 0^o$. A set of Figs. 5.19 and 5.20 show them in the same manner when $\chi = 45^o$ and a set of Figs. 5.21 and 5.22 when $\chi = 90^o$. The critical components are mostly those of columns. As in the case of the Hutton TLP, subsequently failed components following the first failed one lie in the section where the first failed one lies.

As shown in Figs. 5.17, 5.19 and 5.21, the total load factors, λ_T varies from 2.13 for Mode-2 when $\chi = 45^o$, to 4.05 for Mode-3 when $\chi = 90^o$, and average of λ_T's is 2.82. This is about 7.2% greater than that of the Hutton TLP.

From the results of TLP-A, one can see that TLP-A also possesses considerable reserve strength, and comparison of β_{sys} in Table 5.21 and β_{path} in Table 5.22 implies that the model also possesses appreciable residual strength like the Hutton TLP. A higher average value of λ_T's compared to that of the Hutton TLP implies that the structures having ring- and stringer-stiffened cylinders can more efficiently sustain the environmental loading than the structure having ring-stiffened cylinders.

Table 5.18 Identified Important Failure Modes of TLP-A for $\chi = 0^o$

mode no.	failed components	β_{path} $[(P_f)_{path}]$
Mode-1	85, 64, 61, 72, 53, 69, 77, 3, 4	6.10 [0.550×10^{-9}]
Mode-2	85, 64, 61, 72, 53, 69, 77, 3, 46	6.69 [0.112×10^{-10}]
Mode-3	85, 64, 61, 72, 53, 69, 77, 3, 14	6.69 [0.109×10^{-10}]
Mode-4	85, 64, 61, 72, 53, 69, 77, 3, 35	6.90 [0.264×10^{-11}]

Bounds of β_{sys} and $(P_f)_{sys}$:

$\beta_{sys,lower}$ and $(P_f)_{sys,upper}$ = 6.09 and 0.575×10^{-9}

$\beta_{sys,upper}$ and $(P_f)_{sys,lower}$ = 6.09 and 0.575×10^{-9}

Table 5.19 Identified Important Failure Modes of TLP-A for $\chi = 45^o$

mode no.	failed components	β_{path} $[(P_f)_{path}]$
Mode-1	61, 69, 53, 64. 72, 77, 56, 80, 85, 88	7.21 [0.291×10^{-12}]
Mode-2	61, 69, 53, 64. 72, 77, 56, 80, 85, 93	7.21 [0.291×10^{-12}]
Mode-3	61, 69, 53, 64. 72, 77, 56, 80, 85, 62	7.72 [0.574×10^{-14}]
Mode-4	61, 69, 53, 64. 72, 77, 56, 80, 85, 70	7.89 [0.148×10^{-14}]

Bounds of β_{sys} and $(P_f)_{sys}$:

$\beta_{sys,lower}$ and $(P_f)_{sys,upper}$ = 7.20 and 0.299×10^{-12}

$\beta_{sys,upper}$ and $(P_f)_{sys,lower}$ = 7.20 and 0.299×10^{-12}

Table 5.20 Identified Important Failure Modes of TLP-A for $\chi = 90^o$

mode no.	failed components	β_{path} $[(P_f)_{path}]$
Mode-1	64, 77, 69, 61, 53, 93, 35, 43	6.69 [0.112×10^{-10}]
Mode-2	64, 77, 69, 61, 53, 93, 35, 56	8.08 [0.342×10^{-15}]
Mode-3	64, 77, 69, 61, 53, 93, 35, 44	8.34 [0.388×10^{-16}]
Mode-4	64, 77, 69, 61, 53, 93, 35, 46	7.93 [0.115×10^{-14}]

Bounds of β_{sys} and $(P_f)_{sys}$:

$\beta_{sys,lower}$ and $(P_f)_{sys,upper}$ = 6.69 and 0.112×10^{-10}

$\beta_{sys,upper}$ and $(P_f)_{sys,lower}$ = 6.69 and 0.112×10^{-10}

Table 5.21 Summary of System Reliability Analysis of TLP-A

χ	$\beta_{sys,lower}$ [$(P_f)_{sys,upper}$]	$\beta_{sys,upper}$ [$(P_f)_{sys,lower}$]	average β_{sys} [average $(P_f)_{sys}$]
0	6.09 [0.575×10^{-9}]	6.09 [0.575×10^{-9}]	6.09 [0.575×10^{-9}]
45	7.20 [0.299×10^{-12}]	7.20 [0.299×10^{-12}]	7.20 [0.299×10^{-12}]
90	6.69 [0.112×10^{-10}]	6.69 [0.112×10^{-10}]	6.69 [0.112×10^{-10}]
Total Average of	β_{sys}	= 6.26	
	$(P_f)_{sys}$	= 0.195×10^{-9}	

Table 5.22 Component Reliability Index and Probability of Failure for TLP-A

χ	first failed component	Component 61
0	1.25 [0.105]	3.37 [0.373×10^{-3}]
45	4.61 [0.200×10^{-5}]	4.61 [0.200×10^{-5}]
90	5.28 [0.654×10^{-7}]	5.54 [0.156×10^{-7}]

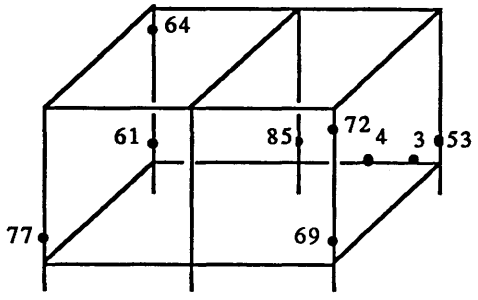

(1) Mode-1

failed components

: 85, 64, 61, 72, 53, 69, 77, 3, 4

β_{path} = 6.10 λ_T = 2.89

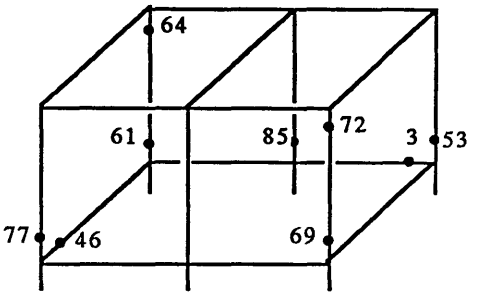

(2) Mode-2

failed components

: 85, 64, 61, 72, 53, 69, 77, 3, 46

β_{path} = 6.69 λ_T = 2.43

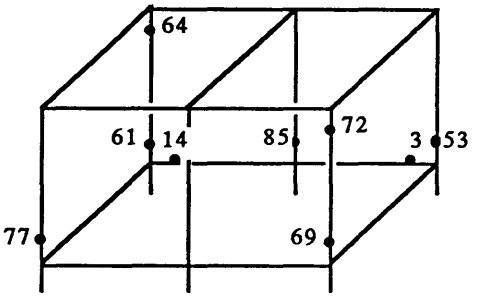

(3) Mode-3

failed components

: 85, 64, 61, 72, 53, 69, 77, 3, 14

β_{path} = 6.70 λ_T = 2.67

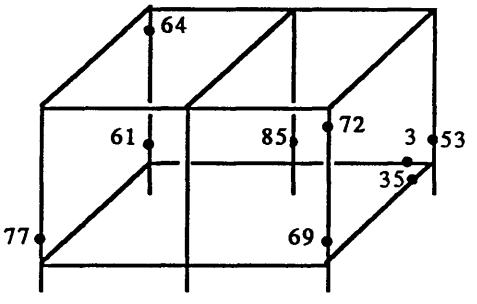

(4) Mode-4

failed components

: 85, 64, 61, 72, 53, 69, 77, 3, 14

β_{path} = 6.90 λ_T = 2.27

Fig. 5.17 Structural Failure States of TLP-A for $\chi = 0^o$

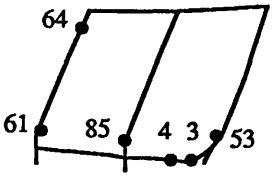

Section A-1

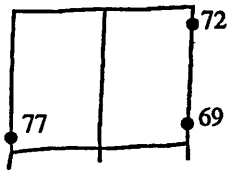

Section A-2

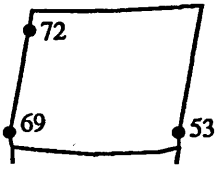

Section B-1

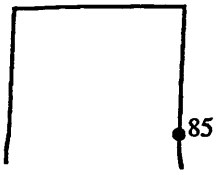

Section B-2

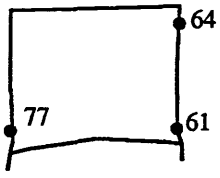

Section B-3

(1) Mode-1

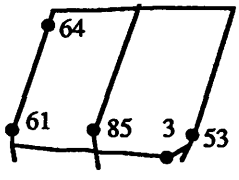

Section A-1

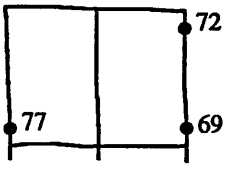

Section A-2

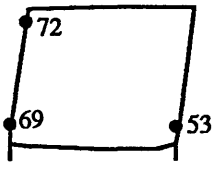

Section B-1

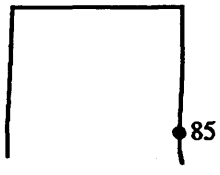

Section B-2

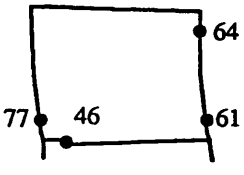

Section B-3

(2) Mode-2

Fig. 5.18 Collapse Modes of TLP-A for $\chi = 0^{o}$

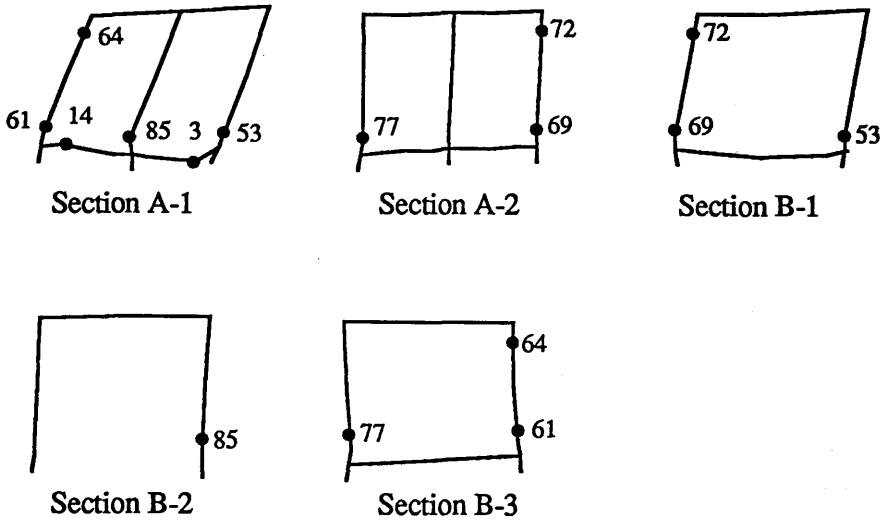

(3) Mode-3

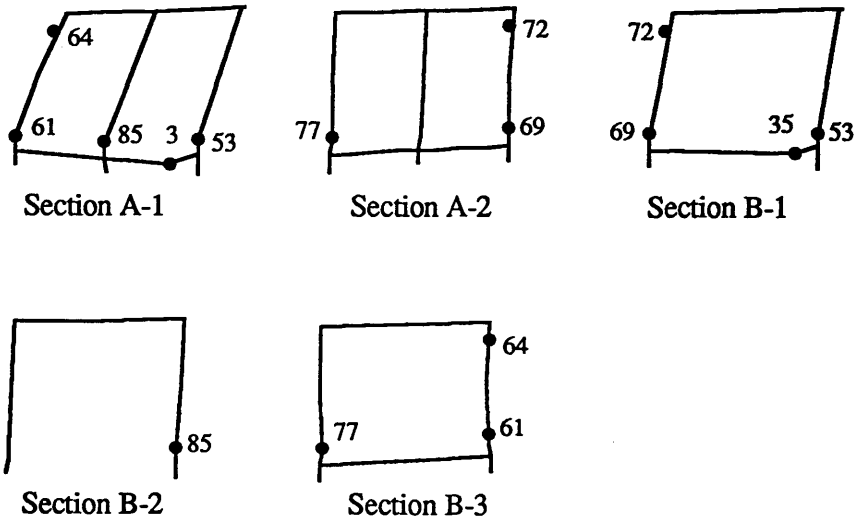

(4) Mode-4

Fig. 5.18 Collapse Modes of TLP-A for $\chi = 0^0$ (continued)

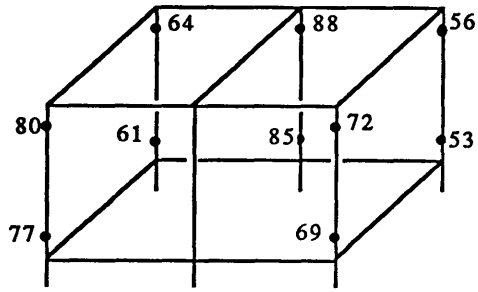

(1) Mode-1

failed components

: 61, 69, 53, 64, 72, 77, 56, 80, 85, 88

β_{path} = 7.21 λ_T = 2.32

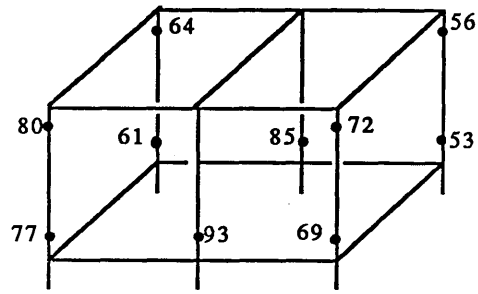

(2) Mode-2

failed components

: 61, 69, 53, 64, 72, 77, 56, 80, 85, 93

β_{path} = 7.21 λ_T = 2.13

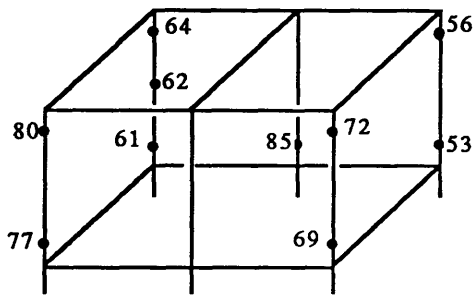

(3) Mode-3

failed components

: 61, 69, 53, 64, 72, 77, 56, 80, 85, 62

β_{path} = 7.72 λ_T = 3.17

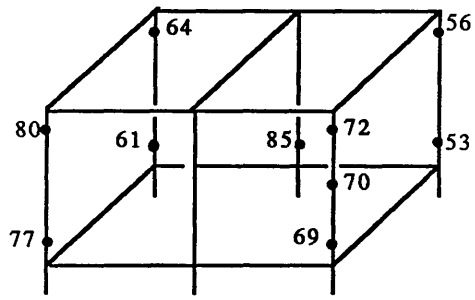

(4) Mode-4

failed components

: 61, 69, 53, 64, 72, 77, 56, 80, 85, 70

β_{path} = 7.89 λ_T = 3.39

Fig. 5.19 Structural Failure States of TLP-A for $\chi = 45^o$

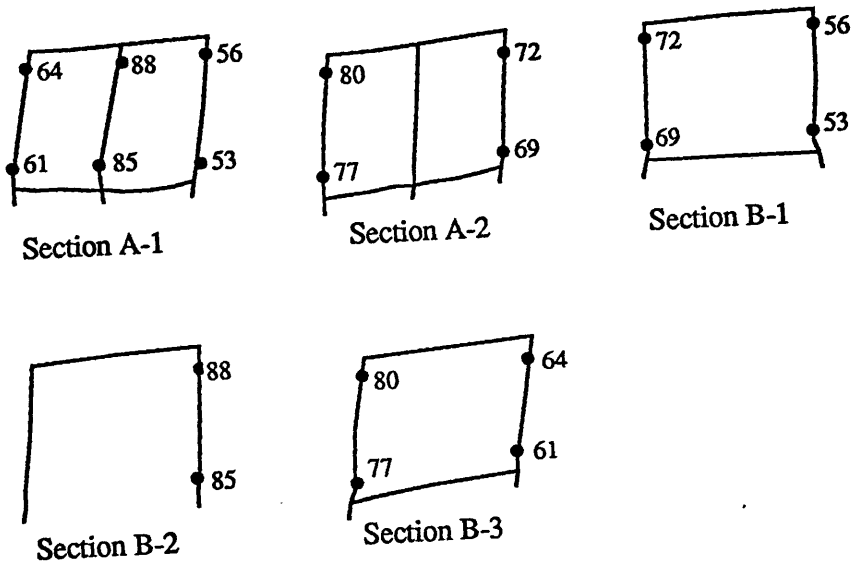

(1) Mode-1

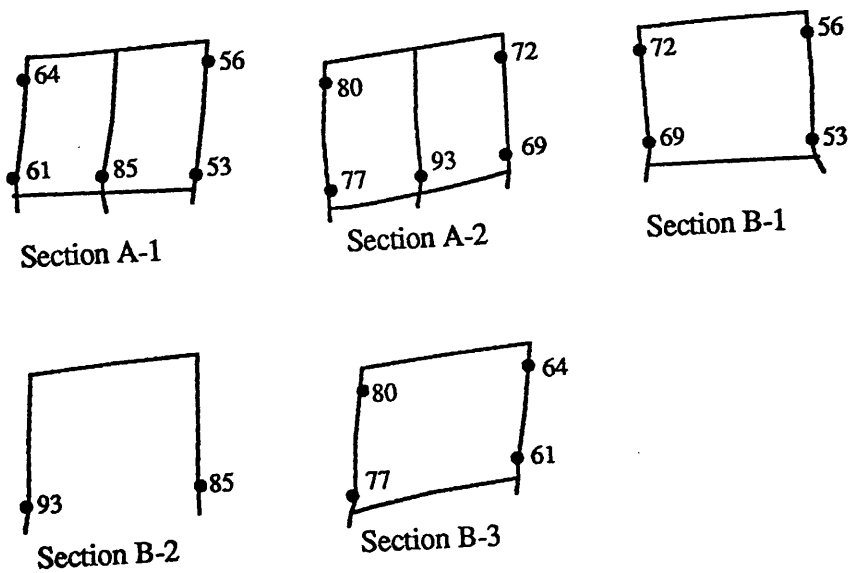

(2) Mode-2

Fig. 5.20 Collapse Modes of TLP-A for $\chi = 45^{o}$

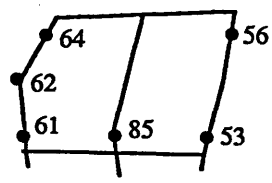

Section A-1

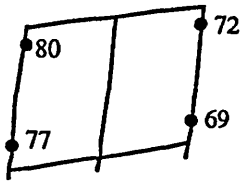

Section A-2

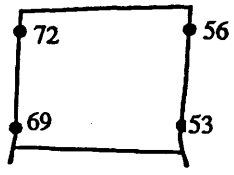

Section B-1

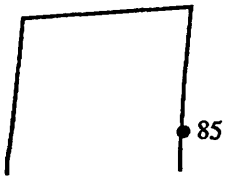

Section B-2

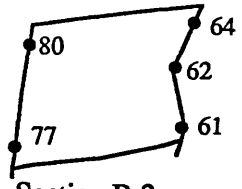

Section B-3

(3) Mode-3

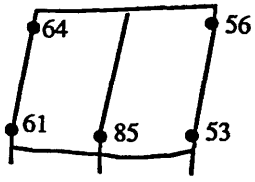

Section A-1

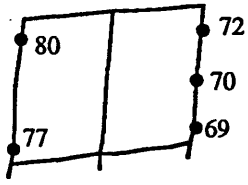

Section A-2

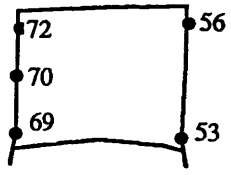

Section B-1

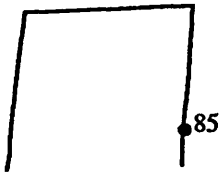

Section B-2

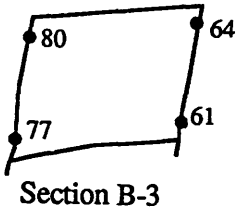

Section B-3

(4) Mode-4

Fig. 5.20 Collapse Modes of TLP-A for $\chi = 45^{o}$ (continued)

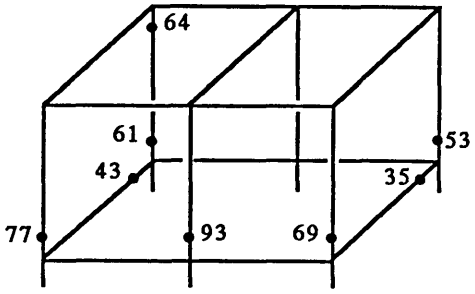

(1) Mode-1

failed components

: 64, 77, 69, 61, 53, 93, 35, 43

β_{path} = 6.69 λ_T = 3.22

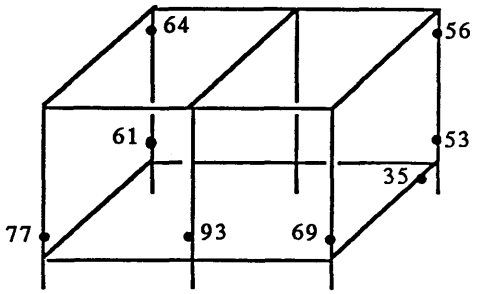

(2) Mode-2

failed components

: 64, 77, 69, 61, 53, 93, 35, 56

β_{path} = 8.08 λ_T = 2.34

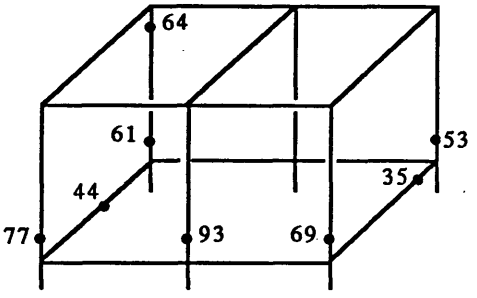

(3) Mode-3

failed components

: 64, 77, 69, 61, 53, 93, 35, 44

β_{path} = 8.34 λ_T = 4.05

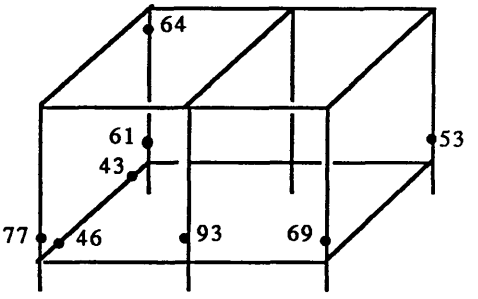

(4) Mode-4

failed components

: 64, 77, 69, 61, 53, 93, 35, 46

β_{path} = 7.93 λ_T = 3.00

Fig. 5.21 Structural Failure States of TLP-A for $\chi = 90^o$

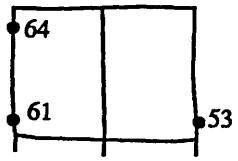

Section A-1

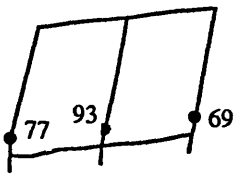

Section A-2

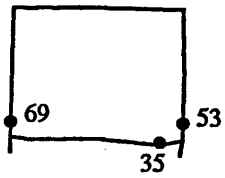

Section B-1

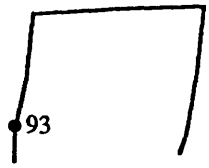

Section B-2

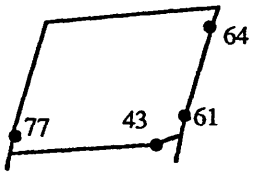

Section B-3

(1) Mode-1

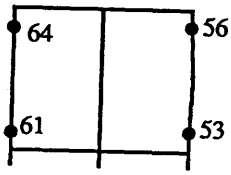

Section A-1

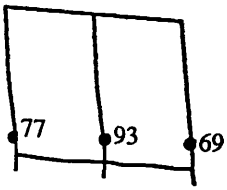

Section A-2

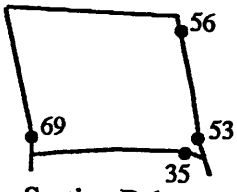

Section B-1

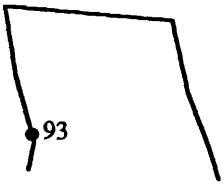

Section B-2

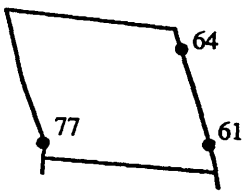

Section B-3

(2) Mode-2

Fig. 5.22 Collapse Modes of TLP-A for $\chi = 90^{o}$

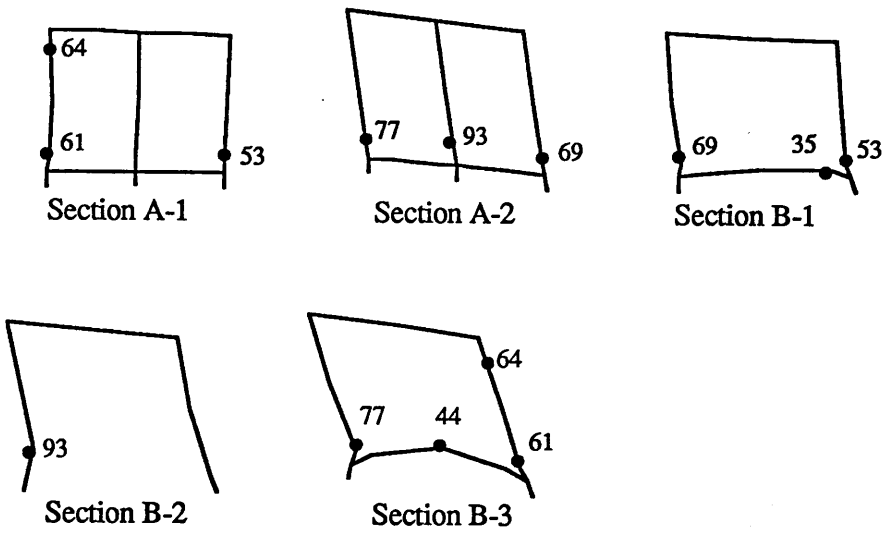

(3) Mode-3

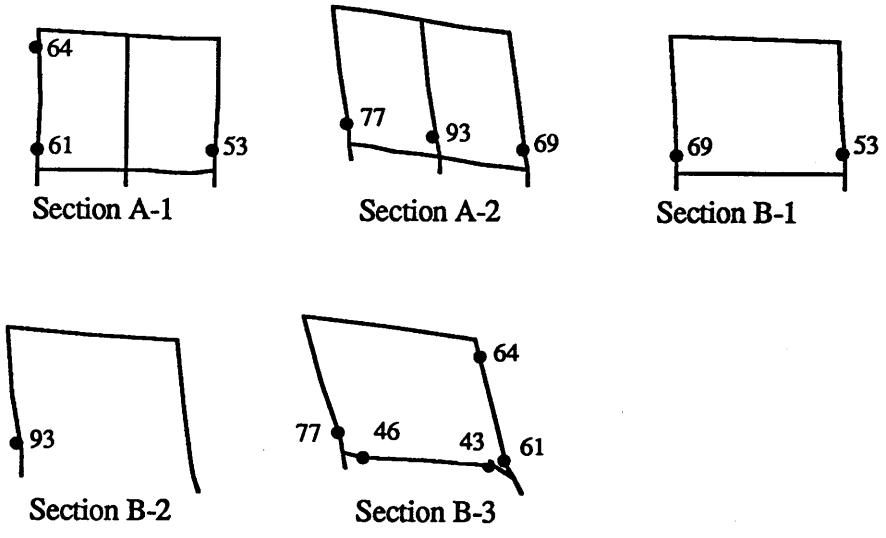

(4) Mode-4

Fig. 5.22 Collapse Modes of TLP-A for $\chi = 90^{o}$ (continued)

5.4.3 TLP-B

As described in Section 5.3, TLP-B is a variant of the Hutton TLP modelled by by removing the mid-columns and replacing corner columns with ring- and stringer-stiffened cylinders or removing the two mid-columns in TLP-A [see Table 5.10]. The model has four corner columns and its overall structural dimensions are the same as for the Hutton TLP and TLP-A but the structural weight and its distribution are different from those of the other models and, consequently, the distribution of load and load effects is different from the previous TLP models.

Figs. 5.23 and 5.24 show the RAOs of surge and heave motion and forces when wave direction is 0^o, 45^o and 90^o. TLP-B shows similar motion characteristics to the Hutton TLP.

The strength formula given as Eq.(3.53) has been used for the components of columns. The same values of control parameters for the procedure of identifying the important failure modes are used as for the previous TLP models [Table 5.12]. Four failure modes have been found for all wave directions as in the case of the previous models. The results of system reliability analysis for this model are presented in Tables 5.23, 5.24 and 5.25 when wave direction is 0^o, 45^o and 90^o, respectively. Failure modes for all wave directions have been generated in increasing order of path reliability index (in decreasing order of failure probability). As for the Hutton TLP and TLP-A, no differences can be seen between bounds of β_{sys} and $(P_f)_{sys}$ and it can be seen that the bounds are dominated by the first failure mode.

Table 5.26 shows the summarised results together with the total average value of $(P_f)_{sys}$ and corresponding β_{sys}. When $\chi = 0^o$, average β_{sys} is lowest as for TLP-A but average of β_{sys}, when $\chi = 45^o$, is followed. The average β_{sys}, when $\chi = 45^o$ and when $\chi = 90^o$ are about 5.3% and 8.1% greater than β_{sys} when $\chi = 0^o$. The total average β_{sys} is 6.91. That is, TLP-B shows about 7.3% and 10.3% higher β_{sys} than the Hutton TLP and TLP-A, respectively, in spite of there being much less structural material.

When considering only column weight, the structural weight of TLP-B has been reduced by about 43.7% and 31.4% compared to the designs of the Hutton TLP and TLP-A, respectively. When equipment installed in mid-columns of the Hutton TLP and TLP-A is installed in corner columns of TLP-B, including their weight and effect on loading and load effects, this causes the scantlings to increase, e.g. increase of shell thickness and hence, the weight difference between TLP-B and the other TLPs may, of course, be reduced. But these considerations may not be expected to cause the structural weight to appreciably increase and, hence, the weight differences of TLP-B against the Hutton TLP and TLP-B, say, 43.7% and 31.4% may not be reduced. The experience from the Jolliet TLP indirectly supports this comment. Even the case that the expected increase of structural weight is accounted for, the actual weight can be saved by perhaps at least 40% comparing the design of TLP-B with the design of the Hutton TLP. This can be supported by the higher value of average β_{sys} of TLP-B than that of the Hutton TLP.

Table 5.27 illustrates the reliability indices of the first failed component in the failure modes and of the component located at the same position as in the Hutton TLP and TLP-A. The component is designated Component 45 [shaded part in Fig. 5.7 and see also Fig. 5.8]. Structural failure states and collapse modes for all identified failure modes are shown in Figs. 5.25 to 5.30 in the same manner as for the Hutton TLP and TLP-A. Critical components are mainly those of columns but relatively more components of pontoons have failed compared to the previous two TLP models. For this model λ_T varies from 2.21 for Mode-1, when $\chi = 90^o$ to 4.23 for Mode-4 when $\chi = 90^o$, and their average is 2.96. This is about 12.5% greater than that of the Hutton TLP, of which average of λ_T's was 2.63, and about 5% than that of TLP-A, of which average of λ_T's was 2.82. This also denotes that the ring- and stringer-stiffened cylinder can more efficiently resist external load than the ring-stiffened cylinder.

For comparison of the system reliability indices when using the different strength models, Eq.(3.58) proposed by Faulkner[161] is chosen for the components of columns. The same values of parameters controlling the procedure of identifying the important failure modes are used except that the required minimum number of failure modes to be

identified is given as 2, i.e., $M_{min} = 2$. The results of TLP-B when using Eq.(3.58) are summarised in Table 5.28 and Table 5.29 illustrates comparisons of systems and components reliability indices with the results when using Eq.(3.53) (or alternatively Eq.(3.11)).

As is expected, the strength model given by Eq.(3.58) gives a somewhat different level of system and component reliability. The average β_{sys} has been increased by about 1.3%, 12.2% and 26.6% for each wave direction, and component reliability indices by about 18.5% to 71.1% depending on component number and wave direction. The total average β_{sys} is about 1.6% greater than that when using Eq.(3.53). From Table 5.29, λ_T varies from 2.29 for Mode-2 when $\chi = 45^o$, to 3.48 for Mode-2 when $\chi = 90^o$. When λ_T's of only the first two modes for each wave direction are taken, using Eq.(3.53) gives the average λ_T of 2.74 for TLP-B [Figs. 5.26, 5.28 and 5.30] and 2.43 for the Hutton TLP [Figs. 5.12, 5.14 and 5.16], whereas using Eq.(3.58) gives the average λ_T of 2.76 which has increased by about 0.7% and 13.5% compared to the averages for TLP-B and for the Hutton TLP, respectively, when using Eq.(3.53). This comparison implies that TLP-B could provide a weight saving of more than 40 to 45% compared to the Hutton TLP design if columns of TLP-B were designed according to the strength model given by Eq.(3.57).

The comparison of reliabilities for the different strength models shows that using a more improved strength model must be the way to achieve appreciable weight saving with retaining the required level of reliability. The position of strength modelling parameter within the safety margin equation (2.103) means that reducing the uncertainties in strength model must be important. The results of system analysis and discussions about this point will be presented in the next chapter.

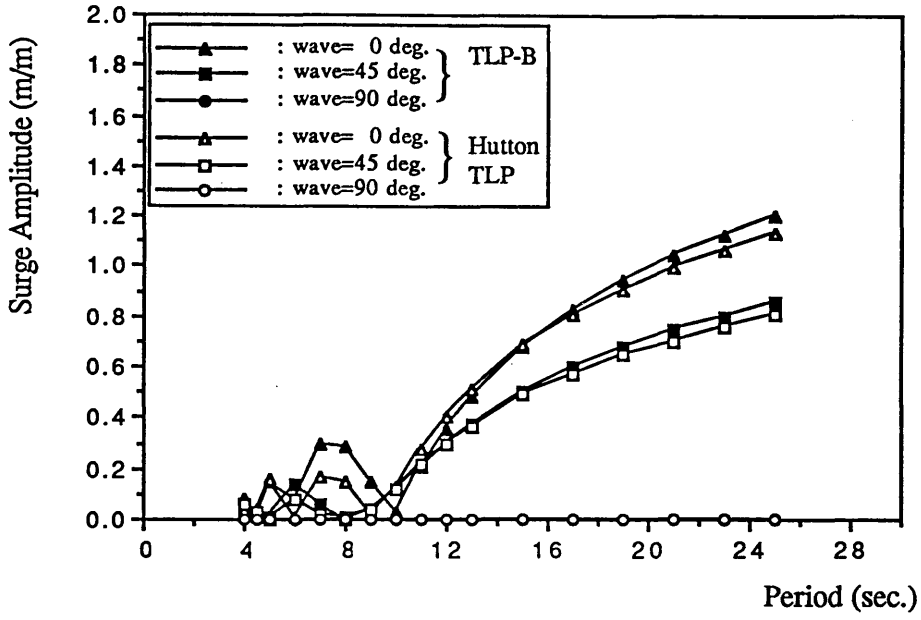

(a) Surge

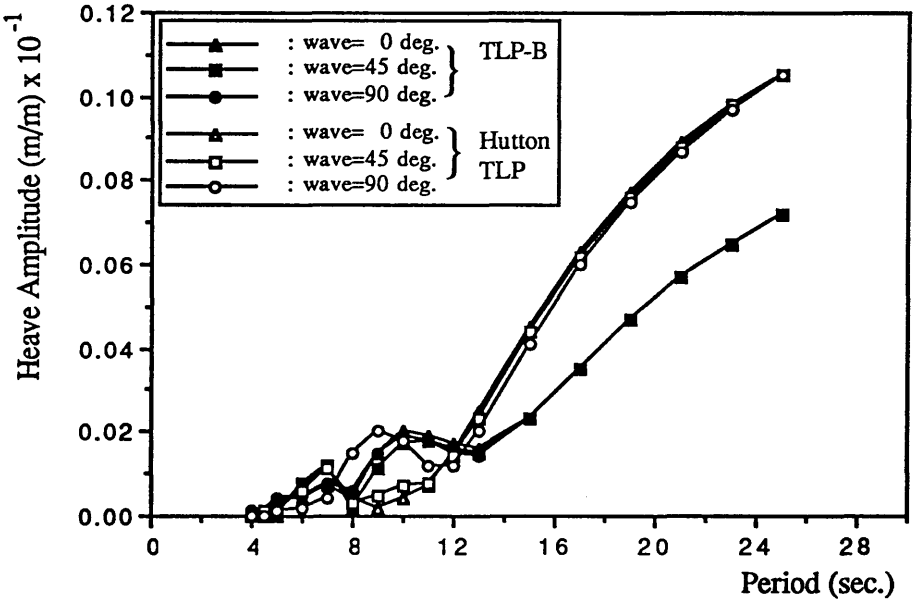

(b) Heave

Fig. 5.23 Motion RAOs of TLP-B at 32 m Draft

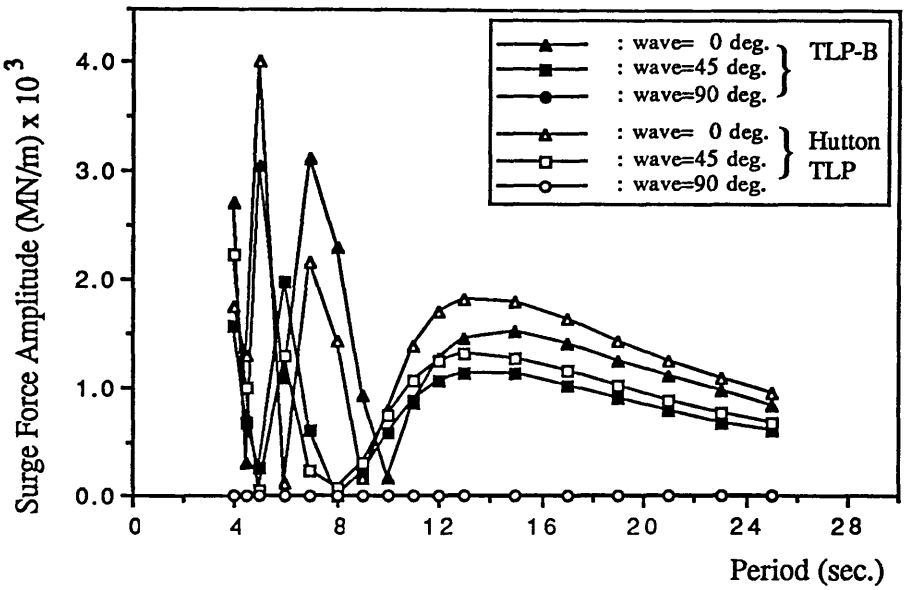

(a) Surge

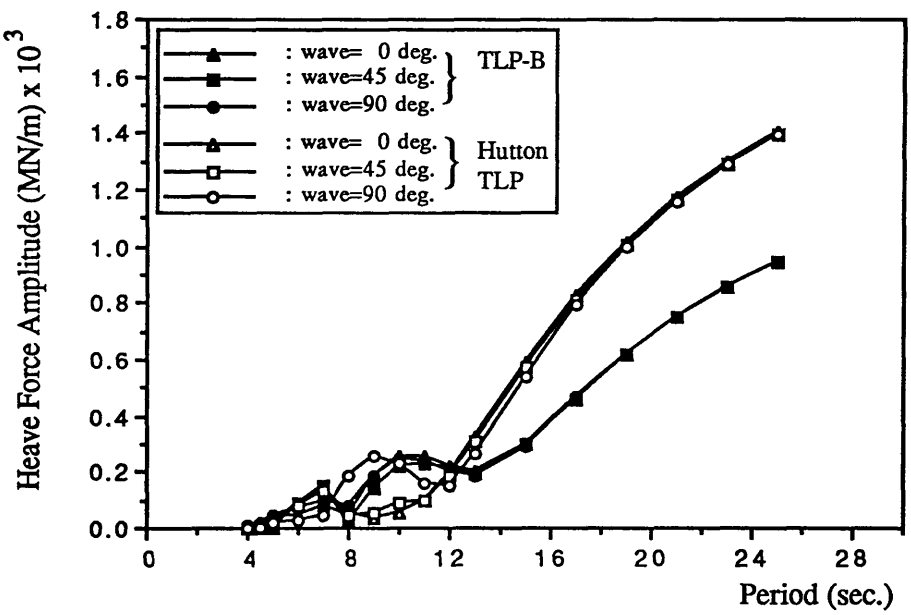

(b) Heave

Fig. 5.24 Force RAOs of TLP-B at 32 m Draft

Table 5.23 Identified Important Failure Modes of TLP-B for $\chi = 0^o$

mode no.	failed components	β_{path} $[(P_f)_{path}]$
Mode-1	48, 61, 53, 37, 45, 3, 64, 56	6.77 [0.640×10^{-11}]
Mode-2	48, 61, 53, 37, 45, 3, 64, 11	7.74 [0.515×10^{-14}]
Mode-3	48, 61, 53, 37, 45, 3, 64, 46	8.02 [0.528×10^{-15}]
Mode-4	48, 61, 53, 37, 45, 3, 64, 22	8.06 [0.396×10^{-15}]

bounds of β_{sys} and $(P_f)_{sys}$:

$\beta_{sys,lower}$ and $(P_f)_{sys,upper}$ = 6.77 and 0.640×10^{-9}

$\beta_{sys,upper}$ and $(P_f)_{sys,lower}$ = 6.77 and 0.640×10^{-9}

Table 5.24 Identified Important Failure Modes of TLP-B for $\chi = 45^o$

mode no.	failed components	β_{path} $[(P_f)_{path}]$
Mode-1	40, 48, 37, 61, 45, 3, 64, 56	7.14 [0.464×10^{-12}]
Mode-2	40, 48, 37, 61, 45, 3, 64, 46	7.46 [0.445×10^{-13}]
Mode-3	40, 48, 37, 61, 45, 3, 64, 38	7.95 [0.931×10^{-15}]
Mode-4	40, 48, 37, 61, 45, 3, 64, 54	7.99 [0.662×10^{-15}]

bounds of β_{sys} and $(P_f)_{sys}$:

$\beta_{sys,lower}$ and $(P_f)_{sys,upper}$ = 7.13 and 0.510×10^{-12}

$\beta_{sys,upper}$ and $(P_f)_{sys,lower}$ = 7.13 and 0.510×10^{-12}

Table 5.25 Identified Important Failure Modes of TLP-B for $\chi = 90^o$

mode no.	failed components	β_{path} [$(P_f)_{path}$]
Mode-1	37, 53, 14, 45, 61, 30, 64, 56	7.37 [0.888×10^{-13}]
Mode-2	37, 53, 14, 45, 61, 30, 64, 40	7.49 [0.342×10^{-13}]
Mode-3	37, 53, 14, 45, 61, 30, 64, 48	8.24 [0.900×10^{-16}]
Mode-4	37, 53, 14, 45, 61, 30, 64, 27	8.49 [0.101×10^{-16}]

bounds of β_{sys} and $(P_f)_{sys}$:

$\beta_{sys,lower}$ and $(P_f)_{sys,upper}$ = 7.32 and 0.123×10^{-12}

$\beta_{sys,upper}$ and $(P_f)_{sys,lower}$ = 7.32 and 0.123×10^{-12}

Table 5.26 Summary of System Reliability Analysis of TLP-B

χ	$\beta_{sys,lower}$ [$(P_f)_{sys,upper}$]	$\beta_{sys,upper}$ [$(P_f)_{sys,lower}$]	average β_{sys} [average $(P_f)_{sys}$]
0	6.77 [0.640×10^{-11}]	6.77 [0.640×10^{-11}]	6.77 [0.640×10^{-11}]
45	7.13 [0.510×10^{-12}]	7.13 [0.510×10^{-12}]	7.13 [0.510×10^{-12}]
90	7.32 [0.123×10^{-12}]	7.32 [0.123×10^{-12}]	7.32 [0.123×10^{-12}]

Total Average of β_{sys} = 6.91

$(P_f)_{sys}$ = 0.234×10^{-11}

Table 5.27 Component Reliability Index and Probability of Failure for TLP-B

χ	first failed component	Component 45
0	3.14 [0.853 x 10^{-3}]	3.75 [0.874 x 10^{-4}]
45	3.05 [0.113 x 10^{-2}]	3.79 [0.747 x 10^{-4}]
90	4.91 [0.454 x 10^{-6}]	4.89 [0.506 x 10^{-6}]

Table 5.28 Results of TLP-B When Using Strength Model, Eq.(3.58)

(1) $\chi = 0^o$

mode no.	failed components	β_{path} $[(P_f)_{path}]$	λ_T
Mode-1	40, 45, 48, 64, 37, 61, 3	6.86 [0.341 x 10^{-11}]	2.35
Mode-2	40, 45, 48, 64, 37, 61, 6	7.75 [0.470 x 10^{-14}]	2.82

$\beta_{sys,lower}$ and $(P_f)_{sys,upper}$ = 6.86 and 0.345 x 10^{-11}
$\beta_{sys,upper}$ and $(P_f)_{sys,lower}$ = 6.86 and 0.345 x 10^{-11}

(2) $\chi = 45^o$

mode no.	failed components	β_{path} $[(P_f)_{path}]$	λ_T
Mode-1	56, 37, 45, 40, 48, 61, 53	8.30 [0.532 x 10^{-16}]	2.30
Mode-2	56, 37, 45, 40, 48, 61, 64, 53	8.00 [0.619 x 10^{-15}]	2.29
Mode-3	56, 37, 45, 40, 48, 61, 64, 3	9.63 [0.310 x 10^{-21}]	2.40

$\beta_{sys,lower}$ and $(P_f)_{sys,upper}$ = 7.99 and 0.645 x 10^{-15}
$\beta_{sys,upper}$ and $(P_f)_{sys,lower}$ = 8.00 and 0.637 x 10^{-15}

Table 5.28 (continued)

(3) $\chi = 90^o$

mode no.	failed components	β_{path} $[(P_f)_{path}]$	λ_T
Mode-1	56, 48, 61, 53, 45, 37, 54	9.31 [0.635×10^{-20}]	3.33
Mode-2	56, 48, 61, 53, 45, 37, 46	9.39 [0.305×10^{-20}]	3.48

$\beta_{sys,lower}$ and $(P_f)_{sys,upper}$ = 9.27 and 0.940×10^{-20}

$\beta_{sys,upper}$ and $(P_f)_{sys,lower}$ = 9.27 and 0.940×10^{-20}

Table 5.29 Comparisons of Reliability Indices for Different Strength Models

	system reliability indices		component reliability indices			
			Eq.(3.53)		Eq.(3.58)	
χ	Eq.(3.53)	Eq.(3.58)	first failed component	Component 45	first failed component	Component 45
0	6.77	6.86	3.14	357	4.90	5.54
45	7.13	8.00	3.05	3.79	5.22	5.59
90	7.32	9.27	4.91	4.89	5.82	6.68

total average of β_{sys} = 6.91 by Eq.(3.53)

= 7.02 by Eq.(3.58)

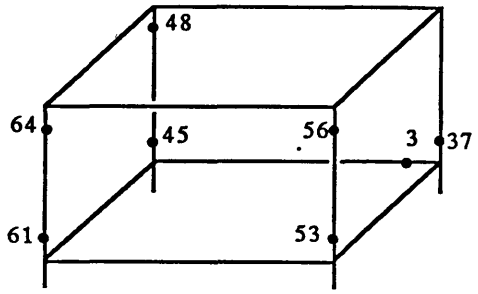

(1) Mode-1

failed components

: 48, 61, 53, 37, 45, 3, 64, 56

β_{path} = 6.77 λ_T = 2.56

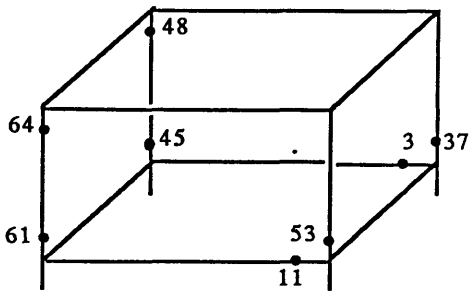

(2) Mode-2

failed components

: 48, 61, 53, 37, 45, 3, 64, 11

β_{path} = 7.74 λ_T = 3.55

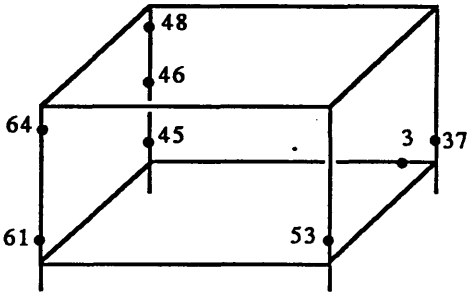

(3) Mode-3

failed components

: 48, 61, 53, 37, 45, 3, 64, 46

β_{path} = 8.02 λ_T = 2.93

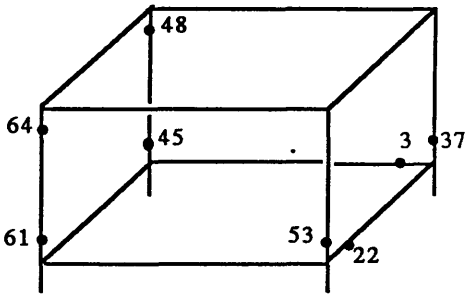

(4) Mode-4

failed components

: 48, 61, 53, 37, 45, 3, 64, 22

β_{path} = 8.06 λ_T = 3.56

Fig. 5.25 Structural Failure States of TLP-B for $\chi = 0^o$

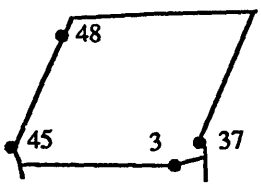

Section A-1

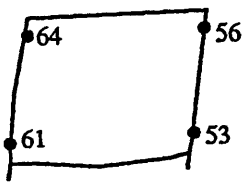

Section A-2

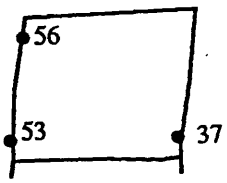

Section B-1

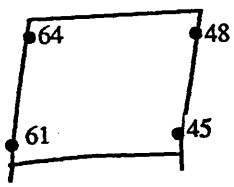

Section B-2

(1) Mode-1

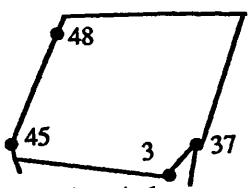

Section A-1

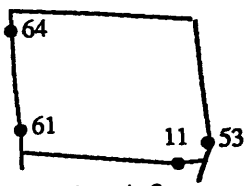

Section A-2

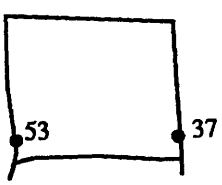

Section B-1

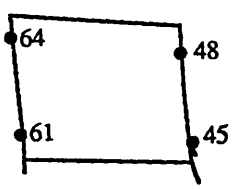

Section B-2

(2) Mode-2

Fig. 5.26 Collapse Modes of TLP-B for $\chi = 0^o$

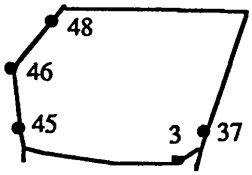

Section A-1

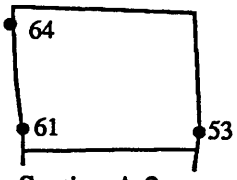

Section A-2

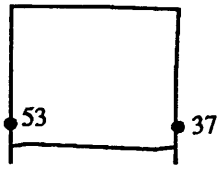

Section B-1

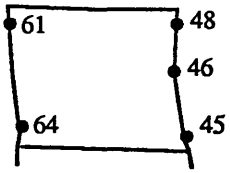

Section B-2

(3) Mode-3

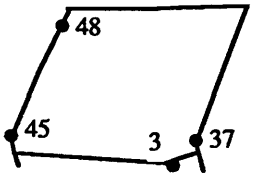

Section A-1

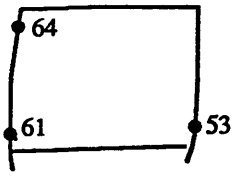

Section A-2

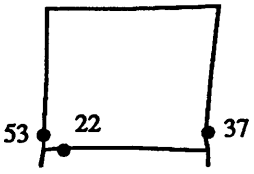

Section B-1

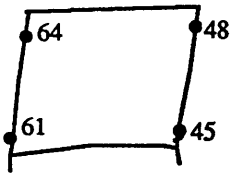

Section B-2

(4) Mode-4

Fig. 5.26 Collapse Modes of TLP-B for $\chi = 0^0$ (continued)

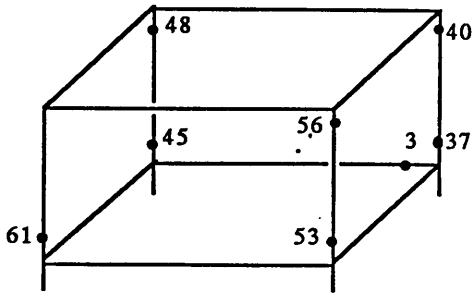

(1) Mode-1

failed components

: 40, 48, 37, 61, 45, 53, 56, 3

β_{path} = 7.14 λ_T = 2.62

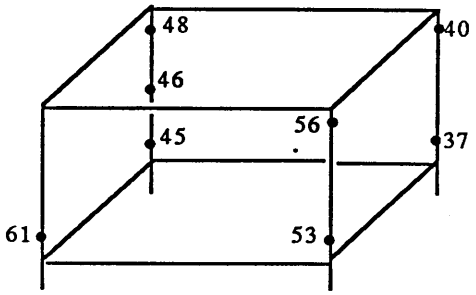

(2) Mode-2

failed components

: 40, 48, 37, 61, 45, 53, 56,46

β_{path} = 7.46 λ_T = 2.82

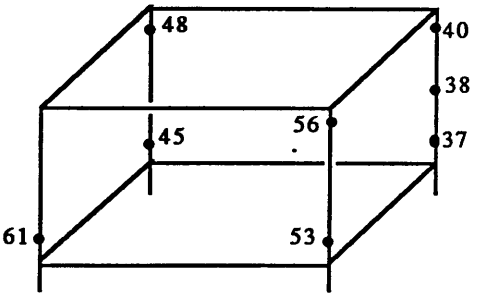

(3) Mode-3

failed components

: 40, 48, 37, 61, 45, 53, 56, 38

β_{path} = 7.95 λ_T = 2.72

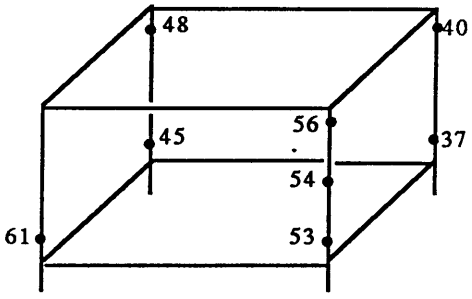

(4) Mode-4

failed components

: 40, 48, 37, 61, 45, 53, 56, 54

β_{path} = 7.99 λ_T = 3.02

Fig. 5.27 Structural Failure States of TLP-B for $\chi = 45^o$

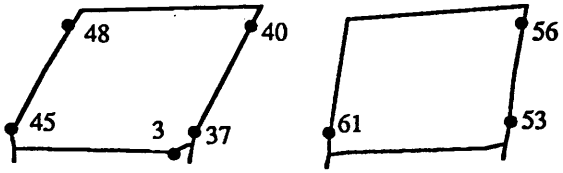

Section A-1 Section A-2

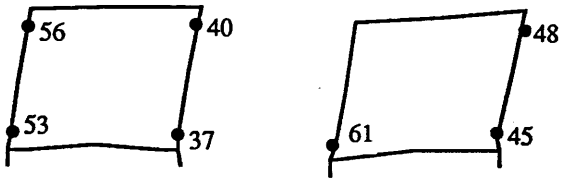

Section B-1 Section B-2

(1) Mode-1

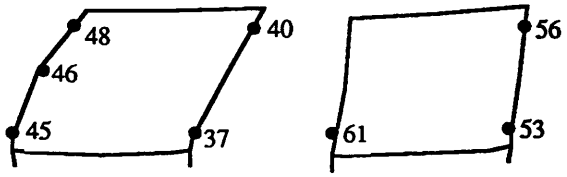

Section A-1 Section A-2

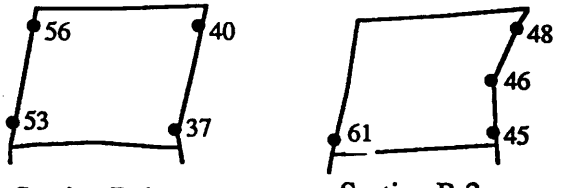

Section B-1 Section B-2

(2) Mode-2

Fig. 5.28 Collapse Modes of TLP-B for $\chi = 45^{o}$

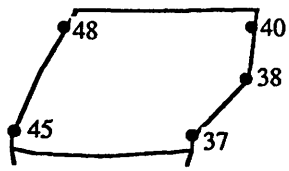

Section A-1

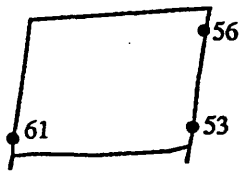

Section A-2

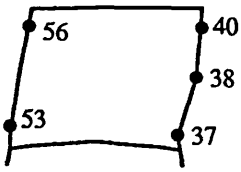

Section B-1

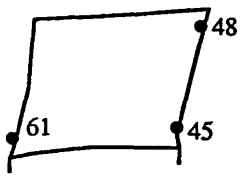

Section B-2

(3) Mode-3

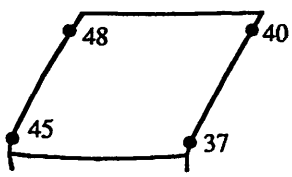

Section A-1

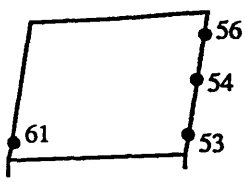

Section A-2

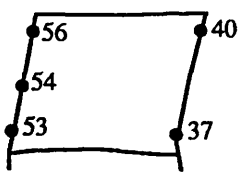

Section B-1

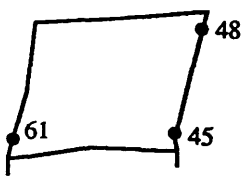

Section B-2

(4) Mode-4

Fig. 5.28 Collapse Modes of TLP-B for $\chi = 45^{o}$ (continued)

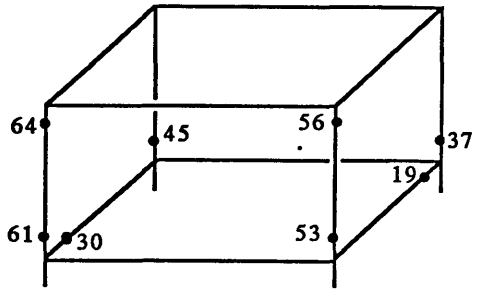

(1) Mode-1

failed components

: 37, 53, 19, 45, 61, 30, 64, 56

β_{path} = 7.37 λ_T = 2.21

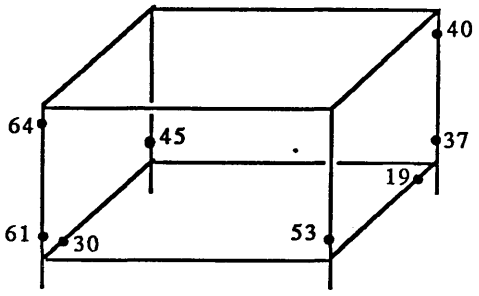

(2) Mode-2

failed components

: 37, 53, 19, 45, 61, 30, 64, 40

β_{path} = 7.49 λ_T = 2.69

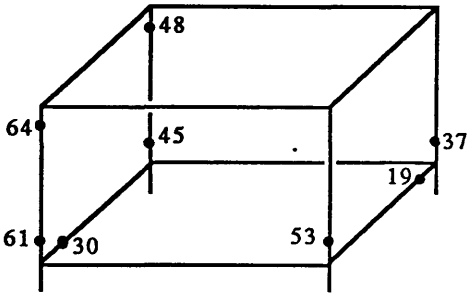

(3) Mode-3

failed components

: 37, 53, 19, 45, 61, 30, 64, 48

β_{path} = 8.24 λ_T = 2.61

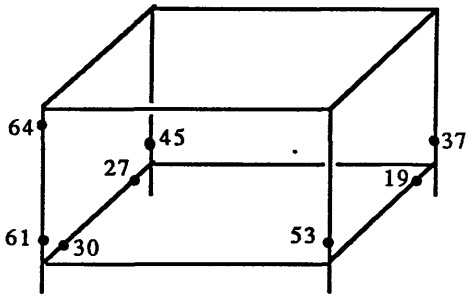

(4) Mode-4

failed components

: 37, 53, 19, 45, 61, 30, 64, 27

β_{path} = 8.49 λ_T = 4.23

Fig. 5.29 Structural Failure States of TLP-B for $\chi = 90^o$

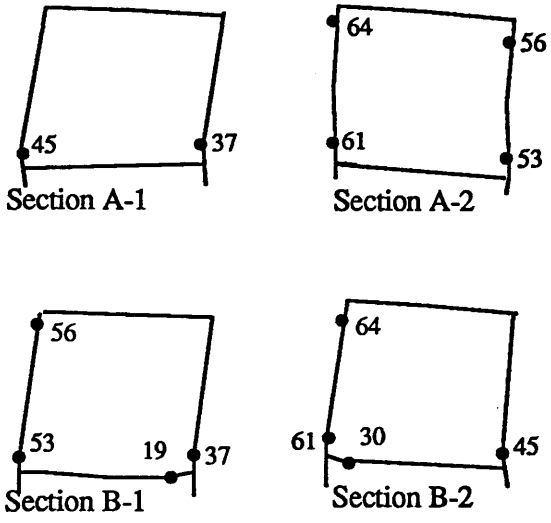

(1) Mode-1

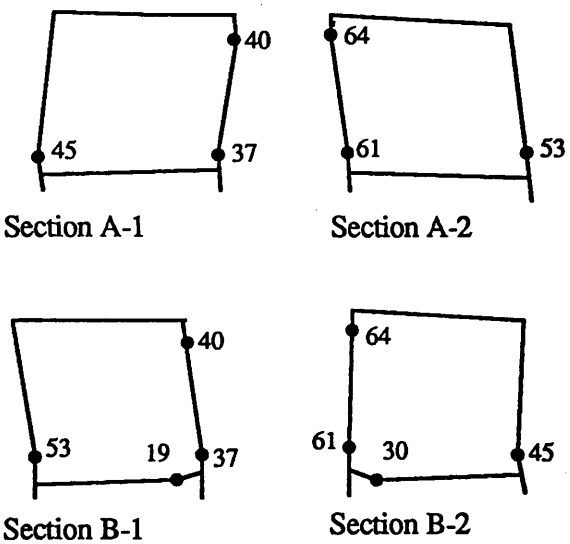

(2) Mode-2

Fig. 5.30 Collapse Modes of TLP-B for $\chi = 90^{o}$

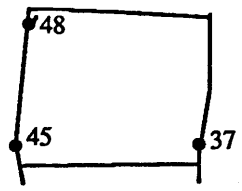

Section A-1

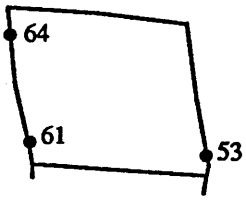

Section A-2

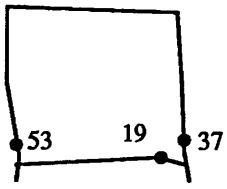

Section B-1

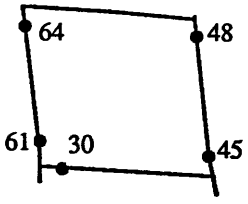

Section B-2

(3) Mode-3

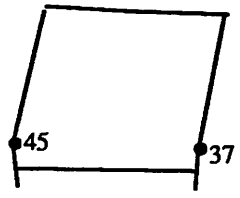

Section A-1

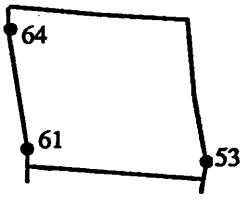

Section A-2

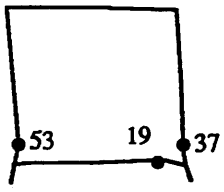

Section B-1

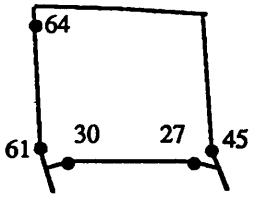

Section B-2

(4) Mode-4

Fig. 5.30 Collapse Modes of TLP-B for $\chi = 90^{o}$ (continued)

5.4.4 Comparison and Discussion of the Reliability Study Results

From Table 5.16 for the Hutton TLP, 5.21 for TLP-A and 5.26 TLP-B, results of three TLP models are compared in Table 5.30. The Hutton TLP and TLP-A show nearly the same level of system safety (average β_{sys} of TLP-A is about 3% lower than that of the Hutton TLP), whereas the system safety of TLP-B is 7.3% greater than that of the Hutton TLP. The lower value of TLP-A may be due to the fact that the components on the mid-columns of the ring-stiffened cylinder have a higher chance of failing than other components and, therefore, the load acting on the components is re-distributed earlier on to the other components. The higher value of TLP-B may be due to the fact that the load level acting on this structure is lower than the other two models and the load re-distribution of the failed components on the mid-columns is removed, i.e. in the cases of the Hutton TLP and TLP-A, the load acting on the failed components on the mid-columns, which has a higher probability of failing, is re-distributed to the remaining components of the corner columns and pontoons, and this may cause a lower reliability index than that of TLP-B. But in the case of TLP-B, this re-distribution effect does not occur. This might be the main reason that TLP-B shows a higher system reliability index in spite of there being much less structural material. From the results it can be said that the orthogonally stiffened cylinder is more efficient and reliable from both the system's and component's point of view and hence more weight saving can be achieved, say at least 40% compared to the Hutton TLP as designed.

The total load factors (λ_T) and the path reliability indices (β_{path}) of three TLP models [see figures for collapse modes in the previous three sections] are summarised in Table 5.31, and the relation between λ_T and β_{path} of three TLP models is plotted in Fig.5.31. As described in Section 2.1.2, λ_T is related to the reserve strength of a structure. The average values of λ_T's of 2.63, 2.82 and 2.96 for the Hutton TLP, TLP-A and TLP-B imply appreciable reserve strength of the TLP structural system. Based on these values, TLP-B seems to possesses more reserve strength than the other two TLPs in such a way that its average λ_T is about 12.5% and 5% greater than those of the Hutton TLP and TLP-A, respectively, in spite of there being much less structural material. From Table 5.31 and Fig. 5.31, it can be seen that as β_{path} increases, λ_T usually increases,

although the higher β_{path} does not always have the higher load factor.

When we choose the β measure, RDI_β given by Eq.(2.13), which is related to the residual strength, as a measure of the probabilistic structural redundancy, it can be easily calculated as illustrated in Table 5.32 for three TLP models. When calculating the β measure from Eq.(2.13), β_{comp} is that of the first failed component in any failure mode and β_{sys} is the path reliability index, β_{path} of the mode.

The Hutton TLP and TLP-A show higher RDI_β's for $\chi = 0^o$ because of small β_{comp}'s , whereas TLP-B for $\chi = 45^o$. RDI_β's of TLP-B are more uniform and their average is greater than those of the Hutton TLP and TLP-A. The averages of RDI_β's for TLP-A and TLP-B are 22% and 27% greater than that of the Hutton TLP, respectively.

These comparisons and discussions also show that the structure having ring- and stringer-stiffened cylinders is more efficient than the structure having ring-stiffened cylinders in the light of residual strength as well as in the light of reserve strength.

As mentioned before, with regard to the relation between the total load factor and the path reliability index, the higher β_{path} does not always have the higher λ_T. This implies that the deterministically important mode is not identical with the probabilistically important mode as was also found for the simple frame model in Section 2.6.2. As can be seen in Table 5.31, the deterministically most important modes are:

Mode-2 with $\lambda_T = 1.87$, when $\chi = 0^o$ for the Hutton TLP

Mode-2 with $\lambda_T = 2.13$, when $\chi = 45^o$ for TLP-A

Mode-1 with $\lambda_T = 2.21$, when $\chi = 90^o$ for TLP-B

whereas the probabilistically most important ones are:

Mode-1 with $\beta_{path} = 6.31$, when $\chi = 0^o$ for the Hutton TLP

Mode-1 with $\beta_{path} = 6.10$, when $\chi = 0^o$, for TLP-A

Mode-1 with $\beta_{path} = 6.77$, when $\chi = 0^o$ for TLP-B

In the case of the Hutton TLP the ratio of β_{path} of the deterministically most important mode to that of the probabilistically most important one is 1.128, and for the two variants the ratios are 1.182 for TLP-A and 1.089 for TLP-B. The ratios of λ_T of the deterministically most important mode to that of the probabilistically most important one is 0.609 for the Hutton TLP, and for two variants 0.737 and 0.863, respectively, i.e. in the case of the Hutton TLP, the deterministically most important mode has 12.8% higher β_{path} than that of the probabilistically most important one, while 39.1% lower λ_T, and in the case of two variants, 18.2% and 8.9% higher β_{path} and 26.3% and 13.7% lower λ_T, respectively.

Table 5.30 Comparison of β_{sys} for Three TLP Models

χ	Hutton TLP	TLP-A	TLP-B
0	6.55 [0.293×10^{-10}]	6.09 [0.575×10^{-9}]	6.77 [0.640×10^{-11}]
45	6.30 [0.147×10^{-9}]	7.20 [0.299×10^{-12}]	7.13 [0.510×10^{-12}]
90	7.32 [0.411×10^{-11}]	6.69 [0.112×10^{-10}]	7.32 [0.123×10^{-12}]
Total	[6.44]	[6.26]	[6.91]
Average	[0.602×10^{-10}]	[0.195×10^{-9}]	[0.234×10^{-11}]

note : Figure in [ ] is the probability of failure.

Table 5.31 β_{path} vs λ_T for Three TLP Models

χ	mode no.	Hutton TLP		TLP-A		TLP-B	
		β_{path}	λ_T	β_{path}	λ_T	β_{path}	λ_T
0	1	6.55	2.13	6.10^{P}	2.89	6.77^{P}	2.56
	2	7.12	1.87^{D}	6.69	2.43	7.74	3.55
	3	7.66	2.29	6.70	2.67	8.02	2.93
	4	7.82	2.15	6.90	2.27	8.06	3.56
45	1	6.31^{P}	3.07	7.21	2.32	7.14	2.62
	2	6.71	2.53	7.21	2.13^{D}	7.46	2.82
	3	7.24	4.13	7.72	3.17	7.95	2.72
	4	7.31	2.48	7.89	3.39	7.99	3.02
90	1	6.84	2.63	6.69	3.22	7.37	2.21^{D}
	2	8.28	2.38	8.08	2.34	7.49	2.69
	3	8.52	2.48	8.34	4.05	8.24	2.61
	4	6.98	3.48	7.93	3.00	8.49	4.23
average λ_T :			2.63		2.82		2.96

D : deterministically most important mode

P : probabilistically most important mode

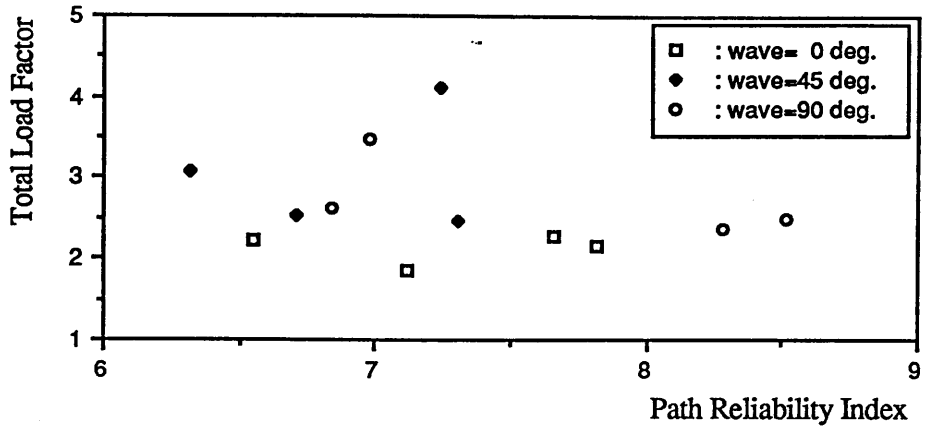

(1) Hutton TLP

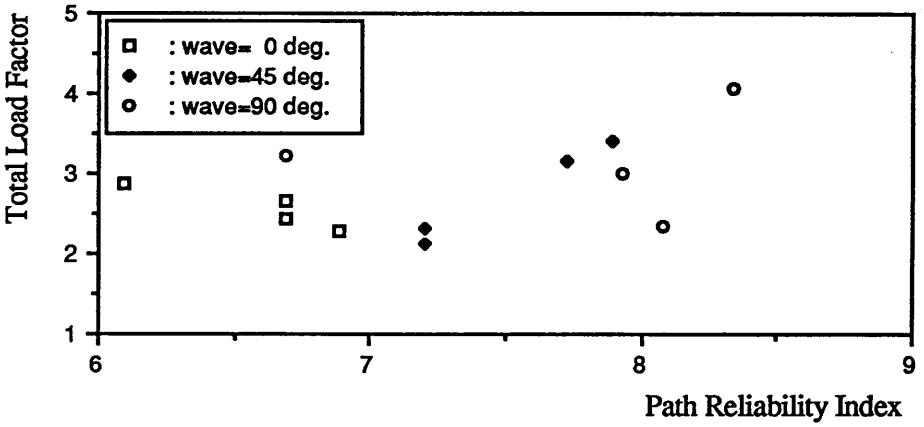

(2) TLP-A

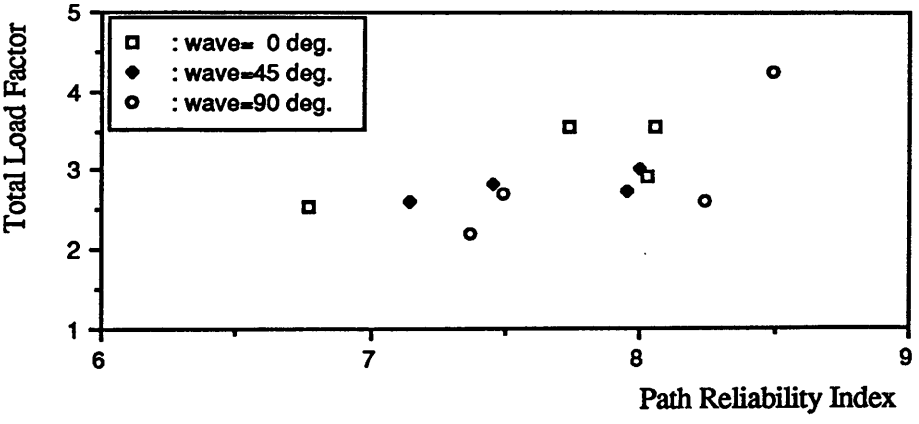

(3) TLP-B

Fig. 5.31 Path Reliability Index (β_{path}) vs Total Load Factor (λ_T)

Table 5.32 β Measure of Structural Redundancy (RDI_β) for Three TLP Models

(1) Hutton TLP

χ	mode no.	Hutton TLP			TLP-A			TLP-B		
		β_{comp}	β_{sys}	RDI_β	β_{comp}	β_{sys}	RDI_β	β_{comp}	β_{sys}	RDI_β
0	1	2.14	6.55	0.67	1.25	6.10	0.78	3.14	6.77	0.54
	2	2.14	7.12	0.70	1.25	6.69	0.81	3.14	7.74	0.59
	3	2.14	7.66	0.72	1.25	6.70	0.81	3.14	8.02	0.61
	4	2.14	7.82	0.73	1.25	6.90	0.82	3.14	8.06	0.61
45	1	5.31	6.31	0.16	4.61	7.21	0.36	3.05	7.14	0.57
	2	5.31	6.71	0.21	4.61	7.21	0.36	3.05	7.46	0.59
	3	5.31	7.24	0.27	4.61	7.72	0.40	3.05	7.95	0.62
	4	5.31	7.31	0.27	4.61	7.89	0.42	3.05	7.99	0.62
90	1	5.36	6.84	0.22	5.28	6.69	0.21	4.91	7.37	0.33
	2	5.36	8.28	0.35	5.28	8.08	0.35	4.91	7.49	0.34
	3	5.36	8.52	0.37	5.28	8.34	0.37	4.91	8.24	0.40
	4	5.36	6.98	0.23	5.28	7.93	0.33	4.91	8.49	0.42
			min.	0.16		min.	0.21		min.	0.33
			max.	0.73		max.	0.82		max.	0.62
			average.	0.41		average.	0.50		average.	0.52

A similar situation can be found from the results of the system analysis by others. For example, Murotsu et al proposed, so called, the central load factor (or central limit load factor or central safety factor) for considering the deterministically dominant modes of structural failure to the probabilistically dominant modes[130,155]. For the m the failure mode the central load factor, λ_{CLF} is given as:

$$\lambda_{CLF} = \frac{\sum_{k=1}^{r_m} C_{mk} \underline{R}_k}{\sum_{l=1}^{L} B_{ml} \underline{P}^{(l)}} \tag{5.1}$$

where $\underline{R}_k$ and $\underline{P}^{(l)}$ are the mean values of resistance of component k and of the l th load and r_m is the number of failed components contained in the mode. The numerator means the sum of the mean load effects and the denominator the sum of the resistance of the components in the mode.

Fig. 5.32 shows a three-bay frame structure[155] and Fig. 5.33 transverse structure of a semi-submersible[130] of which structural and loading data are given as Table 5.33. Fig. 5.34 shows the collapse modes for the three-bay frame structure and Fig. 5.35 for the transverse structure of the semi-submersible. Table 5.34 illustrates the values of the central load factors obtained from Eq.(5.1) for the three-bay frame structure and the transverse structure of the semi-submersible. β_{path}'s are plotted against λ_{CLF}'s as shown in Fig. 5.36. For the three-bay frame structure the deterministically most important failure mode is Mode 13 with λ_{CLF} =1.72. On the contrary, the failure modes having the lowest β_{path} are Mode 1 and 4 with β_{path} = 2.91. For the transverse structure of the semi-submersible, the deterministically most important mode is Mode C-1 with λ_{CLF} =1.53, whereas the the probabilistically most important one is Mode A-1 with β_{path} =5.58.

These results also indicate that the deterministically dominant failure mode is not

identical to the probabilistically dominant failure modes and for this reason the load factor may not be proportional to the level of path reliability index.

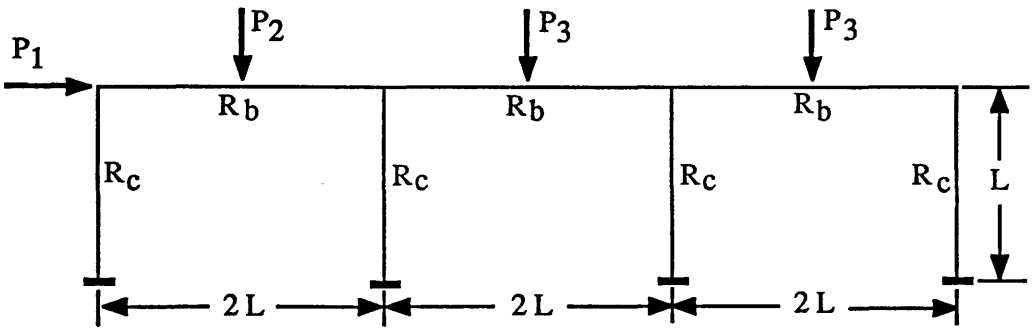

$L = 5$ m $\quad \underline{P_1} = 50$ kN $\quad \underline{P_2} = \underline{P_3} = \underline{P_4} = 40$ kN

$\underline{R_b} = 101.2$ kN m $\quad \underline{R_c} = 75$ kN m

Fig. 5.32 Three-Bay Frame Structure[155]

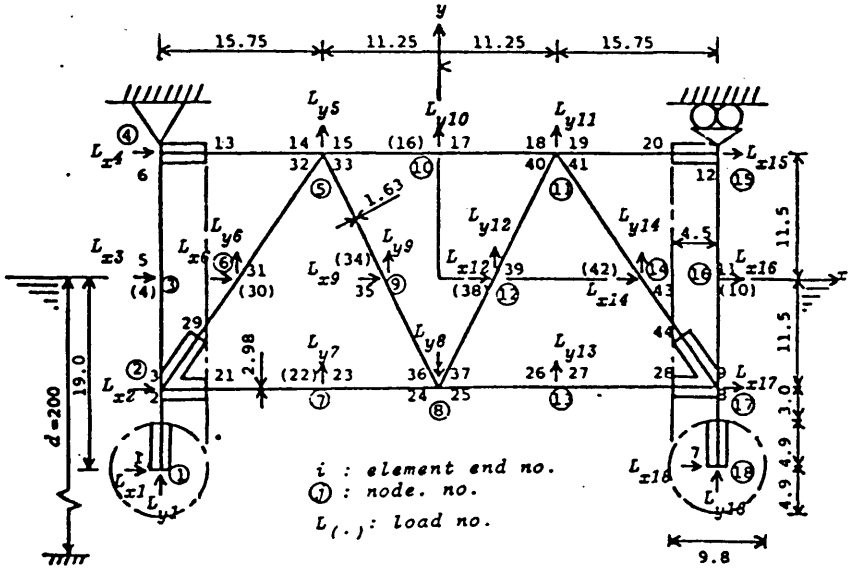

Fig. 5.33 Transverse Structure of Semi-Submersible[130]

Table 5.33 Data for Semi-Submersible[130]

(1) Postulated Extreme Sea-State and Morison's Coefficient

significant wave height	$H_S = 13$ m	duration of sea-state	$T = 3600$ sec.
wave period	$T_W = 3.55\ H^{0.559}$ sec.		
mass coefficient	mean = $\underline{C}_M = 0.8$,	COV = $V_{C_a} = 30\%$	
drag coefficient	mean = $\underline{C}_d = 0.8$,	COV = $V_{C_a} = 30\%$	
correlation coefficient between C_M and C_d	$\rho_{C_M C_a} = -0.9$		

(2) Structural Data

member	element end no	cross-sec area A_{pi} (m^2)	moment of inertia I_i (m^4)	reference strength R_i	length of rigid body (m) s_1	s_2
column	1, 2, 7, 8				4.9	—
(D=9 m)	3-6, 9-12	0.4804	4.864	493.6	—	—
deck	13, 14				4.5	—
	15-18	0.1931	0.0985	41.36	—	—
	19, 20				—	4.5
diagonal	29, (30)				4.5	—
brace	31-36,37-(42)	0.1554	0.5099	27.65	—	—
(D=1.63 m)	43,44				—	4.5
horizontal	21,22				4.5	—
brace	23-(26)	0.1404	0.1558	47.48	—	—
(D=2.98 m)	27,28				—	4.5

Reference strength	R_i = plastic bending moment
Elastic modulus	$E = 210$ GPa
Yield stress	σ_Y : mean = 360 MPa, COV = 8%

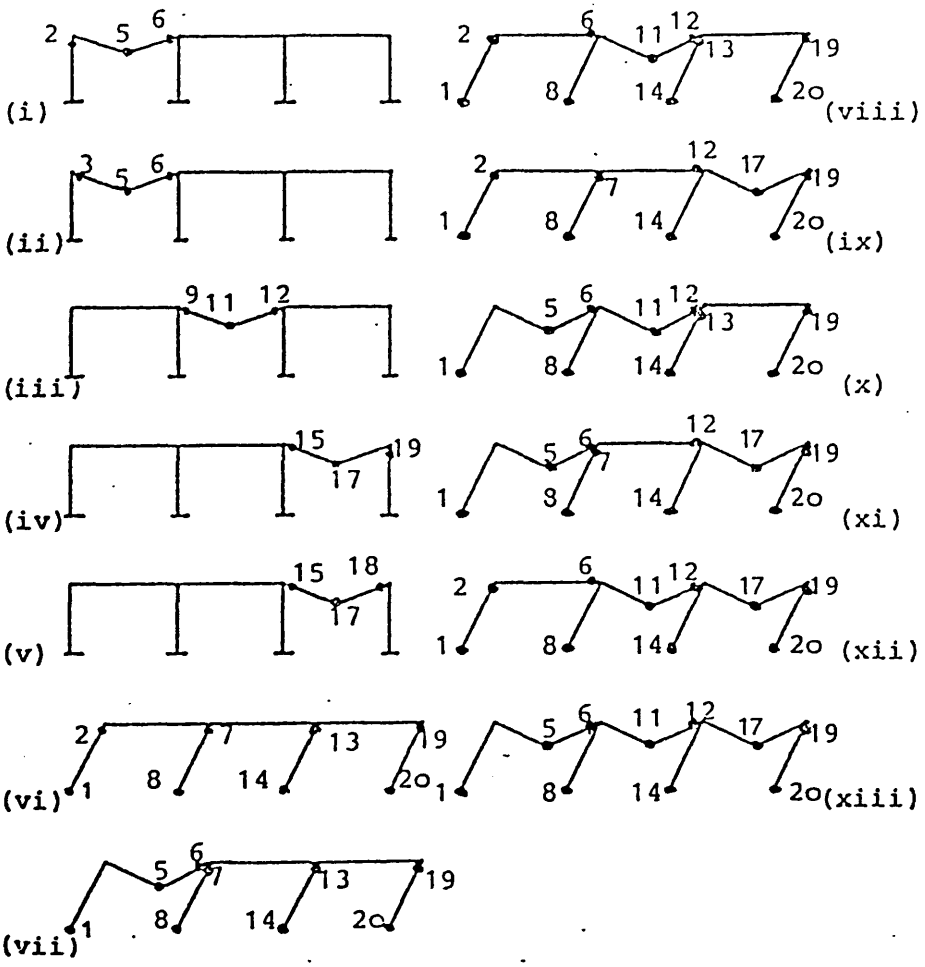

Fig. 5.34 Collapse Modes for Three-Bay Frame Structure[155]

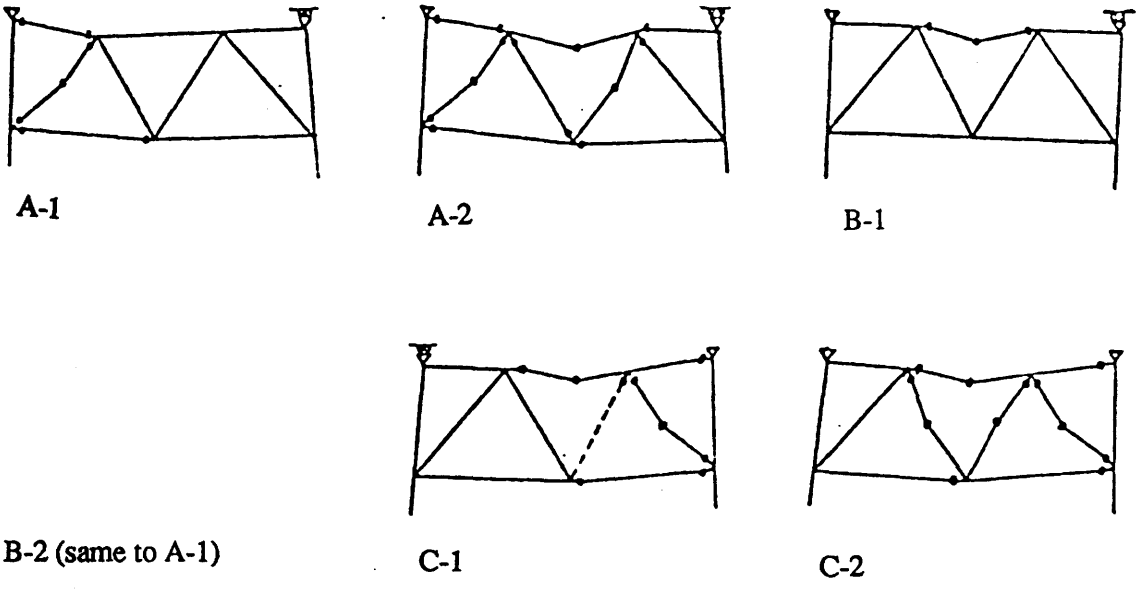

Fig. 5.35 Collapse Modes for Semi-Submersible[130]

Table 5.34 Central Load Factors Calculated from Eq.(5.1)

(1) Three-Bay Frame Structure[155]

mode no.	β_{path}	λ_{CLF}	mode no.	β_{path}	λ_{CLF}
1	2.91^{P}	1.89	8	4.92	2.06
2	3.33	2.02	9	4.65	2.01
3	3.33	2.02	10	4.41	1.78
4	2.91^{P}	1.89	11	4.19	1.74
5	3.33	2.02	12	5.05	1.90
6	4.62	2.40	13	4.67	1.72^{D}
7	3.89	1.84			

average of λ_{CLF} = 1.95

(2) Semi-Submersible[130]

mode no.	β	λ_{CLF}	mode no.	β	λ_{CLF}
A-1	5.58^{P}	1.55	C-1	6.32	1.53^{D}
A-2	7.46	1.65	C-2	7.44	1.65
B-1	8.48	2.15			
B-2	9.60	2.05			

average of λ_{CLF} = 1.76

D : deterministically most important mode

P : probabilistically most important mode

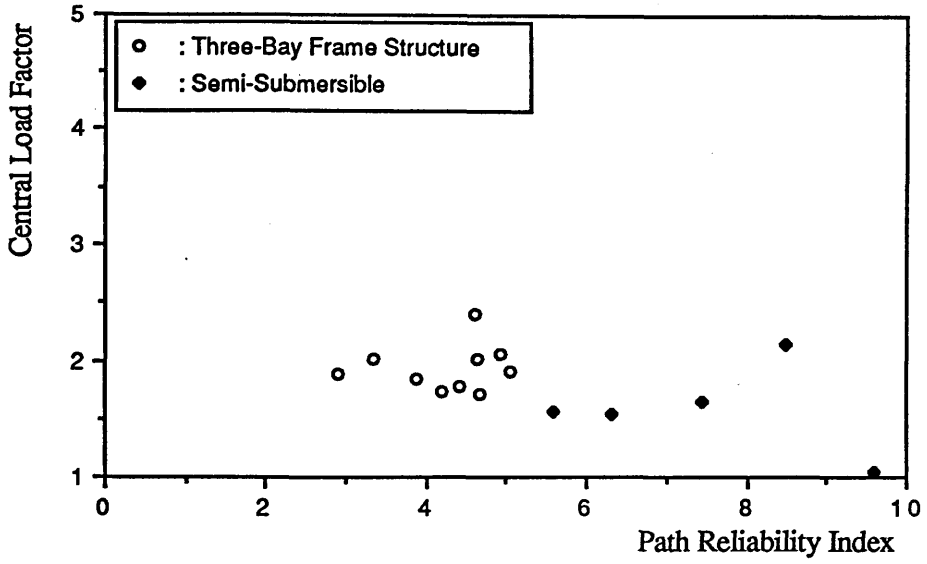

Fig. 5.36 Central Load Factor vs β_{path}

Two load factors, λ_T given as Eq.(2.95) and λ_{CLF} as Eq.(5.1), have different definitions from each other, i.e., the total load factor, λ_T in Eq.(2.95) can represent the ratio of the collapse load to the mean applied load as mentioned in Section 2.1.2. This was given by:

$$\lambda_T = \frac{\text{System Collapse Load}}{\text{Mean Applied Load}} \tag{2.15.b}$$

while the central load factor λ_{CLF} in Eq.(5.1) can represent the ratio of the mean strength for system to the mean applied load:

$$\lambda_{CLF} = \frac{\text{Mean Strength for System}}{\text{Mean Applied Load}} \tag{5.2}$$

Although two load factors are derived from the different definitions, their actual meanings

are similar, that is, both factors are related to reserve strength and can represent the system safety factors.

Calculation of the load factors from Eqs.(2.95) and (5.1) is illustrated in Appendix-B for the simple frame model.

5.4.5 System Reliability to Changes in Control Parameters of Identifying Procedure

The number of important failure modes to be identified and, consequently, the system reliability to be evaluated should be affected by the various parameters controlling the procedure of identifying the important failure modes [Section 2.5.6 and also refer to Table 5.12].

ε_{sys} and M_{min} may affect the number of failure modes. Decreasing ε_{sys} and increasing M_{min} can lead the identifying procedure to find a great number of failure modes to be identified. Increasing ε_{utr} can reduce the number of possible interim modes. N_{det} of closer to unity can lead the procedure so that the identified important failure modes closer to true solution are to be generated. However, as mentioned in Section 2.5.6, this requires very expensive computational cost. The parameter, N_{Limit} can reduce the number of possible interim modes as ε_{utr}, when searching procedure has progressed to a certain stage. At the same time, the parameter can affect the quality of the generated failure modes and, consequently, the evaluated system reliability. The parameter, ε_{det} should be one of the most influential ones affecting the evaluated system reliability because the occurrence of a structural collapse is approximately judged from Eq.(2.111) for a large and complex system. Hence, the parameter has close relation to the number of failed components in any failure mode in such a way that as its value decreases, more components will participate in the associated collapse mechanism and vice versa.

In this section the effects of the values of N_{Limit} and ε_{det} upon the system reliability level (β_{sys}) are investigated. For this some computations have been carried out to changes in their values.

o Effect of N_{Limit} :

Two typical values of N_{Limit} are chosen to investigate its effect upon the system reliability level, namely, N_{Limit} = 6 and 1 with retaining values of other parameters as the same values shown in Table 5.12. When N_{Limit} = 1, the identifying procedure is nearly the same as that of the marginal failure probability-based method proposed by Murotsu et al[41] [Section 2.5.3]. Table 5.35 illustrates comparison between the results of two cases for the three TLP models. In the case of the Hutton TLP and TLP-A, using N_{Limit} of 1 gives the average β_{sys} of about 3% and 0.5% lower than using N_{Limit} of 6, respectively, but the differences are negligibly small. While in the case of TLP-B, when N_{Limit} = 1, the average β_{sys} of about 11% higher than when N_{Limit} = 1 has been obtained. Based on these results, when N_{Limit} = 1, the Hutton TLP and TLP-A have nearly the same β_{sys} (the difference of the average β_{sys} between two TLP models is 0.5%), while TLP-B has β_{sys} about 22.7% greater than the other TLP models. However, the results may be far from the true solution.

Table 5.35 β_{sys} to Change in N_{Limit} Value

χ	Hutton TLP		TLP-A		TLP-B	
	$N_{Limit}=6$	$N_{Limit}=1$	$N_{Limit}=6$	$N_{Limit}=1$	$N_{Limit}=6$	$N_{Limit}=1$
0	6.55	6.70	6.09	6.04	6.77	7.58
45	6.30	6.08	7.20	7.86	7.13	7.67
90	6.83	6.88	6.69	6.68	7.32	8.36
total average	6.44	6.25	6.26	6.22	6.91	7.67

o Effect of ε_{det} :

When the structural collapse is judged from Eq.(2.111), it can be easily supposed that the number of failed components and, consequently, the system reliability, depends on the selected value of ε_{det}. In order to investigate the relation between β_{sys} and ε_{det},

two more cases of ε_{det} values, say $\varepsilon_{det} = 10^{-6}$ and 10^{-10}, are selected in addition to $\varepsilon_{det} = 10^{-8}$. The system reliability index is evaluated when wave direction, χ is 0^{o} only. For the Hutton TLP and TLP-B, β_{sys} are plotted against to $Log_{10}\varepsilon_{det}$ as shown in Fig. 5.37.

As is expected, change of β_{sys} is very much sensitive to the selected value of ε_{det}. In the case of the Hutton TLP, when $\varepsilon_{det} = 10^{-6}$, β_{sys} has decreased by about 19% and when $\varepsilon_{det} = 10^{-10}$, increased by about 15% compared to β_{sys} when $\varepsilon_{det} = 10^{-8}$ in Table 5.12. In the case of TLP-B, when $\varepsilon_{det} = 10^{-6}$, β_{sys} has decreased by about 16% and when $\varepsilon_{det} = 10^{-10}$, increased by about 12% compared to β_{sys} when $\varepsilon_{det} = 10^{-8}$. The average number of failed components contained in the failure modes is listed in Table 5.36.

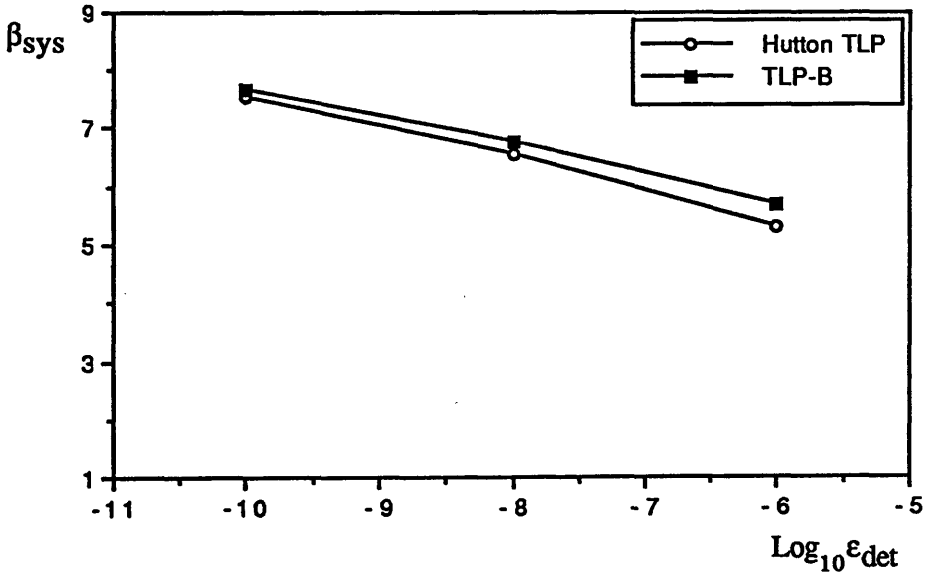

Fig. 5.37 β_{sys} vs ε_{det}

Table 5.36 Average Number of Failed Components vs ε_{det}

ε_{det}	10^{-6}	10^{-8}	10^{-10}
Hutton TLP	9	10	12
TLP-B	6	8	9

5.5 Discussion

This chapter has mainly stressed the system reliability studies of the Hutton TLP and its two variants. As far as the present numerical results are concerned, the two variants were found to be more efficient than the Hutton TLP. TLP-B especially showed higher β_{sys} than the other TLP models in spite of there being much less structural weight. The comparison of its design to the design of the Hutton TLP indicated that the design of at least 40% weight saving could perhaps be achieved. In general, it can be said that under the environmental loading condition found in TLPs, the structure having the ring- and stringer-stiffened cylinders is more efficient than the structure having the ring-stiffened cylinders from the system's point of view as well as from the component's point of view. Since the post-ultimate behaviour of any failed component was assumed to be ductile, the actual β_{sys}'s may be expected to be lower than the evaluated ones in Section 5.4. For the same structure, β_{sys} of the structure with components of brittle behaviour is usually less than the structure with components of ductile behaviour. β_{sys}, under the assumption that all components are brittle behaviour, is likely the lower bound of the system reliability. Further investigation and discussion about the effect of the post-ultimate behaviour of components will be given in Section 6.4.

The relation between the total load factor (λ_T) and the path reliability index (β_{path}) of the three TLP models indicated that the deterministically most important failure mode was not identical with the probabilistically most important one. A similar situation

could be found from the results of others as illustrated in Section 5.4.4. Because of this, the identifying procedure based on utilisation ratio could not perhaps provide the probabilistically important failure modes.

With regard to the structural redundancy of TLPs, it was shown that TLP structural systems possessed appreciable reserve (in the deterministic sense) and residual strength (in the probabilistic sense) as can be seen from the total load factors in Table 5.31, which are related to the reserve strength, and the β measure of structural residual strength (RDI_β) in Table 5.32. The average λ_T was obtained as 2.63 for the Hutton TLP, 2.82 for TLP-A and 2.96 for TLP-B. These seem to be higher than the expected value by Faulkner[8,136], who stated that the reserve strength index (RSI) given as Eq.(2.11) would be greater than 2. Lloyd and Clawson[91] also stated that well-designed platforms could resist greater than twice design environmental load without collapse.

The reliability study for the transverse structure of a semi-submersible by Murotsu et al[130] showed somewhat less reserve strength than the present TLP structures (the average load factor was 1.76). Amdahl et al[132] presented the results of reserve and residual strength for the Aker H3.2 type 8 column semi-submersible shown in Fig. 5.38 through the non-linear structural analysis using the idealised structural unit method (ISUM) in which non-linear geometric and material behaviour was included. A typical collapse mode is illustrated in Fig. 5.39 and numerical results are listed in Table 5.37. In contrast to Murotsu et al[130], it is shown that the semi-submersible of Amdahl et al[132] possesses more reserve strength than Murotsu et al and also considerable residual strength.

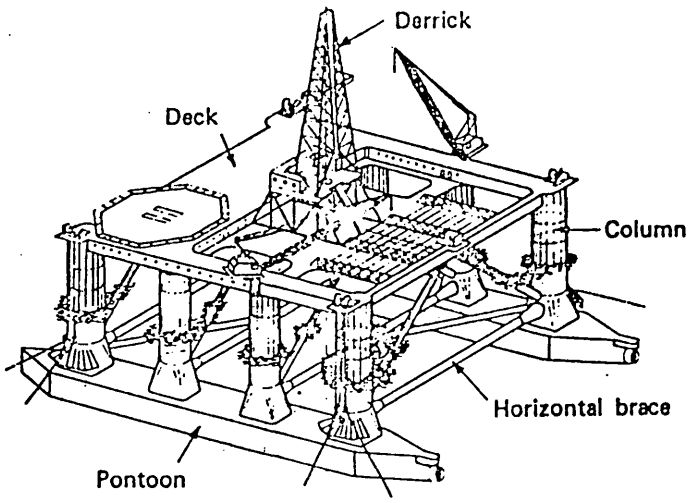

Fig. 5.38 Semi-Submersible Model of Amdahl et al[132]

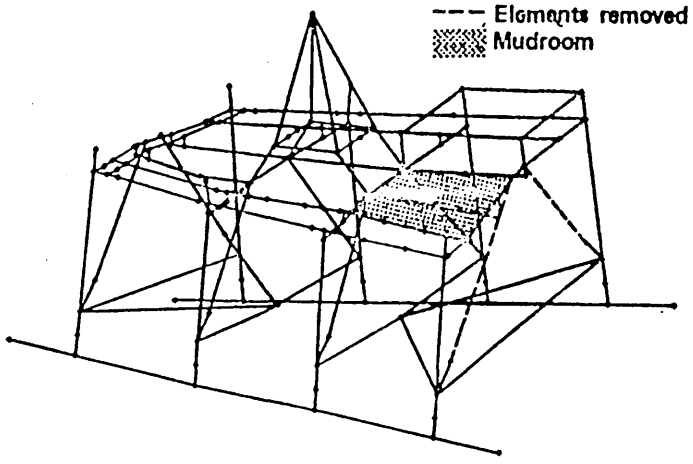

Fig. 5.39 Collapse Mode of Semi-Submersible of Amdahl et al[132]

Table 5.37 Numerical Results for Semi-Submersible by Amdahl et al[132]

Case	Condition	First yield	Load factor at collapse	Reserve strength factor	Residual strength factor
1	Undamaged	1.28	3.76	3.76	--
2	Explosion mud room Elements removed	0.18	1.86	--	0.49
3	Explosion mud room Reduced capacity	1.1	3.45	--	0.92
4	Explosion main leg	1.0	3.08	--	0.82

From the above discussions it can be drawn that floating platforms, especially TLPs, may possess considerable reserve and residual strength. As mentioned in Section 2.1.2, the structural redundancy is dependent upon various factors and hence, further study is required in this area.

The investigation into the relation between β_{sys} and control parameters of identifying procedure for generation the important failure modes, namely, N_{Limit} and ϵ_{det}, showed that the β_{sys} to be evaluated was very sensitive to their selected values. In order to obtain a reasonable level of system reliability, the appropriate values of control parameters must perhaps be determined by accumulating experience from the application of the methods for system reliability analysis to real structures. Additionally, the parameter values should be consistently kept throughout the system reliability analysis to provide reasonable information for the comparison of different structures and for a sensitivity study to investigate the effect of various variables affecting the β_{sys} (and β_{comp}).The sensitivity study will be shown in the next chapter.

CHAPTER 6 SENSITIVITY STUDIES

6.1 Introduction

A sensitivity study to changes in stochastic parameters (mean and COV) and distribution types of design variables must precede the optimisation procedure[135], and it is an important and valuable task in the light of that:

- it can provide useful information about the relative importance of design variables with regard to their effects on safety and then, the variable which is comparatively less important and influential on safety can be treated as a deterministic one.
- it can provide the designer with useful information to intelligently modify structures.
- it can illustrate the accuracy needed in describing the structural data required in probabilistic computations which is a major goal in limit state design.

Here the sensitivity study is mainly concerned with the effect on system safety to changes in stochastic parameters, namely, mean and COV, of design variables and the effect of post-ultimate behaviour of failed components. Results will be shown in the relevant figures representing the relation of the system reliability index to stochastic parameters. Their effects on the component safety will also be illustrated as a by-product for comparison with their effects on the system reliability.

For the present purpose the Hutton TLP has been chosen as an existing TLP and TLP-B as its variant to compare the safety level of the structures having different types of principle component, i.e. ring-stiffened cylinder (the Hutton TLP) and ring- and stringer-stiffened cylinder (TLP-B).

Design variables are divided into two groups: resistance variables and loading variables. There must be many variables (or factors) affecting the safety level of a

structure. For the present sensitivity study, selecting the important variables, which are supposed to have comparatively much influence on safety level, has been determined with reference to results of component reliability analysis by others[114,116,155,213].

As a resistance variable, the strength modelling parameter (X_M) must be one of the most important and influential variables with regard to their effect on safety, as can be expected from its important position within the safety margin equation [Eq.(2.103)]. Yield stress (σ_Y) is known to be more influential than the elastic modulus (E). The elastic modulus usually has comparatively small influence on safety and sometimes is treated as a deterministic variable. The influence of geometric properties is also comparatively small because of their small COV. But for a cylindrical member results of component reliability analysis by Das et al[114,116] indicated that radius and thickness of cylinder could be influential on safety. As it has been well recognised, the post-ultimate behaviour of failed components is one of the major factors which affect the system reliability and determine the residual strength of a structural system. When any particular component, of which post-ultimate behaviour is not ductile, its failure can greatly affect the re-distribution of load effects of other components and structural stiffness. Further discussion on this will be shown in Section 6.4.

Loading variables are known to be more influential on safety than resistance ones mainly because of their position within the safety margin equation and their high COVs. The effect of changes in mean bias and COV of three category load effects (dynamic, static and quasi-static) on system and component safety have been investigated.

A range of the design variables selected for the present sensitivity study are listed in Table 6.1 except parameters for the post-ultimate behaviour [see Section 6.4]. Throughout the numerical analysis the system reliability index is the total average one corresponding to the total average probability of system failure as described in Chapter 5. The component reliability index is always referred to that of the component of column 2 located just above pontoon, when χ =0 deg. The component is designated as Component 61 for the Hutton TLP [Fig. 5.1] and Component 45 for TLP-B [Fig.5.9]. The same

values of control parameters in the procedure of identifying the important failure modes are consistently used as shown in Table 5.13.

Table 6.1 Ranges of Variables for the Sensitivity Study

[1] Strength modelling parameter (X_M)

mean bias ($\underline{X}_M$) : 0.90, 0.95, 0.99, 1.05, 1.10

COV (V_{X_M} : %) : 5.0, 7.5, 10.0, 13.0, 15.0, 17.5, 20.0

[2] Yield stress (σ_Y)

COV (%) : 4.0, 8.0, 12.0

[3] Radius and thickness of cylinder (R and t)

COV (%) : 2.0, 4.0, 6.0, 8.0

[4] Mean bias of load effect

dynamic component : 0.6*, 0.8, 1.0, 1.2

static component : 0.6, 0.8, 1.0

quasi-static component : 0.0, 0.8, 1.0

[5] COV bias of load effect (%)

dynamic component : 5.0, 10.0, 15.0, 20.0, 25.0, 30.0

static component : 5.0*, 10.0, 15.0, 20.0, 25.0*, 30.0*

quasi-static component : 10.0, 20.0, 30.0

* : for TLP-B only

6.2 Influence of Resistance Variables

6.2.1 Strength Modelling Parameter

As proposed in Section 2.4, the safety margin equation is given as Eq.(2.103) in the modified form of Eq.(2.86). As mentioned before, the strength modelling parameter plays a major role as a resistance variable and may have much influence on the system

resistance and consequently, the system reliability.

As mentioned in Chapter 1, the incremental load method can be easily applied to evaluating the system safety for the sensitivity study when the failure paths are pre-defined. In order to investigate the influence of mean bias, $\underline{X}_M$ and modelling uncertainty, V_{X_M} (COV of bias) on the system reliability, the failure modes already identified when $\underline{X}_M$ and V_{X_M} have the values of the standard case [Table 5.3] are used to evaluate the system safety level when they have different values. $\underline{X}_M$ and V_{X_M} of cylindrical components only are to be varied. The identified failure paths are listed in Tables 5.13 - 5.15 for the Hutton TLP and Tables 5.23 - 5.25 for TLP-B.

When $\underline{X}_M$ and V_{X_M} have different values from the standard case, the failure sequences of the important failure modes to be identified differ, of course, and hence, there is a difference between the evaluated system reliability indices when the pre-defined paths are followed and when the probabilistic searching procedure is passed through. The difference may be expected to be small and therefore can be neglected at least for the purpose of sensivitivity studies. For example, Table 6.2 compares the system reliability index (β_{sys}) of the Hutton TLP by the two procedures which show nearly the same tendencies.

As listed in Table 6.1, five cases of mean bias, $\underline{X}_M$ and seven cases of modelling uncertainty, V_{X_M} by varying them within the practical range including the standard case [Table 5.3] have been carried out for the Hutton TLP and TLP-B. Fig. 6.1 shows the relation between β_{sys} and $\underline{X}_M$, and Fig. 6.2 the relation between β_{sys} and V_{X_M} for the Hutton TLP. Figs. 6.3 and 6.4 are for TLP-B. The relation of β_{comp} to $\underline{X}_M$ and V_{X_M} are illustrated in Figs. 6.5 to 6.8, respectively, in the same way.

As can be seen in Figs. 6.1 to 6.4, β_{sys} is more sensitive to V_{X_M} than to $\underline{X}_M$ for both TLP models. When V_{X_M} is small, say less than 7.5%, there is no change of β_{sys} to $\underline{X}_M$. The effect of $\underline{X}_M$ on β_{sys} becomes significant when V_{X_M} is greater than 10%. β_{comp} is also sensitive to the change in both $\underline{X}_M$ and V_{X_M} as illustrated in Figs. 6.5 to

6.8. It can be seen that β_{comp} of both TLP models is more sensitive to change in both $\underline{X}_M$ and V_{X_M} than β_{sys} and varies linearly to change in $\underline{X}_M$. The effect of $\underline{X}_M$ on β_{comp} is significant within the low range of V_{X_M} differently from its effect on β_{sys}.

Figs. 6.9 to 6.12 show comparisons of β_{sys} and β_{comp} to change in $\underline{X}_M$ when V_{X_M} has the value of standard case (=10% for the Hutton TLP, =13% for TLP-B) and in V_{X_M} when $\underline{X}_M$ has the value of standard case (=0.99 for two TLPs).

Even though the effects of $\underline{X}_M$ and V_{X_M} on β_{sys} and β_{comp} may differ depending on several factors, e.g. the structural configurations, the component types of the structure, etc, from the results it can be drawn that regardless of structural configuration or component types, developing the strength formula having low modelling uncertainty may be one of the easiest ways to raise the system safety and, therefore, to achieve the weight saving with retaining the same level of β_{sys}.

The sensitivity factors of β_{sys} and β_{comp} to changes in $\underline{X}_M$ and V_{X_M} are calculated to show the relative importance between $\underline{X}_M$ and V_{X_M},which are regarded as random variables. The sensitivity factors can be calculated from Eq.(6.1)[5] using the slopes of curves in Figs. 6.9 to 6.12, where $\{X\}=\{X_1, X_2\} =\{\underline{X}_M, V_{X_M}\}$ and slopes are evaluated at the standard values of $\underline{X}_M$ and V_{X_M} [see Table 5.3].

$$\alpha_i = \frac{\left(\frac{d\beta}{dx_i}\right)_{\mathbf{x}}}{\sqrt{\sum_j \left[\left(\frac{d\beta}{dx_j}\right)_{\mathbf{x}}\right]^2}} \qquad i = 1, 2 \qquad (6.1)$$

where $\mathbf{X} = \{\underline{X}_1, \underline{X}_2\}$ =standard value of $\underline{X}_M$ and V_{X_M} as in Table 5.3 and β is β_{sys} or β_{comp}.

The calculated sensitivity factors are listed in Table 6.3, in which α_1 and α_2 are sensitivity factors of reliability index (β_{sys} or β_{comp}) to $\underline{X}_M$ and V_{X_M}, respectively. From Table 6.3 it can be seen that β_{sys} and β_{comp} of both TLPs are much more

sensitive to V_{X_M} than to $\underline{X}_M$. β_{comp} is more sensitive to $\underline{X}_M$ than β_{sys}.

These results confirm that the modelling uncertainty of the strength formula is relatively more important than the mean bias and much more influential not only on the system reliability but also on the component reliability which is the usual basis for most designs. Therefore, as pointed out in references [119] and [163] it is required to have to keep V_{X_M} as low as possible to gain a higher level of β_{sys} and β_{comp} with keeping $\underline{X}_M$ close to unity.

Table 6.2 Comparison of β_{sys} by Two Procedures : Hutton TLP

$(\underline{X}_M, V_{X_M})$	(0.90, 0.10)	(1.05, 0.10)	(0.99, 0.05)	(0.99, 0.15)
procedure following the pre-defined failure modes	5.96	6.18	6.74	5.18
probabilistic searching procedure	6.12	5.73	6.80	5.33

Table 6.3 Sensitivity Factors of β_{sys} and β_{comp} to Changes in $\underline{X}_M$ and V_{X_M}

sensitivity factor	β_{sys}		β_{comp}	
	Hutton TLP	TLP-B	Hutton TLP	TLP-B
α_1 for $\underline{X}_M$	0.077	0.173	0.332	0.300
α_2 for V_{X_M}	-0.997	-0.985	-0.943	-0.954

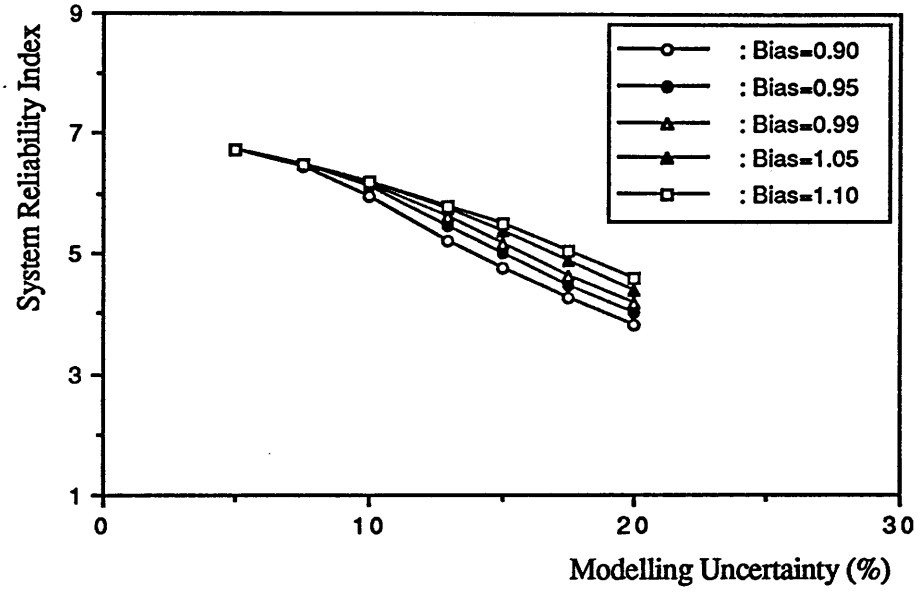

Fig. 6.1 β_{sys} vs $\underline{X}_M$: Hutton TLP

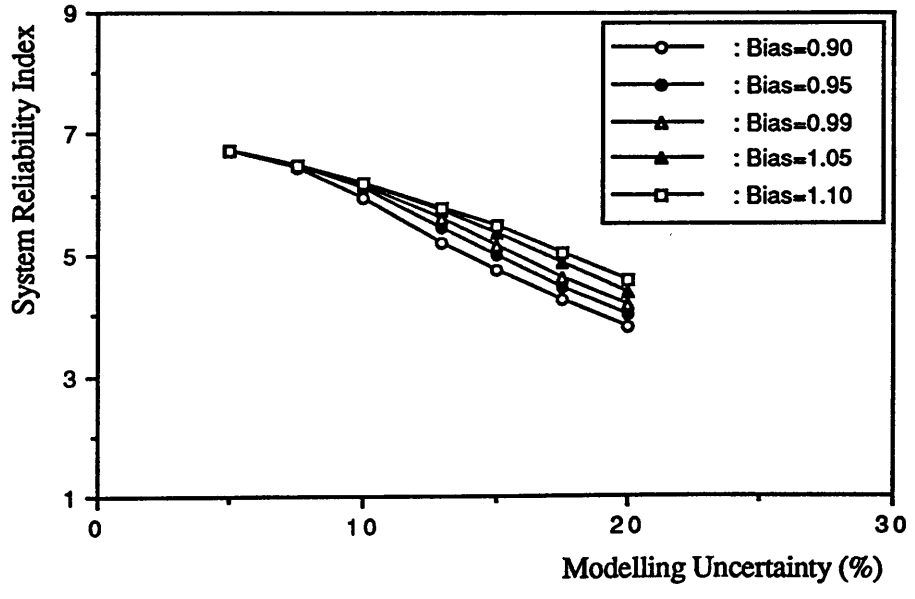

Fig. 6.2 β_{sys} vs V_{X_M} : Hutton TLP

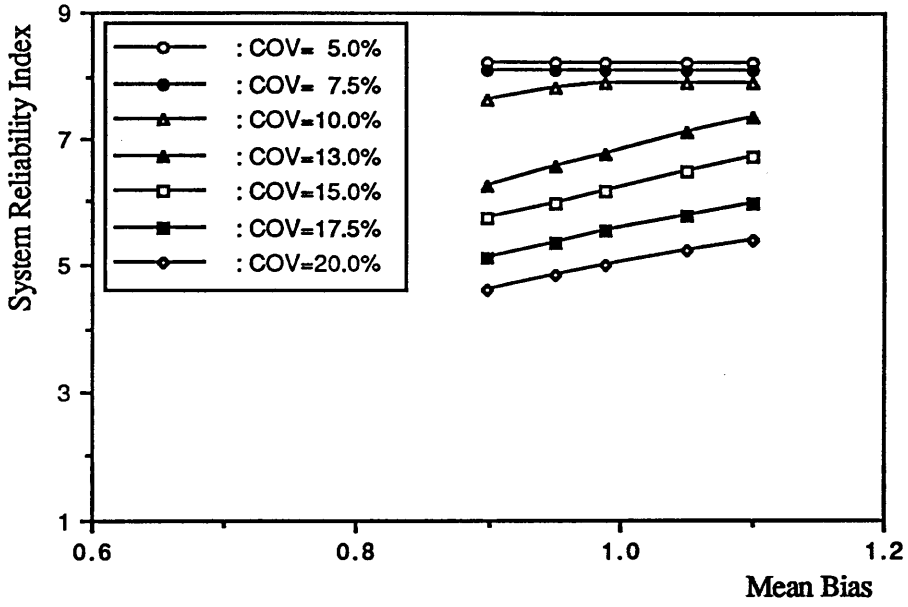

Fig. 6.3 β_{sys} vs $\underline{X}_M$: TLP-B

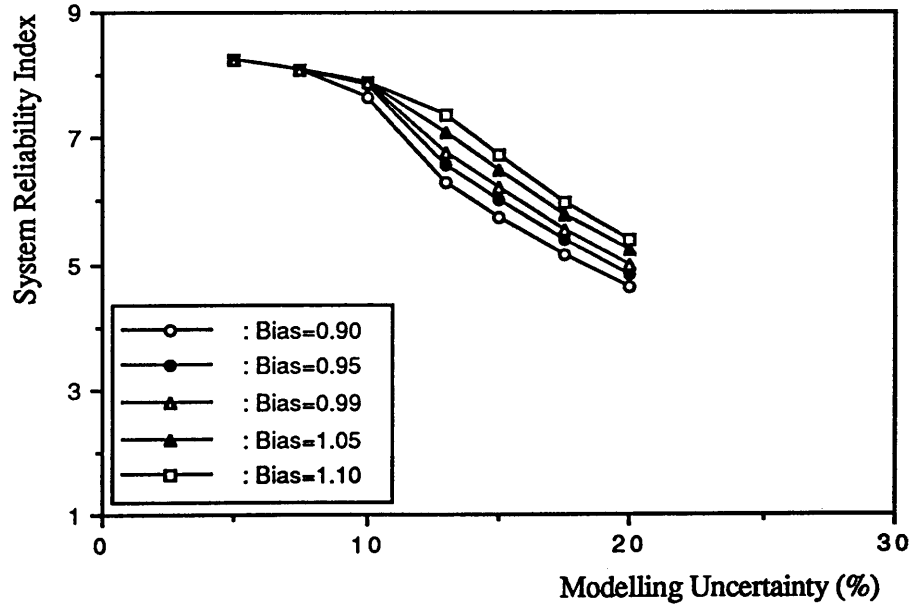

Fig. 6.4 β_{sys} vs V_{X_M} : TLP-B

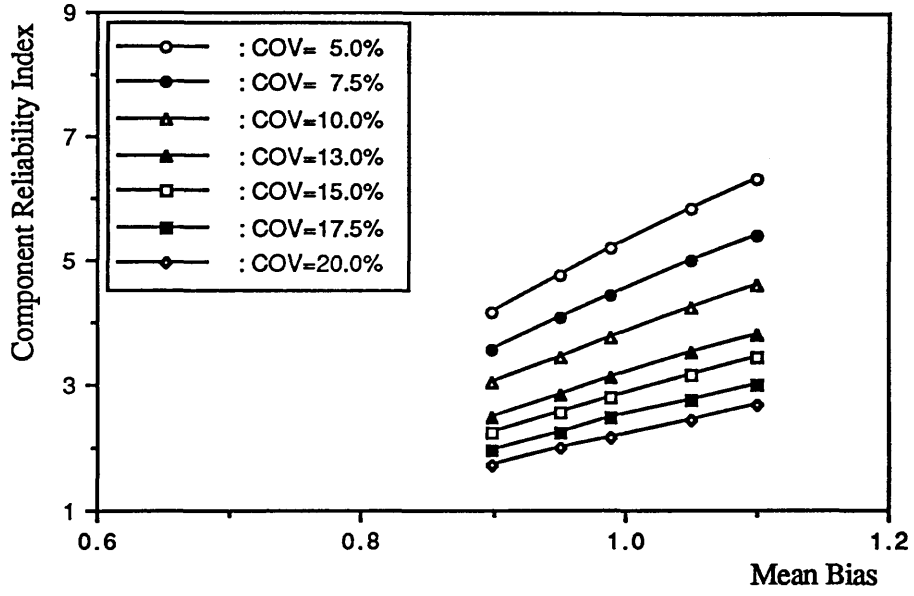

Fig. 6.5 β_{comp} vs $\underline{X}_M$: Hutton TLP

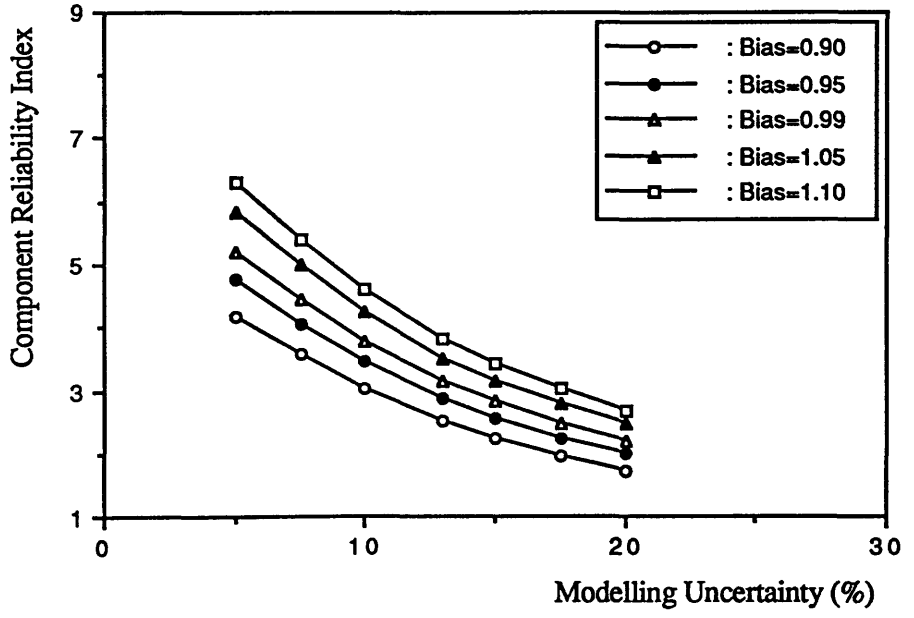

Fig. 6.6 β_{comp} vs V_{X_M} : Hutton TLP

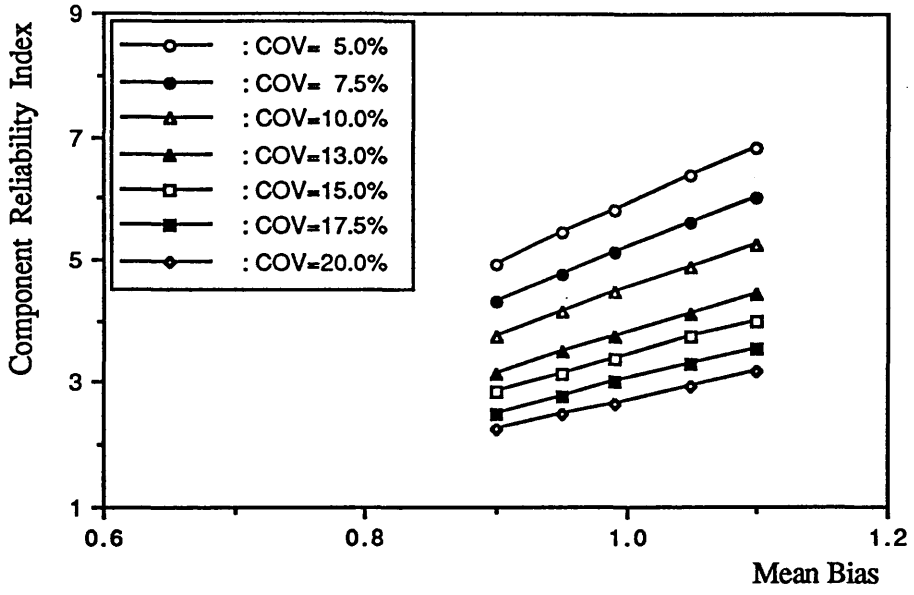

Fig. 6.7 β_{comp} vs $\underline{X}_M$: TLP-B

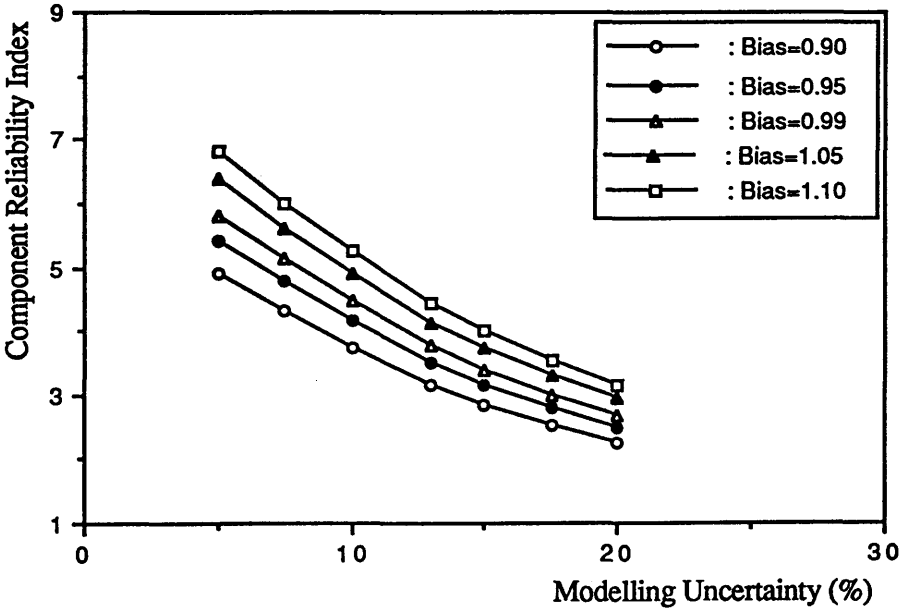

Fig. 6.8 β_{comp} vs V_{X_M} : TLP-B

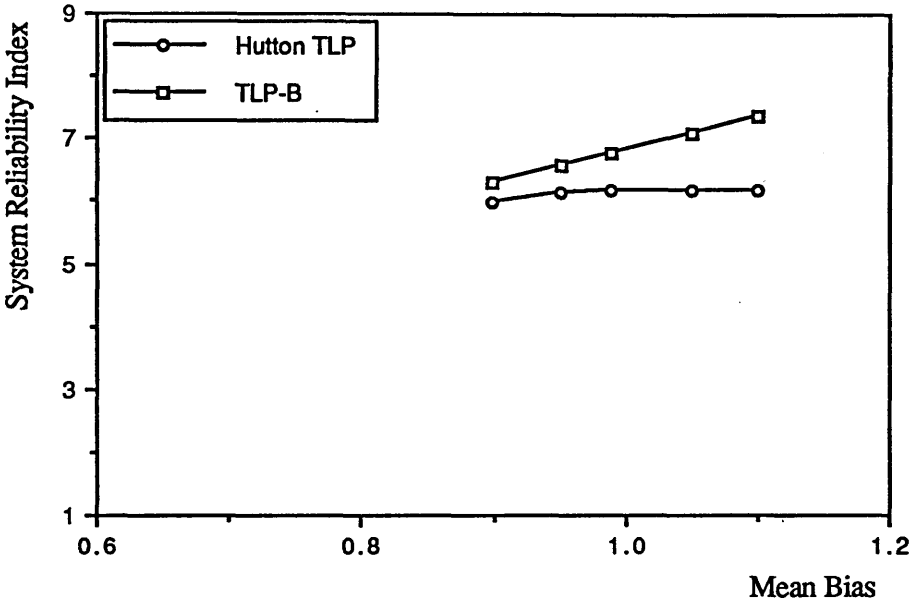

Fig. 6.9 Comparison of β_{sys} to Changes in $\underline{X}_M$

: V_{X_M} = 10.0% for the Hutton TLP and 13.0% for TLP-B

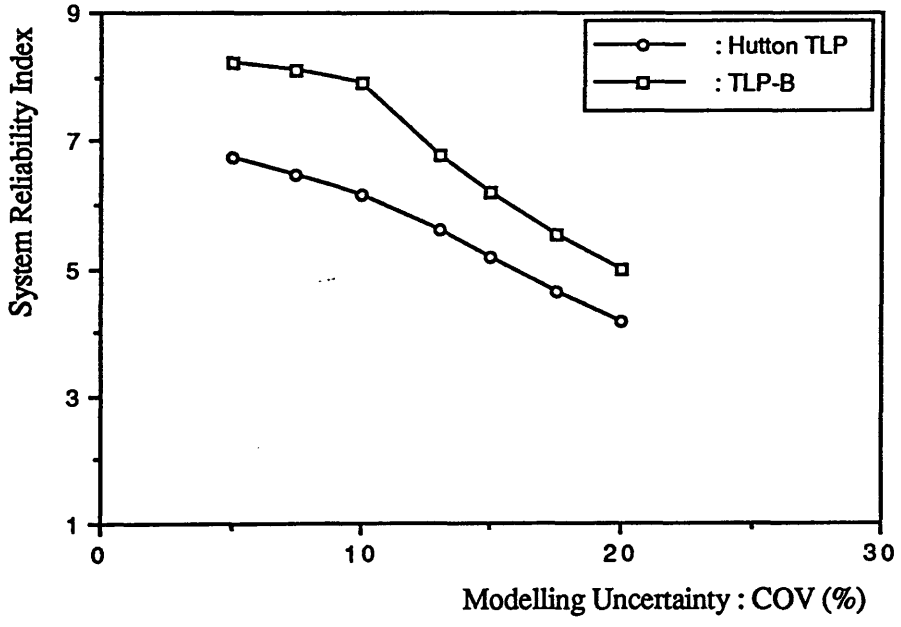

Fig. 6.10 Comparison of β_{sys} to Changes in V_{X_M}

: $\underline{X}_M$ = 0.99 for the Hutton TLP and TLP-B

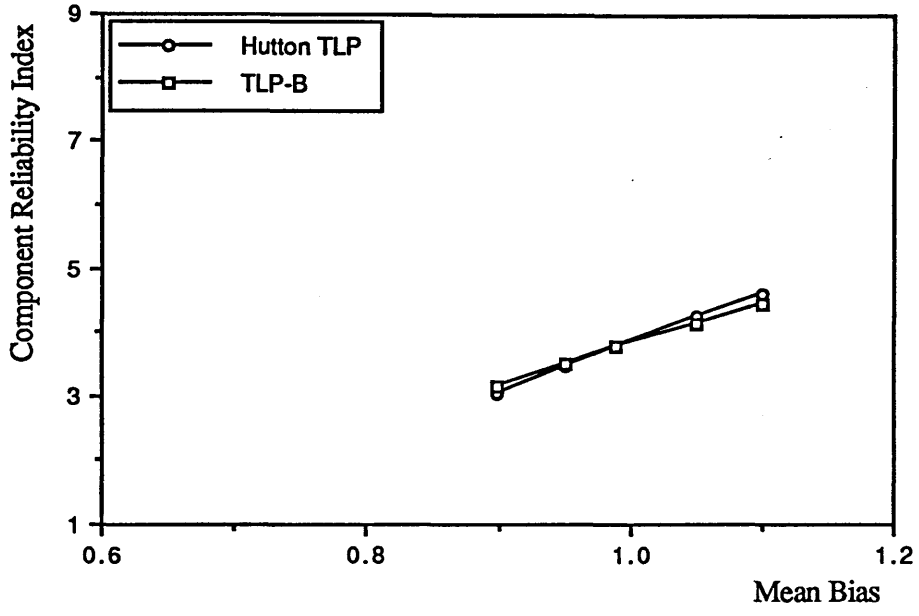

Fig. 6.11 Comparison of β_{comp} to Changes in $\underline{X}_M$

: V_{X_M} = 10.0% for the Hutton TLP and 13.0% for TLP-B

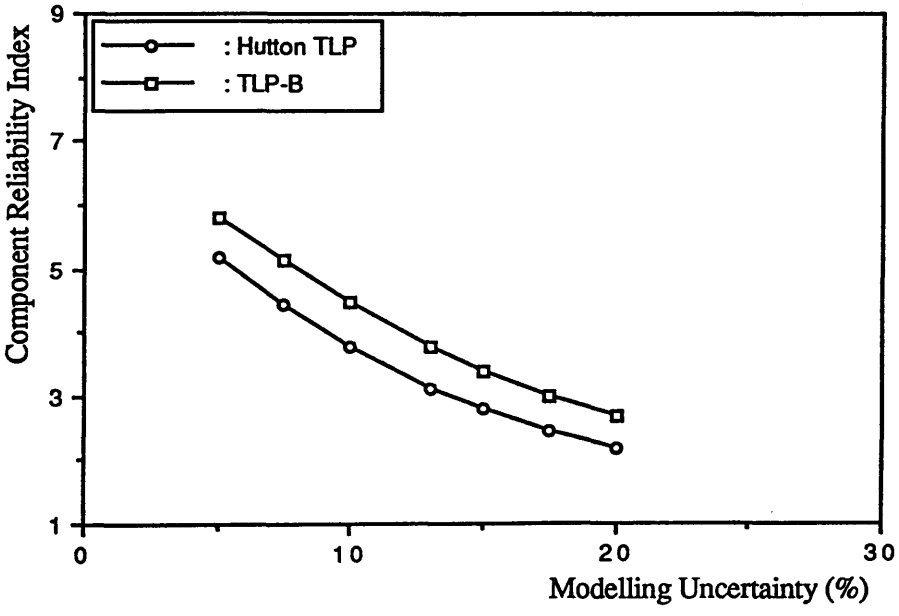

Fig. 6.12 Comparison of β_{comp} to Changes in V_{X_M}

: $\underline{X}_M$ = 0.99 for the Hutton TLP and TLP-B

6.2.2 Material and Geometric Properties

According to the results of component reliability analysis in references yield stress (σ_Y) and radius and thickness of the cylinder (R and t) are important variables affecting the component reliability.

Figs. 6.13 and 6.14 show the β_{sys} and β_{comp} to change in COV of σ_Y, respectively, for the Hutton TLP and TLP-B. Both TLPs show nearly the same tendencies of changes of β_{sys} and β_{comp} to COV of σ_Y and R and t, and two reliability indices are not sensitive.

The effect of σ_Y is such that, in the case of the Hutton TLP, the difference of β_{sys} between when COV of σ_Y is 8% and when 4 and 12% are about $\pm$ 3%, whereas in the case of TLP-B, the difference is less than 1%. The difference of β_{comp} lies between $\pm$ 1% for the Hutton TLP and $\pm$ 5% for TLP-B. The effect of R and t of cylindrical components on β_{comp} is small, as can be seen in Fig. 6.16. COV of 2 and 6% of R and t gives the difference of within $\pm$ 3% compared to β_{comp} when the COV is 4% and COV of 8% gives about 6% lower β_{comp}. Meanwhile their effects on β_{sys} are somewhat greater than on β_{comp} in such a way that for the Hutton TLP, β_{sys} has increased by about 5 and 10% when the COV is 6 and 8%, respectively, and for TLP-B, it has decreased by about 9% when the COV is 8%.

Fig. 6.17 shows comparison between the effect of COV of σ_Y and that of COV of R and t upon β_{sys} for the Hutton TLP and Fig. 6.18 upon β_{comp}. Figs. 6.19 and 6.20 for TLP-B. The figures show that R and t are more influential on resistance and safety than σ_Y. But, this may be due to the fact that COV of R and t were given as the same value and their effects were probably more reflected in the form of combined action on safety COV of σ_Y. β_{comp} was less sensitive to change in COV's of R and t than β_{sys}.

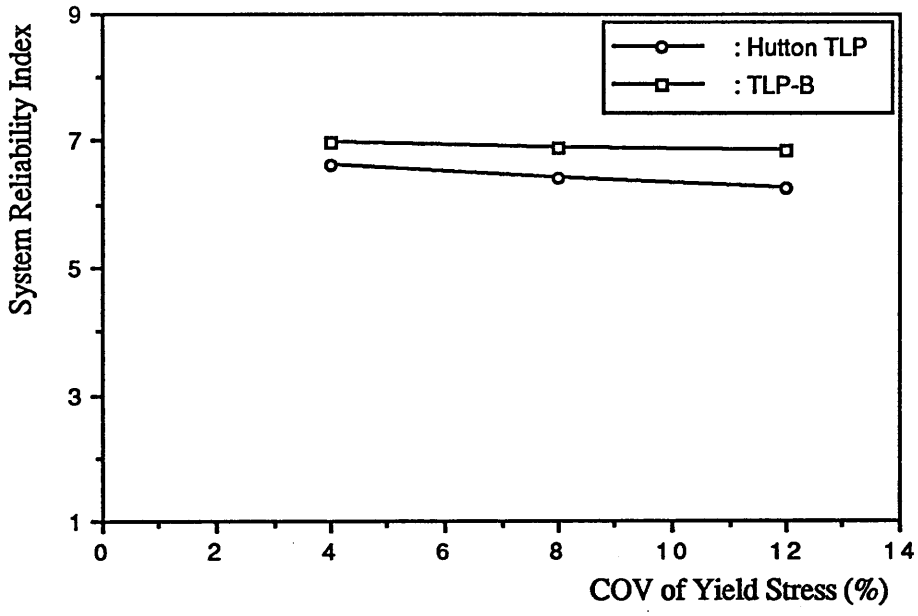

Fig. 6.13 β_{sys} vs COV of σ_Y

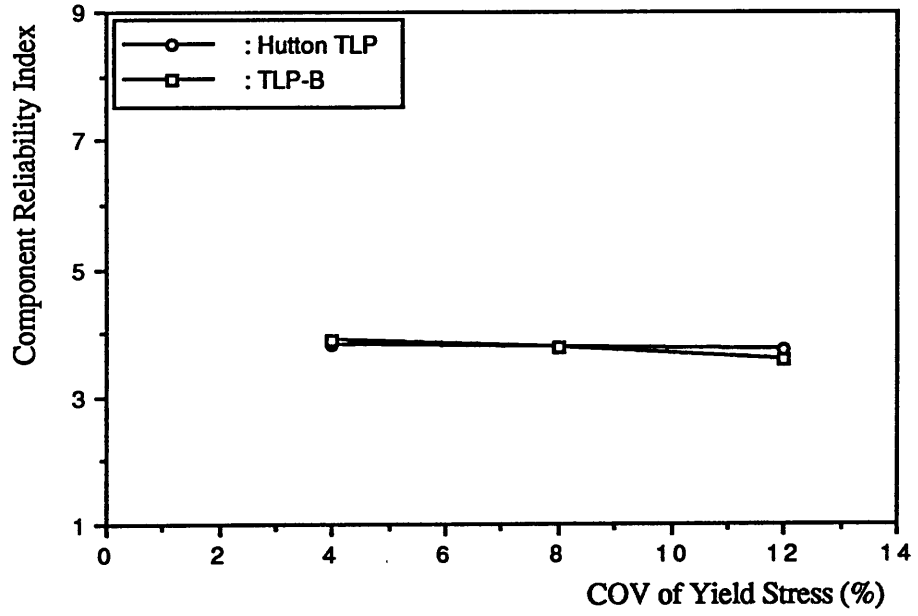

Fig. 6.14 β_{comp} vs COV of σ_Y

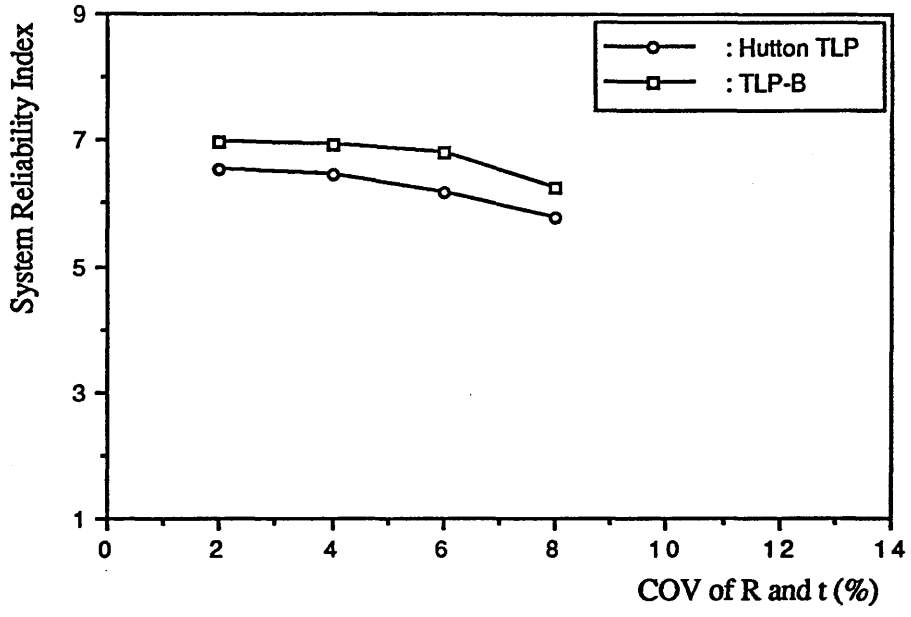

Fig. 6.15 β_{sys} vs COV of R and t of Cylindrical Components

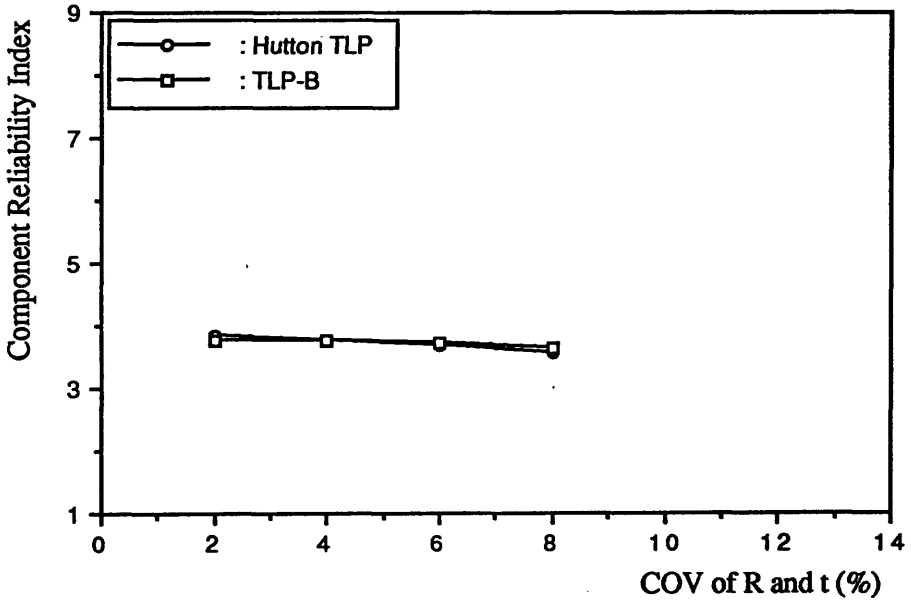

Fig. 6.16 β_{comp} vs COV of R and t of Cylindrical Components

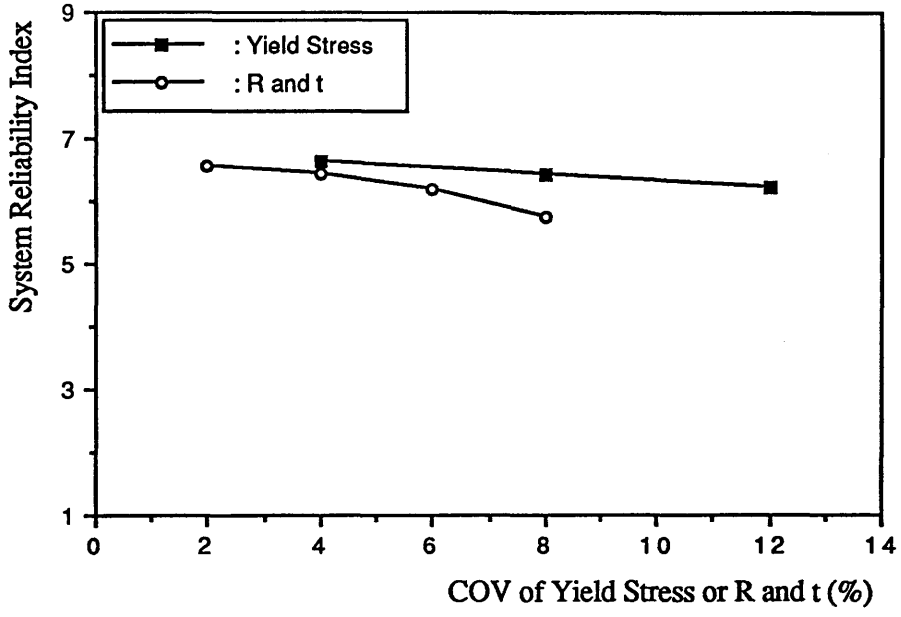

Fig. 6.17 β_{sys} vs COV of σ_Y and R and t of Cylindrical Components : Hutton TLP

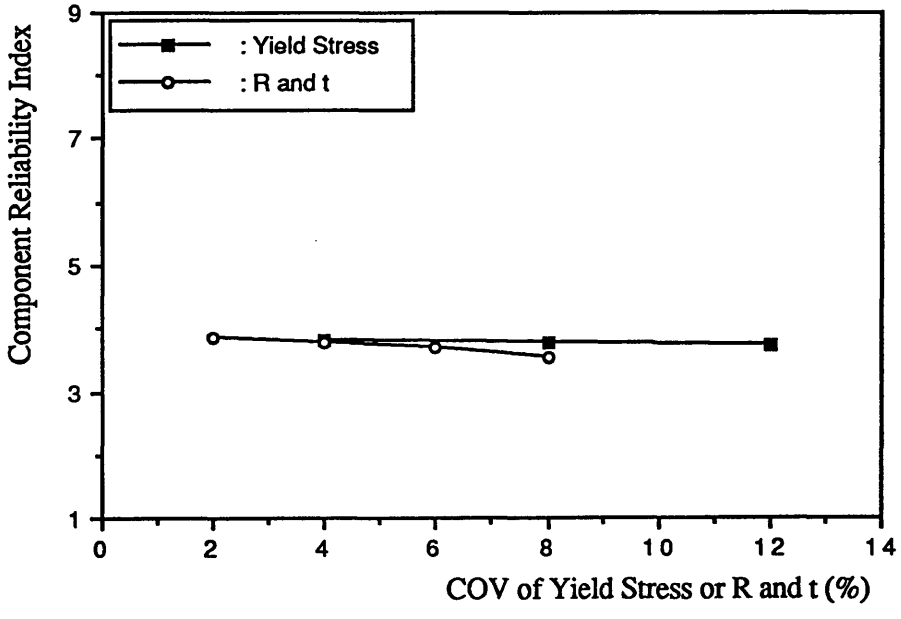

Fig. 6.18 β_{comp} vs COV of σ_Y and R and t of Cylindrical Components : Hutton TLP

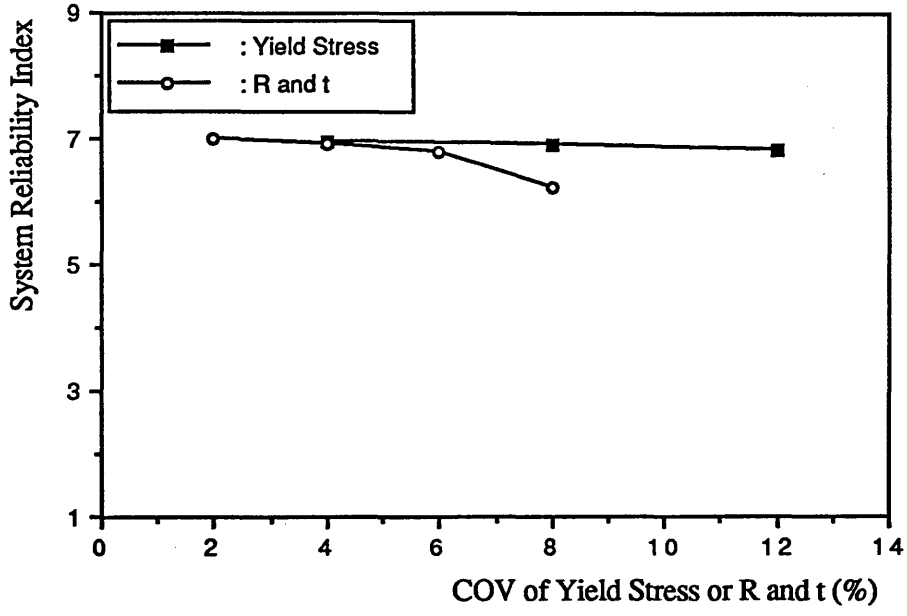

Fig. 6.19 β_{sys} vs COV of σ_Y and R and t of Cylindrical Components : TLP-B

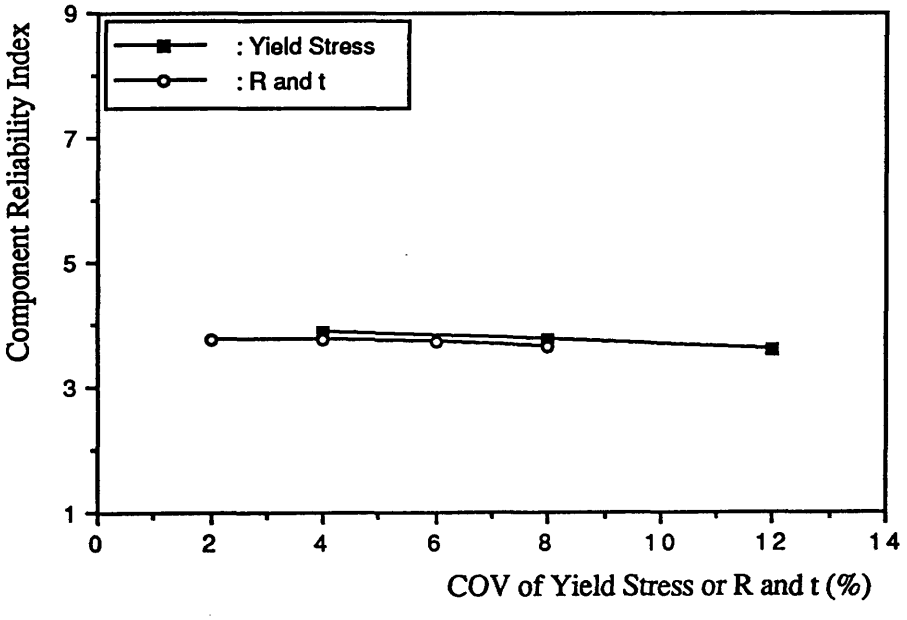

Fig. 6.20 β_{comp} vs COV of σ_Y and R and t of Cylindrical Components : TLP-B

6.3 Influence of Loading Variables

6.3.1 Mean Bias of Load Effect

To investigate the influence of mean bias of load effects system analysis has been carried out with three postulated cases for mean bias of predicted load effects as listed in Table 6.1.

Results for the Hutton TLP are shown in Figs. 6.21 and 6.22 relating the reliability index to mean bias of load effect. Mean bias has more influence on β_{comp} than β_{sys}.Two reliability indices are more sensitive to mean bias of static component than to dynamic and quasi-static components. When mean bias of static component is 0.6 and 0.8, β_{sys} has increased by about 8% and 6%, respectively and β_{comp} by about 25% and 53%, respectively. Meanwhile, when mean bias of dynamic component is 0.8, β_{sys} and β_{comp} have increased by about 4% and 20%, respectively. With regard to the effect of quasi-static component, when its mean bias is 0.0, i.e. when there is no quasi-static component, both reliability indices are increased by about 8%. This implies that safety is not sensitive to mean bias of quasi-static component.

The results for TLP-B are illustrated as Figs. 6.23 and 6.24, where one more case is added when mean bias of dynamic component is 0.6. For this model β_{comp} shows more sensitivity to mean biases of load effects than β_{sys}. Static component is most influential upon both reliability indices followed by dynamic component. Regarding the influence of dynamic component on safety, when its mean bias is 0.6, 0.8 and 1.0, β_{sys} has increased by about 17%, 6% and 1%, respectively, and β_{comp} by about 16%, 9% and 2%, respectively. Meanwhile the influence of static component is such that the mean bias of 0.6 and 0.8 give about 18% and 10% higher β_{sys}, respectively. When only static and dynamic component are acting, β_{sys} has increased by about 10% to β_{sys} of about 7.6 and β_{comp} by about 4% to β_{comp} of 4.0.

To illustrate the comparison of effects of mean biases of load effects upon safety between two TLP models, results are re-drawn as shown in Fig. 6.25 for β_{sys} and in

Fig. 6.26 for β_{comp}. In Fig. 6.25 TLP-B shows more sensitivity to changes in static and dynamic components than the Hutton TLP. Two models show nearly the same changes to quasi-static component.

As far as the present results are concerned, it can be drawn that the mean bias of load effect give much influence upon the safety, system level as well as component level, and static component is most influential followed by dynamic component, and quasi-static component is relatively less influential than the other two load effects.

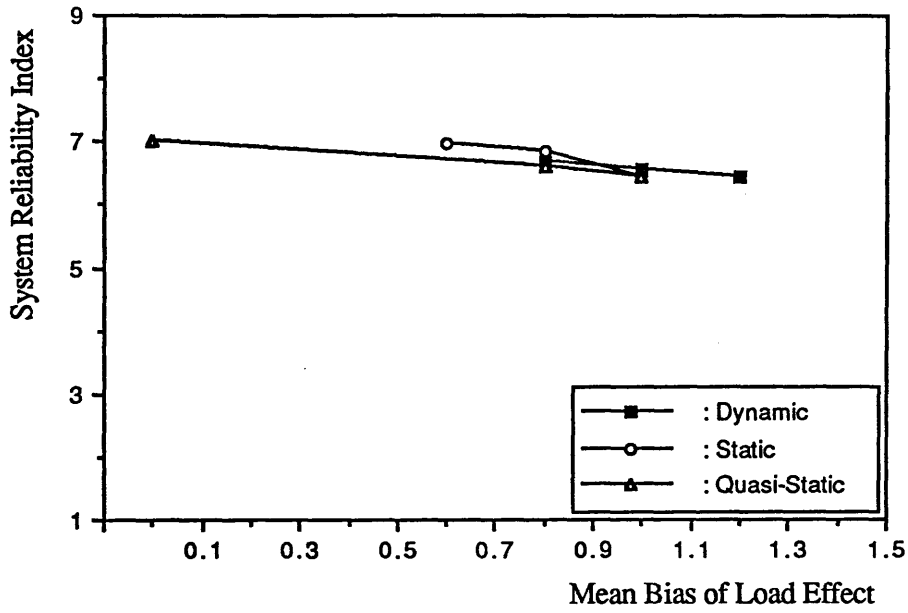

Fig. 6.21 β_{sys} vs Mean Bias of Load Effects : Hutton TLP

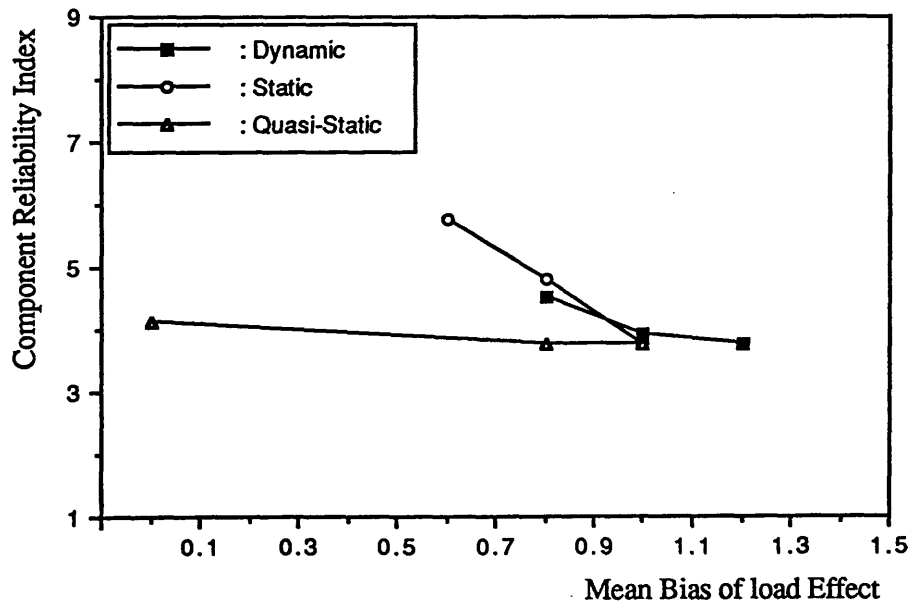

Fig. 6.22 β_{comp} vs Mean Bias of Load Effects : Hutton TLP

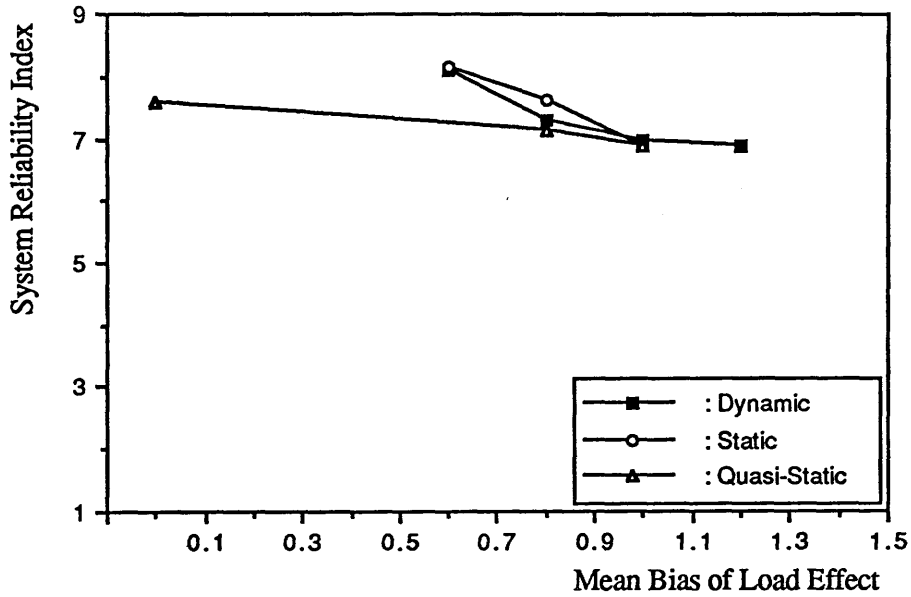

Fig. 6.23 β_{sys} vs Mean Bias of Load Effects : TLP-B

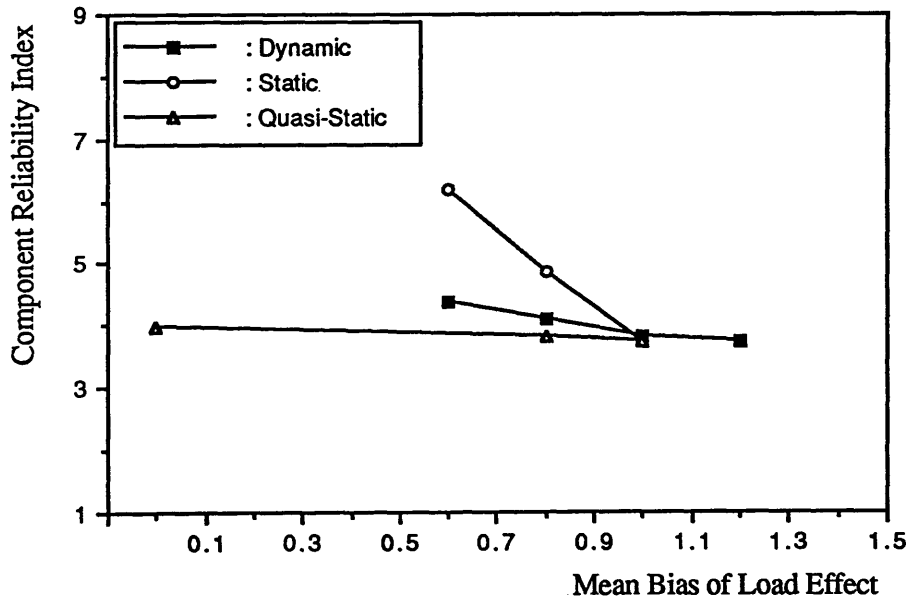

Fig. 6.24 β_{comp} vs Mean Bias of Load Effects : TLP-B

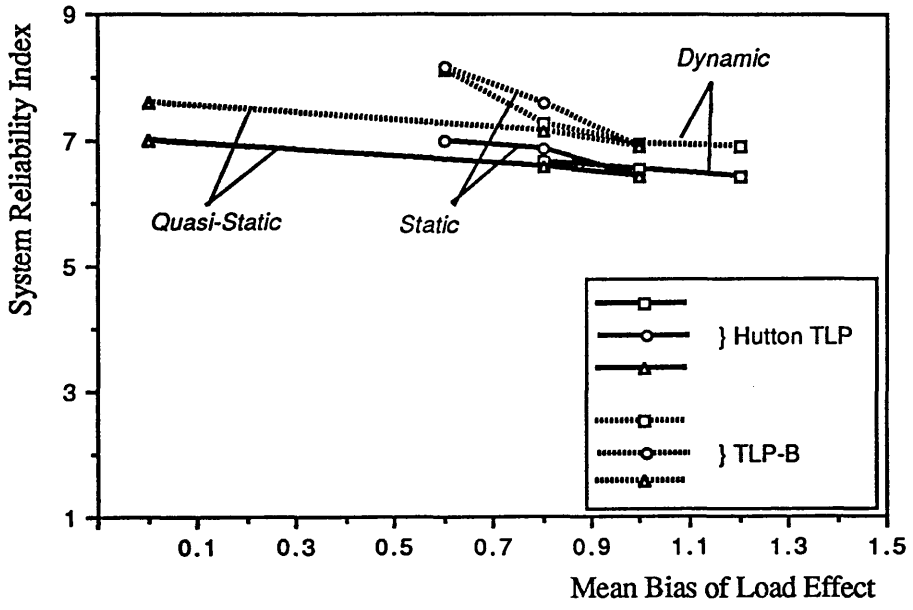

Fig. 6.25 Comparison of β_{sys} vs Mean Bias of Load Effects

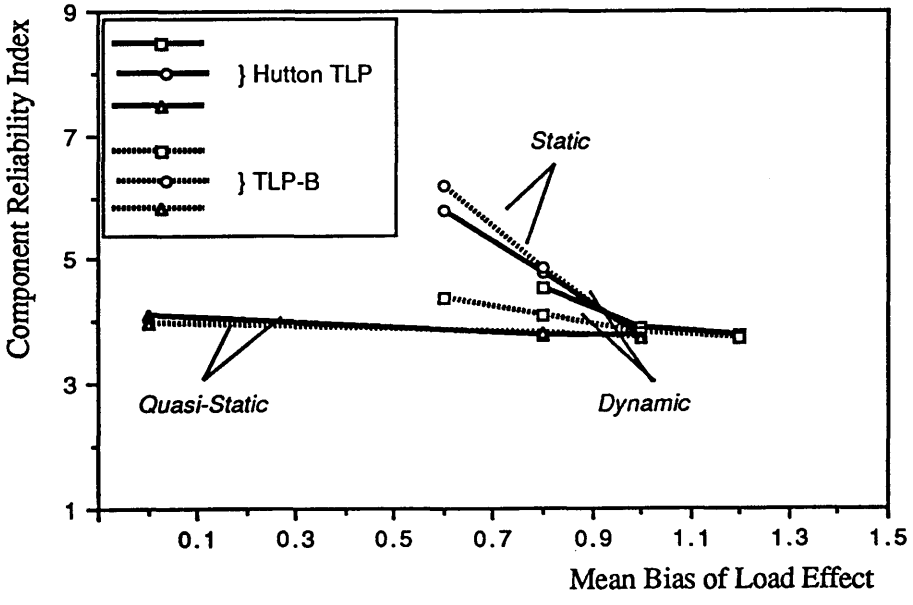

Fig. 6.26 Comparison of β_{comp} vs Mean Bias of Load Effects

6.3.2 Coefficient of Variation of Load Effect

According to the results for component safety by others[114,116,135,213] coefficients of variation of load effects were shown to affect the safety level. To investigate the influence of COV of load effects upon safety, system and component level, several case studies have been carried out by varying COV values for static, dynamic and quasi-static components: three cases for static component, six cases for dynamic component and three cases for quasi-static component as shown in Table 6.1.

The results can be seen in Figs. 6.27 to 6.32 plotted in the same way as before. As is expected, it can be found in Fig. 6.27 that the effect of COV of dynamic component upon β_{sys} becomes significant as the COV increases. For the Hutton TLP increase of the COV to 20%, 25% and 30% results in decrease of β_{sys} by about 15%, 25% and 30%, respectively compared to when the COV is 10% and for TLP-B by about 18%, 32% and 40%, respectively. With regard to its effect on β_{comp}, in the case of the Hutton TLP, when the COV is 20, 25 and 30%, β_{comp} is about 13, 21 and 28% less than that when the COV is 10%. The change of TLP-B's β_{comp} to the COV is relatively small. When the COV is 30%, β_{comp} is about 8% less than that when the COV is 10%.

From Figs. 6.29 and 6.30 effect of static component upon two reliability indices is shown to be greater than that of dynamic component. β_{comp} of the Hutton TLP and TLP-B varies in nearly the same manner, whereas β_{sys} of the Hutton TLP varies within a wider range than that of TLP-B. For the Hutton TLP, when COV of static component has increased to 15% and 20%, β_{sys} has dropped down by about 20% and 32%, respectively and for TLP-B by about 12% and 18%, respectively. The effect of quasi-static component on safety, as can be seen in Figs. 6.31 and 6.32, is comparatively small compared to those of static and dynamic components and particularly its effect on β_{comp}.

To compare the effects of changes in COVs of three types of load effects, the results are re-drawn in Figs. 6.32 and 6.34 for the Hutton TLP and in Figs.6.35 and 6.36 for TLP-B. In the case of TLP-B, three more cases of changes in static component, i.e. when the COV is 5%, 25% and 30%, are added to show more extensively its effect

upon safety but the two cases of 25% and 30% are unlikely to be practical in TLP structures. From Fig. 6.35 it can be shown that in the case of TLP-B, when COV of static component is 5%, β_{sys} has decreased by about 12%, and β_{comp} by about 7%. Meanwhile, when the COV is 25 and 30%, β_{sys} is about 32% and 40% less than β_{sys} when the COV is 10%, respectively. β_{comp} has decreased by about 28% and 35%, respectively.

Conclusively speaking, the effects of three types of load effects upon the safety, as far as present results are concerned, it was shown that static load effect (mean bias and COV) was most influential on the system reliability index as well as component reliability index followed by the dynamic load effect. This may be due to the greater magnitude of static component acting on components than that of dynamic component. But considering the practically more degree of uncertainty in dynamic component than in static component, it can be said that dynamic component may be the more important loading variable. Quasi-static component was found to be relatively less influential than the other two components. This is probably due to its relative less magnitude than the other two components and negligence of the load due to wave drifting. However, its effects on the system safety may not be significant. Additionally, when quasi-static load effect of any particular component is of the same order as static or dynamic load effects, β_{comp} may be sensitive to quasi-static load effect from the component's side. But the situation may not always be applied for the system reliability because when any component has failed, there occurs the load effect re-distribution of failed components and it may change the magnitude of load effects on the other components, i.e. the influence of the component on the system reliability (or probability of system failure), on which is acting the same order of quasi-static component as static or dynamic component, can be overwhelmed by the other components of which static and dynamic load effects are greater than the quasi-static component and has higher probability of failing after one or more components have failed.

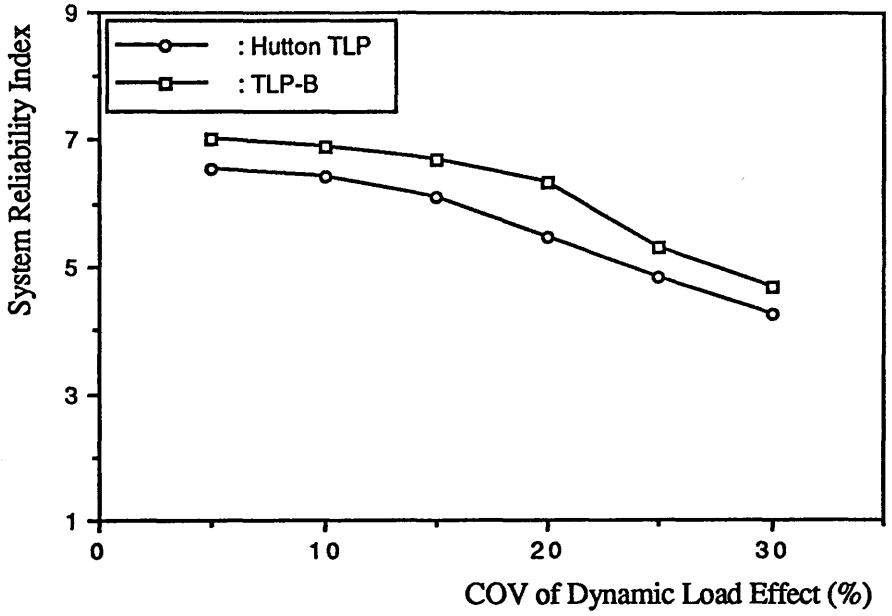

Fig. 6.27 β_{sys} vs COV of Dynamic Load Effect

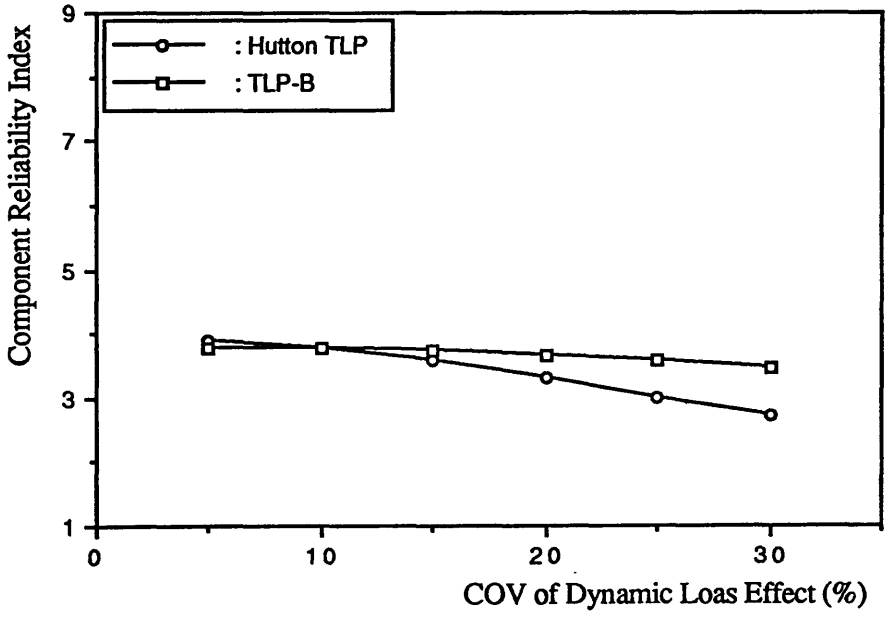

Fig. 6.28 β_{comp} vs COV of Dynamic Load Effect

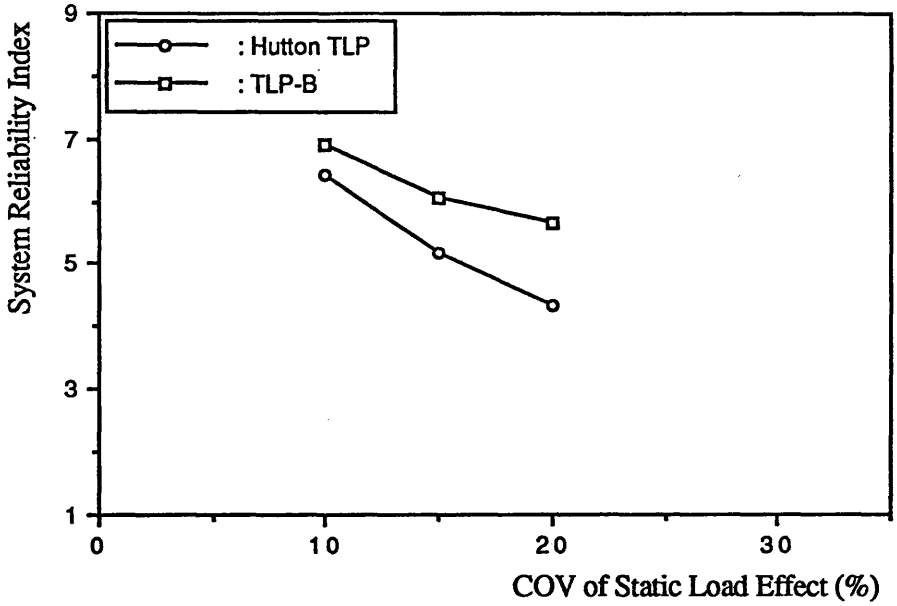

Fig. 6.29 β_{sys} vs COV of Static Load Effect

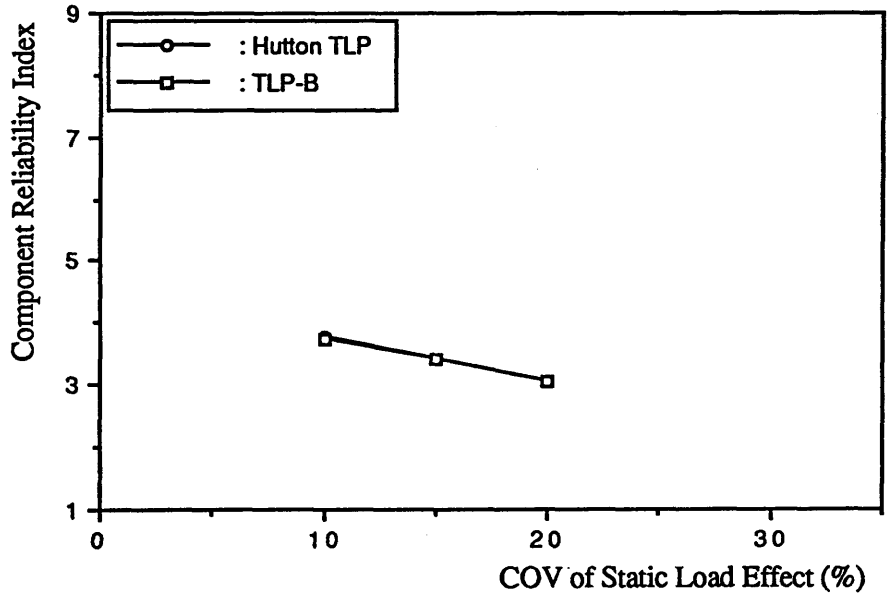

Fig. 6.30 β_{comp} vs COV of Static Load Effect

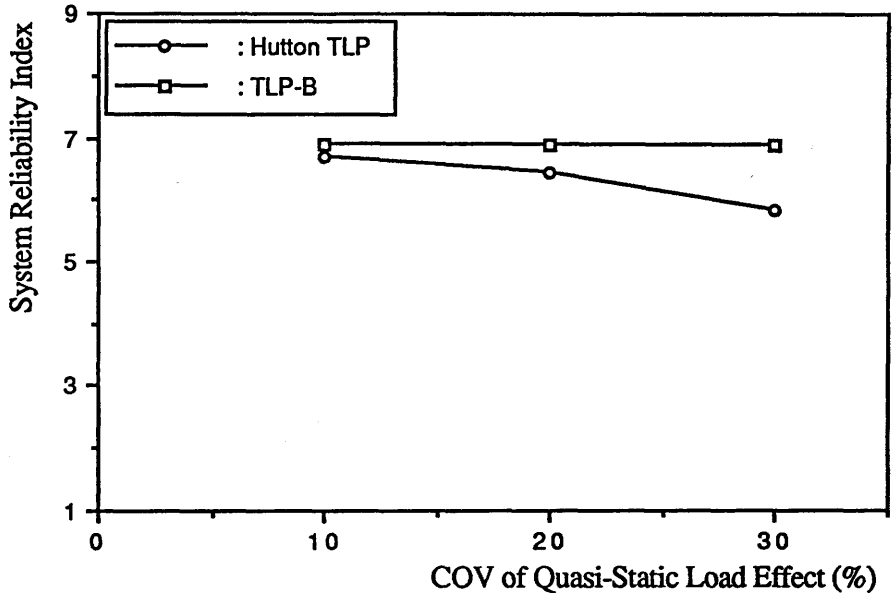

Fig. 6.31 β_{sys} vs COV of Quasi-Static Load Effect

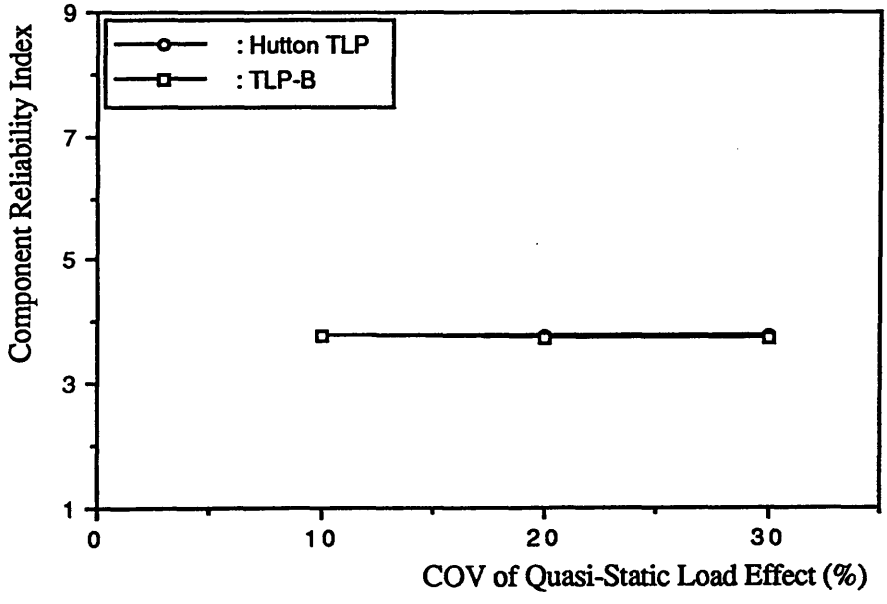

Fig. 6.32 β_{comp} vs COV of Quasi-Static Load Effect

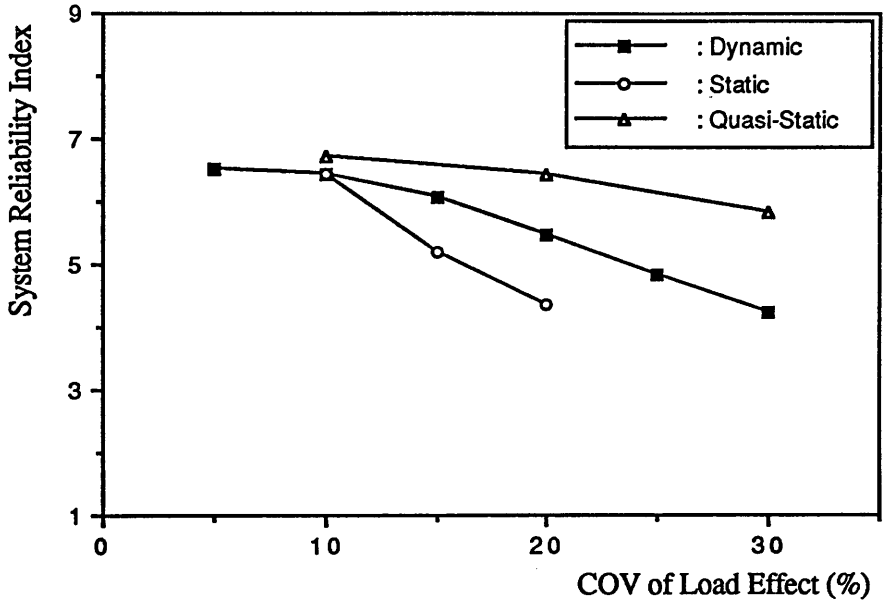

Fig. 6.33 β_{sys} vs COV of Load Effects : Hutton TLP

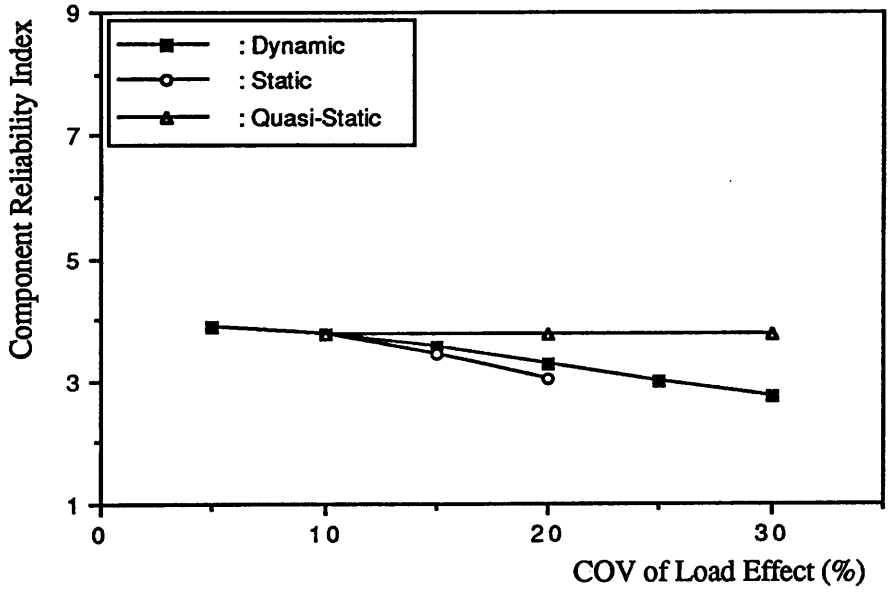

Fig. 6.34 β_{comp} vs COV of Load Effects : Hutton TLP

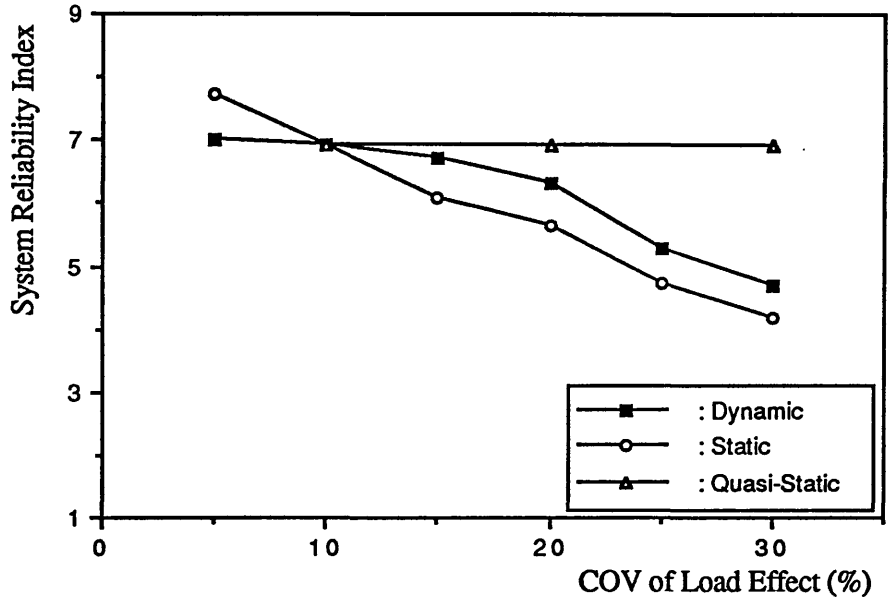

Fig. 6.35 β_{sys} vs COV of Load Effects : TLP-B

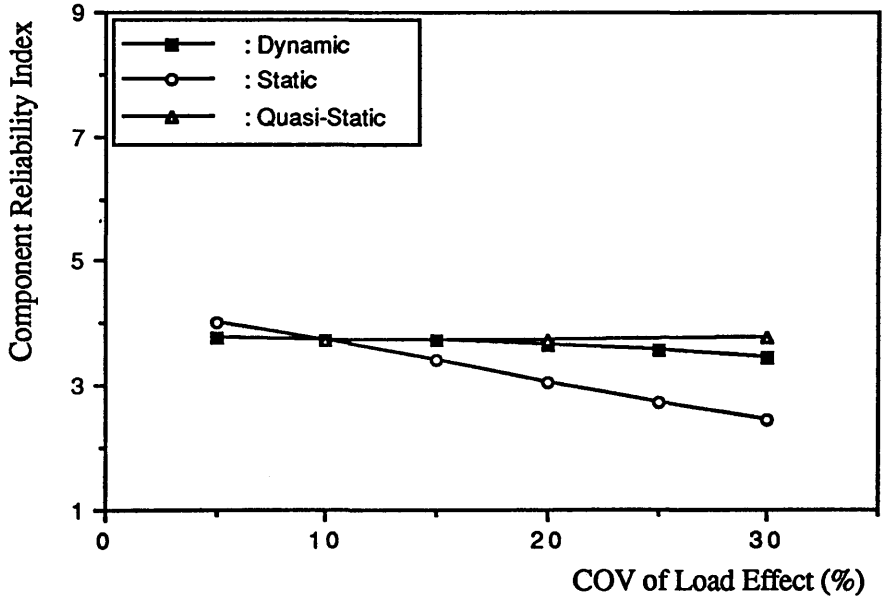

Fig. 6.36 β_{comp} vs COV of Load Effects : TLP-B

6.4 Influence of Post-Ultimate Behaviour

It has been well recognised that the post-ultimate behaviour after failure of any component can greatly influence the load effects re-distribution of survival components and the structural stiffness. It also affects the residual strength of a structural system. The non-linearity of a failed component is usually modelled as a two-state behaviour as in Fig. 6.37(a). At present there is no adequate algorithm which is able to accurately include this non-linearity in sufficient generality in the system reliability analysis.

Corotis et. al.[27,28,74] proposed the load (or load effect) space formulation to evaluate the system safety of frame structure through non-linear structural analysis in which the incremental load method was used to evaluate the system resistance. A load space approach was adopted to obtain the failure probability by numerical integration. Hohenbichler and Rackwitz[152] proposed the imposed deformation approach. Bennett[78] proposed the method based on the imposed deformation approach and the stable configuration approach[77]. These have allowed the reliability of a more general structure to be evaluated. However, these approaches have limitations to be applied to the practical structures. The method proposed by Corotis et al requires the non-linear structural analysis and the method by Bennett finds the stable configuration of a structure (survival modes) rather than failure modes. The structural analysis usually takes a great portion of computational time in system reliability analysis, two approaches may not be suitable for a large and complex practical structure such as fixed and floating platforms.

As described in Chapter 1, the simple two-state model in Fig. 6.37(a) give a reasonable solution in some cases, but in solving most structural problems a better post-ultimate (or post-failure) behaviour is required. For this purpose the incremental load method is adequate because it can more realistically allow for the post-ultimate behaviour than the element replacement method [see Table 1.1].

Moses and Rashed[66] used a two-state model with no residual strength which

could represent the work softening. Melchers et al[72,73] used a three state model [see Fig.6.44] which could represent the work softening and work hardening after component failure. Both used a plane truss structure in which only axial load effects in members were considered using the incremental load method. When load effects are combined it must be a very complicated problem to involve the post-ultimate behaviour in system reliability analysis of real structures with a more realistic post-ultimate behaviour model.

6.4.1 Simplified Model of Non-Linear Behaviour

6.4.1.1 Three-State model

In this study, use is made of the idea using the concept of mean load factor that can be obtained when structural failure has progressed up to any particular failure stage to predict the strain state and the stiffness of an element which contains a failed component.

The three-state model, shown in Fig. 6.38(a), is employed to account for the post-ultimate behaviour in system reliability analysis. In Fig. 6.38(a) σ' and ε' are the stress and strain normalised by the ultimate state (ε_u), i.e. $\varepsilon' = \varepsilon / \varepsilon_u$ and $\sigma' = \sigma / \sigma_u$ in which σ and ε is the actual stress and strain. Hence, at point A, $(\varepsilon', \sigma')_A = (1.0, 1.0)$. $E' = E_T / E$ represents the post-ultimate slope (non-dimensional) which is related to the work softening (or work hardening) tangential stiffness. η is the residual strength parameter which is the ratio of residual strength to the ultimate strength. In modelling component load end-shortening the following assumptions are adopted:

[1] A three-state model is assumed to represent the load end-shortening behaviour, as Fig. 6.38 (a): when an element is in the intact state the behaviour is assumed to be elastic (line OA). ; when one or both nodes of a finite element fail, they are assumed to follow the line AB.; beyond B, zero stiffness is assumed with residual strength represented by the parameter, η.

[2] Axial load effect is assumed to be dominant and the same behaviour is assumed for all actions (in the normalised form by their ultimate state), e.g., for bending action its behaviour is the same as that for axial action by replacing ε' and σ' by the associated bending moment and the associated curvature.

[3] The behaviour of the critical portion of the cross-section is assumed to represent

the behaviour of the whole cross-section.

When E' and η are given, the coordinate of point B in Fig. 6.38 (a) are:

$$(\varepsilon', \sigma')_B = \left(\frac{\eta - 1}{E'} + 1, \eta\right) \tag{6.2}$$

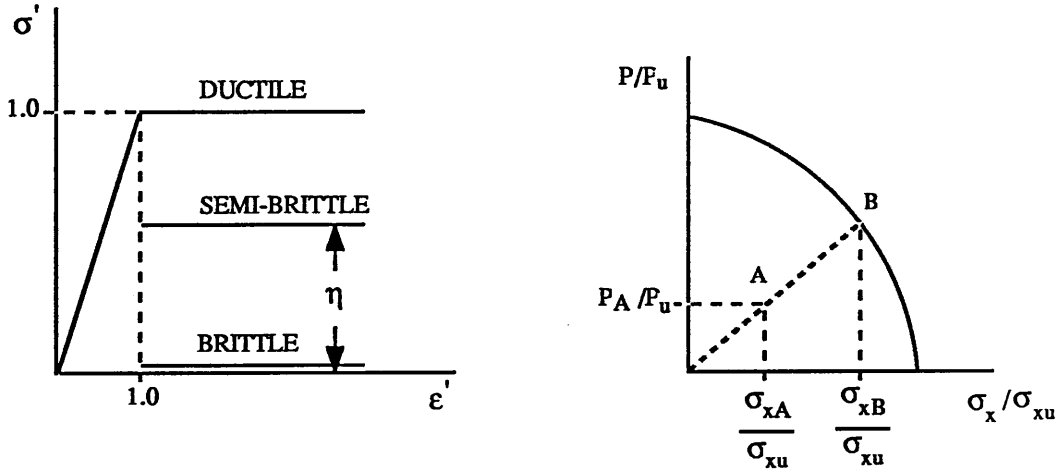

(a) Non-dimensional Stress=Strain Curve (b) Failure Surface

Fig. 6.37 Two-State Model for Non-linear Behaviour

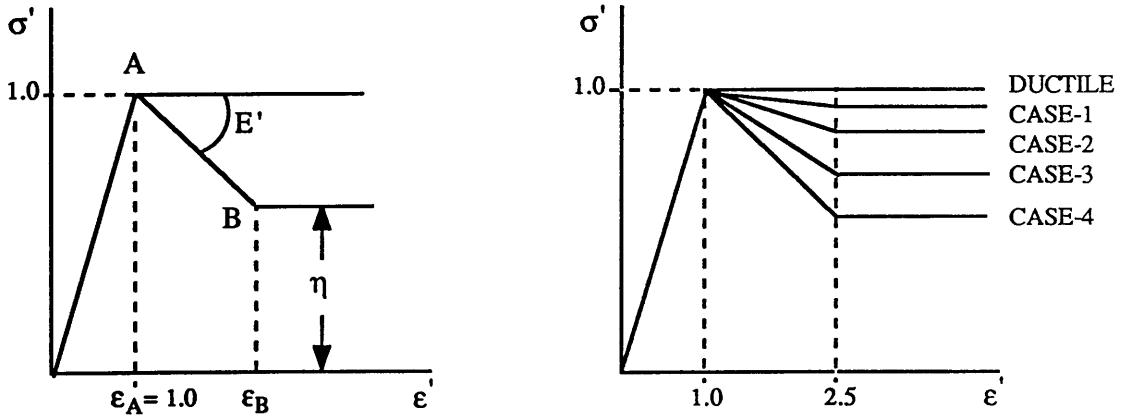

(a) Non-dimensional Stress-Strain Curve (b) Non-dimensional Stress-Strain Curves for Case Study

Fig. 6.38 Three-State Model for Non-linear Behaviour

6.4.1.2 Two-State model

When using the simple two-state model shown in Fig. 6.37 (a), the equivalent nodal forces (or artificial nodal forces) due to the unloading process of a failed component of which post-ultimate behaviour is not ductile, i.e. semi-ductile or ductile ($\eta < 1.0$) act as external forces. Calculation of the equivalent nodal force can be obtained with the strength formula used in system reliability analysis. The calculating procedure suggested herein is similar to that proposed by Murotsu et al[13,69]. The equivalent force vector can be given as the following equations:

[1] when node i in any particular element fails [see Fig. 2.5]

$$\{f_i\}_{eq} = \frac{R_i [k_o] \{a\}}{\{a\}^T [k_o] \{a\}} \tag{6.3.a}$$

where $\{f_i\}_{eq}$ is the equivalent force vector acting on the node i of the element. the force acting on node j is naturally zero, i.e. $\{f_j\}_{eq} = \{0\}$ and hence the force vector action on the element is $\{f\}_{eq} = [\,[f_i]_{eq}\,[0]\,]^T$.

[2] when both nodes, i and j, fail

$$\{f\}_{eq} = [H]^T [G]^{-1} \begin{Bmatrix} R_i \\ R_j \end{Bmatrix} \tag{6.3.b}$$

where $\{f\}_{eq}$ is the equivalent force vector acting on nodes i and j of the element. In the above equations R_i and R_j are the reference strength of a component considered, {a} is the flow vector given by Eqs.(2.106) and (2.107), and [H] and [G] are given below Eq.(2.109).

The equivalent forces given as Eq.(6.3) are equivalent to the forces against which the associated element resists. Therefore, the artificial nodal force actually applied on the

nodal points is obtained by multiplying the residual strength parameter, η, as a fraction of the ultimate strength of the element[39]:

$$\text{Applied Artificial Nodal Force} = (1-\eta) \times \{f\}_{eq} \qquad (6.4)$$

In the present approach, because the strength formula (interaction equation) is directly used to obtain the utilisation ratio and hence, to obtain the resistance coefficient and loading coefficient, the artificial force vector can be calculated with the given strength formula. For illustration, Fig. 6.37(b) shows the two dimensional failure surface. The force corresponding to point A in Fig. 6.37(b) acting on any failed component is proportionally increased until point A reaches point B. This approach is based on the assumption that the forces are proportionally increased until the limit state is reached. After then, the artificial forces are applied in the worst direction by checking the magnitude of the force vector of each type of loading. The artificial force vector to be applied is obtained from Eq.(6.4) in the usual way.

The load effects due to this artificial force vector are calculated, and then from the interaction equation used in the analysis, the elements of the unloading matrix, [B] in Eq.(2.73) for other survival components are calculated, of which elements also represent the utilised strength of survival components.

6.4.2 Application to TLP

In practice the value of E' and η of an element will depend on the geometric and material properties, e.g. R/t, s/t, etc in the case of a cylindrical component, stiffener spacing, yield stress, etc., on the initial imperfections due to welding, such as initial stress and deflection and on the component types, i.e. the ring-stiffened cylinder, the ring- and stringer-stiffened cylinder or the rectangular box-girder. When the two-state model [Fig. 6.37 (a)] is used, it is usually assumed that no other component fails during the unloading process. When the multi-state model [more than two states as Fig. 6.38 (a)] is used, this assumption is eliminated. But the failure tree increases both in depth (i.e. more events in a failure mode) and in width (i.e. a broader tree).

In this study TLP-B is chosen to investigate the effect of the post-ultimate behaviour on the system safety. Four cases of behaviour, as shown in Fig. 6.38(b), have been carried out. Values of their E' and η are listed in Table 6.4.

For illustration, the results when χ = 0 deg, are also summarised in Table 6.4 with the result of ductile behaviour. As it is expected, the system reliability indices of Case 1 to Case 4 are been reduced by about 8%, 12%, 31% and 38%, respectively, compared with that of the ductile behaviour. Even Case 1 which is very close to ductile behaviour (E' = -0.05, η = 0.925) shows a significant reduction of β_{sys}. This may be due to the combined effect of E' and η. The post-ultimate slope, E', may give the effect of reducing the structural stiffness as well as load effect re-distribution of survival components and η may give the effect of load re-distribution.

The post-ultimate behaviour can affect the residual strength of a structural system. When Component 48 which is located at the bottom bay of Column 2 [see Fig. 5.7] has failed, of which reliability index (β_{comp}) was 3.14 [see Table 5.32], the consequence of the component failure can be assessed by using the β-measure of residual strength, RDI_β, given by Eq.(2.13). For example, when component behaviour follows the behaviour of Case 4, the lowest path reliability index is $\beta_{path} \cong 4.21$. From Eq.(2.13) RDI_β is (4.21 - 3.14) / 4.16 $\cong$ 0.25 and this value is more than 50% less than that of the ductile behaviour of which RDI_β was 0.54 [see the 1st row in Table 5.32], i.e. system residual strength of Case 4 has been very much reduced. For Cases 1 to 3 β-measure is:

RDI_β = 0.49 for Case 1 $\qquad$ RDI_β = 0.33 for Case 3

RDI_β = 0.47 for Case 2

These values of RDI_β imply that the post-ultimate behaviour of failed components give much influence upon the residual strength of the structural system. β_{sys} in Table 6.4 (the 3rd column) is plotted against the residual strength parameter, as shown in Fig. 6.40. In the figure β_{sys} when χ = 45 and 90 deg. and the total average β_{sys} are also included. For the behaviour of Cases 1 to 4, the total average β_{sys} is decreased by about 12%, 18%, 32% and 40%, respectively, compared with that of the ductile system.

When using the two-state model in Fig.6.37(a) the results for the semi-brittle system Cases 1 to 4 in Table 6.4 are also summarised in the same table when $\chi = 0$ deg. β_{sys} of the system with the two-state model is always less than that of the system with the three-state model. Fig. 6.41 show the relation between β_{sys} and η in which the results when $\chi = 45$ and 90 deg and the total average β_{sys} are also included. Results for three more cases when $\eta = 0.40$, 0.225 and 0.0 are included in the same figure to more extensively show the effect of the components residual strength. When Component 48 has failed, the β-measures of semi-brittle systems with the two-state model are:

$RDI_\beta = 0.43$ for Case 1 $\qquad$ $RDI_\beta = 0.05$ for Case 3

$RDI_\beta = 0.25$ for Case 2 $\qquad$ $RDI_\beta = 0.00$ for Case 4

which are less than those with the three-state model. For TLP-B, when cylindrical components follow the bahaviour of Case 4, there is no residual strength, i.e. the failure of Component 48 results in the failure of the entire structure.

The total average β_{sys} is re-drawn against η in Fig. 6.42. It can be seen that when the residual strength parameter is less than about 0.5, the change of β_{sys} to the parameter is negligibly small and its effect becomes significant as the parameter is closer to unity.

Table 6.4 Case Study of the Semi-brittle Systems

case	(E' , η)	β sys (χ = 0 deg.)	
		three-state model	two-state model
ductile	(0.0 , 1.0)	6.77	6.77
SM* - case 1	(-0.05,0.925)	6.20	5.51
SM* - case 2	(-0.10, 0.85)	5.93	4.19
SM* - case 3	(-0.20, 0.70)	4.66	3.30
SM* - case 4	(-0.30, 0.55)	4.21	3.14

SM* : semi-brittle system

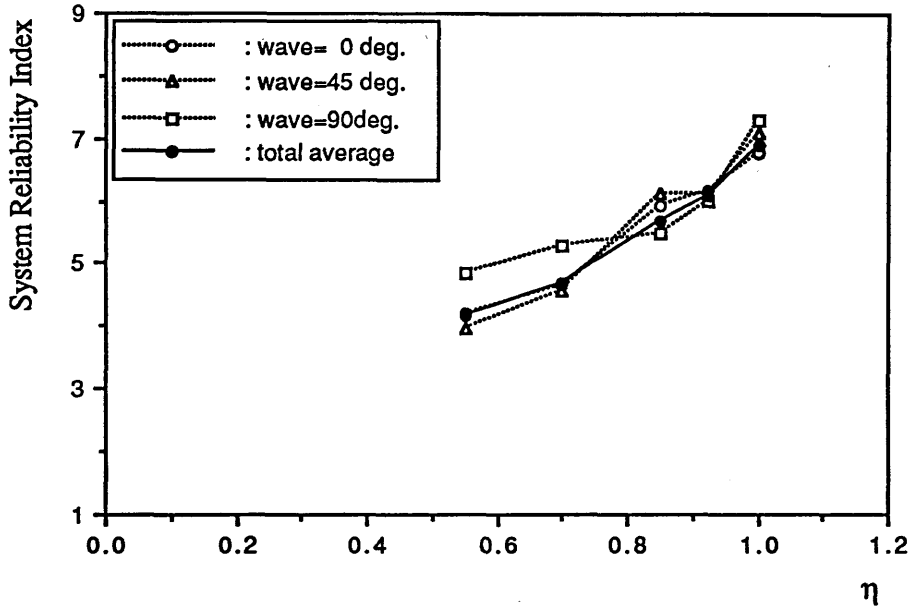

Fig. 6. 40 β_{sys} of TLP-B by Three-State Model : β_{sys} vs η

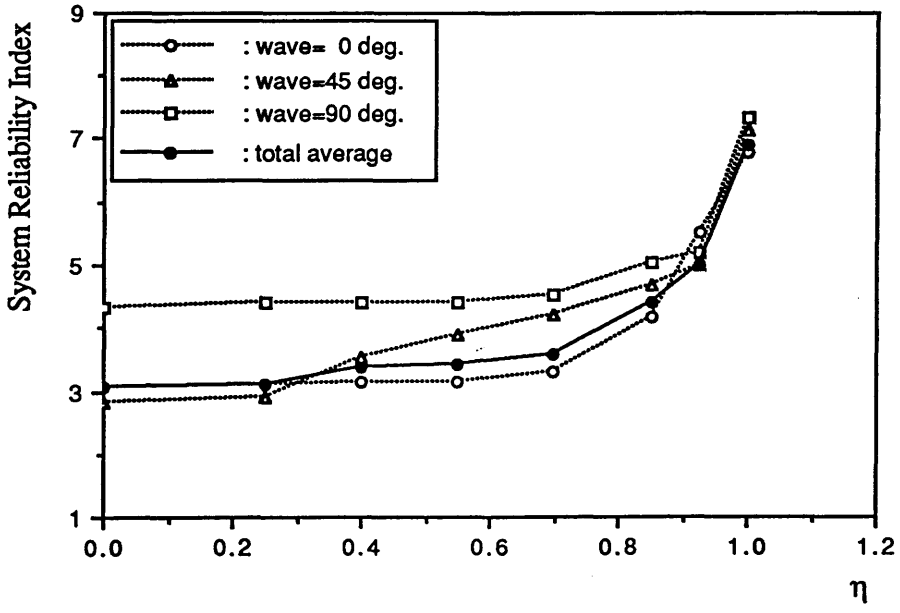

Fig. 6. 41 β_{sys} of TLP-B by Two-State Model : β_{sys} vs η

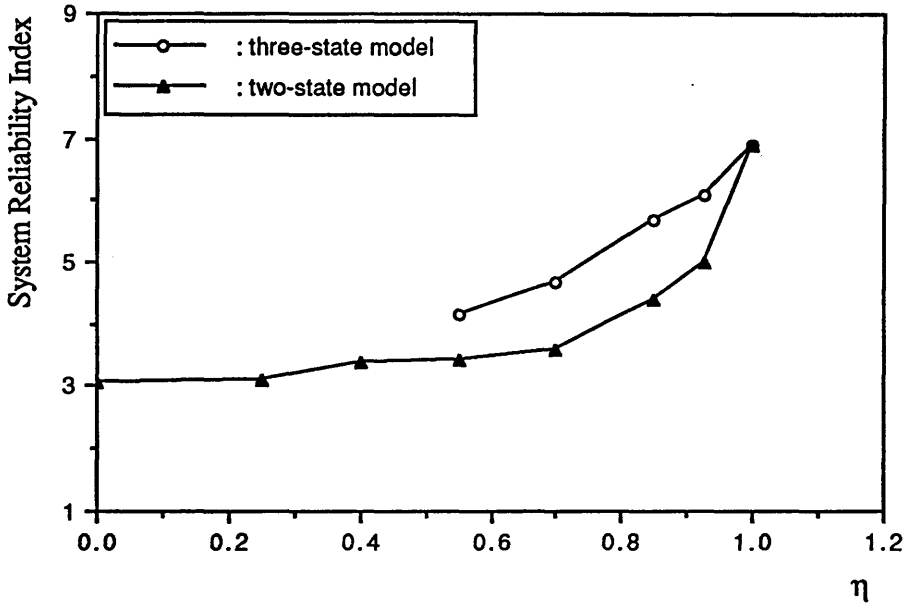

Fig. 6. 42 Comparison of β_{sys} of TLP-B by Two- and Three-State Model : β_{sys} vs η

To illustrate the change of β_{sys} to the post-ultimate behaviour for a discrete structure the plane truss structure shown in Fig. 6.43 by Melchers and Tang[72] is selected. They used the three-state model in Fig. 6.43 (b) for the non-linear behaviour of a member. Their results are illustrated in Table 6.6 using the present notations.

Case 3 is ductile behaviour and Case 10 brittle behaviour. The difference between two extreme cases is about 18%. The truss structure shows less change of β_{sys} to η and the post-ultimate slope than the present TLP model.

As an another example of discrete structure, the two-dimensional tower model (fixed platform model) of Chan and Melchers[73] is selected, as shown in Fig. 6.45. The model was modified from the spatial truss tower studied by Bjerager[214]. They assumed that the member behaviour was described by the two-state model [Fig. 6.37(a)] and the wave was a sinusoidal pattern of which the length was 350 m. The wave height

was the only uncertain parameter. They carried out a system reliability analysis for the model by varying the wave position relative to the structure [designated θ in Fig. 6.45]. Table 6.7 shows their results [refer to the reference for numerical data about wave loads and member resistance]. It is evident that the unloading effect of a non-ductile system is significant for this structure in such a way that from ductile system to brittle system, bounds of β_{sys} is lowered by about 32% and 40%.

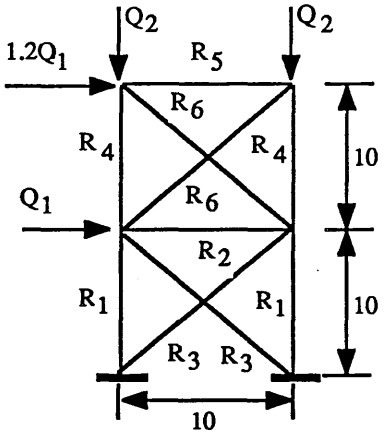

$\underline{R}_1 = 60$, $\underline{R}_2 = 6$, $\underline{R}_3 = 32$, $\underline{R}_4 = 14$, $\underline{R}_5 = 10$, $\underline{R}_6 = 20$
$\underline{Q}_6 = 12$, $\underline{Q}_6 = 4$ $V_R = 0.15$, $V_{Q_1} = 0.3$ $V_{Q_2} = 0.2$

Fig. 6.43 Two-degree Redundant Truss[72]

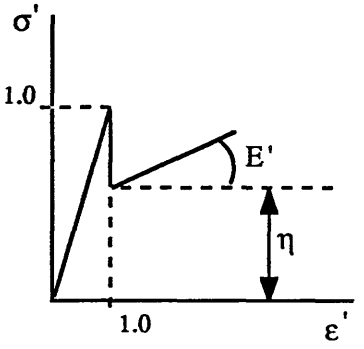

Fig. 6.44 Post-Ultimate Behaviour Model of Melchers[72]

Table 6.6 System Bounds for Non-linear Members of Truss Model[72].

case	E'	η	bounds for β_{sys}	case	E'	η	bounds for β_{sys}
1	0.2	1.0	3.78 - 3.83	6	0.1	0.75	3.31 - 3.37
2	0.1	1.0	3.66 - 3.76	7	0.0	0.75	2.65 - 2.73
3	0.0	1.0	3.08 - 3.10	8	-0.1	0.75	2.50 - 2.62
4	-0.1	1.0	2.92 - 2.99	9	0.0	0.5	2.53 - 2.55
5	-0.2	1.0	2.74 - 2.81	10	0.0	0.0	2.54 - 2.54

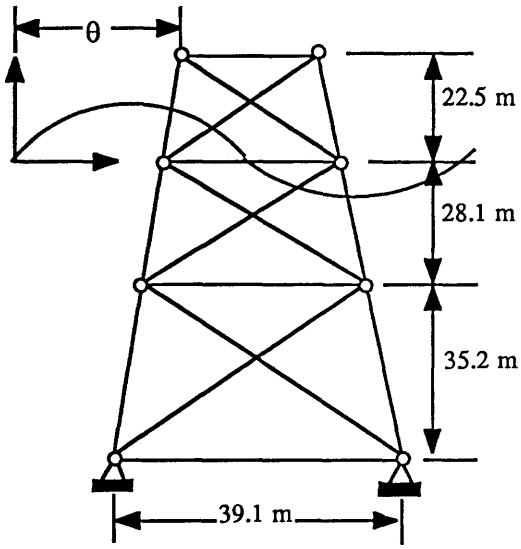

Fig. 6.45 Two-dimensional Truss Tower

Table 6.7 Bounds of β_{sys} : Truss Tower [73]

η	Bounds of β_{sys}	
1.0	1.49	1.47
0.9	1.14	1.00
0.75	1.05	0.86
0.5	1.03	0.86
0.0	1.02	0.88

From the results of the present study and others, it was shown that changing the component behaviour from ductile to semi-brittle or brittle has a significant effect on the structural system reliability and residual strength of the TLP. The significant influence of the post-ultimate behaviour on system safety can also be seen from the works about discrete structures as illustrated.

At present there are no similar result for continuous structures. But the present findings confirm that the post-ultimate behaviour of failed components give much influence upon the system safety and upon residual strength of a structural system, continuous or discrete, and should be taken into account in assessing the system safety. This implies the necessity and the importance of realistic component behaviour modelling.

6.5 Discussion

In this Chapter a sensitivity study for TLP structural systems has been

investigated by placing emphasis on investigating the influence of stochastic parameters of the important design variables in strength and loading, say mean and COV, on system safety as well as component safety: the strength modelling parameter (X_M), geometric properties (R and t of cylindrical component), material property (σ_Y) and load effects. The post-ultimate behaviour of failed components on system safety level has also been investigated.

The strength modelling parameter (or error), X_M represented by its mean bias, $\underline{X}_M$ and the coefficient of variation (modelling uncertainty), V_{X_M} was found to have much influence on the system reliability and the component reliability (β_{sys} and β_{comp}). The main reason for this is due to its important position within the safety margin equation (2.103) and, hence, its effect upon strength and safety. It was shown that the modelling uncertainty (V_{X_M}) is much more influential not only on the system reliability but also on the component reliability than the mean bias ($\underline{X}_M$).

Apart from the effect of the strength modelling parameter on β_{sys} and β_{comp} the modified safety margin equation given as Eq.(2.103) can flexibly allow the different strength models in system reliability assessment. In the extreme case, when any particular strength model has been developed based on the lower bound of strength, $\underline{X}_M$ naturally becomes much greater than unity [mean bias is the ratio of actual strength to predicted strength, see Eq.(2.97)]. Hence, the failure surface is much shifted away from the original one [see Fig. 2.4] and, consequently, a higher β_{sys} and β_{comp} can be obtained under the same load effects. In the opposite extreme case vice versa. But as seen from the results in Section 6.2.1, when V_{X_M} has a low value, say, less than about 7.5%, there is no change of β_{sys} to $\underline{X}_M$. As recommended in references [119] and [163], in order to achieve the economic benefit in the design V_{X_M} should, therefore, be kept as low as possible with the mean bias being kept close to unity from both the systems side and from the components side.

From the results in Section 6.2.2, it was found that R and t were more influential on resistance and safety than σ_Y. But, as described there, this may be due to the fact that

since the same COV values were given for R and t, their effect on strength and safety was perhaps more reflected in the form of combined action than the effect of COV of σ_Y. β_{comp} was shown to be less sensitive to change in COV's of R and t than β_{sys}.

With regard to the influence of three types of load effects on safety, say, static, dynamic and quasi-static load effects, from the results in Section 6.3 it was shown that static load effect (both its mean bias and COV) was most influential on the system reliability index as well as component reliability index followed by the dynamic load effect. Quasi-static component was found to be relatively less influential than the other two components. This may be due to the greater magnitude of static and dynamic component acting on components than the magnitude of quasi-static component. Neglecting the wave drifting induced force may be another reason. But it may not have much influence on safety. Considering that, in practice, dynamic component the more degree of uncertainty than static component, dynamic component can have more influence upon safety than static component. This implies that COVs of load effects must be an important factor. The effect of quasi-static component on β_{sys} seemed to be overwhelmed by static and dynamic components from the system's point of view although quasi-static load effect of any particular component can be greater than static or dynamic load effects.

As is expected, the post-ultimate behaviour of failed components, which was characterised by post-ultimate slope (E') and residual strength (η), very much affects the safety level and residual strength of a structural system. It may have more influence on the safety of a structural system than the strength modelling parameter and loading variables. It can, therefore, be said that the post-ultimate behaviour of failed components should be accounted for in assessing the system safety and residual strength with a more refined and realistic model.

Residual strength of a structural system depends on several factors, such as non-linear behaviour of a component, especially the post-ultimate behaviour, structural configuration, loading types acting on a structure, etc. Component behaviour itself

depends on factors such as component type, type of loading acting on a component, component strength, etc. With regard to its effects on safety of structures with different component types, from the test experiences, the ring- and stringer-stiffened cylinder shows closer to the ductile behaviour and less sensitive to the initial imperfections than the ring stiffened cylinder. The behaviour of the stringer-stiffened cylinder may be modelled as the three-state model [Fig. 6.38(a)], whereas the behaviour of ring-stiffened cylinder (and unstiffened cylinder) may be modelled as the two-state model [Fig. 6.37(a)] or Melchers' model [Fig. 6.44]. Therefore, the actual TLP structure will be expected to be more efficient and reliable when using the ring- and stringer-stiffened cylinder rather than the ring-stiffened cylinder from the system's point of view.

As far as the present sensitivity results are concerned, because of the influence of resistance variables upon the safety, β_{sys} as well as β_{comp}, the strength modelling parameter is an important resistance variable affecting the system resistance and, consequently, the safety level. This is mainly due to its position within the safety margin [Eq.(2.103)] as mentioned before. Its effect was shown to be greater than those of geometric and material properties. The modelling uncertainty, V_{X_M}, rather than the mean bias, X_M, is more influential on both β_{sys} and β_{comp}.

The post-ultimate behaviour seems to be more influential and important than the strength modelling parameter from the systems side. It must be the most important resistance variable and a key factor to determine the residual strength of a structural system. Hence, it should be considered in the analysis using a more refined and realistic model and a more extensive study, including model and/or full scale test about this area, is required. Loading variables have a great influence on the reliability because of the uncertainties with these variables. From this point it can be drawn that dynamic load effect may be most influential.

The sensitivity study shown in this chapter is useful in assessing the parameters perturbation effects on the component and system reliability index, and the results, such as the relation of the reliability index to variables and sensitivity factors, can provide

useful information about the relative importance of design variables in the context of reliability-based design. Finally, in order to provide the designer with a useful criteria or information as an aid to decision making in the design stage, it can be recommended that certain type of sensitivity studies, as illustrated in this chapter, must be useful to intelligently modify the structural design.

CHAPTER 7 RELIABILITY-BASED DESIGN

7.1 Design Code Format

In reliability-based design we seek to obtain uniform or consistent reliabilities over the range of potential utilisation. In conventional design practice there is a single safety factor in the safety check equation whereas, on the basis of the Level II reliability approach it is possible to derive partial safety factors (PSFs) for use in safety check equations. This provides the basis of the Level I method for use in design which makes little, if any, reference to statistical properties beyond those necessary for defining the more important variables such as nominal yield stress etc. This safety checking format with PSFs can allow for flexibility since they can reflect the overall uncertainties in loading and strength as well as the overall target reliability index.

In its simplest form the safety check equation can be written as:

$$\sum_i \gamma_{f_i} Q_{k_i} \leq \frac{R_k}{\gamma_m \gamma_c} \tag{7.1}$$

which essentially relate nominal or characteristic values of extreme load effects Q_k and ultimate strength, R_k, of the structural component. The γ's are the partial safety factors which reflect the uncertainties in load, γ_{f_i}, in as built strength, γ_m, and also the nature of the structure and the seriousness of the consequences of failure, γ_c, which is linked to socio-economic factors.

API Recommended Practice which dominates the design of offshore platforms in the U.S. uses the Load and Resistance Factor Design (LRFD) format[110]. In this format a safety check equation is of the form:

$$\sum_{k} \gamma_k Q_k \leq \phi_{sys} \phi_i R_i \qquad (7.2)$$

where R_i is the nominal strength, Q_k the nominal loading, ϕ_i respective strength factor of the nominal loading and γ_k load factor. System factor, ϕ_{sys} is also added in the partial safety equation to represent the system consequences of a component failure and would be greater than unity. However, in the present LRFD format ϕ_{sys} is taken as unity.

The actual form of safety check equation adopted by the TLP RCC in the model code for structural design of TLPs[9] is somewhat more complex than Eqs.(7.1) and (7.2) and checking for component safety is generally done with a three term interaction equation.

$$\sum_{i=1,2,3} \left\{ \frac{\gamma_s Q_{s_i} + \gamma_q Q_{q_i} + \gamma_d B Q_{d_i}}{R_{k_i} / \gamma_m \gamma_i \phi_{sys}} \right\}^{j_i} \leq 1 \qquad (7.3)$$

where subscripts s, q and d refer to static, quasi-static and dynamic load effect components and B is a systematic modelling or bias factor for the dynamic component. Subscripts i = 1, 2, and 3 refer to the equivalent or resolved axial, shear and pressure load and resistance effects, γ_s, γ_q and γ_d are partial safety factors for load effects and are greater than unity. γ_m accounts for uncertainties in the material properties, the γ_i's are modelling uncertainties for the three strength components, and j_i is an interaction exponent for each of these three strength components. ϕ_{sys} is the system factor normally less than unity but which is taken as unity for the present TLP model code. γ_c for socio-economic consequences of failure has been omitted because the more rational approach of selecting the target reliability index from a minimisation of total costs is preferred. This in turn would lead to an adjustment of all the PSFs[136].

7.2 Significance for Design

7.2.1 Redundancy Considerations

An efficient structure is one which does not fail, has adequate but not excessive safety and which minimises cost. Inevitably cost is very closely linked to safety factors (reliability index), especially in structures whose scantlings are governed by ultimate strength considerations. So aiming at the lower safety envelope of accepted past designs has considerable merit. Reliability-based design is aimed at achieving designs in which reliability is uniformly distributed. But the present component reliability-based design approach cannot always give uniform distribution of reliability over the entire structure and in some cases the design can be such that failure of any single component causes the structure to catastrophically collapse as a total system. This may be due to lack of redundancy and lack of knowledge about the re-distribution of load effects after failure of any component. These facts have perhaps stimulated the need to introduce system reliability into design.

System performance has been recognised as a part of structural design thinking. A major benefit from incorporating the system capacity into design is the additional structural reserve strength often found due to design symmetry, multiple load conditions, fabrication requirements and design approximations. These additional margins should be examined in assessing the reliability against extreme load and accident conditions.

Specifications in recent years recommend the designer to provide redundancy. Additional members can also raise the degree of structural redundancy. Hence, in the context of system reliability-based design, one should consider structural redundancy characterised as by reserve strength and residual strength.

For ultimate strength collapse a four legged jacket structure which has horizontal chords and single diagonal or K bracings is statically determinate and has very little residual strength when a bracing member is severely damaged or removed. The only source of residual strength is from secondary bending at the ends of the remaining braces

or the portal action of the vertical members. X braced systems are much more redundant and have high reserve strengths. Their residual strengths will generally also be high but this will be depend on the column slenderness of the compression braces and will be low for slender columns. Multi-leg systems will be stronger still in those planes where three or more legs occur. Then, the choice as to whether the diagonal braces are all oriented in the same direction or are opposed at their connections with the legs has to be made[36] the former generally being preferred if the worst environmental loading is likely to come from one predominant direction. If the braces are then designed to be mostly in tension then their fatigue design at node joints would be more important than if they are mostly in compression. In the latter case low column slenderness and high punching static strength at the node are desirable. Reserve strength ratios (n) in most fixed jacket structures are sometimes less than 2.0 but probably average around 2.5. A reserve strength index for well-designed floating offshore structures is recommended to be about 2.0[91].

7.2.2 Relation between Safety and Redundancy

The system factor (often called system partial safety factor), ϕ_{sys}, has close correlation with structural redundancy because the redundancy should play a major role in choosing the value of ϕ_{sys} and can represent the system consequences of a component or member failure.

As Moses[11,110] and Faulkner[8,136] stated, the system factor should perhaps be incorporated in the safety check equation and should be examined alongside the more logical (in principle) use of a system reliability index, β_{sys} , to derive all the PSFs as the best way of including safety and redundancy considerations in the design process. When using the safety check equation given as Eq.(7.2), ϕ_{sys} is normally greater than unity while, when using the safety check equation given as Eq.(7.3), ϕ_{sys} is normally less than unity which is, however, taken as unity in the present codes in use.

Faulkner[136] proposed a simple procedure of calculating the system factor, ϕ_{sys}, with the assumption that the distributions of component strength (or resistance) and lifetime load effect are normal. With this assumption the reliability index is defined in

terms of the central safety factor as Eq.(2.10).

When reliability index, β, is given, the central safety factor is obtained by solving Eq.(2.10) as:

$$\theta = f(\beta, V_R, V_Q) = \frac{1 \pm \sqrt{1 - (1 - \beta^2 V_R^2)(1 - \beta^2 V_Q^2)}}{(1 - \beta^2 V_R^2)} \tag{7.4}$$

When the sign before the root is negative, Eq.(7.4) gives a trivial solution. From Eq.(7.4) the central safety factor for component, θ_{comp}, and system, θ_{sys}, is obtained as given β_{comp} and β_{sys}:

$$\begin{aligned} \theta_{comp} &= f(\beta_{comp}, V_{R_{comp}}, V_Q) && \text{for component} \\ \theta_{sys} &= f(\beta_{sys}, V_{R_{sys}}, V_Q) && \text{for system} \end{aligned} \tag{7.5}$$

in which β_{comp} and $V_{R_{comp}}$ are component reliability index and COV of component resistance, and β_{sys} and $V_{R_{sys}}$ system reliability index and COV of system resistance. Then, assuming the mean values are characteristic values, it follows that an acceptable multiplicative resistance partial safety factor, ϕ_R, is defined by:

$$\phi_R = \frac{R^*}{\underline{R}} = 1 - \beta \alpha_R V_R \tag{7.6}$$

where R^* is the "design point" value for maximum probability of failure and α_R is the representative sensitivity parameter given as:

$$\alpha_R = \frac{\theta V_R}{\sqrt{(\theta V_R)^2 + V_Q^2}} \tag{7.7}$$

If the central safety factor for system, θ_{sys}, is defined as being n times that for a component, i.e., $\theta_{sys} = n\,\theta_{comp}$, the system reliability index, β_{sys} , can be evaluated from Eq.(2.10) with replacing θ by θ_{sys}. The representative sensitivity parameter, $\alpha_{R_{sys}}$, and resistance partial safety factor, $\phi_{R_{sys}}$, can be obtained from Eqs.(7.7) and (7.6), respectively. An approximation to the system factor, ϕ_{sys}, to use with a design based on component failure can be estimated from:

$$\phi_{sys} = \frac{\phi_{R_{sys}}}{\phi_{R_{comp}}} = \frac{1 - \beta_{sys}\alpha_{R_{sys}} V_{R_{sys}}}{1 - \beta_{comp}\alpha_{R_{comp}} V_{R_{comp}}} \tag{7.8}$$

For the ranges of n = 1.05 to 3.0 and β_{comp} = 0.1 to 5.0, when typical values of $V_Q = 0.2$ and $V_{R_{comp}} = V_{R_{sys}} = 0.15$ are assumed, Figs. 7.1 and 7.2 show the relation of β_{comp} and n to β_{sys} and ϕ_{sys}, respectively.

The total load factor, λ_T, is defined as the ratio of the system collapse load to the design load. Let F_{comp} be the ratio of a component failure load to the design load. The parameter, n, is defined as the ratio of the mean system collapse load to the mean component collapse load. Thus:

$$n = \frac{\lambda_T}{F_{comp}} \tag{7.9}$$

and n is referred to as the reserve strength ratio for system (or reserve strength factor).

Consider the case when R and Q are lognormal. Then, ln R and ln Q are normal with means, λ_R and λ_Q, and standard deviations, ζ_R and ζ_Q, given by[5,45] :

$$\lambda_R = \ln \underline{R} - \frac{1}{2}\zeta_R^2 , \qquad \lambda_Q = \ln \underline{Q} - \frac{1}{2}\zeta_Q^2$$

$$\zeta_R^2 = \ln (1 + V_R^2) , \qquad \zeta_Q^2 = \ln (1 + V_Q^2) \tag{7.10}$$

The safety margin, $Z = R - Q$, is equivalent to a non-dimensional form:

$$Z' = \frac{R}{Q} - 1 = \theta - 1 \tag{7.11}$$

where θ is the central safety factor and also a lognormal variate with parameters:

$$\lambda_\theta = \lambda_R - \lambda_Q = \ln \frac{\theta}{\left[\frac{1+V_R^2}{1+V_Q^2}\right]^{1/2}} \tag{7.12.a}$$

$$\zeta_\theta^2 = \zeta_R^2 + \zeta_Q^2 = \ln (1+V_R^2)(1+V_Q^2) \tag{7.12.b}$$

Therefore, ln θ is also normal with mean, λ_θ, and standard deviation, ζ_θ. Then, the corresponding reliability index to Eq.(7.11) is given by:

$$\beta = \frac{\lambda_\theta}{\zeta_\theta} \tag{7.13}$$

Assume the same value of V_R and V_Q for component and system as the case when R and Q are normal. Then,

$$\zeta_{\theta_{sys}} = \zeta_{\theta_{comp}} \tag{7.14.a}$$

If the central safety factor for the system, θ_{sys}, is defined as n times that for a component, θ_{comp}, as before, the parameter λ_θ for system, $\lambda_{\theta_{sys}}$, is expressed from Eq.(7.12.a) as:

$$\lambda_{\theta_{sys}} = \ln \frac{\underline{\theta}_{sys}}{\left[\frac{1+V_R^2}{1+V_Q^2}\right]^{1/2}} = \ln \frac{n\,\underline{\theta}_{comp}}{\left[\frac{1+V_R^2}{1+V_Q^2}\right]^{1/2}}$$

$$= \ln n + \lambda_{\theta_{comp}} \qquad (7.14.b)$$

With Eqs.(7.14) Eq.(7.13) gives the system reliability index as:

$$\beta_{sys} = \frac{\lambda_{\theta_{sys}}}{\zeta_{\theta_{sys}}} = \frac{\ln n + \lambda_{\theta_{comp}}}{\zeta_{\theta_{sys}}} = \frac{\ln n}{\zeta_\theta} + \beta_{comp} \qquad (7.15)$$

That is, β_{sys} is ($\ln n / \zeta_\theta$) greater than β_{comp}. Eq.(7.15) is the relation between the reserve strength for system and component and system safety. From this equation the probabilististic measure of residual strength, RDI_β, given by Eq.(2.13) can easily be derived as:

$$RDI_\beta = \frac{\ln n}{\zeta_\theta} \frac{1}{\beta_{comp}} \qquad (7.16)$$

This shows the relation between the residual strength and the reserve strength for system to component safety. RDI_β is inversely proportional to component safety index.

In order to evaluate the system factor from Eq.(7.8), ϕ_{sys}, R_{comp} and R_{sys} are assumed to have means of $\underline{\theta}_{comp}$ and $\underline{\theta}_{sys}$ and COV of V_R, and Q is assumed to have mean of unity and COV of V_Q.

For the same ranges of n and β_{comp} and with the same values of V_R and V_Q as before Figs. 7.3 and 7.4 show the relation of n and β_{comp} to β_{sys} and ϕ_{sys},

respectively. Comparing Figs. 7.3 and 7.4 with Figs. 7.1 and 7.2, it can be seen that lognormal distributions of R and Q give higher β_{sys} and especially, ϕ_{sys} than for normal distributions. Moreover ϕ_{sys} has a very different tendency from that of ϕ_{sys} for normal distributions such that ϕ_{sys} increases as β_{comp} increases with lognormal distributions, whereas it decreases when R and Q are normal. Within practical ranges of n = 1.5 to 3.0 and and β_{comp} of 2.0 to 5.0 Table 7.1 illustrates β_{sys} and ϕ_{sys} when R and Q are assumed normal and lognormal.

The above approximations have merit, because of their simplicity, that the relation of component and system safety to redundancy can easily be predicted for a structure in the initial design stage. However, the system factors should probably be determined from a more rigorous system analysis for the intact and/or a damaged model of the structure. One reflects the reserve strength, while the other the residual strength.

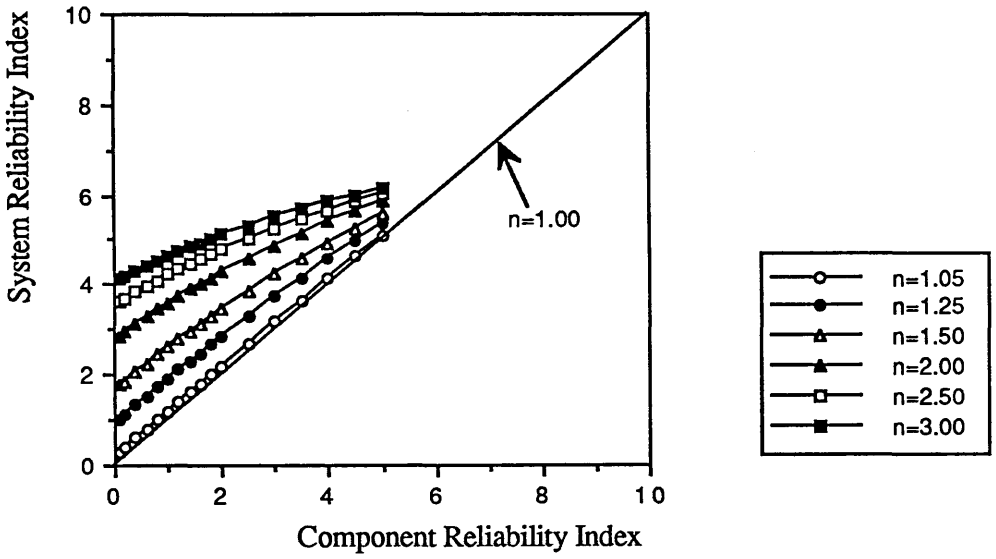

Fig. 7.1 Relation between n, β_{comp} and β_{sys} (R & Q are normal)

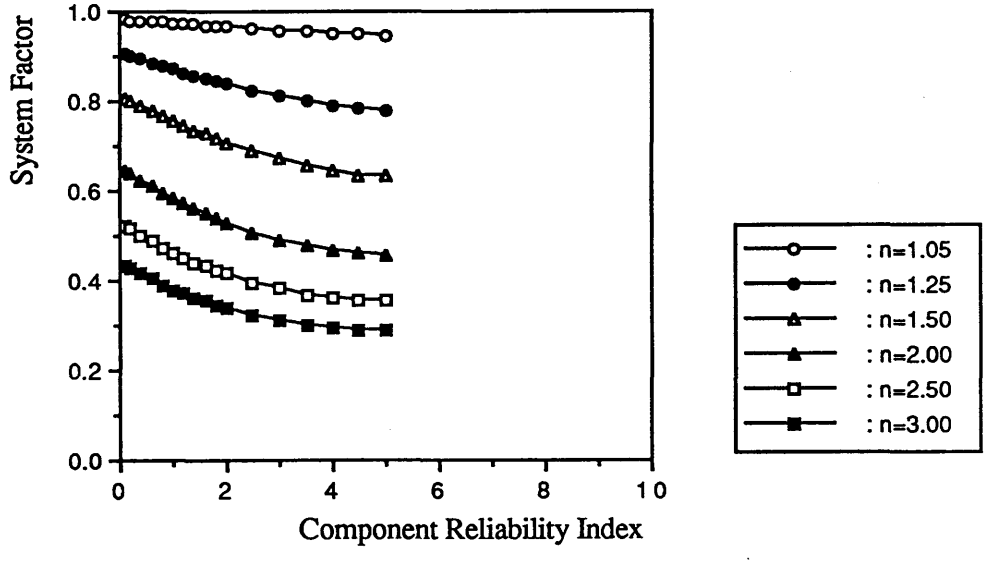

Fig. 7.2 Relation between n, β_{comp} and ϕ_{sys} (R & Q are normal)

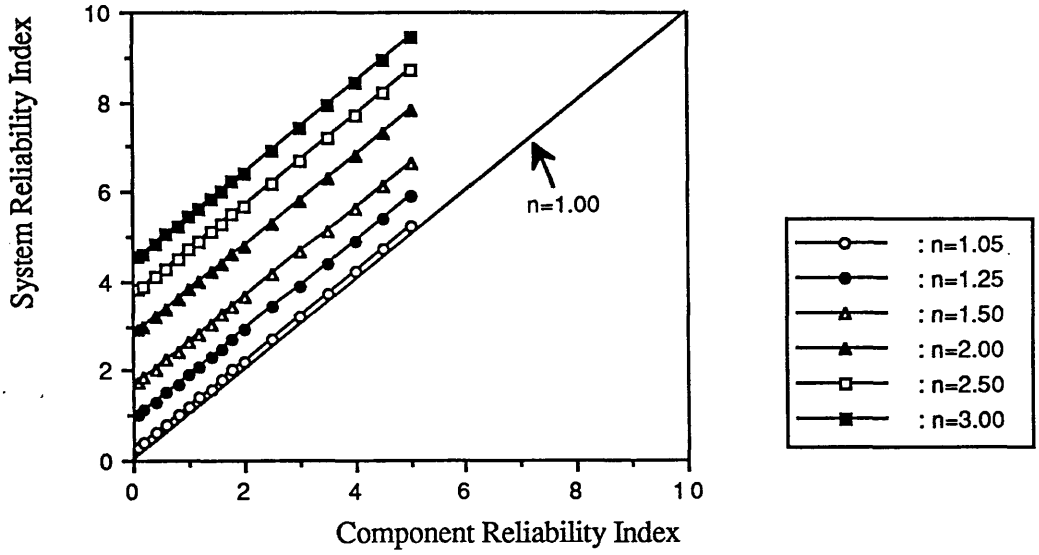

Fig. 7.3 Relation between n, β_{comp} and β_{sys} (R & Q are lognormal)

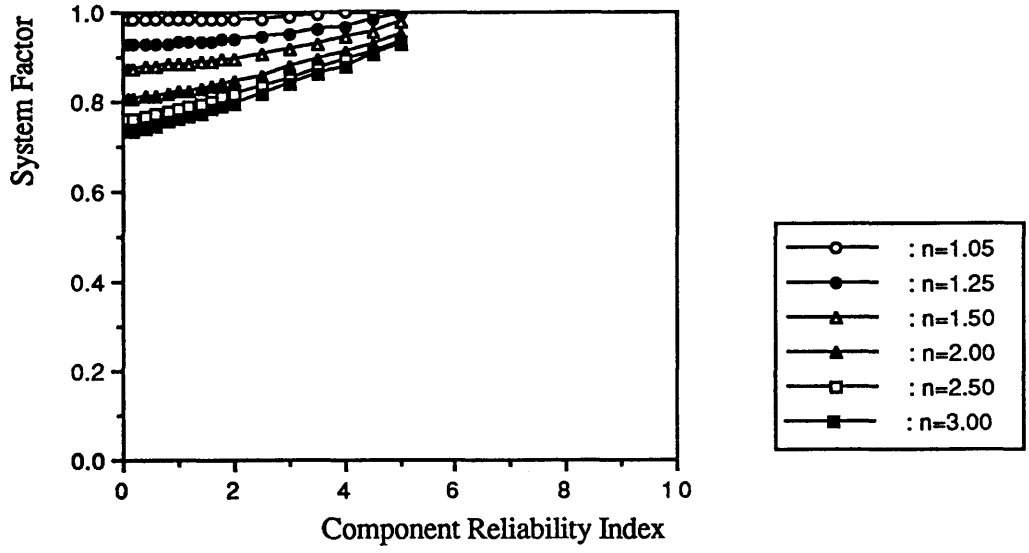

Fig. 7.4 Relation between n, β_{comp} and ϕ_{sys} (R & Q are lognormal)

Table 7.1 β_{sys} and ϕ_{sys} to β_{comp}

(1) when R and Q are normal

β_{comp}	n = 1.5		n = 2.0		n = 2.5		n = 3.0	
	β_{sys}	ϕ_{sys}	β_{sys}	ϕ_{sys}	β_{sys}	ϕ_{sys}	β_{sys}	ϕ_{sys}
2.0	3.46	0.71	4.28	0.53	4.78	0.41	5.12	0.34
2.5	3.86	0.69	4.59	0.51	5.03	0.40	5.32	0.32
3.0	4.23	0.67	4.87	0.49	5.25	0.38	5.51	0.31
3.5	4.58	0.66	5.14	0.48	5.46	0.37	5.68	0.30
4.0	4.93	0.64	5.39	0.47	5.66	0.36	5.84	0.29
4.5	5.26	0.64	5.64	0.46	5.86	0.36	6.00	0.29
5.0	5.59	0.63	5.88	0.46	6.04	0.36	6.15	0.29

(2) when R and Q are lognormal

β_{comp}	n = 1.5		n = 2.0		n = 2.5		n = 3.0	
	β_{sys}	ϕ_{sys}	β_{sys}	ϕ_{sys}	β_{sys}	ϕ_{sys}	β_{sys}	ϕ_{sys}
2.0	3.64	0.89	4.80	0.84	5.70	0.82	6.43	0.80
2.5	4.14	0.90	5.30	0.86	6.20	0.83	6.93	0.82
3.0	4.64	0.92	5.80	0.88	6.70	0.85	7.43	0.84
3.5	5.14	0.93	6.30	0.89	7.20	0.87	7.93	0.86
4.0	5.64	0.94	6.80	0.91	7.70	0.89	8.43	0.88
4.5	6.14	0.96	7.30	0.93	8.20	0.91	8.93	0.90
5.0	6.64	0.98	7.80	0.95	8.70	0.94	9.43	0.93

7.2.3 Acceptable Safety Levels

In design we should recognise that rational safety levels must pay some regard to the definition of safety as applied in judicial proceedings. This pertains to collapse of the overall structural system when the economic and human consequences become significant. Nevertheless by tradition and for convenience, specifications have to be prepared which deal with components, beams, columns, connections and so on. Recognising also that formal prescribed notional safety has very little if any correlation with actuarial safety for most structures the way would seem open to:

(a) Progressively lower component notional safety levels, especially as our knowledge of loading and response steadily improves.

(b) Introduce system safety in design on a consistent basis which recognises the hierarchical type of structure and components being considered, the degree of residual strength and reserve strength present, and a start should now be made to formalise in design codes.

(c) Develop a rational relation between component and system safety. A non-redundant structure would need a higher safety margin than a redundant one to achieve the same acceptable level of damage tolerance.

Of course it will always be important to ensure that with the lowering of component safety the probability of fatigue or overload damage in service is kept to an acceptable level mainly to reduce the need for repair costs. Nevertheless, from (a) there could be significant scope for cost and weight savings.

If one examines present practice, Table 7.2 attempts to give the present relation between average component safety indices and reserve strength ratio, n, beyond first component failure for a variety of steel structures[19]., in which the present three TLPs are included. Some of the values are judgements to aid discussion. β_{comp} of the present TLPs are taken as the averages for three wave directions. Calculation of their n is illustrated in Table 7.3.

It would seem that with the exception of Naval ships there is already a rough

correlation between low β_{comp} and high n (and even higher λ_T) and it would seem there is merit in pursuing such studies. They might lead ultimately, for example, to relations for use in designs as[19]:

$$\beta_{comp} + n \leq 5.0 \tag{7.17}$$

In the discussion of reference [19] a lower value of 4.5 was suggested by Frieze for the right hand side, and certainly the inequality was suggested as an upper limit. From Eq.(7.5) or (7.15) we can obtain the reserve strength ratio, n, given that β_{comp} and β_{sys}. That is:

(1) when R and Q are normal, from Eq.(7.5)

$$n = \frac{f(\beta_{comp}, V_{R_{comp}}, V_Q)}{f(\beta_{sys}, V_{R_{sys}}, V_Q)} \tag{7.18}$$

function f is evalusted from Eq.(7.4).

(2) when R and Q are lognormal, from Eq.(7.15)

$$n = Exp[\zeta_\theta(\beta_{sys} - \beta_{comp})] \tag{7.19}$$

When β_{sys} is 4.0 to 6.0, n values by Eq(7.18) and (7.19) are plotted against β_{comp} as shown in Fig. 7.5, in which the points corresponding to various structures of Table 7.2 and Eq.(7.17) are also included. Comparison of Eq.(7.19) to (7.18) shows that lognormal distributions of R and Q may give more realistic predictions for comparison with n than normal distributions especially for the higher β_{sys} values. By reference to Eq.(7.17) in Fig. 7.5 semi-submersibles and the North Sea TLP seem to be overdesigned. For floating offshore structures, if the allowable β_{sys} (β^o_{sys}) is provisionally chosen to be not greater than 6.0, well-designed structures possibly lie

within the region determined the inequality equation, (7.17) and the following equation derived from Eq.(7.19):

$$\beta_{comp} + \frac{\ln n}{\zeta_\theta} \leq \beta^o_{sys} \quad (= \text{say } 6.0) \tag{7.20}$$

The thick solid line in Fig. 7.5 represents the boundary determined by Eqs.(7.17) and (7.20).

In order to show the relation of component safety to residual strength, the probabilistic measure, RDI_β, given by Eq.(7.16) is plotted against β_{comp} in Fig. 7.6 taking typical n value of 1.5 and 1.7 with the positions of various steel structures taken from Table 7.2. From the figure offshore structures possess higher residual strength indices than naval ships, bridges and merchant ships. Nevertheless this latter group give good service performance and therefore the concept of residual strength may be less meaningful in continuous structures than for discrete ones. It is notable that the predicted RDI_β's of three TLPs by Eq.(7.16), say 0.38, 0.53 and 0.58 for the Hutton TLP, TLP-A and TLP-B, respectively, are close to the average values found in Table 5.32, which were derived from the results of a system reliability analysis. Of course, RDI_β is very dependent upon post-ultimate behaviour (as was found in Section 6.4) which needs to be better defined and validated for continuous structures. The above illustrations and discussions are to show the relation of component and system reliability to redundancy.

Table 7.4 is an attempt to show the system factor, ϕ_{sys}, for three TLP models which are derived when $V_R = 0.15$ and $V_Q = 0.20$, and when $V_R = V_{X_M}$ and V_Q has been obtained using FORM with the safety margin equations of the identified failure modes [see Section 5.4.1 to 5.4.3]. In the latter case it can be seen that ϕ_{sys} is decreased by about 0.1 compared to the former case. From a careful consideration of this the author would propose that ϕ_{sys} of 0.85 or 0.90 might be used for the design of the design of TLP structures.

The use of n, the system strength to component strength ratio, is preferred rather than the more popular reserve strength factor, λ_T[19]. This is because λ_T inevitably contains the safety factor of the most critical component within it and therefore would cloud the "high - low" relationship which Table 7.2 seems to establish. The choice of β_{sys} would then follows naturally from such studies. Alternatively, a system factor, ϕ_{sys}, could be applied in component design as recommended by Moses[11,110] and by Faulkner[8,136].

The inequality sign in Eqs.(7.17) and (7.19) recognises that some acceptable safety levels may very well be lower than these limits, and also the passage of time would naturally require safety levels to reduce in a rational code. Moreover, it recognises that perhaps the most rational safety level should really be chosen on economic grounds unless massive human life were really at risk - as they are in aircraft.

Table 7.2 Component Safety and Subsequent System Redundancy
(average values only)

Structure	Component β	category	System n	category
Fixed Platforms	2.3	low	1.7	high
Buildings	3.0 - 3.5	average	1.5	average
Bridges	3.7	average	< 1.2	low
	4.8	high	< 1.2	low
Merchant Ships	3.5 - 4.0	average	< 1.2	low
Semi-Submersibles	> 4.0	high	> 1.5	average
North Sea TLP	> 4.5	high	1.5	average
Naval Ships	2.2	low	< 1.2	low
Present TLPs				
TLP-A	3.7	average	1.6	average to high
TLP-B	3.7		1.7	

Table 7.3 Illustration of Calculating Reserve Strength Ratio, n, for Three TLP Models

χ	Hutton TLP			TLP-A			TLP-B		
	λ_T	F_{comp}	n	λ_T	F_{comp}	n	λ_T	F_{comp}	n
0°	2.13	1.32	1.61	2.89	1.18	2.45	2.56	1.63	1.57
	1.87	1.32	1.42	2.43	1.18	2.06	3.55	1.63	2.18
	2.29	1.32	1.73	2.67	1.18	2.26	2.93	1.63	1.80
	2.15	1.32	1.63	2.27	1.18	1.92	3.56	1.63	2.18
45°	3.07	2.02	1.52	2.32	2.08	1.12	2.62	1.61	1.63
	2.53	2.02	1.25	2.13	2.08	1.02	2.82	1.61	1.75
	4.13	2.02	2.04	3.17	2.08	1.52	2.72	1.61	1.69
	2.48	2.02	1.23	3.39	2.08	1.63	3.02	1.61	1.88
90°	2.63	1.99	1.32	3.22	2.26	1.42	2.21	2.10	1.10
	2.38	1.99	1.20	2.34	2.26	1.04	2.69	2.10	1.34
	2.48	1.99	1.25	4.05	2.26	1.79	2.61	2.10	1.30
	3.48	1.99	1.75	3.00	2.26	1.33	4.23	2.10	2.10
average n:			1.50			1.63			1.71

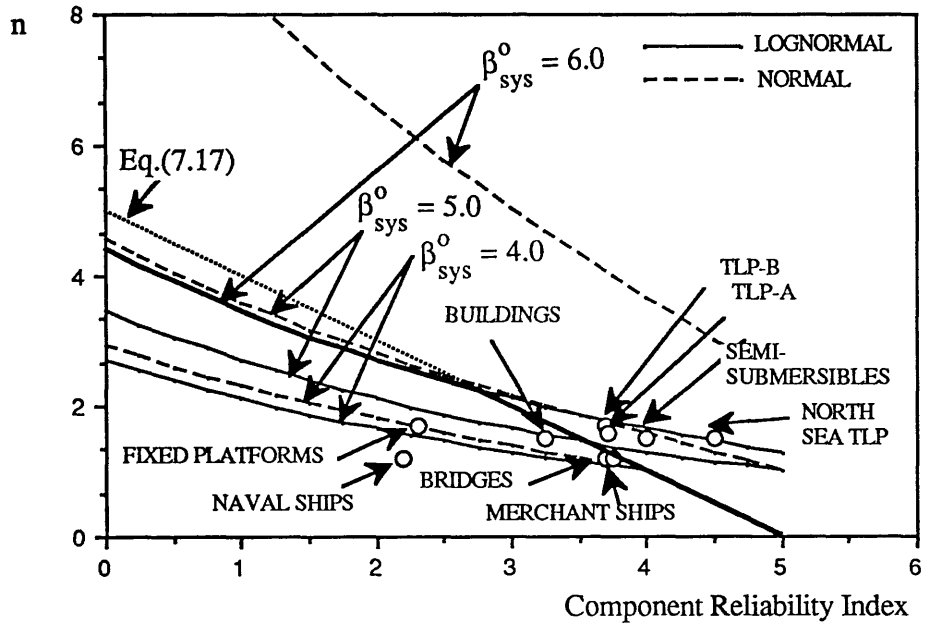

Fig. 7.5 β_{comp} and n

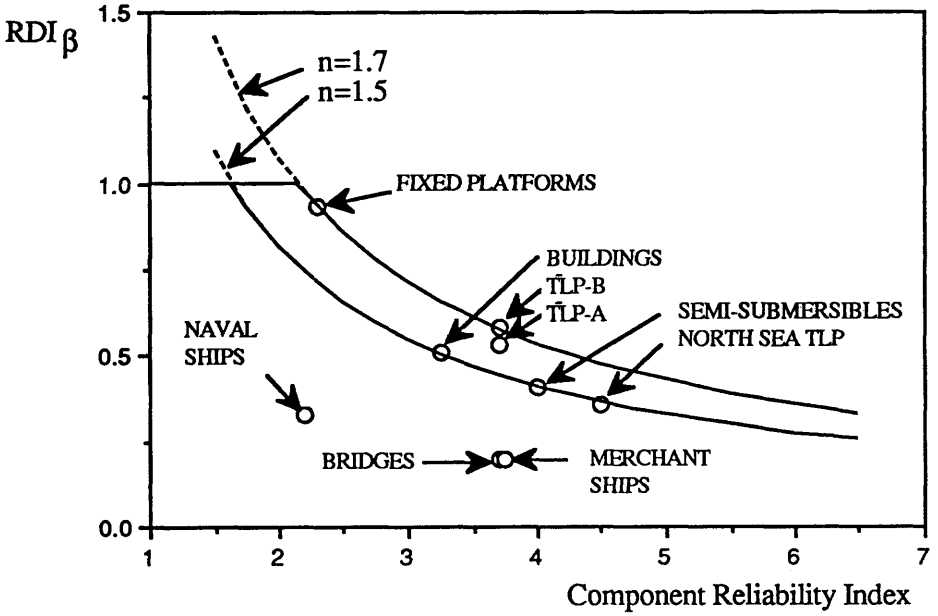

Fig. 7.6 RDIβ and β_{comp}

Table 7.4 ϕ_{sys} of Three TLP Models

TLP model	$V_R = 0.15,\ V_Q = 0.20$	$V_R = V_{X_M},\ V_Q$ by FORM
Hutton TLP	0.95	0.86
TLP-A	0.92	0.82
TLP-B	0.91	0.81

7.3 Reliability-Based Optimal Design

In the context of reliability-based structural design, the optimum design is to distribute the material within the entire structure to obtain a harmonised design having the minimum weight or cost within a prescribed acceptable safety level. This is not the place to go into the detail of reliability-based optimal design. A general idea may be helpful. Development of models for reliability-based optimisation apparently initiated from Forsell[26] who formulated the optimisation problem as minimisation of total cost. Hilton and Feigen[215] were the first to propose a reliability-based weight minimisation formulation. During the last two decades reliability-based optimum design has been developed in conjunction with the classical deterministic optimisation formulation. It has been proposed for some time that a more rational criterion for structural design is that safety be represented by reliability or alternatively by the probability of failure and that the reliability constraints should be included in re-design and optimisation procedure to achieve lower weight and/or cost [21-28,112,137]. In this sense the optimisation problem is probabilistic and not deterministic.

Deterministic optimum design procedures have enjoyed their popularity. But In some cases, with regard to the safety of structure, the optimum design may not be a safe one. For example, Das and Frieze[114] found that designs optimised on a weight basis were not the most reliable. They compared the reliabilities of stringer-stiffened cylinders

as designed based on reliability and with deterministically optimised designs on a weight basis. Table 7.5 illustrates their results. It is shown that the minimum weight designs are much less reliable than the reliability-based designs.

The general idea of optimisation is to minimise (or maximise) the objective function subjected to reliability (or probability of failure) constraints. The possible objective function may be structural weight, total cost, in which the cost due to failure is often included, probability of unserviceability and utility function. Structural weight or total cost is usually taken as an objective function just as for deterministic optimisation. For the sake of economy of any particular structure, the total cost is naturally more preferable as the objective in the optimisation formulation than structural weight, because this can be implicitly accounted for in the cost optimisation procedure. The total cost may include the initial construction cost, maintenance cost and the cost arising from the consequence of structural failure. For this purpose, several formulation procedures have been proposed[13,26,138]. In recent years, system reliability methods have been applied to the optimum design of the structural system[31-33] and to finding the optimum strategy of inspection and repair of a structure[30-32]. Although its application is at the early developing stage and still has many difficulties, it has potential applications, especially in the offshore engineering field.

Table 7.5 Comparison of Reliability Index Between Reliability-Based Design and DeterministicMinimum Weight Design[114] : β_{comp} [P_f]

COV of axial compressive force	10%	20%
reliability-based design (non-optimum)	2.62 [4.4 x 10^{-3}]	1.75 [4.0 x 10^{-2}]
minimum weight design	1.84 [3.8 x 10^{-2}]	1.18 [0.119]

In the reliability-based optimisation, the design variables to be optimised are:

- size of members, e.g., for cylindrical components, cylinder radius (R) and thickness (t), stiffener scantlings (h_w, t_w,b_f, t_f), number of stiffeners (N), spacing of ring frames (L)
- geometric layout of component
- material to be used
- structural topology

The design variables are herein signified as X_i , i = 1 to n. Consider the optimisation problem to minimise the total cost subject to reliability constraints and to design requirements specified in any particular design code as sub-constraints. The problem is:

Find X_i such that minimise the total cost given by:

$$f(X_i) = C_T = C_0(X_i) + C_f * P_f(X_i) \tag{7.21}$$

subject to reliability constraints :

$$\beta \leq \beta^0 \tag{7.22}$$

and

$$X_{i,l} < X_i < X_{i,u} \tag{7.23}$$

In Eq.(7.21), C_T is the expected total cost in present worth terms, C_0 the initial cost (e.g., sum of all costs associated with design and construction), C_f the expected cost of failure in which inspection and repair cost, re-construction cost, compensation cost, cost due to social consequences, etc. and P_f is the risk, i.e. the probability of failure in appropriate annual or life time values. In Eq.(7.22) β is the reliability index to be evaluated and may be a component reliability index or system reliability index, and β^0 is its allowable value, i.e. target component reliability index or some target system reliability

index. The total cost and reliability index are functions of design variables. In Eq.(7.23), $X_{i,l}$ and $X_{i,u}$ are lower and upper bounds of the design variables specified in a design code or by the designer.

A sensitivity study of the design variables[135] and selection of the target reliability index[136] for the component or system level, must precede the optimisation procedure so the important variables to optimise are identified.

An illustration of total cost as a function of P_f is shown in Fig. 7.7. Increased initial cost results in a decreased risk and a reduction in the cost of failure, $C_f * P_f$ in Eq.(7.21), and vice versa. An optimum design is reached when an increase of initial cost is balanced by a reduction in expected cost of failure times the probability of failure.

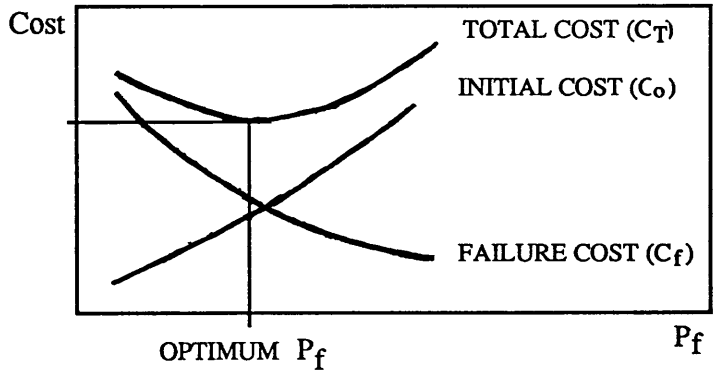

Fig. 7.7 Total Cost, Initial Cost and Failure Cost vs Risk

Reliability-based optimisation studies using Eqs. (7.21) to (7.23) are generally a constrained non-linear problems. Since the design goal is to achieve the minimum total cost (or weight) and maximum safety, a more general problem can be the multi-objective optimisation one[29,138,216] with multiple constraints, in which a preference solution, e.g., to maximise the decision makers utilities, is chosen from the so-called Pareto optimum set. This can also include design requirements specified in any particular design code as constraints.

The deterministic optimisation methods which are linear and non-linear programming techniques[217-219] are also generally suitable for solving reliability-based optimisation problems including constrained formulation problems. Most experience has been gained using the method of feasible directions. This method solves the constrained problem as a sequence of useable feasible steps in the design space[137,220]. It may also be effectively solved by using Sequential Linear Programming (SLP). SLP uses a (Linear Programming (LP) algorithm sequentially in such a way that in the limit the successive solutions of the LP problems converge with those of non-linear programming[13]. The original programming problem can be reduced to the linearised problem by linearising the non-linear objective function and constraints via the first-order Taylor series expansion. Many other solution methods, such as penalty function method, dynamic programming method[20] and stochastic programming method[221] have been used for solving reliability-based optimisation problems. Recently more sophisticated methods (e.g., generalised reduced gradient method, robust feasible direction method) have been used. More discussion about solution methods can be found in various text books, e.g. references [217] to[219].

The following algorithmic procedure based on the method of feasible directions can be used to obtain the optimum solution with reliability constraints [see Fig. 7.8].

Step 1 Specify the target reliability index, β^o, and select the design variables and set their initial values, X_{oi}. The initial values of design variables can be determined according to the design code in use for the design of the structure considered under the given structural configuration and the design environmental conditions. A reliability-based design code would be preferred.

Step 2 Change the design variables in the objective function gradient direction

Step 3 Evaluate the reliability index, β (components or systems level), and check if the reliability constraint is satisfied. If yes, go to Step 4, otherwise go back to Step 2.

Step 4 Check that the design requirements of the code are satisfied. If satisfied, go to Step 5, otherwise, change the design variables to satisfy these constraints and go to Step 2

Steps 2 to 4 are to be continued until reliability constraints and design requirements are satisfied.

Step 5 A move is made in the direction which continues to reduce the objective function without violating the reliability constraints, i.e. find a vector of feasible direction, {s} for design variables such that it satisfies the following relations:

$$\nabla\{R(X_i)\}^T \{s\} > 0 \qquad \nabla\{f(X_i)\}^T \{s\} < 0$$

where $\nabla\{R(X_i)\}$ is the normal vector to the reliability constraint, $\nabla\{f(X_i)\}$ the normal vector to the object function and {s} the vector of direction in which the move should be made.

Step 6 Find a feasible point, X_i such that $X_i = X_{oi} + \alpha s_i$ in which α is a constant to be determined to satisfy $\|X_i - X_{oi}\| > \varepsilon$. ε is the prescribed small number.

Step 7 Check convergence of the solution. If the solution satisfies

$$\left| \frac{\nabla f}{|\nabla f|} \right| < \varepsilon$$

then the point is optimum, otherwise go to Step 2.

This procedure continues until the optimum is reached, or when the movement in the feasible directions produces no decrease in the objective function. Because the optimum point may be a local minimum, the design procedure should be started from a number of different initial points. A high degree of confidence in the optimum solution is achieved when (nearly) the same design point, or at least points with almost equal objective function, are determined from several starting points. The above procedure is

shown in Fig. 7.9.

A more ambitious task is to incorporate structural redundancy with system reliability-based design, the reserve strength can be reflected by the system reliability index, β_{sys} of the structure in the intact condition, and the residual strength by the residual system reliability index, $\beta_{sys,R}$, of the structure in the damaged condition. $\beta_{sys,R}$ is the system reliability index given that any critical component has failed [see text at Eq.(2.12)]. In general, the system reliability-based optimisation problem is to find design variables to minimise the total costs given by Eq.(7.21) or minimum structural weight subject to the reliability constraints. The constraints might well include

$$\begin{aligned} \beta_{comp} &> \beta^{o}_{comp} \\ \beta_{sys} &> \beta^{o}_{sys} \\ \beta_{sys,R} &> \beta^{o}_{sys,R} \end{aligned} \tag{7.24}$$

where β^{o}_{comp}, β^{o}_{sys} and $\beta^{o}_{sys,R}$ are the specified target reliability of component and of the system when the structure is intact and damaged. Solving this problem must be very complicated for practical structures.

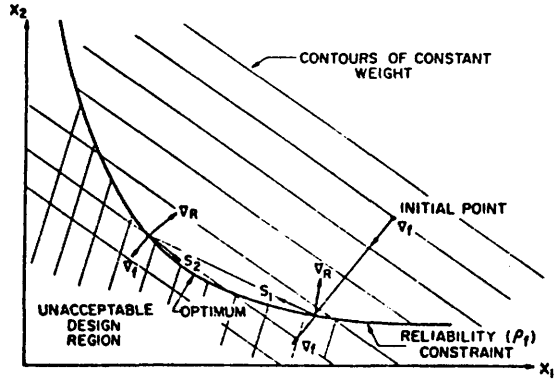

Fig. 7.8 Design Space with Reliability Constraint

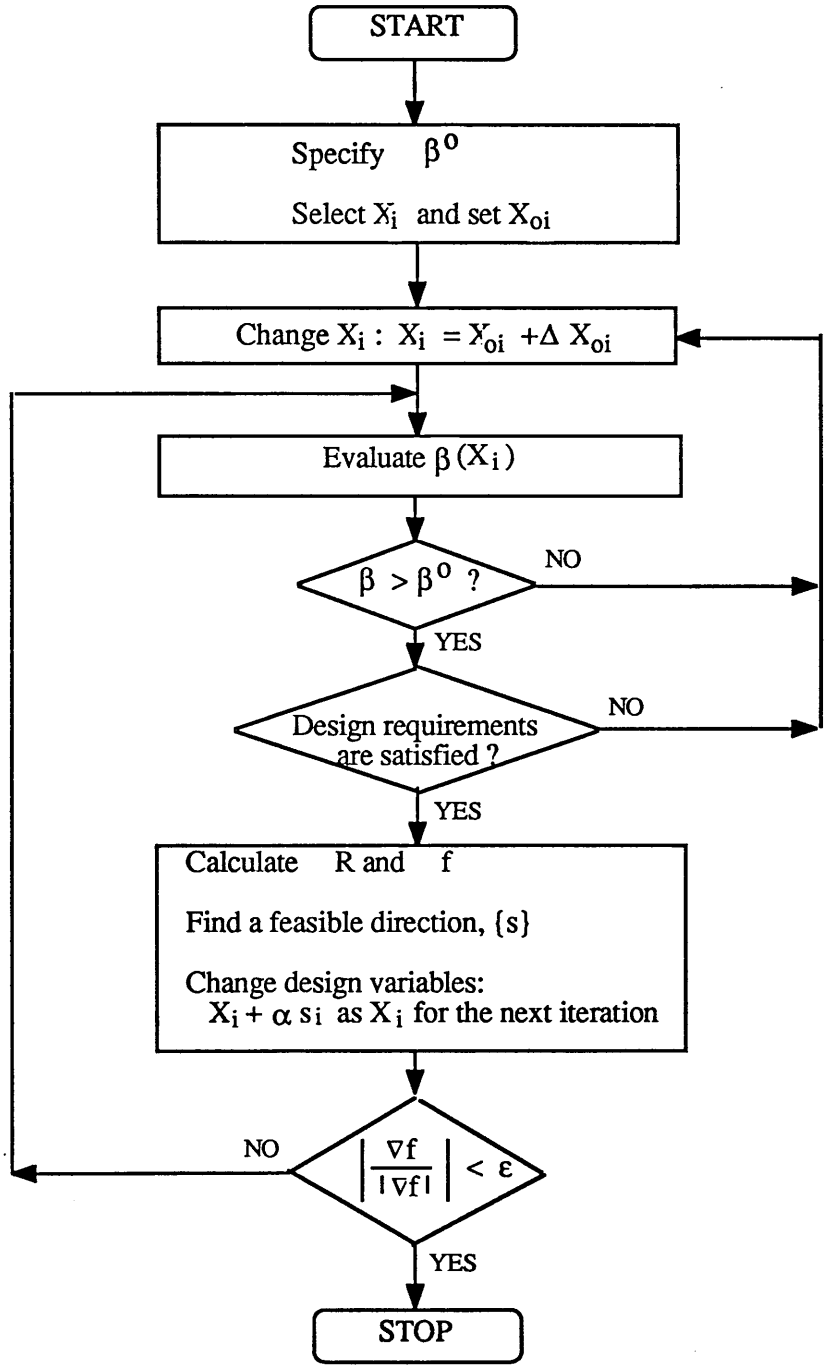

Fig. 7.9 Procedure of Reliability-Based Optimisation

7.4 In-service Reassessment

Another application of the system reliability methods is to find the optimum inspection and maintenance strategy[31-33]. For offshore platforms it is important to make in-place inspections so that structural damage or structural degradation is repaired to ensure safety and thereby not only protect investment but also prevent pollution of the environment and loss of life. Inspection and maintenance strategies used today are based on experience rather than rationality. Still this does not imply that they are not adequate. However, it should be noted that the total cost for inspection and repair is generally high and must therefore be maintained as an economic level. Thus, it seems rational to try to use the recently developed system reliability methods to improve these strategies.

The strategies are the non-prescriptive engineering approach to the re-qualification of existing platforms and in recent years have been incorporated with the deterministic optimum theories. The objective is to find the optimum strategy such that inspection and repair costs are minimum subjected to the reliability constraints. The strategy is sometimes referred to as AIM (Assessment, Inspection and Maintenance)[33]. Let the cost of inspection be C_I and the cost of repair C_R. Then, the total costs for inspection and repair is simply:

$$C_{IR} = C_I + C_R \tag{7.25}$$

The cost C_I depends on the quality and number of the inspections. The optimisation variables are the time interval between inspections and the quality of the inspections and repairs.

The inspection cost is usually both very expensive and difficult to implement. It is important to stress that it is usually much better to design the platform in such a way that sufficient safety, but not excessive, is ensured during the lifetime of the structure than to rely on repair when needed. Therefore, a more general problem of system reliability-based optimisation is to find the design which minimises the expected total cost which

includes all costs during the lifetime of the structure subjected to system and component reliability constraints. Recently, an attempt at this was made of by Søresen and Thoft-Christensen[31].

7.4 Discussion

The simple procedures introduced in Section 7.1 may be helpful to roughly predict the system safety level and structural reserve and residual strengths, and also to choose an acceptable safety level in the design stage. Levels of safety vary quite widely depending on structural type and behaviour of component in a structure, especially on the post-ultimate behaviour of a failed component. It has been suggested that they may sensibly be linked to the reserve strength ratio for the system, n, and component strength, as given by Eqs.(7.17) and (7.20). It should be pointed out that first generation semi-submersibles and TLP structures would appear to be significantly overdesigned in the light of the present studies [see Fig. 7.5]. Therefore, acceptable safety levels may be lowered than those used in present design, and this would also appear to be justified in the light of service experience.

Reliability-based optimisation is still at an early development stage because of its complex nature in applying it to practical problems. The difficulties are:

[1] As is well-known, there are various methods for handling the uncertainties in similar structural design situations, e.g. first-order second moment methods, full-distribution methods and combined methods of these two. Even the reliability index to be evaluated differs in various methods [see references in Section 1.2.2]. Lacking a single method, individuals are likely to adopt separate strategies for handling the uncertainties in their particular problems. This affords the possibility of non-uniform reliability levels in a similar structural design situation[26].

[2] There are diverging options on many basic issues, from the very definition of reliability-based optimisation, including the definition of the optimum solution, the objective function and the constraints, to its application in structural design

practice[26].

Particular difficulties, with regard to the system-based design are:

[3] it is not an overstatement to say that any single method for system reliability analysis cannot claim to have a significant advantage over others and the identified important failure modes and the evaluated system reliability level can differ for various algorithms and can be far from "true" solutions for practical structures.

[4] There are many factors affecting the system reliability whose effects are not yet clearly known to us. As a typical example, the post-ultimate behaviour including the residual strength characteristics of component under the multiple load effects.

[5] System reliability analysis itself is computationally very expensive work.

[6] Selecting the target system reliability indices, β_{sys}^{o} and $\beta_{sys,R}^{o}$, must precede system reliability-based optimum design.

Hence, it is not likely that a fully automatic optimum design procedure can yet be obtained. However, these difficulties do not always lie on the pessimistic side. System reliability methods have matured and efforts to apply them to the design practice have already been started in such a way that the system factor (system partial safety factor) which could be added in the safety check format, as can be found in API LRFD (Load and Resistance Factor Design) format, Eq.(7.2), and TLP RCC (Rule Case Committee) format, Eq.(7.3). This system factor, ϕ_{sys} can and should be obtained through the system reliability analysis. It may differ depending on the structure, component type, load combination, etc. But, it is taken as unity in the present code formats. It is advantageous to have an interactive system so that it is possible manually to make decisions and thereby to intelligently modify the design. It seems to be reasonable to use expert system techniques for this purpose.

The use of system reliability methods in decision making for existing platforms is in progress. Such decisions may concern extended life time, planning for inspection, repair or demolition. Achieving an optimal strategy for inspection and repair based on

system reliability considerations is a relatively new area with potential applications in the offshore engineering field. Rational practical application, however, requires further research, and investigation e.g. into deterioration of platforms.

In conclusion, in spite of there being many unsolved problems, considering that structural design problems are substantially probabilistic, reliability-based design procedures should perhaps be incorporated with optimisation techniques to achieve the design for minimum cost (or weight) for a given safety level. This must be an attracting area to develop with many potential applications, especially in offshore engineering.

CHAPTER 8 CONCLUSIONS AND RECOMMENDATIONS

8.1 Review of the Work

This thesis has been mainly concerned with the system reliability analysis of continuous structures, and especially, TLP structural systems. Various methods and procedures for identifying the important failure modes developed for structural system reliability analysis were reviewed. The proposed method, called herein the "Extended Incremental Load Method", was introduced as another approximate method which an extended the conventional incremental load method. This extension included system analysis of structures under multiple loading together with a proposed modified non-dimensional safety margin equation (2.103) which allows the use of strength models in system analysis. The method has been successfully applied to discrete structures and continuous structures such as TLP structural systems. A sensitivity study to changes in statistical parameters of the design variables in strength and in loading has been carried out to show their relative importance with regard to their effects on safety at component and system levels. Reliability-based design was briefly described. From this the following conclusions can be drawn:

o Method Used:

The proposed method for system reliability analysis, together with the modified safety margin equation (2.103), is a new method in that:

- The method can be applied to the structure under multiple loading.
- The method can directly use strength models generally given in the form of interaction equations under combined load effects and hence, the method can allow for the use of different strength models in the system analysis for the same structure.
- The strength modelling parameter can be incorporated into the safety margin equation proposed herein which has a non-dimensional form. Doing this can

represent the randomness of the failure surfaces of components and also flexibly to reflect the effect on safety of changes in the statistical parameters of the strength models used in the analysis, in particular to their mean biases and modelling uncertainties (COV). In this way, the derived system reliability can be re-evaluated when its mean bias and COV have changed as test data are progressively accumulated.

- The method can more realistically allow for the post-ultimate behaviour of failed components by using the multi-state linearised model for non-linear behaviour.

The method has been coupled with the procedure for identifying the most important failure modes in which several control parameters were used to reduce the computational time when applied to a large and complex structure. In the present approach, a computer program has been developed which can cover the estimation of environmental loadings and their effects on strength and reliability, at systems level as well as at components level, especially for floating offshore platforms.

o Applications to Discrete Structures:

The validity of the present method and the modified safety margin equation together with the identifying procedure was illustrated by applying the present approach to discrete structures. Failure modes were obtained in increasing order of reliability and the proposed safety margin equation gave reasonable results compared with those from the conventional equation [Eq.(2.86)].

o Applications to TLP Structures:

To illustrate application to a continuous structure, the method has been successfully applied to a TLP structural system. The Hutton TLP was chosen as an existing TLP model which has 6 columns of ring-stiffened cylinders and pontoons of rectangular box girders. Its two variants, TLP-A and TLP-B, were chosen to compare the system reliability with different types of principle components, i.e. ring- and stringer-stiffened cylinder against the Hutton TLP, and different structural configurations. TLP-A

was modelled by replacing the four corner columns of the Hutton TLP by ring- and stringer-stiffened cylinders whose design followed the TLP RCC design code and whose structural weight was about 25% less than the original ring-stiffened cylinder. TLP-B was modelled by removing the two mid-columns of TLP-A. When considering only the weights of columns, the structural weight of TLP-A and TLP-B were about 18% and 43.7% less than that for the Hutton TLP, respectively.

From the results of the system reliability analyses for these three TLP models it was found that TLP-A showed nearly the same level of system safety as the Hutton TLP (average β_{sys} of TLP-A is about 3% lower), whereas TLP-B showed a significantly higher level of system safety with average β_{sys} 7.3% and 10.4% greater than those of the Hutton TLP and TLP-A respectively. The higher system safety level of TLP-B is surprising and may be due to the quite different first failure load and the pattern of load effect re-distributions of the failed components from the pattern for the other two TLP models. That is, in the cases of the Hutton TLP and TLP-A, the mid-columns components have a higher probability of failing than the other components (corner columns and pontoons). When any component of the mid-columns fails its load is re-distributed to the remaining components. This appears to cause the Hutton TLP and TLP-A to have a lower level of system safety than TLP-B in which the re-distribution effect arising from the failed component of the mid-columns does not occur. This might be the main reason that TLP-B shows a higher system reliability index in spite of there being much less structural material. This difficult point requires further investigation.

When using the incremental load method, one can obtain the total load factor (λ_T) when structural collapse occurs. The factor is the ratio of collapse load to mean applied design load and is related to the reserve strength of a structural system. The average λ_T values are 2.63, 2.82 and 2.96 for the Hutton TLP, TLP-A and TLP-B, respectively. This implies, perhaps surprisingly to some, that TLP structural systems possess considerable reserve strength in the deterministic sense. The values of RDI_β (a measure of the probabilistic structural redundancy) which appear in Section 5.4.3, and which are related to the residual strengths, also show the appreciable residual strength of TLP

structural systems. From the redundancy analysis, it was found that the deterministically most important failure mode was not identical to the probabilistically most important failure mode as it was found from the simple frame structure in Section 2.6.2 and from the results of others.

Comparing the redundancy measure for the three TLP models it was seen that TLP-B also possessed a higher reserve strength and residual strength than the Hutton TLP and TLP-A. Hence, it could be said that the structure having ring- and stringer-stiffened cylinders could more efficiently resist the external load and possessed more reserve strength and residual strength than the structure having ring-stiffened cylinders. Therefore, compared to the design of the Hutton TLP, a design with at least 40% weight saving in the columns could perhaps be achieved using the ring- and stringer-stiffened cylinders as principle components rather than using ring-stiffened alone.

As was shown in Section 5.4.3, using different strength models in the analysis gave different levels of system safety. The model given by Eq.(3.58) gave a higher system reliability index than Eq.(3.53). This indicated that further weight saving must be possible with the more advanced strength models.

o Sensitivity Study:

A sensitivity study for TLP structural systems has been carried out to investigate the influence of the mean and the COV of the important parameters and variables in strength and loading upon the system reliability as well as component reliability. These were the component strength modelling parameter (or error, X_M), geometric properties (R and t : radius and thickness of cylindrical components), material property (σ_Y) and load effects. The influence of the post-ultimate behaviour of failed components on the system reliability and residual strength was also investigated.

The component strength modelling parameter represented by its mean bias ($\underline{X}_M$) and the coefficient of variation (modelling uncertainty, V_{X_M}) was found to greatly affect the system reliability (β_{sys}) as well as the component reliability (β_{comp}). In physical

terms this is explained by the much higher mean values of strength terms to loading terms so that for any given COV a much higher spread occurs in strength distribution than for loading. It was found that this was mainly due to its important position within the safety margin equation (2.103) proposed in this study and, consequently, its effect upon strength and safety. It was also shown that the modelling uncertainty was much more influential, not only on the system reliability, but also on the component reliability than the mean bias. Therefore, the modelling uncertainties (randomness) of strength models should be kept as low as possible with the mean bias also being kept close to unity to achieve economic benefit in the design from the viewpoint of both the system and the component.

As resistance variables, the material and geometric properties showed comparatively less effect than the strength modelling parameter.

With regard to the influence of static, dynamic and quasi-static load effects, it was found from the results in Section 6.3 that static load effects (both its mean bias and COV) was most influential on the system reliability index as well as component reliability index followed by the dynamic load effects. The effect of the quasi-static load component was found to be relatively less influential. It was found that this was mainly due to the comparatively greater magnitudes of static and dynamic load components acting on the structure than that of the quasi-static component. Neglecting wave drift induced forces might be another reason, but its effect upon safety is not expected to be significant. Considering the much greater degree of random uncertainty with the dynamic component than with the static component, the dynamic component can in some applications have more effect on the safety. Hence, it can be said that the COVs of load effects may be a more important factor affecting safety than mean biases in many designs.

The post-ultimate behaviour of a failed component was modelled into the simplified linearised model, namely, the three-state model, which was characterised by post-ultimate slope (E') and residual strength parameter (η). As was expected, it was shown that the post-ultimate behaviour of failed components had much influence upon

the safety level and residual strength of a structural system. Its effect upon safety was greater than those of the strength modelling parameter and loading variables. Comparison of the results using the three-state model against the two-state model showed that as expected the three-state model gave higher system reliability indices for the same residual strength parameter, η. This arises from the effect of the post-ultimate slope on the pattern of load effects re-distribution. The post-ultimate behaviour of a failed component should therefore be accounted for in assessing the system safety and residual strength with a more refined and realistic model, perhaps achieved initially with a wider choice of E' and η.

The sensitivity study as presented here is important in that it provides useful information about the relative importance of design variables. Consequently, such information must be helpful to the designer in intelligently modifying the design. One important point to be stressed from the sensitivity study is that the control parameters used in the identifying procedure should be consistently kept throughout the numerical analysis because they can greatly affect the failure probability of the structural system and, consequently, the system reliability index to be evaluated.

o Reliability-Based Design Design:

An attempt has been made to show the correlation between structural safety and redundancy for use in design. The present relation between the average component safety indices and the reserve strength ratio for the system for a variety of steel structures shows a rough correlation between low component safety and high reserve strength. Although the need for system safety is well recognised in judicial proceedings when structural catastrophes occurs, most emphasis in design is placed on component safety. To link the two a design correlation between β_{comp} and n, for example, as given by Eq.(7.17) is put forward for consideration. The author suggests that the boundary determined by Eqs.(7.17) and (7.20) be considered as a criterion to achieve balanced designs with adequate safety and redundancy.

It was also found that the first generation semi-submersibles and TLP structures

were significantly overdesigned in the light of the present studies. It might be suggested that β_{sys} could be chosen as 6.0 for floating offshore structures. With regard to the distribution type of resistance and loading variable, as pointed out in Section 7.2 (e.g., see Fig. 7.5), their lognormal distribution seems to better represent the uncertainties associated with resistance and loading and gives more realistic predictions of the safety level than the normal distribution, especially for higher levels of safety.

Within the context of the reliability-based limit-state design, the major goal should be to achieve reliability-based optimum design. Although no results about this subject were presented, the algorithmic procedure illustrated in Section 7.3 is applicable to obtain the optimum solution. Additionally, since structural design problems are generally non-deterministic it follows that engineering optimum design should cope with uncertainties. It is not an overstatement to affirm that reliability-based design procedures incorporated with optimisation techniques must be the best way to achieve the harmonised design for minimum cost (or weight) within any prescribed safety level. This must be a promising area with potential applications, especially for offshore engineering design.

8.2 Main Conclusions

The proposed method for system reliability analysis, together with the modified safety margin equation and the procedure of identifying the most important failure modes, can be used in assessing the system reliabilities under multiple loading conditions, of floating or fixed offshore platforms or other types of structures, and whose components behaviour is a ductile, brittle or two-state unloading manner. Developed strength models for principle components of the structure can be directly used with the method in the system analysis.

Incorporating the strength modelling parameter with the proposed modified form of safety margin equation, given by Eq.(2.103), can flexibly allow for the use of different strength models regardless of the magnitude of their mean biases and random

uncertainties, and can effectively reflect the change of system safety level when strength models are updated as more experimental data are available.

A sensitivity study of structural reliability, at the system level and component level, to design variables must precede the optimisation procedure for several reasons, e.g. to investigate the relative importance of design variables with regard to their effect on safety. The outcome is at the same time useful when modifying the design as an aid to decision making. The post-ultimate behaviour of failed components must be accounted for in the system reliability analysis with a more realistic model to provide the designer with insight into the effective residual strength of structural systems.

The study to attempt to link the structural safety to redundancy recognises the acceptability of relatively low component safety when there is appreciable reserve strength, as in most jacket structures, and vice versa. It would seem that there is a merit in pursuing such studies and perhaps refining Fig. 7.5. For example, for TLP structures the component safety index can then be lowered to about 3.0 with a corresponding system safety index of about 6.0, and the combination may then be acceptable.

Since the reliability method is the best way to treat the uncertainties in load and strength in a more rational way, the optimisation procedure should be on the basis of system reliability to achieve the design of minimum cost for a given safety level. However, this subject is at an early stage in development and there has not been much work reported. Its application to practical structures, including obtaining the optimum strategy for inspection and repair, has many problems still to be solved. In spite of this, the application of system reliability analysis to design code development based on reserve strength and residual strength, strategies for inspection and quality assurance and optimum balance between life-cycle costs and expected risk loss, must be an important future task.

8.3 Recommendations for Future Research

System reliability analysis and its application to design is a relatively new area and has several problems still to be solved before it can be seriously introduced into general design practice. Nevertheless, its application to design and to re-assessment of existing structures is undoubtfully the best way towards achieving a balanced design for economy and safety within the entire structure, especially in the offshore engineering field. The following areas are recommended for more research on the subject and as a future extension of the present work in the future:

[1] System reliability method :

It is necessary to develop a more efficient method for system reliability analysis which should be applicable to a wider range of real structure with general component behaviour, together with the procedure for more efficiently identifying the probabilistically most important failure modes. This can be achieved by refining the available methods to ensure their validity by comparing the results, e.g. load factors of the pre-defined failure modes, to the results of model tests (or wherever possible large scale test) and/or to the results of rigorous non-linear structural analysis (deterministic). This would provide cross check between system reliability methods and results from model tests or more rigorous non-linear analysis.

An important area closely linked to the development or refinement of the system reliability analysis method is to derive the explicit form of the post-ultimate behaviour of principle components in a structure, especially the post-ultimate behaviour. For this, it may be more reasonable to derive more realistic multi-state post-ultimate models, since it is impractical to consider the material and geometric non-linearity through the rigorous non-linear structural analysis in the system reliability analysis of real offshore structures.

[2] Assessment of residual system reliability ($\beta_{SYS,R}$):

This is necessary to ensure the structure survives in the damaged state. For this, formulation of the strength models of components for the damaged state is an important

area to be undertaken..

[3] Fatigue consideration:

The real problem involves deterioration of the component strengths due to environmental actions. Deterioration arises from combinations of temperature and humidity, but the most serious deterioration is closely related to fluctuating loading acting on the structural components. This can cause fatigue failure of components in a structure and may result in the catastrophic collapse of the entire structure. Therefore, fatigue problems should be considered in the system reliability analysis. One way of incorporating the safety margin equation is to progressively reduce the mean bias of strength modelling parameter, i.e. progressively shift the failure surface in the direction of its origin.

[4] Code development and calibration:

The design code to be developed and calibrated should be able to reflect the consequence of failure of any component, and the reserve strength and residual strength of the structural system. Adding the system factor (or system partial safety factor) in the safety check format must be an attractive way of doing that. The safety factor must be obtained through rigorous system reliability analysis. Alternatively, the assessment of system reliability may be carried out at the design stage. For this, it is necessary to gain experience of the reliability assessment by applying the developed methods or algorithms to real structures.

[5] System reliability-based optimum design:

The optimisation procedure should be based on reliability, more generally system reliability as well as component reliability wherever possible. The total cost is preferable than weight as an objective function which may include the initial cost, expected cost of failure and costs of inspection and repair. An important sub-part of this ambitious subject is to obtain the optimum strategy of inspection.

The pre-solved problem, to obtain the optimum design for practical structure, is to

select the target system reliability with acceptable level, when a structure is intact or damaged condition (β^{o}_{sys} or $\beta^{o}_{sys,R}$).

[6] Consideration of gross error

Most structural failure is due to gross error (human error) and therefore it is very desirable to explicitly account for this error in reliability assessment with a realistic model.

[7] Marine growth

When an offshore structure is in-service, marine growth effects on the loading acting on the submerged part of the structure and the distribution of load effects, and hence on the safety level of the structure. This may also be considered in the reliability assessment with a realistic model.

Finally, as a fundamental but important area in the context of reliability-based design, effort should be made towards the development of more advanced strength models which must be derived based on the limit-state analysis and have modelling uncertainty as low as possible. A parallel effort toward achieving more realistic three-dimensional wave, current and wind loading models for design is also needed.

8.4 Closing Remarks

Because of many assumptions adopted herein and the uncertainty with the method itself, the results of the present reliability study may not be the "true" solution, but a reasonable solution. Some of the gaps have been pointed out in these conclusions, but those that are judged to be most important are emphasised here:

- It has not been proved absolutely that the procedure developed for identifying the most important failure modes will always identify kinematically admissible failure mechanisms.

- The post-ultimate strength of structural components appears to be a very crucial parameter in systems reliability, and this requires to be more fully addressed. Its associated modelling uncertainty and the systems modelling uncertainty are, again, important parameters that need further consideration.
- The very strong dependence of the reliability index on the post-ultimate strength, shown in Chapter 6, is emphasised. The implication of this Chapter is that following collapse of critical components if their residual strengths are less than 75% of their ultimate strength they may not contribute significantly to the load-carrying capacity of the system.
- The effects of boundary condition mode of unloading following attainment of ultimate load, etc, of component response in a real structure, in contrast to experimentally observed response under idealised laboratory conditions needs to be highlighted. They could be important factors given the sensitivity of the reliability index to the post-ultimate response of important components.
- Some of these factors would require careful experiments to validate modelled behaviour, including ideally the sequence of failure under idealised multiple loads. Such experiments, of course, would be very expensive to conduct, but they are nevertheless important to consider if system analysis is to be used for continuous spatially distributed structures.
- It is emphasised that the reliability index corresponds to the life of the structure and not to an annual reliability.

Finally, the author would like to close this thesis with the hope that it may provide one corner stone of system reliability analysis and its application to the design of practical structures in the future. System reliability analysis is intended more to provide useful information as criteria for decision making in the design stages and in-service assessment.

REFERENCES

[1] Ellingwood, B. and Galambos, T.V. ,"Probability-Based Criteria for Structural Design", Structural Safety, Vol.1, 1982, pp.15-26

[2] Ang, A.H-S and Cornell, C.A. ,"Reliability Bases of Structural Safety and Design", J. of Struct. Div., ASCE, Vol.100, No.ST9, Sept. 1974, pp.1755-1769

[3] Faulkner, D. ,"Development of a Code for the Structural Design of Compliant Deep Water Platforms", Dept. of Naval Arch. and Ocean Engineering, Univ. of Glasgow Report, NAOE-84-65, Dec. 1984

[4] Planeix, J.-M.,"Recent Progress in Probabilistic Structure Design - An Elementary Discussion of Developments", Proc. Advances in Marine Structures, ARE, Dunfermline, Scotland, 20-23 May 1986, Paper No.31

[5] Thoft-Christensen, P. and Baker, M.J. ,*Structural Reliability Theory and its Applications*, Springer-Verlag, 1982

[6] Pugsley, A.G. ,"A Philosophy of Aeroplane Strength Factors", Report and Memo No.1906, British Aeronautical Research Committee, 1942

[7] Ditlevsen, O. and Bjerager, P. ,"Methods of Structural System Reliability", Structural Safety, Vol.3, 1986, pp.195-229

[8] Faulkner, D. ,"Reliability of Offshore Structures", SERC Marine Technology Seminar, 9-10 April 1984, London

[9] ABS-Conoco ,"Model Code for Structural Design of Tension Leg Platforms",

Conoco-ABS TLP Rule Case Committee, Final Report, ABS, N.Y., Feb. 1984

[10] Moses, F. ,"Utilization of a Reliability-Based API RP2A Format on a Platform Design", Final Report, API PRAC 81-22, American Petroleum Institute, Nov. 1982

[11] Moses, F. ,"System Reliability Developments in Structural Engineering", Structural Safety, Vol.1, 1982, pp.3-13

[12] Edwards, G.E., Heidweiller, A., Kerstens, J. and Vrouwenvelder, A. , "Methodologies for Limit State Reliability Analysis of Offshore Jacket Platforms", Proc. 4th Intl. Conf. on Behaviour of Offshore Structures, Delft, The Netherland, July 1-5, 1985, pp.315-324

[13] Thoft-Christensen, P. and Murotsu, Y. ,*Application of Structural Systems Reliability Theory*, Springer-Verlag, 1986

[14] Madsen, H.O., Krenk, S. and Lind, N.C. ,*Methods of Structural Safety*, Prentice-Hall, Inc., 1986

[15] de Oliveira, J.G. and Zimmer, R.A. ,"Redundancy Consideration in the Structural Design of Floating Offshore Platforms", in 'The Role of Design, Inspection and Redundancy in Marine Structural Reliability', D. Faulkner et al ed., National Academic Press, 1984, pp.293-327

[16] Marshall, P.W. ,"The Design-Inspection-Redundancy Triangle", in 'The Role of Design, Inspection and Redundancy in Marine Structural Reliability', D. Faulkner et al ed., National Academy Press, 1984, pp.1-10

[17] Frangopol, D.M. ,"Sensitivity Studies in Reliability-Based Analysis of Redundant Structures", Structural Safety, Vol.3, 1985, pp.13-22

[18] Frangopol, D.M. ,"Computer-Automated Sensitivity Analysis in Reliability-Based Plastic Design", Computers & Structures, Vol.22, No.1, 1986 pp.63-75

[19] Lee, J.-S. and Faulkner, D. ,"System Design of Floating Offshore Structure", RINA Spring Meeting, 1989, Paper No.8

[20] Kalaba, R.E. ,"Design of Minimum Weight Structures Given Reliability and Cost", J. of the Aerospace Science, Vol.29, 1962, pp.355-356

[21] Moses, F. ,"Structural System Reliability and Optimization", Computers & Structures, Vol.7, 1977, pp.283-290

[22] Feng, Y.S. and Moses, F. ,"Optimum Design, Redundancy and Reliability of Structural Systems", Computers & Structures, Vol.24, No.2, 1986 pp.239-251

[23] Feng, Y.S. and Moses, F. ,"A Method of Structural Optimization Based on Structural System Reliability", J. of Struct. Mech., Vol.14, No.4, 1986, pp.437-453

[24] Murotsu, Y., Kishi, M., Okada, H., Yonezawa, M. and Taguchi, K. , "Probabilistically Optimum Design of Frame Structure", Proc. 11th IFIP Conf. System Modelling and Optimization, Copenhagen, Denmark, July 25-29, 1983, pp.545-554

[25] Frangopol, D.M. ,"Multicriteria Reliability-Based Structural Optimization", Structural Safety, Vol.3, 1985, pp.23-28

[26] Frangopol, D.M. ,"Structural Optimization Using Reliability Concepts", J. of Struct. Engg., ASCE, Vol.111, No.ST11, 1985, pp.2288-2301

[27] Corotis, R.B. and Soltani, M. ,"Structural System Reliability : Limit States and Modal Consequences", Proc. 4th Intl. Conf. on Structural Safety and Reliability, Vol.1, Kobe, Japan, May 1985, pp.107-116

[28] Kishi, M., Murotsu, Y., Okada, H. and Taguchi, K. ,"Probabilistically Optimum Design of Offshore Platforms Considering Maintenance Costs", Proc. 4th Intl. Conf. on Structural Safety and Reliability, Vol.2, Kobe, Japan, May 1985, pp.557-563

[29] Soltani, M. and Corotis, R.B. ,"Load Space Reduction of Random Structural Systems and Failure Cost Design", Proc. 5th Intl. Conf. on Applications of Statistics and Probability in Soil and Structural Engineering, Vol.1, Univ. of British Columbia, Vancouver, B.C., Canada, May 25-29, 1987, pp.111-118

[30] Murotsu, Y., Shao, X., Miki, M. and Okada, H. ,"On a Reliability-Based Shape Optimization of Truss Structures", Proc. 2nd Working Conf. on Reliability and Optimization of Structural Systems, London, U.K., Sept. 26-28, 1988
(paper presented)

[31] Sørensen, J.D. and Thoft-Christensen, P. ,"Integrated Reliability-Based Optimal Design of Structures", Proc. 1st Working Conf. on Reliability and Optimization of Structural Systems, Aalborg, Denmark, May 6-8, 1987, pp.385-398

[32] Thoft-Christensen, P. ,"Application of Structural Systems Reliability Theory in Offshore Engineering, State-of Art", Proc. 3rd Intl. Conf. on Integrity of Offshore Structures, Univ. of Glasgow, Sept. 28-29, 1987, Paper No.1, pp.1-24

[33] Bea, R.G. and Smith, C.E. ,"AIM (Assessment, Inspection, Maintenance) and Reliability of Offshore Platforms", Proc. Marine Structural Reliability Symposium, The Ship Structure Committee and SNAME, Arlington, VA, Oct. 5-6, 1987, pp.57-75

[34] Lind, N.C. ,"Models of Human Error in Structural Reliability", Structural Safety, Vol.1, 1983, pp.167-175

[35] Melchers, R.E. and Harrington, M.V. ,"Structural Reliability as Affected by Human Error", Proc. 4th Intl. Conf. on Applications of Statistics and Probability in Soil

and Structural Engineering, Vol.1, Univ. of Firenze, Italy, June 13-17, 1983, pp.683-694

[36] Nowak, A.S. and Carr, R.I. ,"Errors in Structural Models", Proc. 4th Intl. Conf. on Structural Safety and Reliability, Vol.2, Kobe, Japan, May 1985, pp.107-116

[37] Madsen, H.O. ,"Model Updating in Reliability Theory", Proc. 5th Intl. Conf. on Applications of Statistics and Probability in Soil and Structural Engineering, Vol.1, Univ. of British Columbia, Vancouver, B.C., Canada, May 25-29, 1987, pp.564-577

[38] Baker, M.J. ,"The Reliability Concept as an Aid to Decision Making in Offshore Engineering", Proc. 4th Intl. Conf. on Behaviour of Offshore Structures, Delft, The Netherland, July 1-5, 1985, pp.75-94

[39] Guenard, Y.F. ,"Application of System Reliability Analysis to Offshore Structures", John A. Blume Earthquake Engineering Centre, Stanford Univ., U.S.A., Report No.71, Nov. 1984

[40] Moses, F. and Stahl, B. ,"Reliability Analysis Format for Offshore Structures", Proc. 10th Offshore Technology Conf., OTC 3046, Houston, Texas, 1978, pp.29-38

[41] Lee, J.-S. and Faulkner, D. ,"System Reliability Analysis of Structural System", Dept. of Naval Arch. and Ocean Engineering, Univ. of Glasgow Report, NAOE-88-33, May 1988

[42] Murotsu, Y. ,"Reliability Analysis of Framed Structure Through Automatic Generation of Failure Modes" in 'Reliability Theory and its Application in Structural and Soil Mechanics', P.Thoft-Christensen ed., Martinus Nijhoff Pub., 1983, pp.525-540

[43] Crohas, H. and Tai, A.A. ,"Reliability Analysis of Offshore Structures Under Extreme Environmental Loading", Proc. 16th Offshore Technology Conf., OTC 4826,

Houston, Texas, 1984, pp.417-426

[44] Melchers, R.E. and Tang, L.K. ,"Dominant Failure Modes in Stochastic Structural Systems", Structural Safety, Vol.2, 1984, pp.127-143

[45] Ang, A.H.-S. and Tang, H.T. ,*Probability Concepts in Engineering Planning and Design - Vol.II ; Decision, Risk and Reliability*, John Wiley & Sons, Inc., 1984

[46] Task Committee on Structural Safety ,"Structural Safety - A Literature Review", J. of Struct. Div., ASCE, 1972, Vol.98, No.ST4, pp.845-884

[47] Freudenthal, A.M., Garrelts, J.M. and Shinozuka, M. ,"The Analysis of Structural Safety", J. of Struct. Div., ASCE, Vol.92, No.ST1, Feb. 1966, pp.267-325

[48] The Committee on Reliability of Offshore Structures of the Committee on Structural Safety and Reliability of Structural Division ,"Application of Reliability Methods in Design and Analysis of Offshore Platforms", J. of Struct. Engg., ASCE, Vol.109, No.10, Oct. 1983, pp.2265-2291

[49] Moses, F. ,"Reliability of Offshore Structures", Proc. of Ocean Structural Dynamics, Oregon State Univ., Corvallis, Sept. 1986

[50] Stiansen, S.G. and Thayamballi, A.K. ,"Lessons Learnt from Structural Reliability Research and Applications in Marine Structures", Proc. Marine Structural Reliability Symposium, The Ship Structure Committee and SNAME, Arlington, VA, Oct. 5-6, 1987, pp.1-13

[51] "Report on Structural Safety", with Discussion, The Structural Engineer, Vol.33, No.5, May 1955

[52] Cornell, C.A. ,"Probability-Based Structural Code", J. of ACI, Dec. 1969

[53] Hasofer, A.H. and Lind, N.C. ,"Exact and Invariant Second-Moment Code Format", J. of Engg. Mech. Div., ASCE, Vol.100, No. EM1, Feb. 1974, pp.111-121

[54] Rackwitz, R. and Fiessler, B. ,"Structural Reliability Under Combined Random Load Sequences", Computers & Structures, Vol.9, 1978, pp.489-494

[55] Gollwitzer, S. and Rackwitz, R. ,"Equivalent Components in First-Order System Reliability", Reliability Engineering, Vol.5, 1983, pp.99-115

[56] Veneziano, D. ,"New Index of Reliability", J. of Engg. Mech. Div., ASCE, Vol.105, No.EM2, 1979, pp.277-296

[57] Ditlevsen, O. ,"Generalized Second Moment Reliability Index", J. of Struct. Mech., Vol.7, No.4, 1979, pp.435-451

[58] Chen, X. and Lind, N.C. ,"Fast Probability Integration by Three-Parameter Normal Tail Approximation", Structural Safety, Vol.1, No.4, 1983, pp.269-276

[59] Wu, Y.-T. and Wirsching, P.H. ,"New Algorithm for Structural Reliability Estimation", J. of Engg. Mech., Vol.113, No.9, Sept. 1987, pp.1319-1336

[60] Ayyub, B.M. and White, G.J. ,"Reliability-Conditioned Partial Safety factors", J. of Struct. Engg., Vol.113, No.2, Feb. 1987, pp.279-294

[61] White, G.J. and Ayyub, B.M. ,"Reliability-Based Design for Marine Structures", J. of Ship Research, Vol.31, No.1, March 1987, pp.60-69

[62] Gollwitzer, S. and Rackwitz, R. ,"First-Order System Reliability of Structural Systems", Proc. 4 th Intl. Conf. on Structural Safety and Reliability, Vol.1, Kobe, Japan, May 1985, pp.171-218

[63] Madsen, H.O. ,"First Order vs Second Order Reliability Analysis of Series Structures", Structural Safety, Vol.2, 1984, pp.207-214

[64] Kiureghian, A.D., Lin, H-Z and Hwang, S-J ,"Second-Order Reliability Approximations", J. of Engg. Mech., ASCE, Vol.113, No.8, Aug. 1987, pp.1208-1225

[65] Tvedt, L. ,"Second Order Probability by an Exact Integral", Proc. 2nd Working Conf. on Reliability and Optimisation of Structural Systems, London, U.K., Sept. 26-28, 1988 (paper presented)

[66] Moses, F. and Rashedi, M.R. ,"The Application of System Reliability to Structural Safety", Proc. 4 th Intl. Conf. on Applications of Statistics and Probability in Soil and Structural Engineering, Vol.1, Univ. of Firenze, Italy, June 13-17, 1983, pp.573-584

[67] Gorman, M. ,"Automatic Generation of Collapse Mode Equation", J. of Struct. Div., ASCE, Vol.107, No.ST7, July, 1981, pp.1350-1354

[68] Murotsu, Y., Okada, H., Yonezawa, M. and Taguchi, K. ,"Reliability Assessment of Redundant Structure", 3 rd Intl. Conf. on Structural Safety and Reliability, 1981, pp.315-329

[69] Murotsu, Y., Okada, H., Matsuzaki, S. and Katsura, S. ,"Reliability Assessment of Marine Structures", College of Engineering, Univ. of Osaka Prefecture, Japan, July 1985

[70] Thoft-Christensen, P. and Sørensen, J.D. ,"Reliability Analysis of Elasto-Plastic Structures", Proc. 11th IFIP Conf. System Modelling and Optimization, Copenhagen, Denmark, July 25-29, 1983, pp.555-565

[71] Ditlevsen, O. and Bjerager, P. ,"Reliability of Highly Redundant Plastic Structures", J. of Engg. Mech., ASCE, Vol.110, No.5, May 1984, pp.671-693

[72] Melchers, R.E. and Tang, L.K. ,"Failure Modes in Complex Stochastic Systems", Proc. 4 th Intl. Conf. on Structural Safety and Reliability, Vol.1, Kobe, Japan, May 1985, pp.97-106

[73] Chan, H.Y. and Melchers, R.E. ,"Reliability of Complex Structures Under Wave Loads", Proc. 5th Intl. Conf. on Applications of Statistics and Probability in Soil and Structural Engineering, Vol.1, Univ. of British Columbia, Vancouver, B.C., Canada, May 25-29, 1987, pp.166-173

[74] Lee, J.-S. and Faulkner, D. ,"Reliability Analysis of TLP Structural Systems", 8th Intl. Symp. on OMAE, The Hague, Netherland, 1989

[75] Kam, T-Y, Corotis, R.B. and Rossow, E.C. ,"Reliability of Nonlinear Framed Structures", J. of Struct. Engg., ASCE, Vol.109, No.7, July 1983, pp.1585-1601

[76] Lin, T.S. and Corotis, R.B. ,"Reliability of Ductile Systems with Random Strength", ASCE, J. of Struct. Engg., Vol.111, No.ST6, 1985, pp.1306-1325

[77] Bennett, R.M. ,"Reliability Analysis of Frame Structures with Brittle Components", Structural Safety, Vol.2, 1985, pp.281-290

[78] Bennett, R.M. ,"Reliability of Nonlinear Brittle Structures", J. of Struct. Engg., ASCE, Vol.112, No.9, Sept. 1986, pp.2027-2040

[79] Bennett, R.M. and Ang, A. H.-S. ,"Formulation of Structural System Reliability", J. of Engg. Mech., ASCE, Vol.112, No.11, Nov,1986, pp.1135-1151

[80] Cornell, C.A. ,"Bounds on the Reliability of Structural Systems", J. of Struct. Div., ASCE,Vol.66, No.ST1, Feb. 1967

[81] Ditlevsen, O. ,"Narrow Reliability Bounds for Structural Systems", J. of Struct.

Mech., Vol.7, No.4, 1979, pp.453-472

[82] Vanmarcke, E.H. ,"Matrix Formulation of Reliability Analysis and Reliability Based Design", Compters & Structures, Vol.3, 1973, pp.757-770

[83] Chou, K.C., McIntosh, C. and Corotis, R.B. ,"Observations on Structural System Reliability and the Role of Modal Correlations", Structural Safety, Vol.1, 1983, pp.189-198

[84] Frangopol, D.M. ,"Accuracy of Methods for System Reliability Analysis", Proc. of the Intl. Conf. on Reliability of Methods for Engineering Analysis, University College, Swansea, July 9-11, 1986, pp.255-270

[85] Grimmeit, M.J. and Schueller, G.I. ,"Benchmark Study on Methods to Determine Collapse Failure Probabilities of Redundant Structures", Structural Safety, Vol.1, 1982/1983, pp.93-106

[86] Schueller, G.I. ,"Current Trends in System Reliability", Proc. 4th Intl. Conf. on Structural Safety and Reliability, Vol.1, Kobe, Japan, May 1985, pp.139-148

[87] Hohenbichler, M. and Rackwitz, R. ,"First-Order Concept in System Reliability", Structural Safety, Vol.1, 1983, pp.177-188

[88] Karamchandani, A. ,"Structural System Reliability Analysis Method", John A. Blume Earthquake Engineering Centre, Stanford Univ., U.S.A., Report No.83, July 1987

[89] Marshall, P.W. and Bea, R.G. ,"Failure Modes of Offshore Platforms", Proc. 1st Intl. Conf. on Behavior of Offshore Structures (BOSS '76), Vol.2, the Norweigian Institute of Technology, Trondheim, 1976, pp.579-635

[90] Marshall, P.W. ,"Cost-Risk Trade-offs in Design, M.I.R.V., and Fracture Control for Offshore Platforms", Proc. 7th Intl. Ship Structures Congress, Joint Session, Paris, 1979

[91] Lloyd, J.R. and Clawson, W.C. ,"Reserve and Residual Strength of Pile Founded Offshore Platforms" in 'The Role of Design, Inspection and Redundancy in Marine Structural Reliability', D. Faulkner et al ed., National Academy Press, 1984, pp.157-198

[92] Paliou, C., Shinozuka, M. and Chen, Y-N. ,"Reliability Analysis of Offshore Structures", Proc. Marine Structural Reliability Symposium, The Ship Structure Committee and SNAME, Arlington, VA, Oct. 5-6, 1987, pp.143-157

[93] Nordal, H., Cornell, C.A. and Karamchandani, A. ,"A Structural System Reliability Care Study of an Eight-leg Steel Jacket Offshore Production Platform", Proc. Marine Structural Reliability Symposium, The Ship Structure Committee and SNAME, Arilington, VA, Oct. 5-6, 1987, pp.193-216

[94] Mistree, F. ,"Design of Damage Tolerant Structural Systems", Euromech Colloquium 164, Univ. of Siegan, W. Germany, 1982

[95] Mistree, F., Lyou, T.D. and Shupe, J.A. ,"Design of Damage Tolerant Offshore Structures", Proc. MTS - IEEE Oceans '82 Conf., Washington DC., Sept. 1982

[96] Plane, C.A., Cowling, M.J., Nwegbu, V. and Burdekin, F.M. ,"The Determination of Safety Factors for Defect Assessment Using Reliability Analysis Methods", Proc. 3rdIntl. Conf. on Integrity of Offshore Structures, Univ. of Glasgow, Sept. 28-29, 1987, Paper No.19, 1988, pp.395-420

[97] "Report of Committee 10 on Design Philosophy and Procedure", Proc. 7th Intl. Ship Structures Congress, Oslo, 1967

[98] Mansour, A.E. and Faulkner, D. ,"On Applying the Statistical Approach to Extreme Sea Loads and Ship Hull Strength", Trans. RINA, Vol.115, 1973, pp.277-314

[99] Faulkner, D. and Sadden, J.A. ,"Toward a Unified Approach to Ship Structural Safety", Trans. RINA, Vol.120, 1979, pp.1-28

[100] Faulkner, D. ,"Semi-Probabilistic Approach to the Design of Marine Structures", Intl. Symp. on the Extreme Loads Response, SNAME, Arlington, Va., Oct. 1981, pp.213-230

[101] Stiansen, S.G., Mansour, A., Jan, H.Y. and Thayamballi, A. ,"Reliability Methods in Ship Structures", Trans. RINA, Vol.121, 1980, pp.381-406

[102] Aldwinckle, D.S. and Pomery, R.V. ,"A Rational Assessment of Ship Reliability and Safety", Trans. RINA, Vol.124, 1983, pp.269-288

[103] Akita, Y. ,"Reliability Analysis of Ship Strength (4th Report) - Ultimate Longitudinal Strength due to Successive Collapse of Deck Plates Having Initial Deflection -", Trans. Society of Naval Arch. of Japan, No.158, Nov. 1986, pp.301-309 (in Japanese)

[104] Guedes Soares, C. and Moan, T. ,"Uncertainty Analysis and Code Calibration of the Primary Load Effects in Ship Structures", Proc. 4th Intl. Conf. on Structural Safety and Reliability, Vol.3, Kobe, Japan, May 1985, pp.501-512

[105] Mansour, Jan, H.Y., Zigelman, C.I., Chen, Y.N. and Harding,S.J. , "Implementation of Reliability Methods to Marine Structures", Trans. SNAME, Vol.92, 1984, pp.353-382

[106] Mansour, A.E. ,"Comparison of Three Reliability Methods as Applied to Ocean

Vessels", Proc. 4th Intl. Conf. on Structural Safety and Reliability, Vol.3, Kobe, Japan, May 1985, pp.523-532

[107] Thayamballi, A., Kutt,L. and Chen, Y.N. ,"Advanced Strength and Structural Reliability Assessment of the Ship's Hull Girder", Proc. Advances in Marine Structures, ARE, Dunfermline, Scotland, 20-23 May 1986, Paper No.7

[108] Edwards, G. ,"Some Recent Applications of Reliability Theory in Offshore Structural Engineering", Proc. 16th Offshore Technology Conference, OTC 4827, Houston, Texas, 1984, pp.427-432

[109] Moses, F. and Russell, L. ,"Applicability of Reliability Analysis in Offshore Design Practice", Final Report, API PRAC 79-22, American Petroleum Institute, 1980

[110] Moses, F. ,"Guidelines for Calibrating API RP2A for Reliability-Based Design", Final Report, API PRAC 80-22, American Petroleum Institute, Oct. 1981

[111] Moses, F. ,"Load and Resistance Factor Design - Recommended Practice for Approval", Final Report, API PRAC 86-22, American Petroleum Institute, Dec. 1986

[112] Bea, R.G. ,"Reliability Considerations in Offshore Platform Criteria", J. of Struct. Div., ASCE, Vol.106, No.ST9, 1980, pp.1835-1853

[113] Faulkner, D., Chen, Y.N. and de Oliveira, J.G. ,"Limit State Design Criteria for Stiffened Cylinders of Offshore Structures", ASME 4th National Congress of Pressure Vessels and Piping Technology, Portland, Or., June 1983, pp.1-11

[114] Das, P.K. and Frieze, P.A. ,"Application of an Advanced Level-II Reliability Analysis Procedure to the Safety Assessment of Stiffened Cylinders", Dept. of Naval Arch. and Ocean Engineering, Univ. of Glasgow Report, NAOE-82-08, March, 1982

[115] Det norske Veritas ,"Rules for the Design, Construction and Inspection of Offshore Structures, Appendix C: Steel Structures", DnV, Hovik, 1982

[116] Das, P.K. and Faulkner, D. ,"Safety Factor Evaluation for Cylindrical Components of Floating Platforms in Extreme Loads", Centenary Conf. on Marine Safety, Univ. of Glasgow, Sept. 1983, Paper No.17

[117] Maes, M.A. and Muir, L.R. ,"Choice of Design Formats for Offshore Codes", 6th Intl. Symp. on OMAE, Houston, Texas, March 1-6, 1987, pp.259-265

[118] Kenny, J.P. and Partners ,*Buckling of Offshore Structures*, Gulf Pub. Co., 1984

[119] Warwick, D.M. and Faulkner, D. ,"Strength of Tubular Members in Offshore Structures", Dept. of Naval Arch. and Ocean Engineering, Univ. of Glasgow Report, NAOE-88-36, June 1988

[120] Faulkner, D. ,"Compression Strength of Welded Grillages", Chapter 21 of 'Ship Structural Design Concepts', J.H.Evans ed., Cornell Maritime Press Inc., 1975, pp.633-712

[121] Crisfield, M.A. ,"Full-Range Analysis of Steel Plates and Stiffened Plating under Uni-axial Compression", Proc. Inst. of Civil Engrs., Part 2, Vol.59, 1975, pp.595-624

[122] Lee, J.-S. and Koo, J.-D. ,"Non-Linear Analysis of Ship's Structures", J. of Society of Naval Arch. of Korea, Vol.20, No.1, 1983, pp.11-20 (in Korean)

[123] Fujita, Y. ,"On the Non-linear Response of Ship Structural Elements", Univ. of Tokyo, 1977

[124] "Report of Committee II.2 on Non-Linear Structural Response", Proc. 9th Intl. Ship Structures Congress, Genova, 1985

[125] Lin, Y.T. ,"Ship Longitudinal Strength Modelling", Ph.D. Thesis, Dept. of Naval Arch. and Ocean Engineering, Univ. of Glasgow, March. 1985

[126] Ostapenko, A. ,"Strength of Ship Hull Girders under Moment, Shear and Torque", Intl. Symp. on the Extreme Loads Response, SNAME, Arlington, VA, Oct. 1981, pp.149-166

[127] Faulkner, J.A., Clarke, J.D., Smith, C.S. and Faulkner, D. ,"The Loss of HMS COBRA - A Reassessment", Trans. RINA, Vol.126, 1985, pp.125-151

[128] Lee, J.-S. ,"Pre- and Post-Ultimate Behaviour Analysis and Derivation of Strength Model of Rectangular Box Girder", Dept. of Naval Arch. and Ocean Engineering, Univ. of Glasgow Report, NAOE-87-27, May 1987

[129] Murotsu, Y., Kishi, M., Okada, H., Ikeda, Y. and Matsuzuki, S. ,"Probability Analysis of Ultimate Strength for Jacket-Type Offshore Platform", Trans. The West-Japan Society of Naval Arch., No.195, Dec. 1984, pp.95-106 (in Japanese)

[130] Murotsu, Y., Okada, H., Ikeda, Y. and Matsuzaki, S. ,"On the System Reliability of Semi-Submersible Platform", Proc. 3rd Intl. Symp. on Practical Design in Shipbuilding, Trondheim, June 1987, pp.752-764

[131] Frieze, P.A. ,"Design Implications of Reliability and Collapse Analysis of Mobile Units", Proc. 3rd Intl. Symp. on Practical Design in Shipbuilding , Trondheim, June 1987, pp.773-782

[132] Amdahl, J., Taby, J. and Granli, T. ,"Progressive Collapse Analysis of Mobile Platforms", Proc. 3rd Intl. Symp. on Practical Design in Shipbuilding , Trondheim, June 1987, pp.1060-1072

[133] Prucz, Z. and Soong, T.T. ,"Reliability and Safety of Tension Leg Platforms",

Engineering Structures, Vol.6, April 1984, pp.142-149

[134] Baker, M.J. and Ramachandran, K. ,"Reliability Analysis as a Tool in the Design of Fixed Offshore Platforms", Proc. 2 nd Intl. Symp. on Integrity of Offshore Structures, Glasgow, 1981, pp.135-153

[135] Smith, D., Csenki, A. and Ellinas, C.P. ,"Ultimate Limit State Analysis of Unstiffened and Stiffened Structural Components", Proc. 3 rd Intl. Conf. on Integrity of Offshore Structures, Univ. of Glasgow, Sept. 28-29, 1987, Paper No.7, pp.145-168

[136] Faulkner, D. ,"On Selecting a Target Reliability for Deep Water Tension Leg Platforms", Proc. 11th IFIP Conf. System Modelling and Optimization, Copenhagen, Denmark, July 25-29, 1983, pp.490-513

[137] Moses, F. and Stevenson, D. ,"Reliability-Based Structural Design", J. of Struct. Div., ASCE, Vol.96, No.ST2, Feb. 1970, pp.221-244

[138] Murotsu, Y. ,"Development in Structural Systems Reliability Theory", Nuclear Engineering and Design, Vol.94, 1986, pp.101-114

[139] Harbitz, A. ,"Efficient and Accurate Probability of Failure Calculation by Use of the Importance Sampling Technique", Proc. 4th Intl. Conf. on Applications of Statistics and Probability in Soil and Structural Engineering, Vol.2, Univ. of Firenze, Italy, June 13-17, 1983, pp.825-836

[140] Wirsching, P.H. and Chen, Y.N. ,"Considerations of Probability Based Fatigue Design for Marine Structures", Proc. Marine Structural Reliability Symposium, The Ship Structure Committee and SNAME, Arlington, VA, Oct. 5-6, 1987, pp.31-43

[141] Yamamoto, M. and Ang, A.H.-S. ,"Significance of Gross Errors on Reliability Structures", Proc. 4th Intl. Conf. on Structural Safety and Reliability, Vol.3, Kobe,

Japan, May 1985, pp.669-674

[142] Nessim, M. and Jordaan, I. ,"Models for Human Error in Structural Reliability", J. of Struct. Engg, Vol.111, No.6, 1985, pp.1358-1376

[143] Melchers, R.E. ,"Structural Reliability Assessment and Human Error", Proc. 5th Intl. Conf. on Applications of Statistics and Probability in Soil and Structural Engineering, Vol.1, Univ. of British Columbia, Vancouver, B.C., Canada, May 25-29, 1987, pp.46-54

[144] Shirashi, N., Furuta, H. and Sugimoto, M. ,"Effects of Gross Errors on Structural Design", Structural Safety, Vol.2, 1985, pp.245-250

[145] Shiraishi, N. and Furuta, H. ,"Reliability Analysis of Damaged Structures", Proc. 5th Intl. Conf. on Applications of Statistics and Probability in Soil and Structural Engineering, Vol.1, Univ. of British Columbia, Vancouver, B.C., Canada, May 25-29, 1987, pp.190-197

[146] Handa, K. and Anderson, K. ,"Application of Finite Element Methods in the Statistical Analysis of Structures", Proc. 3rd Intl. Conf. on Structural Safety and Reliability, Trondheim, 1981, pp.409-417

[147] Hisada, T. and Nakagiri, S. ,"Stochastic Finite Element Method Developed for Structural Safety and Reliability", Proc. 3rd Intl. Conf. on Structural Safety and Reliability, Trondheim, 1981, pp.395-408

[148] Vanmarcke, E.H., Shinozuka, M., Nakagiri, S., Schueller, G.I. and Grigoriu,M. ,"Random Field and Stochastic Finite Elements", Structural Safety, Vol.3, 1986, pp.143-166

[149] Chryssanthopoulos, M., Baker, M.J. and Dowling, P.J. ,"Reliability-Based

Design of Stringer-Stiffened Cylinders Under Axial Compression", 6th Intl. Symp. on OMAE, Houston, Texas, March 1-6, 1987, pp.403-411

[150] Vilmann, D. and Bjerager, P. ,"Boundary Element Method in Structural Reliability", Proc. 5th Intl. Conf. on Applications of Statistics and Probability in Soil and Structural Engineering, Vol.1, Univ. of British Columbia, Vancouver, B.C., Canada, May 25-29, 1987, pp.528-537

[151] Amdahl, J., Leira, B. and Wu, Y-L., "On the Application of a Non-linear Finite Element Formulation in Structural System Reliability", Proc. 1st Working Conf. on Reliability and Optimization of Structural Systems, Aalborg, Denmark, May 6-8, 1987, pp.1-19

[152] Hohenbichler, M. and Rackwitz, R. ,"Reliability of Parallel Systems Under Imposed Uniform Strain", J. of Engg. Mech., ASCE, Vol.109, No.3, June 1983, pp.896-907

[153] Der Kiureghian, A. and Taylor, R.L. ,"Numerical Methods in Structural Reliability", Proc. 4th Intl. Conf. on Applications of Statistics and Probability in Soil and Structural Engineering, Vol.2, Univ. of Firenze, Italy, June 13-17, 1983, pp.769-784

[154] Lee, J.-S. ,"Basic Study on the System Reliability Analysis of Floating Offshore Structures", Dept. of Naval Arch. and Ocean Engineering, Univ. of Glasgow, Progress Report, Nov. 1987 (unpublished)

[155] Murotsu, Y., Okada, H., Taguchi, K., Grimmeit, M. and Yonezawa, M. , "Automatic Generation of Stochastically Dominant Failure Modes of Frame Structures", Structural Safety, Vol.2, 1984, pp.17-25

[156] Guenard, Y., Goyet, J., Labeyrie, J. and Remy, B. ,"Structural Safety Evaluation

of Steel Jacket Platforms", Proc. Marine Structural Reliability Symp., The Ship Structure Committee and SNAME, Arlington, VA, Oct. 5-6, 1987, pp.169-183

[157] Ditlevsen, O. ,"Principle of Normal Tail Approximation", J. of Engg. Mech. Div., ASCE, Vol.107, No.EM6, Dec. 1981, pp.1191-1208

[158] Anderberg, M.R. ,*Cluster Analysis for Applications*, Academic Press, New York, 1973

[159] Ang, A. H-S. ,"Structural Risk Analysis and Reliability-Based Design", J. of Struct. Div., ASCE, Vol.99, No.ST9, Sept. 1973, pp.1891-1910

[160] Odland, J. and Faulkner, D. ,"Buckling of Curved Steel Structures - Design Formulations", Proc. 2nd Intl. Symp. on Integrity of Offshore Structures, Univ. of Glasgow, 1981, pp.419-443

[161] Faulkner, D. ,"Inelastic Interactive (Shell) Buckling", ABS-Conoco RCC Note, 13 Sep. 1983 (unpublished)

[162] Faulkner, D. and Warwick, D.M. ,"Predicting the Strength of Welded Stiffened Cylinders", Proc. Intl. Symp. Developments in Deep Waters, RINA, London, Oct. 1986

[163] Faulkner, D., Guedes Soares, C. and Warwick, D.M. ,"Modelling Requirements for Structural Design and Assessment", Proc. 3rd Intl. Conf. on Integrity of Offshore Structures, Univ. of Glasgow, Sep. 28-29, 1987, Paper No.2, pp.25-54

[164] Yim, S.-J., Kwak, B.-M. and Lee, J.-S. ,*Introduction to the Finite Element Method*, Dong-Myung Pub. Co., Jan. 1985 (in Korean)

[165] Ranganathan, R. and Deshpande, A.G. ,"Generation of Dominant Modes and

Reliability Analysis of Frames", Structural Safety, Vol.4, 1987, pp.217-228

[166] Lee, J.-S. and Faulkner, D. ,"Answer to the Questions by Reviewers on Reference [74]", Nov., 1988

[167] Timoshenko, S.P. and Wonowsky-Krieger, S. ,*Theory of Plate and Shell*, McGraw-Hill, Inc., 1956

[168] Chajes, A. ,*Principles of Structural Stability Theory*, Prentice-Hall, Inc., 1974

[169] Odland, J. ,"Buckling of Unstiffened and Stiffened Circular Cylindrical Shell Structures", Norwegian Maritime Research, Vol.6, No.3, 1978, pp.2-22

[170] Frieze, P.A., Cho, S.-R. and Faulkner, D. ,"Strength of Ring Stiffened Cylinders Under Combined Loads", Proc. 16th Offshore Technology Conf. OTC 4714, Houston, Texas, 1984

[171] Cho, S.-R. and Frieze, P.A. ,"Derivation of a Strength Formulation for Ring Stiffened Shells Subjected to Combined Axial Loading and Radial Pressure", Dept. of Naval Arch. and Ocean Engineering, Univ. of Glasgow Report, NAOE-86-23, Feb. 1986

[172] Guedes Soares, C. and Søreide, T.H. ,"Behaviour and Design of Stiffened Plates under Predominantly Compressive Loads", Intl. Shipbuilding Progress, Vol.30, 1982, pp.13-27

[173] Søreide, T.H. and Czujko, J. ,"Load Carrying Capacities of Plates under Combined Lateral Load and Axial / Biaxial Compression", Proc. 2nd Intl. Symp. on Practical Design in Shipbuilding, 1983, Tokyo and Seoul, pp.493-500

[174] Faulkner, D. ,"A Review of Effective Plating for Use in the Analysis of Stiffened

Plating in Bending and Compression", J. of Ship Research, Vol.19, No.1, March 1975, pp.1-17

[175] Lee, J.-S. ,"Compressive Ultimate Strength Analysis of Plates with Initial Imperfections", J. of Society of Naval Arch. of Korea, Vol.22, No.1, 1985, pp.31-37 (in Korean)

[176] Dowling, P.J., Chatterjee, S. Frieze, P.A. and Moolani, F.M. ,"Experimental and Predicted Collapse Behaviour of Rectangular Steel Box Girders", Proc. Intl. Conf. on Steel Box Girder Bridges, The Inst. of Civil Engrs, London, Feb. 1973

[177] "Report of Committee II.2 on Nonlinear Structural Response", Proc. 7th Intl. Ship Structures Congress, Paris, 1979

[178] Dow, R.S., Hugill, R.C., Clarke, J.D. and Smith, C.S. ,"Evaluation of Ultimate Ship Hull Strength", Intl. Symp. on the Extreme Loads Response, SNAME, Arlington, VA, Oct. 1981, pp.133-148

[179] "British Standard BS 5400 : Part 3 ", 1982

[180] Carlsen, C.A. ,"A Parametric Study of Collapse Behaviour of Rectangular Steel Box Girders", The Structural Engineers., Vol.56b, 1980, pp.33-40

[181] Galambos, T.V. ,"Reliability of Axially Loaded Columns", Engineering Structures, Vol.5, Jan. 1983, pp.73-78

[182] Faulkner, D. ,"Compression Tests on Welded Eccentrically Stiffened Plate Panels" in 'Steel Plated Structures ', P.J. Dowling et al ed., 1977, pp.581-617

[183] Horne, M.R. and Narayanan, R. ,"Ultimate Capacity of Stiffened Plates Used in Box Girders" Proc. Inst. of Civil Engrs., Vol.61, 1976, pp.253-280

[184] Horne, M.R., Montague, P. and Narayanan, R. ,"Influence on the Strength of Compression Panels of Stiffeners Section, Spacing and Welded Connection", Proc. Inst. of Civil Engrs., Vol.63, Part 2, 1977, pp.1-20

[185] Smith, C.S. ,"Compressive Strength of Welded Steel Ship Grillages", Trans. RINA, Vol.117, 1975, pp.325-359

[186] Vasta, J. ,"Lessons Learned from Full Scale Structural Tests", Trans. SNAME, Vol.68, 1973

[187] Caldwell, J.B. ,"Ultimate Longitudinal Strength", Trans. RINA, Vol.107, 1965

[188] Wong, Y.L. ,"Some Consideration in the Ultimate Strength of Ships", M.Sc. Thesis, Dept. of Naval Arch. and Ocean Engineering, Univ. of Glasgow, 1977

[189] Chen, Y.N., Liu, D. and Shin, Y.S. ,"Probabilistic Analysis of Environmental Loading and Motion of a Tension Leg Platform for Reliability-Based Design", Centenary Conference on Marine Safety, Univ. of Glasgow, Sept. 1983, Paper No.17

[190] Maruo, H. ,"The Drift of a Body Floating on Waves", J. of Ship Research, Vol.4, No.3, Dec. 1960, pp.1-10

[191] Morison, J.R., O'Brien, M.P., Johnson, J.W. and Schaaf, S.A. ,"The Force Exerted by Surface Wave on Piles", Petroleum Trans., AIME, Vol.189, 1950, pp.149-157

[192] Zienkiewicz, O.C., Lewis, R.W. and Stagg, K.G. ,*Numerical Methods in Offshore Engineering*, John Wiley & Sons Inc., 1978

[193] Sarpkaya, T. and Isaacson, M. ,*Mechanics of Wave Forces on Offshore Structures*, Van Nostrand Reinhold Co., 1981

[194] Chakrabarti, S.K. ,*Hydrodynamics of Offshore Structures*, Computational Mechanics Pub., 1987

[195] Bea, R.G. and Lai, N.W. ,"Hydrodynamic Loadings on Offshore Platforms", Proc. 10th Offshore Technology Conf., OTC 3064, Houston, Texas, 1978, pp.155-167

[196] Denise, J-P.F. and Heaf, N.J. ,"Comparison between Linear and Non-linear Response of a Proposed Tension Leg Production Platform", Proc. 11th Offshore Technology Conf., OTC 3555, Houston, Texas, 1979, pp.1743-1754

[197] Stiansen, S.G. and Chen, H.H. ,"Computational Methods for Predicting Motions and Dynamic Loads of Tension-Leg Platforms", Proc. 2nd Intl. Conf. on Integrity of Offshore Structures, Univ. of Glasgow, 1981, pp.1-13

[198] Paulling, J.R. ,"The Sensitivity of Predicted Loads and Responses of Floating Platforms to Computational Methods", Proc. 2nd Intl. Conf. on Integrity of Offshore Structures, Univ. of Glasgow, 1981, pp.51-69

[199] Yoshida, K. and Ozaki, M. ,"A Dynamic Response Analysis Method of Tension Leg Platforms", J. of the Faculty of Engineering, Univ. of Tokyo, Vol.37, No.4, 1984, pp.885-919

[200] Eatock Taylor, R. and Jefferys, E.R. ,"Variability of Hydrodynamic Load Predictions for a Tension Leg Platform", Ocean Engineering, Vol.13, No.5, 1986, pp.449-490

[201] Stansby, P.K. and Isaacson, M. ,"Recent Developments in Offshore Hydrodynamics : Workshop Report", Applied Ocean Research, Vol.9, No.3, 1987, pp.118-127

[202] Bishop, R.E.D. and Price, W.G. ,*Hydroelasticity of Ships*, Cambridge Univ. Press, 1979

[203] Malhotra, A.K. and Penzien, J. ,"Nondeterministic Analysis of Offshore Structures", J. of Engg. Mech. Div., ASCE, No.EM6, Dec. 1970

[204] Chakrabarti, S.K. ,"Discussion on Reference [203]", J. of Engg. Mech. Div., ASCE, No.EM3, June 1971

[205] Chou, F.S., Ghosh, S. and Huang, E.W. ,"Conceptual Design Process of a Tension Leg Platform", Trans. SNAME, Vol.91, 1983, pp.275-305

[206] Det norske Veritas ,"Rules for Classification of Mobile Offshore Units", DnV, Oslo, 1981

[207] Faulkner, D. ,"Tension Leg Platforms - From Hutton to Jolliet" or "Deep Water without Deep Pockets", Dept. of Naval Arch. and Ocean Engineering, Univ. of Glasgow Report, NAOE-88-26, April 1988

[208] Chung, J.S. ,"Offshore and Arctic Frontier : Structures, Ocean Mining", Mechanical Engineering, May 1985, pp.55-63

[209] "Tying down the Next Generation of TLP", Offshore Engineer, April, 1987, p.24

[210] Srokosz, M.A. and Challenor, P.G. ,"Joint Distributions of Wave Height and Period : A Critical Comparison", Ocean Engineering, Vol.14, No.4, 1987, pp.295-311

[211] Ellis, N., Tetlow, J., Anderson, D. and Woodhead, L. ,"Hutton TLP Vessel - Structural Configuration and Design Features", Proc. 14th Offshore Technology Conf., OTC 4427, Houston, Texas, 1982, pp.557-571

[212] Mercier, J.A., Leverette, S.J. and Bliault, A.L. ,"Evaluation of Hutton TLP Response to Environmental Loads", Proc. 14th Offshore Technology Conf., OTC 4429, Houston, Texas,1982, pp.585-601

[213] Das, P.K., Frieze, P.A. and Faulkner, D. ,"Structural Reliability Modelling of Stiffened Components of Floating Structures", Structural Safety, Vol.2, 1984, pp.4-16

[214] Bjerager, P. ,"Reliability Analysis of Structural Systems", Ph.D. Thesis, Dept. of Structural Engineering, Technical University of Denmark, Jan. 1984

[215] Hilton, H.H. and Feigen, H. ,"Minimum Weight Analysis Based on Structural Reliability", J. of the Aerospace Science, Vol.27, 1960, pp.641-653

[216] Prasad, B. and Emerson, J.F. ,"Optimal Structural Remodelling of Multi-Objective Systems", Computers & Structures, Vol.18, No.4, 1984, pp.619-628

[217] Gallagher, R.H. and Zienkiewicz, O.C. ,*Optimal Structural Design - Theory and Application* -, John Wiley & Sons, Inc., 1973

[218] *Engineering Design Handbook ; Computer Aided Design of Mechanical Systems*, AMC Pamphlet No.706-192, 1973

[219] Holman, J.P. ,*Numerical Optimization Techniques for Engineering Design*, McGraw-Hill, Inc., 1984

[220] Sadek, E.A. ,"Application of Methods of Feasible Directions to Structural Optimization Problems", Computers & Structures, Vol.17, No.2, 1983, pp.183-191

[221] Gavarini, D. ,"Stochastic Programming - A Discussion", in Reference [217], 1973, pp.261-264

APPENDIX A EXAMPLE OF DERIVATION OF THE SAFETY MARGIN EQUATION

A plane frame in Fig. 2.7 of Section 2.6.2 is taken as a structural model to illustrate the present procedure for deriving the safety margin equation for the structure under the multiple loading condition. The safety margin of one important failure mode for path 4-7-8-2 [see Section 2.6.2] in the structure will be derived in the form of Eqs.(2.86) and (2.103):

$$Z_m = \sum_{k=1}^{j} C_{mk} R_k - \sum_{l=1}^{L} B_{ml} P^{(l)} \tag{2.86}$$

$$Z_m' = X_{M_j} + \sum_{k=1}^{j-1} G_k(\{R\}_k, \{R\}_j) - \sum_{l=1}^{L} G_l(\{Q\}_l, \{R\}_j) \tag{2.103}$$

A.1 Safety Margin in the form of Eq.(2.86)

The utilisation matrices for loading $P^{(1)}$ and $P^{(2)}$ of the failure mode for path 4-7-8-2 and their inverses are given as in Table A.1 in which the element of the utilisation matrix is the bending moment of each component. Firstly, consider the interim path, 4-7-8. Each utilisation matrix is rewritten as follows from Table A.1 (a).

[for $P^{(1)}$]

$$\begin{matrix} 4 \\ 7 \\ 8 \end{matrix}\begin{bmatrix} 0.0013 & & \\ 0.9982 & 0.9996 & \\ 1.4971 & -1.4977 & 2.4973 \end{bmatrix}$$

[for $P^{(2)}$]

$$\begin{matrix} 4 \\ 7 \\ 8 \end{matrix}\begin{bmatrix} 1.5631 & & \\ 0.9369 & 2.5000 & \\ 0.4670 & 1.2460 & 3.7460 \end{bmatrix}$$

The contribution factor for each loading case is calculated as below:

$$\text{for } P^{(1)} : CF^{(1)} = 2.4973 / (2.4973 + 3.7460) = 0.4$$
$$\text{for } P^{(2)} : CF^{(2)} = 3.7460 / (2.4973 + 3.7460) = 0.6 \qquad \text{(A-1)}$$

From Table A.1(b), the inverse of each matrix is:

[for $P^{(1)}$]

	7	4	8
	746.91		
	-745.90	1.0004	
	-0.4033	-0.6000	0.4004

[for $P^{(2)}$]

	7	4	8
	0.6398		
	-0.2398	0.4000	
	0.210E-05	-0.1331	0.2670

For loading $P^{(1)}$, the resistance terms are obtained in the following procedure.

By summing up the elements in each column,

$$0.6067\ R_4 + 0.4004\ R_7 + 0.4004\ R_8 \qquad \text{(A-2)}$$

is obtained and normalising by the coefficient of the last failed component, i.e. coefficient of R_8, (A-2) becomes

$$1.5152\ R_4 + 1.0000\ R_7 + 1.0000\ R_8 \qquad \text{(A-3)}$$

By multiplying the contribution factor, $CF^{(1)} = 0.4$, the resistance terms for load $P^{(1)}$ are obtained as:

$$0.6061\ R_4 + 0.4000\ R_7 + 0.4000\ R_8 \qquad \text{(A-4)}$$

Similarly for load $P^{(2)}$, the resistance terms are obtained as follows:

Sum the elements in each column of the inverse matrix :

$$0.4000\ R_4 + 0.2670\ R_7 + 0.2670\ R_8 \qquad \text{(A-5)}$$

Normalising by the coefficient of the last failed component:

$$1.4981\ R_4 + 1.0000\ R_7 + 1.0000\ R_8 \qquad \text{(A-6)}$$

and multiplying by the contribution factor, $CF^{(2)} = 0.6$ gives the resistance terms for load $P^{(2)}$:

$$0.8989\ R_4 + 0.6000\ R_7 + 0.6000\ R_8 \qquad \text{(A-7)}$$

Sum of (A-4) and (A-7) results in the resistance terms of the safety margin for the interim path 4-7-8.

$$1.5050\ R_4 + 1.0000\ R_7 + 1.0000\ R_8 \qquad \text{(A-8)}$$

Loading terms are easily obtained from the utilisation matrices of path 4-7-8:

$$-\left(2.4973\ P^{(1)} + 3.7460\ P^{(2)}\right) \qquad \text{(A-9)}$$

Combining (A-8) and (A-9) gives the safety margin equation of path 4-7-8:

$$\begin{aligned} Z_{7\text{-}4\text{-}8} = {} & 1.5050\ R_4 + 1.0000\ R_7 + 1.0000\ R_8 \\ & -\left(2.4973\ P^{(1)} + 3.7460\ P^{(2)}\right) \end{aligned} \qquad \text{(A-10)}$$

The corresponding reliability index of path 4-7-8 is $\beta_{4\text{-}7\text{-}8} = 2.07$.

This path does not result in the collapse of the structure. When component 2 has failed, the collapse occurs. The resistance and loading terms are obtained in the same way as before. The safety margin of the mode for path 4-7-8-2 can be derived through the following procedure:

[1] Contribution factor of each loading case is calculated as:

for $P^{(1)}$: $CF^{(1)} = 0.270 \times 10^{-4} / (0.270 \times 10^{-4} + 5.0002) = 0.540 \times 10^{-5}$

for $P^{(2)}$: $CF^{(2)} = 5.0002 / (0.270 \times 10^{-4} + 5.0000)$

$= 0.9999946$ (A-11)

[2] Sum of the elements in each column of the inverse matrices:

for $P^{(1)}$: $75201\ R_4 + 37282\ R_7 + 0.17797\ R_8 + 37282\ R_2$

for $P^{(2)}$: $0.4000\ R_4 + 0.2000\ R_7 + 0.596 \times 10^{-7}\ R_8 + 0.2000\ R_2$

[3] Normalising the coefficients by that of component 2:

for $P^{(1)}$: $2.0171\ R_4 + 1.0000\ R_7 + 0.477 \times 10^{-5}\ R_8 + 1.0000\ R_2$

for $P^{(2)}$: $2.0000\ R_4 + 1.0000\ R_7 + 0.298 \times 10^{-6}\ R_8 + 1.0000\ R_2$

[4] Multiplying by the contribution factors:

for $P^{(1)}$: $0.109 \times 10^{-4}\ R_4 + 0.540 \times 10^{-5}\ R_7 + 0.258 \times 10^{-10}\ R_8$

$+ 0.540 \times 10^{-5}\ R_2$ (A-12)

for $P^{(2)}$: $2.0000\ R_4 + 1.0000\ R_7 + 0.298 \times 10^{-6}\ R_8 + 1.0000\ R_2$ (A-13)

Comparing (A-12) with (A-13), the resistance term for load $P^{(1)}$ can be neglected. This can also be seen from the contribution factors in Eq.(A-11). Therefore, the resistance terms of the safety margin equation for the path 4-7-8-2 is

$2.0000\ R_4 + 1.0000\ R_7 + 0.298 \times 10^{-6}\ R_8 + 1.0000\ R_2$ (A-14)

Loading terms of path 4-7-8-2 from the utilisation matrix are:

$$-\left(0.268 \times 10^{-4}\, P^{(1)} + 5.0002\, P^{(2)} \right) \qquad \text{(A-15)}$$

The resultant safety margin equation of path 4-7-8-2 is obtained by combining (A-14) and (A-15):

$$\begin{aligned} Z_{4\text{-}7\text{-}8\text{-}2} &= 1.0000\, R_2 + 2.0000\, R_4 + 1.0000\, R_7 + 0.298 \times 10^{-6}\, R_8 \\ &\quad - 0.268 \times 10^{-4}\, P^{(1)} - 5.0002\, P^{(2)} \\ &\cong 1.0000\, R_2 + 2.0000\, R_4 + 1.0000\, R_7 - 5.0002\, P^{(2)} \qquad \text{(A-16)} \end{aligned}$$

As seen in this equation the strength of component 8 and load $P^{(1)}$ do not affect the safety margin as random variables. Hence, although the resultant path is 4-7-8-2, the component 8 does participate in the collapse mechanism. This type of hinge is referred to as a non-active hinge and the others are referred to as active hinges [see Fig.2.8]. But at the interim failure stage, i.e. path 4-7-8, component 8 is an active hinge and load $P^{(1)}$ also plays the role of a random variable.

The modes for path 7-4-8-2, 7-4-2, 7-8-4-2 and 4-7-2 have the same safety margin as Eq.(A-16). The corresponding reliability of path 4-7-8-2 is $\beta_{4\text{-}7\text{-}8\text{-}2} = 2.48$. This equation is exactly the same as that derived by the element replacement method (see Table 7.2.4 of reference [13]).

Table A.1 Utilisation Matrix of Frame Model and its Inverse for Path 4-7-8-2 in Terms of Bending Moment

(a) Utilisation Matrix

[for $P^{(1)}$] :

4	0.0013			
7	0.9982	0.9996		
8	1.4971	1.4977	2.4973	
2	-1.0009	-0.9996	0.149E-04	0.268E-04

[for $P^{(2)}$] :

4	1.5631			
7	0.9369	2.5000		
8	0.4670	1.2460	3.7460	
2	0.9369	2.5000	5.0002	5.0002

(b) Inverse of the Utilisation Matrix

[for $P^{(1)}$] :

7	4	8	2
746.91			
-745.90	1.0004		
-0.4033	-0.6000	0.4004	
75200.	37282.	-0.2225	37282.

[for $P^{(2)}$] :

7	4	8	2
0.6398			
-0.2398	0.4000		
0.210E-05	-0.1331	0.2670	
0.284E-06	-0.0669	-0.2670	1.9999

A.2 Safety Margin in the form of Eq.(2.103)

The procedure of deriving the safety margin in form of Eq.(2.103) is the same as in the previous section, except that the elements of the utilisation matrix represent the utilised proportion of component strengths and not any physical quantity, say, bending moments.

Consider the same mode for path 4-7-8-2 as in the previous section. The elements of the utilisation matrix in Table A.1 are bending moments. Let them be denoted as $S_{ki}^{(1)}$ which is the bending moment of component k at the i th incremental stage due to the unit load of $P^{(1)}$. When using Eq.(2.103), the elements of the utilisation matrix are the utilised strengths at any incremental stage and are calculated from the given strength formula. In the model considered, the strength modelling is given as Eq.(2.120) [Section 2.6.2]:

$$Z_k'(X_M, \{R\}, \{Q\}) = X_{M_k} - \frac{Q_k}{R_k} \qquad (2.120)$$

where k is referred to as the component number. The function G in Eq.(2.98.b) [Section 2.4.2] is Q_k / R_k. Then, the element of the utilisation matrix is modified such that it represents the mean utilised proportion of the component strength. Q_k in the above equation is the actual value of bending moment applied on component k due to mean load, i.e. $Q_k = S_{ki}^{(1)} * \underline{P}^{(1)}$. Hence, the elements of the utilisation matrices in Table A.1 (a) are recalculated by the following equation :

$$a_{ki}^{(1)} = \frac{S_{ki}}{\underline{R}_k} \underline{P}^{(1)} \qquad (A\text{-}17)$$

where $\underline{R}_k$ denotes the mean strength of component k and $\underline{P}^{(1)}$ the mean value of $P^{(1)}$, k denotes the failed component numbers, i.e. k = 4, 7, 8 and 2 when i = 1, 2, 3 and 4 respectively. The mean values are given as [see Fig. 2.7]:

$\underline{R}_2 = 0.075$ $\underline{P}^{(1)} = 0.02$

$\underline{R}_4 = 0.101$ $\underline{P}^{(1)} = 0.04$

$\underline{R}_7 = 0.075$

$\underline{R}_8 = 0.075$

By applying Eq.(A-17) to all elements of the utilisation matrices in Table A.1 (a), the new utilisation matrices and their inverses are given in Table A.2.

The contribution factor of each loading case is calculated as:

$$\text{for } P^{(1)}: \; CF^{(1)} = 0.715 \times 10^{-5} / (0.715 \times 10^{-5} + 2.6667)$$
$$= 0.268 \times 10^{-5} \cong 0.0$$
$$\text{for } P^{(2)}: \; CF^{(2)} = 2.6667 / (0.715 \times 10^{-5} + 2.6667)$$
$$= 1.0 - 0.268 \times 10^{-5} \cong 1.0$$

As mentioned in the previous section, the contribution factor for load $P^{(1)}$ is so small that the resistance and loading coefficients associated with the load can be neglected. Hence, the load case is not considered. As before, the safety margin is derived as follow:

[1] Sum of the elements in each column of inverse matrices:

$$1.0100 \; R_4' + 0.3750 \; R_7' + 0.298 \times 10^{-6} \; R_8' + 0.3750 \; R_2'$$

[2] Normalising the coefficients by that of component 2:

$$2.6933 \; R_4' + 1.0000 \; R_7' + 0.795 \times 10^{-6} \; R_8' + 1.0000 \; R_2' \qquad \text{(A-18)}$$

[3] Loading terms are:

$$- (0.715 \times 10^{-5} \; P^{(1)'} + 2.6667 \; P^{(2)'}) \qquad \text{(A-19)}$$

By combining (A-18) and (A-19) the safety margin equation of path 4-7-8-2 is given as:

$$Z'_{4\text{-}7\text{-}8\text{-}2} = 1.0000\,R_2' + 2.6933\,R_4' + 1.0000\,R_7' + 0.795 \times 10^{-6}\,R_8' - (0.715 \times 10^{-5}\,P^{(1)'} + 2.6667\,P^{(2)'}) \cong 1.0000\,R_2' + 2.6933\,R_4' + 1.0000\,R_7' - 2.6667\,P^{(2)'} \quad \text{(A-20)}$$

in which R_k' effectively represents the strength of component k such that the coefficient of R_k' denotes the term associated with component k.

According to Eq.(2.103) the resistance term of the last failed component in the path is replaced by its strength modelling parameter, i.e. R_2' is replaced by X_{M_2}. Hence, the safety margin is finally given by:

$$Z'_{4\text{-}7\text{-}8\text{-}2} = X_{M_2} + 2.6933\,R_4' + 1.0000\,R_7' - 2.6667\,P^{(2)'} \quad \text{(A-21)}$$

In the above equation, each term shows that it is associated with the random variable in strength and load, i.e. each term is treated as a random variable and its coefficient denotes the mean value of each term, e.g. 2.0000 in the second term is the mean value of the term, $2.0000\,R_4'$, because the equation has been derived based on the mean utilisation matrix for each loading case. The corresponding coefficient of variation can be calculated using the first-order reliability concept. The following describes how to calculate COV's of associated terms as random variables.

Eq.(A-21) can be deduced from Eq.(A-16) without any loss of physical meaning. Normalising all terms in Eq.(A-16) by the final term results in:

$$Z'_{4\text{-}7\text{-}8\text{-}2} = 1.0000\left(\frac{R_2}{R_2}\right) + 2.0000\left(\frac{R_4}{R_2}\right) + 1.0000\left(\frac{R_7}{R_2}\right) - 5.0002\left(\frac{P^{(2)}}{R_2}\right) \quad \text{(A-22)}$$

Each term in this equation can be regarded as a random function and its mean and COV are calculated by the first-order reliability method. For this, consider a simple function :

$$G(X, Y) = C - \frac{X}{Y} \tag{A-23}$$

in which C is a constant and X and Y are random variables with mean and standard deviation of ($\underline{X}$, σ_X) and ($\underline{Y}$, σ_Y). The mean of function G is obtained from Eq.(2.104.a):

$$\underline{G}(X, Y) = C - \frac{\underline{X}}{\underline{Y}} \tag{A-24}$$

The variance is obtained from Eq.(2.104.b):

$$\sigma_G^2 = \left[-\frac{CY\sigma_X}{X^2}\right]^2 + \left[\frac{C\sigma_Y}{X}\right]^2 \tag{A-25}$$

Let V_X and V_Y be COVs of X and Y. Putting $\sigma_X = V_X \underline{X}$ and $\sigma_Y = V_Y \underline{Y}$ in the above equation:

$$\sigma_G^2 = \left[\frac{C\underline{Y}}{\underline{X}}\right]^2 + \left[V_X^2 + V_X^2\right]^2 \tag{A-26}$$

Hence, the COV of the function G is given by :

$$V_G = \frac{\sigma_G}{\underline{G}} = \sqrt{V_X^2 + V_Y^2} \tag{A-27}$$

Using Eq.(A-24) and (A-27) the mean and COV of each term in Eq.(A-22) can easily be calculated. Except the first term (which will be replaced by the strength modelling parameter) they are given by:

	Mean	COV
$2.0000 * R_4 / R_2 =$	2.6933	0.0707
$1.0000 * R_7 / R_2 =$	1.0000	0.0707
$5.0002 * P^{(2)} / R_2 =$	2.6667	0.3041

And, let us introduce another set of variables defined as:

$$R_2' = R_2 / R_2 \quad R_4' = R_4 / R_2 \quad R_7' = R_7 / R_2 \quad P^{(2)'} = P^{(2)} / R_2$$

which merely represent the relationship with terms in Eq.(A-22). Eq.(A-22) can be rewritten as:

$$Z_{4\text{-}7\text{-}8\text{-}2}' = 1.0000\, R_2' + 2.6933\, R_4' + 1.0000\, R_7' - 2.6667\, P^{(2)'} \qquad \text{(A-28)}$$

i.e. the coefficients are the mean value of random functions and R_2' etc indicates that they are associated with the first term, etc. of which means and COV's are given as unity and zero so as not to disturb the safety margin equation.

Replacing the first term by its strength modelling parameter, Eq.(A-28) becomes

$$Z_{4\text{-}7\text{-}8\text{-}2}' = X_{M_2} + 2.6933\, R_4' + 1.0000\, R_7' - 2.6667\, P^{(2)'} \qquad \text{(A-29)}$$

This is the same as Eq.(A-21). It can, therefore, be said that Eq.(A-21) is equivalent to Eq.(A-16) and can replace Eq.(A-16) without loss of any physical meaning. Eq.(A-21) gives the path reliability index of $\beta_{4\text{-}7\text{-}8\text{-}2} = 2.46$, which is 1.2% less than than Eq(A-16).

Table A.2 Utilisation Matrix of Frame Model and its Inverse for Path 4-7-8-2 in Terms of Utilised Strength

(a) Utilisation Matrix

[for $P^{(1)}$] :

$$\begin{matrix} 4 \\ 7 \\ 8 \\ 2 \end{matrix} \begin{bmatrix} 0.265E\text{-}03 & & & \\ 0.2662 & 0.2666 & & \\ 0.3992 & 0.3994 & 0.6659 & \\ -0.2669 & -0.2666 & 0.397E\text{-}05 & 0.715E\text{-}05 \end{bmatrix}$$

[for $P^{(2)}$] :

$$\begin{matrix} 4 \\ 7 \\ 8 \\ 2 \end{matrix} \begin{bmatrix} 0.6190 & & & \\ 0.4996 & 1.3333 & & \\ 0.2490 & 0.6645 & 1.9978 & \\ 0.4997 & 1.3333 & 2.6667 & 2.6667 \end{bmatrix}$$

(b) Inverse of the Utilisation Matrix

[for $P^{(1)}$] :

$$\begin{matrix} 7 & 4 & 8 & 2 \end{matrix}$$
$$\begin{bmatrix} 3771.9 & & & \\ -3766.8 & 3.7516 & & \\ -2.0366 & -2.2500 & 1.5017 & \\ 0.380E+06 & 0.140E+06 & -0.8342 & 0.140E+06 \end{bmatrix}$$

[for $P^{(2)}$] :

$$\begin{bmatrix} 1.6154 & & & \\ -0.6054 & 0.7500 & & \\ 0.549E\text{-}05 & -0.2495 & 0.5006 & \\ 0.568E\text{-}06 & -0.1255 & -0.5006 & 0.3750 \end{bmatrix}$$

APPENDIX B EXAMPLE OF CALCULATING TOTAL LOAD FACTOR

Calculation of the total load factor described in Section 2.4.1 is illustrated for the frame model chosen in Appendix-A.

Since the elements of the utilisation matrices in Table A.2(a) are mean utilised strengths, the sum of the two utilisation matrices result in the total mean utilisation matrix as:

$$[\underline{A}] = \begin{bmatrix} 0.6193 & & & \\ 0.7659 & 1.6000 & & \\ 0.6483 & 1.0639 & 2.6637 & \\ 0.2328 & 1.0677 & 2.6667 & 2.6667 \end{bmatrix}$$

and its inverse is:

$$[\underline{A}]^{-1} = \begin{bmatrix} 1.6147 & & & \\ -0.7730 & 0.6251 & & \\ -0.0842 & -0.2497 & 0.3754 & \\ 0.2525 & -0.0004 & -0.3754 & 0.3750 \end{bmatrix}$$

As described in section 2.4.1, the total load factor for a failure mode can be obtained as the sum of all load factors calculated from Eq.(2.90). For the mode of path 7-4-8-2, λ_i (i = 1,4) are calculated as:

$\lambda_1 = 1.6147$ $\lambda_2 = -0.1479$

$\lambda_3 = 0.0415$ $\lambda_4 = 0.2517$

where subscript i = 1, . ., 4 indicates the incremental stage. With these Eq.(2.95) gives the total load factor:

$$\lambda_T = \sum_{i=1}^{4} \lambda_i$$

$$= 1.6147 - 0.1479 + 0.0415 + 0.2517 = 1.76 \qquad \text{(B-1)}$$

The central load factor, λ_{CLF} can be calculated from Eq.(5.1) with the safety margin equation, (A-16) or (A-21). When using Eq.(A-16), the mean values of random variables are to be substituted, whereas they are already included in Eq.(A-21). For the mode considered, λ_{CLF} is obtained from Eq.(5.1) with Eq.(A-21). That is:

$$\lambda_{CLF} = \frac{\underline{X}_{M_2} + 2.6933 + 1.0000}{2.6667} = 1.76 \qquad \text{(B-2)}$$

where $\underline{X}_{M_2}$ is the mean bias of the strength modelling parameter of component 2 and equals 1.0 [Section 2.6.2]. For this example the two factors have the same value.

APPENDIX C EXAMPLE OF IDENTIFICATION OF THE IMPORTANT FAILURE MODES

The plane truss model in Fig. 2.6 of Section 2.6.1 is selected to show the present procedure for identifying the most important failure modes given that $\varepsilon_{sys} = 0.03$ and $\varepsilon_{utr} = 10^{-3}$ [Section 2.5.6]. For this simple structure, specifying the values of ε_{det}, M_{min}, N_{max} etc. may be meaningless. The following, together with Fig. C.1, describes the identifying procedures.

[a] At first, probabilities of failure for components are evaluated, as seen in Fig. C.1(a). Components 3 and 4 have the highest probabilities, and component 3 is selected as a focus component. This is PATH-A as denoted in Section 2.5.6. Because of the comparatively small utilisation of Components 2 and 5, the subsequent modes following these components are discarded.

[b] When component 3 has failed, $N_{max} = 2$ and the possible failure paths of which $N_i = N_{max}$ are 3-1, 3-2, 3-4, 3-5 and 3-6, but path 3-5 and 3-6 are discarded during the formation procedure of the utilisation matrix. Among the remaining paths, path 3-4 has the highest value of failure probability of which $N_i = N_{max}$ and is PATH-A [Fig. C.1(b)]. Then, focus is shifted to the path of Component 4 where its $N_i < N_{max}$. This is PATH-B as denoted in Section 2.5.6. Hereafter, the discarded paths do not appear in the figure.

[c] In Fig.C.1(c), when Component 4 has failed, the paths of which $N_i = N_{max}$ and at the same time have the highest failure probability, are 3-4 and 4-3. When path 3-4 has been selected as the best candidate path (PATH-A), the focus component is No.4, but among the other paths there is no path which has component 4 (as the last failed component) and at the same time of which $N_i < N_{max}$, i.e. $N_i = 1$ because $N_{max} = 2$, and so, structural analysis is performed with failed components 3 and 4. The path leads to collapse and becomes the most important failure mode and the path is closed. The

bounds of β_{sys} are simply its path reliability index:

$$(\beta_{sys,lower})_1 = (\beta_{sys,upper})_1 = 2.25 \qquad \text{(C-1)}$$

[d] Among the remaining paths which are neither closed nor discarded, path 4-3 has the highest probability of failure and focus component is No.3. Since there is no path which has component 3 (as the last failed component) and of which $N_i < N_{max}$, i.e. $N_i = 1$ because $N_{max} = 2$, path 4-3 path is selected. Structural analysis, since Components 4 and 3 have failed, shows that this path also leads to collapse. Hence, path 4-3 becomes the second most important failure mode [Fig. C.1(d)]. With two identified failure modes, the bounds of β_{sys} are calculated as:

$$(\beta_{sys,lower})_2 = 2.16$$
$$(\beta_{sys,upper})_2 = 2.25 \qquad \text{(C-2)}$$

At this stage the convergence check is carried out with Eqs.(C-1) and (C-2). From Eq.(2.113) with m = 2:

$$\text{for lower bound of } \beta_{sys} : \frac{2.25 - 2.16}{2.25} = 0.040 > 0.03$$

$$\text{for upper bound of } \beta_{sys} : \frac{2.25 - 2.06}{2.25} = 0.084 > 0.03$$

i.e. convergence criteria are not satisfied.

[e] From Fig. C.1(d) we can see that component 1 becomes the next focus component, and path 3-1 is selected. There is a path which has component 1 and of which $N_i < N_{max}$.[at the 7th row in Fig. C.1(d)]. When component 1 has failed, there are two paths having the highest probability of failure as seen in Fig. C.1(e). They are paths 3-1 and 4-6.

[f] When path 3-1 is selected as the best candidate path, this path also results in structural collapse, and becomes the third most important path [Fig. C.1(f)]. The bounds of β_{sys} are calculated as with m = 3:

$$(\beta_{sys,lower})_2 = 2.16$$
$$(\beta_{sys,upper})_2 = 2.25 \qquad \text{(C-3)}$$

Convergence checking is carried out again with Eqs.(C-2) and (C-3). Eq.(2.113) gives:

$$\text{for lower bound of } \beta_{sys} : \frac{2.16 - 2.16}{2.16} = 0.000 < 0.03$$

$$\text{for upper bound of } \beta_{sys} : \frac{2.06 - 2.01}{2.06} = 0.024 < 0.03$$

i.e. both Eqs.(2.113.a) and (2.113.b) are satisfied. Therefore, the searching procedure is terminated at this stage.

If $\varepsilon_{sys} < 0.02$, the procedure will continue. Then, the next path to be selected must be path 4-6 and focus is shifted to Component 6.

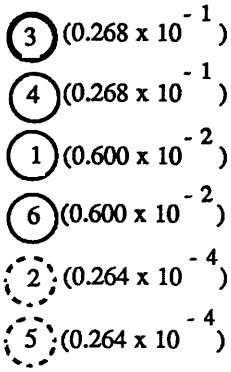

(a) Modes following Component 2 and 5 are discarded. Focus component is Component 3

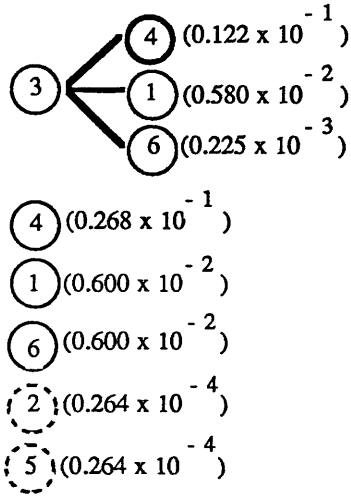

(b) Paths 3-5 and 3-6 are discarded during formation procedure of the utilisation matrix. Focus component is Component 4

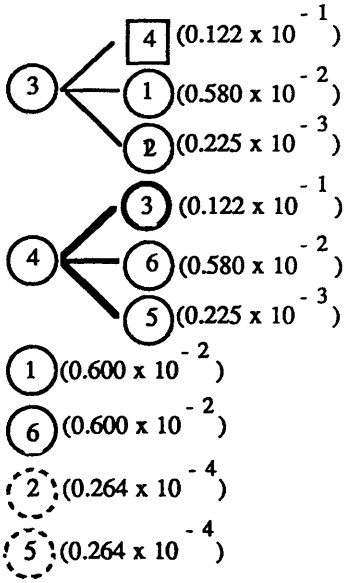

(c) Path 3-4 is selected and it leads to collapse. Focus component. is Component 3

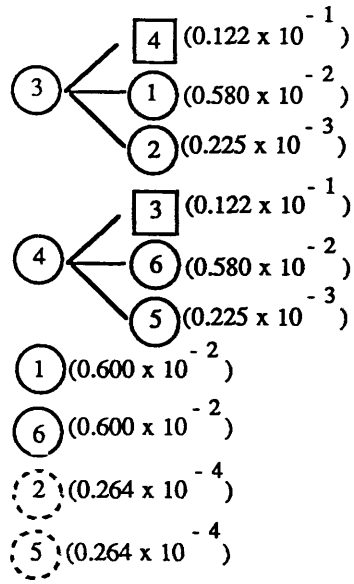

(d) Path 4-3 leads to collapse. Convergence criteria are not satisfied. Focus component is Component 1

Fig. C.1 Failure Path Search Procedure of Plane Truss Model ($\varepsilon_{sys} = 0.03$)

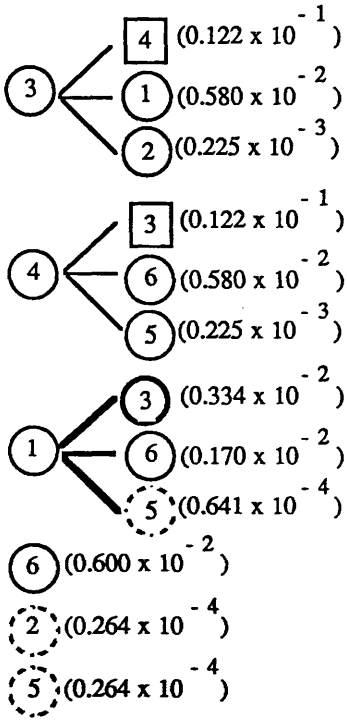

(e) Path 3-1 is selected.

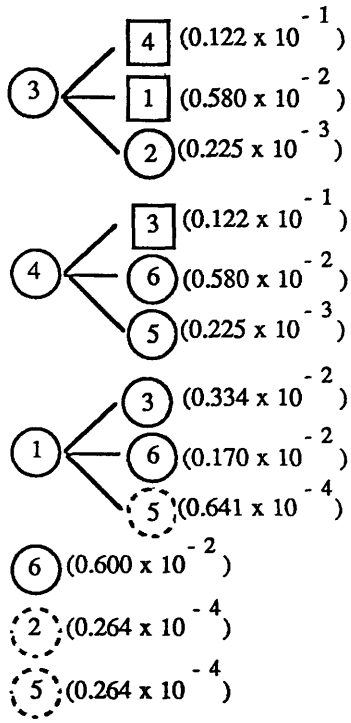

(f) Path 3-1 leads to the collapse and searching procedure is terminated because convergence criteria are satisfied

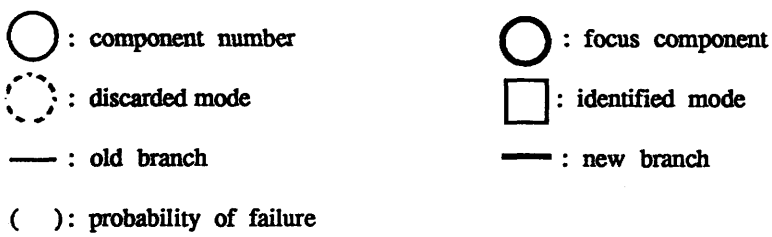

Fig. C.1 (continued)

APPENDIX - D FLOW VECTORS OF PRINCIPLE COMPONENTS

This section deals with the derivation of flow vectors of different types of components using their strength formulae as the failure surface equation according to Section 2.4.3. For illustration, the flow vectors have been derived when the component located at node i has failed [Fig. 2.5]., i.e., in Eq.(2.106) $\{a_j\} = 0$.

D.1 Simple beam element

The failure surface equation (strength formula) given as Eq.(2.120) can be rewritten omitting the strength modelling parameter:

$$\frac{Q_k}{R_k} = 1 \qquad \text{(D-1)}$$

Since Q_k and R_k are the bending moment and the plastic bending moment about the z-axis of component k, M_{z_k} and M_{y_k}, the function G of Eq.(2.107) has the form of:

$$G = \frac{M_{z_k}}{M_{P_k}} = f_6' \qquad \text{(D-2)}$$

From Eq.(2.107) the elements of the flow vector $\{a_i\}$ are obtained as:

$$a_1 = a_2 = a_3 = a_4 = a_5 = 0.0$$

$$a_6 = \frac{dG}{df_6'} = 1.0 \qquad \text{(D-3)}$$

D.2 Cylindrical Components

o Ring- and Stringer-Stiffened Cylinder:

[1] when the failure surface equation is given by Eq.(3.58)

$$\left[\frac{R_x}{\phi_x}\right]^2 + R_x R_\theta \left[\frac{2\sqrt{(1-\phi_x^2)(1-\phi_\theta^2)}}{\phi_x \phi_\theta} - 1\right] + \left[\frac{R_\theta}{\phi_\theta}\right]^2 = 1 \qquad (3.58)$$

Function G is the term on the left hand side of this equation. Using the following notations:

$$R_X / \phi_X = \sigma_X / \sigma_{Xu} = \sigma_X'$$
$$R_\theta / \phi_\theta = \sigma_\theta / \sigma_{\theta u} = \sigma_\theta' \qquad (D\text{-}4)$$

function G can be rewritten in terms of σ_x' and σ_θ' as:

$$G = (\sigma_x')^2 + 2\sigma_x'\sigma_\theta'\sqrt{(1-\phi_x^2)(1-\phi_\theta^2)} + (\sigma_\theta')^2 \qquad (D\text{-}5)$$

The axial stress is the resultant one due to the pure axial compression, σ_{xa}, in which the effect of hydrostatic pressure is included and the effect of the bi-axial bending moment, M_y and M_Z, and can be expressed as:

$$\sigma_x' = \frac{\sigma_x}{\sigma_{xu}} = \frac{1}{\sigma_{xu}}\left\{\sigma_{xa} + \frac{1}{A}\frac{2}{R}\sqrt{M_y^2 + M_z^2}\right\}$$
$$= \sigma_{xa}'' + \sqrt{(M_y'')^2 + (M_z'')^2} \qquad (D\text{-}6)$$

where A and R are the sectional area and the radius of cylinder, and σ_{xa}'' , M_y'' and M_Z''

are defined as:

$$\sigma''_{xa} = \frac{\sigma_{xa}}{\sigma_{xu}} \quad , \quad M''_{y} = \frac{\frac{2}{R}M_{y}}{A\,\sigma_{xu}} \quad , \quad M''_{z} = \frac{\frac{2}{R}M_{z}}{A\,\sigma_{xu}} \tag{D-7}$$

Hence, G becomes the function of σ_{xa}" , M_y" and M_z", which corresponds to f_1' , f_6' and f_5', respectively. Rewriting Eq.(D-6) in terms of f_1' , f_6' and f_5':

$$\sigma'_{x} = f'_{1} + \sqrt{(f'_{6})^2 + (f'_{5})^2} \tag{D-8}$$

Considering that

$$a_k = \frac{dG}{df'_k} \quad \text{and} \quad \frac{dG}{df'_k} = \frac{dG}{d\sigma'_x}\frac{d\sigma'_x}{df'_k} \tag{D-9}$$

the elements of the flow vector are obtained as follows:

$$a_1 = F'$$

$$a_5 = F'\frac{f'_5}{\sqrt{(f'_5)^2 + (f'_6)^2}}$$

$$a_6 = F'\frac{f'_6}{\sqrt{(f'_5)^2 + (f'_6)^2}}$$

and $a_2 = a_3 = a_4 = 0.0$ (D-10)

where

$$F' = \frac{dF}{d\sigma_x'} = 2\sigma_x' + 2\sqrt{(1-\phi_x^2)(1-\phi_\theta^2)} - \sigma_\theta'(\phi_x\phi_\theta)$$

[2] When the failure surface equation is given by Eq.(3.53)

With m = 2 and n = 1, the Eq.(3.53) is:

$$\left[\frac{\sigma_\theta}{\sigma_{\theta u}}\right]^m + \left[\frac{\sigma_x}{\sigma_{xu}}\right]^n = 1 \qquad (3.53)$$

Since the first term is associated with the radial pressure and has nothing to do with the nodal force vector, the function G is:

$$G = \frac{\sigma_x}{\sigma_{xu}} = \sigma_x' = f_1' + \sqrt{(f_6')^2 + (f_5')^2} \qquad (D\text{-}11)$$

Hence, the elements of the flow vector are given by:

$$a_1 = 1.0$$

$$a_5 = \frac{f_5'}{\sqrt{(f_5')^2 + (f_6')^2}}$$

$$a_6 = \frac{f_6'}{\sqrt{(f_5')^2 + (f_6')^2}}$$

and $a_2 = a_3 = a_4 = 0.0$ (D-12)

o Ring-Stiffened Cylinder:

When the strength model of Ring-stiffened cylinder is given as Eq.(3.11), the elements of flow vector are given as Eq.(D-12).

D.3 Rectangular Box-Girder

The failure surface equation is given by Eq.(3.89):

$$\frac{F_x}{F_{xu}} + \left[\left(\frac{M_y}{M_{yu}}\right)^{1.8} + \left(\frac{M_z}{M_{zu}}\right)^{1.8} \right]^2 = 1.0 \qquad (3.89)$$

and function G can be rewritten as Eq.(D-13) putting

$$\frac{F_x}{F_{xu}} = f_1' \quad , \quad \frac{M_y}{M_{yu}} = f_6' \quad , \quad \frac{M_z}{M_{zu}} = f_5'$$

$$G = f_1' + \left[(f_6')^{1.8} + (f_5')^{1.8} \right]^2 \qquad (D\text{-}13)$$

Hence, the elements of the flow vector are given by:

$$a_1 = 1.0$$

$$a_5 = 3.6\,(f_5')^{0.8} \left[(f_5')^{1.8} + (f_6')^{1.8} \right]$$

$$a_5 = 3.6\,(f_6')^{0.8} \left[(f_5')^{1.8} + (f_6')^{1.8} \right]$$

and $a_2 = a_3 = a_4 = 0.0$ (D-14)

Thus, when the component at node i has failed, the flow vector is:

$$\{a\} = \begin{Bmatrix} \{a_i\} \\ \{a_j\} \end{Bmatrix} = \begin{Bmatrix} \{a_i\} \\ \{0\} \end{Bmatrix} \qquad \text{(D-15)}$$

When components at both nodes have failed, the flow vector can be obtained from the above procedure. Once the flow vector is determined, the reduced element stiffness matrix is evaluated from Eq.(2.108) when one node has failed, or from Eq.(2.109) when both nodes have failed. Due to the complex nature of the above procedure, especially in the case of cylindrical components and components of rectangular section, the flow vector and the reduced element stiffness matrix has to be determined numerically.

GLASGOW
UNIVERSITY
LIBRARY